Soil-Driven Self-Healing Concrete: Evaluation of Soil Bacteria, Encapsulated Nutrients, and Environmental Conditions

Submitted in partial fulfilment of the requirements for obtaining a Doctor of Philosophy in Civil Engineering from the University of Derby

Abdurahim Abogdera

University of Derby, College of Science and Engineering

February 2025

Declaration

I declare that this thesis is entirely my own work. I have not submitted it for any other degree at another university. Any ideas or information from other sources have been properly acknowledged and cited in the reference section, following standard academic practices.

Abdurahim Abogdera

Derby, February 2025

Acknowledgement

Throughout my research journey, I would like to express my sincere thanks to my supervisors, Dr. Omar Hamza and Dr. David Elliott. I would like to express my sincere gratitude to the Libyan Embassy as well for their financial support, which gave me the opportunity to complete this project. A special thank you goes out to Richard Duff, Joseph Everington, Giacomo Anderson, and Graham Souch from the laboratory's technical staff. As a result of her constant support and encouragement throughout the years of my studies, I would like to express my deepest gratitude to my wife.

Abstract

Biotechnology opens exciting possibilities for underground concrete structures, such as tunnels and underground storage. Bio-self-healing concrete, which uses bacteria to repair cracks automatically, could enhance the sustainability of these structures by enabling them to self-repair without human intervention. However, a major challenge in bacteria-based self-healing concrete is ensuring bacterial survival and activity, particularly in the harsh chemical environment of concrete, which typically has a high pH that is detrimental to bacterial life.

This research explores a simple yet innovative idea: could the soil surrounding underground structures provide the bacteria needed for self-healing? If successful, this approach could simplify the process, making it more practical and cost-effective. The research addresses this question through a series of lab experiments conducted in three phases, each designed to explore different aspects of the conditions necessary for soil-driven bio-self-healing.

In the first phase, the focus was on understanding the chemical conditions of cement mortar surfaces under which bacteria could survive and function. The research sought to identify the factors that hinder bacterial activity, such as high pH, and to test methods that could improve the conditions for bacteria to thrive. Specifically, experiments were conducted to assess pH levels, electrical conductivity, and calcium ion concentrations in water environments around the mortar. The results revealed that high pH levels resulting from cement mortar leaching hinder bacterial survival. Various techniques were tested, including introducing supplementary materials like GGBS, using flowing water, and accelerating carbonation. These methods created a more bacteria-friendly environment, supporting the growth and activity of bacteria, particularly under conditions mimicking underground structures exposed to water. This phase laid the foundation for understanding how to optimize the chemical environment for bacterial activity.

The second phase explored how to supply the necessary nutrients to attract indigenous soil bacteria to the cement mortar surfaces, thus supporting their activity in the self-healing process. Different nutrient delivery methods were tested to ensure that the addition of nutrients did not compromise the concrete's properties. Nutrient-filled capsules were designed to gradually release nutrients, facilitating bacterial activity to produce calcium carbonate for crack healing. The results showed that calcium carbonate capsules had minimal impact on mortar properties due to their small size and low concentration. In contrast, calcium alginate capsules, which were larger and created voids within the mortar, weakened the material. Various capsule proportions were tested to find an optimal balance, ensuring that the mortar strength remained largely intact while still promoting effective self-healing. This phase answered the research question of how to incorporate nutrients into the mortar without compromising its mechanical properties.

In the third phase, the performance of the self-healing system was tested in a soil environment to simulate real-world underground conditions. Cement mortar samples were exposed to different types of soil as well as water, which acted as a natural source of bacteria and other necessary elements for self-healing. The success of the self-healing process was measured by observing crack closure and the formation of calcium carbonate deposits both near the crack surface and deeper within the mortar. The results demonstrated that the soil environment provided the necessary conditions for bacteria to activate and repair cracks, simulating conditions typically found in underground concrete structures. This phase directly addressed the research question by testing the viability of using natural soil bacteria for self-healing, a cost-effective and sustainable alternative to adding external bacterial cultures.

These findings highlight a practical and sustainable approach to self-healing concrete by harnessing naturally occurring bacteria in organic soil to repair cracks in underground structures. Experimental results showed that modifying the harsh chemical environment of cement mortar—particularly by lowering the pH from >13.5 to a range between 9.2 and 10.5 using GGBS replacement (30–50%), flowing water, and accelerated carbonation—created conditions more conducive to bacterial viability. Bacterial activity was negligible above pH 11.5, but significantly increased when the pH dropped below 10.5, with optimal microbial-induced calcium carbonate precipitation (MICP) occurring near pH 9.5. The use of 50 µm calcium carbonate microcapsules allowed controlled nutrient release without compromising mechanical strength, unlike larger alginate capsules (>300 µm) that reduced compressive strength by up to 15–20%. Notably, mortar samples exposed to organic soil demonstrated visible crack closure up to 0.35 mm within 28 days, with calcium carbonate precipitation reaching 3.1–4.2 g/m² on the crack surfaces, confirming active MICP. Overall, this research presents soil-driven bio-self-healing concrete as a promising, low-cost, and environmentally friendly solution to enhance the resilience and service life of underground infrastructure.

Parts of this work has been published in the following publications

There are the following peer-reviewed papers in which the author is named as the first author or co-author:

1. Abogdera, A., Hamza, O., & Elliott, D. (2024). An examination of how the chemical conditions of concrete surfaces is impacted by the presence of flowing water and additional materials. 4th fib International Conference on Concrete Sustainability. (ICCS2024). ICCS 2024. Lecture Notes in Civil Engineering, vol 574: pp 131–139. Springer, Cham. https://doi.org/10.1007/978-3-031-80724-4_17

2. Abogdera, A., Hamza, O., Elliott D. (2023) Impact of leaching on the chemical composition of concrete solution: the significance of supplementary materials and water conditions. Proceedings of the International Civil Engineering and Architecture Conference (ICEARC23), 12-14 October 2023, Türkiye https://doi.org.10.31461/icearc.2023.mat914

3. Hamza, O., Esaker, M., Abogdera, A., & Elliott, D. (2024). Bio-protection of cementitious materials below ground: The significance of natural soil environments. Developments in the Built Environment, 17, 100331. https://doi.org/10.1016/J.DIBE.2024.100331.

List of contents

1 Contents

List of figures

List of tables

List of abbreviations

PC	Portland cement
PFA	pulverised fuel ash
GGBS	ground granulated blast-furnace slag
C-S-H	Calcium silicate hydrate
Ca ions	Calcium ions
PE	polyethylene
PP	plain mortar
PW	plain mortar in water
PN	particularly mortar with nutrients
PVA	polyvinyl alcohol
EC	Electrical conductivity
MICP	Microbiologically Induced Calcium Carbonate Precipitation.
SCMs	supplementary cementitious materials
SMA	Shape memory alloy
SEM-EDX	Scanning electron microscopy and energy dispersive
SAPs	super absorbent polymers
RGB	red, green, and blue
PSD	Particle Size Distribution
LVDTs	Linear Variable Differential Transducers

1. Chapter 1: Introduction

1.1 Background study

Concrete is a key material in construction, known for its impressive ability to withstand heavy loads. However, it has a natural weakness when it comes to handling tension, which makes it prone to developing cracks. These cracks can have a serious impact on the durability and lifespan of concrete structures (Vijay et al., 2017). Concrete is the backbone of modern construction, but even though it's used everywhere, structures are still prone to cracking. Fixing and maintaining large concrete structures can be both expensive and labour-intensive. How easy it is to repair often depends on where the damage is and how bad it is. In the United States, around $500 billion is spent each year just to keep infrastructure in good shape. In the UK, this figure is about £40 billion annually, with a big chunk of that going toward concrete repairs. (Giang *et al.*, 2011). Similarly, Europe allocates nearly half of its annual construction budget to repair and maintenance, while concrete degradation and steel reinforcement corrosion in China cost nearly 250 billion RMB annually (Sidiq et al., 2019). Cracks in underground concrete structures are influenced by several factors, including groundwater, humidity, acidity, alkalinity, carbonation, corrosion, and frost heave. These factors weaken the structure over time, reducing its lifespan and posing safety risks to pedestrians and vehicles. Repairing and maintaining cracked concrete is not only labour-intensive but also costly, the fees for which can be up to twofold the cost of erecting new structures. Figure 1, adapted from *(TR22 Non-Structural Cracks in Concrete, 2010)*, provides a summary of the primary causes and contributing factors associated with the formation of cracks in concrete. Moreover, as much as 50% of a project's budget could go toward rehabilitating an existing structure that needs to be repaired (de Brito and Kurda, 2021).

Maintaining and inspecting large infrastructure projects, such as tunnels and bridges, comes with significant challenges. These include the high costs involved, the sheer size of the structures, and the difficulty of accessing certain damaged areas. Identifying damage and carrying out routine maintenance require a great deal of money, labour, and planning (Wu, Johannesson, *et al.*, 2012). While bio-concrete holds much promise, making it work in real-world applications is challenging. Adding bacteria to concrete can weaken its compressive strength, and using capsules filled with healing agents can affect the concrete's mechanical performance. The chemical and polymer materials used in these systems can cause weak bonding, and the voids left behind when capsules release their contents can reduce both tensile and compressive strength (Van Tittelboom and De Belie, 2013).

Even though bio-concrete technology has made progress, major obstacles remain, especially when it comes to producing and storing bacterial spores or dormant cells within the concrete over the long term. Developing a practical and reliable self-healing concrete system is still a work in progress.

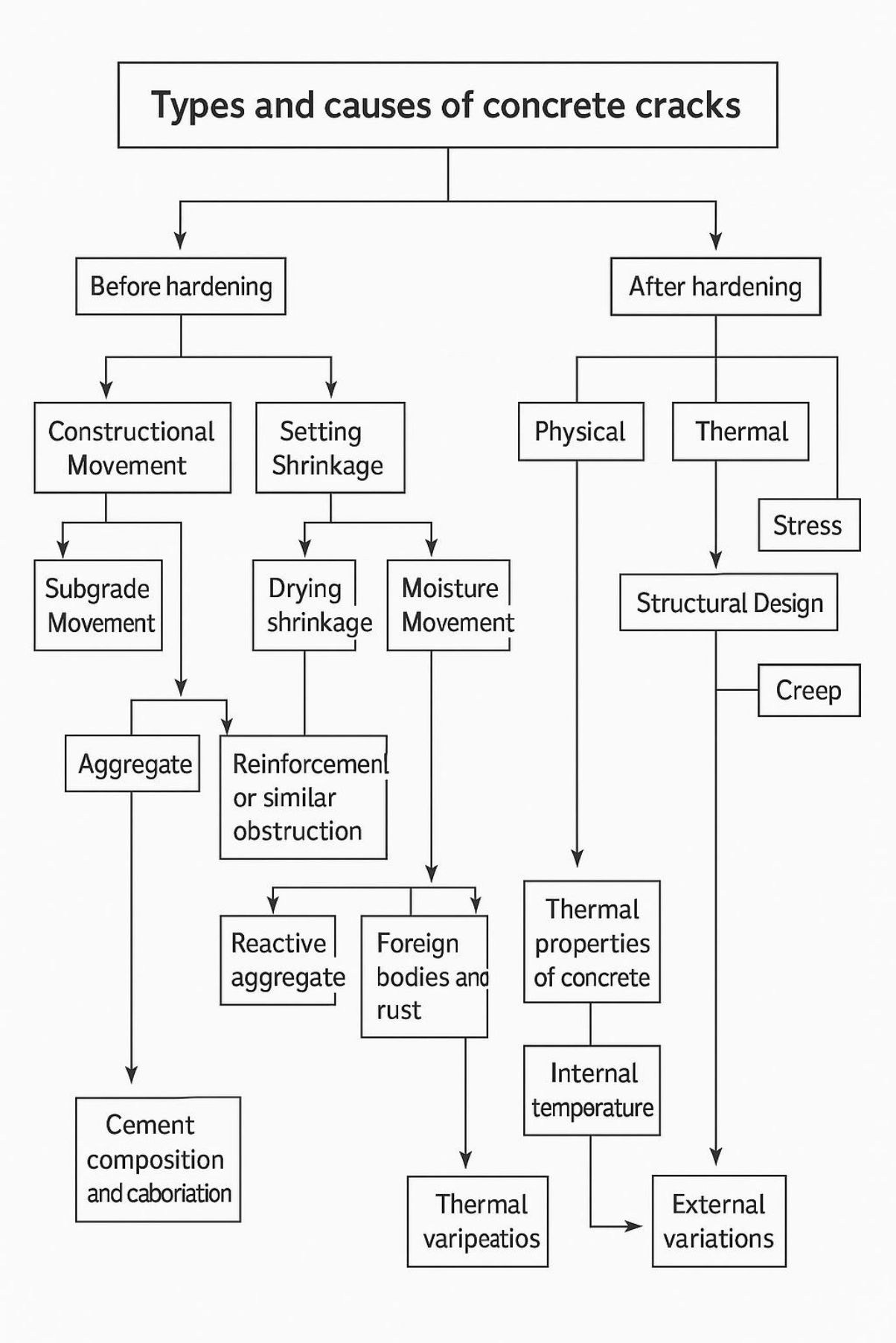

Figure 1: Factors influencing cracks in concrete adopted form (TR22 Non-structural cracks in concrete 2010)

1.2 Research motivation

Autonomous self-healing concrete is an exciting development that could significantly reduce the high costs and labour involved in traditional concrete repair and maintenance (Wu, Johannesson, *et al.*, 2012). This innovative approach has the potential to ease the financial and operational pressures of maintaining concrete infrastructure. Among the various self-healing techniques—such as bacteria, microencapsulation, mineral admixtures, hollow fibres, shape-memory materials, and expansive agents—encapsulating healing agents within concrete stands out as one of the most effective. This method helps restore some of the concrete's strength, blocks harmful substances from penetrating cracks, and fully seals them, ultimately improving the lifespan of concrete structures (Hilloulin *et al.*, 2015).

Wang *et al.* (2019) emphasize the potential of microcapsules, particularly in coastal infrastructure and sustainable self-healing concrete. Tests in both laboratories and real-world conditions have shown that adding microcapsules to concrete can enhance its permeability and improve its ability to repair itself. This is especially useful for tunnels, where controlling permeability is crucial for long-term durability. However, using microcapsule-based self-healing systems in practical applications isn't without challenges. The constantly changing external loads on structures create complex stress conditions, making it harder to manage cracks effectively. To address this, it's important to fine-tune how the healing agents are delivered under different load conditions. Another critical factor is ensuring a strong bond between the concrete and the microcapsules, as a weak bond can compromise the overall strength of the structure (Gupta et al., 2017a). Achieving effective and reliable self-healing in practical concrete applications necessitates an optimal balance between the size and concentration of microcapsules incorporated into the mix. As highlighted by Wang *et al.* (2019), this balance is critical to ensuring that the self-healing system performs efficiently without compromising the mechanical strength and long-term durability of the concrete matrix.

Since the mid-1990s, scientists have been exploring how bacteria can be used in concrete to create more sustainable and environmentally friendly self-healing systems. The idea is to embed bacteria that produce calcium carbonate, which can seal cracks as they form. For this process to work effectively, several factors come into play, including the concentration of dissolved carbon, pH levels, the availability of calcium ions, and nucleation sites (Wu, Johannesson, *et al.*, 2012). However, concrete isn't exactly a welcoming environment for bacteria. Its high alkalinity, with a pH of 12 to 13, and low porosity make it difficult for bacteria to survive (MohdSam *et al.*, 2021). On top of that, the conditions during cement hydration—like high temperatures and limited oxygen—add to the challenge (Lee and Park, 2018a). To tackle these issues, researchers have come up with the idea of using microcapsules to protect the bacteria. These capsules stay intact within the concrete and only release the bacteria when cracks form, exposing them to water and oxygen. Once activated, the bacteria produce calcium carbonate to seal the cracks and stop further damage (MohdSam *et al.*, 2021).

Despite the advancements, the encapsulation of bacteria remains the most effective method for healing cracks up to a maximum width of 970 µm and a depth of 320 µm (Muhammad *et al.*, 2016). Therefore, ongoing research is motivated by the need to overcome the current limitations of self-healing concrete technologies, particularly in optimizing bacterial encapsulation and ensuring effective performance under practical conditions. However, still, the technology of bio-concrete has many challenges, not least those of producing and storing large numbers of spores or senescent cells within the concrete mass for indeterminate periods of time, which

means that a practical and resilient biological self-healing technology for concrete remains out of reach at present. For example, the availability of the microorganisms in soil which should be for geotechnical engineering and researchers, the next transformative practice is harnessing biological processes in soils. It has been suggested, for example, according to Dejong *et al.*, (2013), many chemical processes that are mediated by biology can now be exploited as part of the process. Additionally, as reported by Sari (2015) microorganisms can influence soil's appearance and enhance its ability to resist load applications by precipitating calcite, which binds soil particles together and affects their ability to resist load applications. There is no doubt that microorganisms play a significant role in soil structure and behaviour. Despite being ignored by geotechnical engineers for centuries, microorganisms are ubiquitous in soils and are found in surprisingly high concentrations. This is no matter how saturated, mineralogical, or pH the soil may be. Furthermore, according to Wang *et al.* (2014) the cell concentration from 10^6 to 10^8 cells/mL increased Co_3^{-2} production by over 30%. A concentration of bacterial cells/mL greater than 10^6 is required to obtain a sufficient volume of precipitation, preferably 10^8 cells/ml. Yet, the number of microbes that live near the surface of the soil near the ground surface is more than 10^{12} microbes per kilogram (Sari, 2015). Despite this, as a geotechnical system becomes deeper (e.g., between 2 and 30 m), the microbial population in the system's soil is reduced to a level of about 10^{11} to 10^6 microorganisms per kilogram of soil (Whitman.1998). Consequently, using the existing bacteria in soil to repair cracking concrete may mitigate such problems. There has been extensive research into organic surface treatments, including acrylic, polyurethane, epoxy resins, silanes and siloxanes, and sodium silicates, but these can only be used for a short period of time. Yet, to solve this problem, surface resilient via bio-concrete by using the existing bacteria in soil could be a promising solution.

1.3 Problem statement

The use of bio-concrete would work as a preventative measure to prevent the occurrence of fissures before they develop and would prevent liquids and gases from entering the structure (Gadd and Dyer, 2017a). Currently, there is not much research being done on the topic of bacteria in underground structure. However, several studies have demonstrated that microbially induced calcite precipitation techniques are highly influenced by the concentration of the cementation materials (calcium ions, dissolved organic carbon), the geometric compatibility of the cementation materials, pH, temperature, nutrients, and the availability of nucleation sites (Dhami, and Mukherjee, 2013a). The presence of a significant amount of Ca (OH)2 in the concrete pores makes determining the influence of pH on bacteria activity in concrete critical. Because of the ingress of water from the external environment, the concrete microenvironment is highly alkaline, with pH values as high as 13, while the pH of a concrete crack mouth is predicted to be between 9 and 11, owing to the ingress of water (Dhami et al., 2013a). Additionally, environmental concerns arise from the release of ions such as aluminium, calcium, chromium, magnesium, sodium, potassium, and zinc into the surrounding water, as well as an increase in the pH of the water due to concrete leaching (Wu, Johannesson, *et al.*, 2012). The utilization of self-healing concrete offers immediate benefits such as reducing deterioration, extending infrastructure lifespan, and decreasing repair frequency and costs over time. These advantages can contribute to environmental sustainability by reducing the need for repairs, thereby lowering material consumption, minimizing energy usage, and decreasing pollutant emissions associated with material production and transportation. In addition, the applications of this self-healing concrete could prevent the disruptions of traffic during repair or

reconstruction work in the transport infrastructure. This project proposes to explore the potential for the surrounding soil to supply bacteria needed to bring about self-healing of underground concrete materials, therefore simplifying the self-healing system, and increasing its viability.

1.4 Aim and objectives of the research

This project explores the potential of using the surrounding soil to provide essential materials, like bacteria, to boost the self-healing abilities of underground concrete structures. The goal is to evaluate how effective and practical bio-based self-healing techniques can be in underground environments. By studying the interactions between soil and concrete, the research aims to find out if naturally occurring soil bacteria and other materials can help concrete repair itself. This could make concrete more durable, resilient, and long-lasting, especially in underground structure where maintenance is difficult due to harsh conditions.

The study involves a series of experiments designed to test how well bio self-healing methods work in underground conditions. These experiments will help us understand how soil composition, moisture levels, and chemical interactions between soil and concrete affect the self-healing process. A key focus is on how efficiently materials from the soil, especially bacteria, can activate and sustain self-repair in concrete, ensuring its strength and longevity even in challenging underground environments.

At the heart of this research is the relationship between concrete and the natural environment around it, particularly the role of microorganisms in the soil. Past studies (Amer Algaifi *et al.*, 2020a) have shown that certain bacteria, like Bacillus species, can produce calcium carbonate ($CaCO_3$), which is crucial for self-healing concrete. This project builds on that knowledge by investigating whether bacteria already present in the soil can perform the same function, potentially removing the need to add external bacteria. If successful, this approach could offer a more sustainable and cost-effective solution for self-healing concrete, particularly in critical underground structures like tunnels, foundations, and transportation systems.

The research will explore how the chemical environment impacts the self-healing process, focusing on factors like pH, electrical conductivity, and calcium ions. Understanding these elements is key to adapting bio self-healing techniques to different conditions. This study will also look at how the size of the capsules affects the performance of bio-concrete. These capsules are tiny containers filled with nutrients (like calcium lactate) and are mixed into the concrete. When cracks form in the concrete, the capsules break open and release the nutrients into the cracks. Soil bacteria, which are naturally present in the environment, are attracted to these nutrients. They eat the nutrients and produce carbon dioxide (CO_2) as a byproduct. This CO_2 then reacts with calcium from the concrete itself, forming calcium carbonate—a natural mineral that fills and seals the cracks. This process helps the concrete heal itself over time. The size of the capsules is important because it affects how well the nutrients are spread out in the concrete and how efficiently the cracks get sealed. If the capsules are too small, they might release the nutrients too quickly, and if they're too big, they might not work as effectively. By studying capsule size, it can figure out the best way to make bio-concrete work in real-world situations, in underground structure.

This research aims to deepen our understanding of how bio self-healing methods can be applied to underground structures while exploring new ways to use naturally occurring soil materials to boost concrete's ability to repair itself. The insights gained could lead to innovative

approaches in construction and maintenance, especially for underground infrastructure where repairs are challenging, costly, and difficult to access.

To keep the study focused and thorough, a set of key research questions will guide the process. These questions will shape the experimental design and analysis, focusing on the most important aspects of the investigation.

1. Can soil bacteria colonize and actively participate at the concrete-soil interface? In another word, is the chemical environment at the concrete surface conducive to supporting bacterial activity?
2. If nutrients can be incorporated into concrete to attract indigenous bacteria from the soil, what techniques can be employed to supply these nutrients? Should nutrient delivery rely on encapsulated carriers or direct addition? Additionally, what are the implications of these methods on the strength and durability of the concrete?
3. How does the soil-driven bio-self-healing system function under different conditions? What are the roles of soil bacteria, nutrient delivery, and environmental factors in facilitating calcium carbonate precipitation, and how can the system's design be optimized for efficient crack healing and structural performance?

This study explores an alternative approach: a soil-driven bio-self-healing system that relies on indigenous soil bacteria to repair cracks in concrete. By incorporating nutrients into the concrete matrix, this system aims to attract soil bacteria to the concrete-soil interface, where they can actively participate in the self-healing process. The chemical environment at this interface, along with the method of nutrient delivery, plays a critical role in determining the system's effectiveness. Furthermore, the impact of environmental factors such as moisture, temperature, and pH on the healing process must be understood to optimise the system for real-world applications. The research is structured around three key objectives:

Objective 1: to investigate the potential for soil bacteria to colonise and participate actively at the concrete-soil interface, focusing on the chemical environment's suitability for bacterial activity.

Objective 2: to evaluate techniques for incorporating nutrients into concrete (to attract indigenous soil bacteria), comparing encapsulated carriers and direct addition, and assessing their effects on concrete strength and durability.

Objective 3: to understand the functioning of a soil-driven bio-self-healing system under various conditions, examining the roles of soil bacteria, nutrient delivery, and environmental factors in calcium carbonate precipitation, and optimising system design for effective crack healing and structural performance.

1.5 Thesis outline.

Following is a summary of the contents of the thesis:

Chapter 1: A brief background and introduction to the study is presented, as is a definition of the problem, the purpose of the study, and the objectives that will be addressed as a result of the study.

Chapter 2: Provide a comprehensive critical review of the literature, examining the current advancements in the field related to the types and causes of cracks in concrete structures. Additionally, explore key aspects concerning the classification and evolution of self-healing concrete technologies. Various methodologies utilized to evaluate the effectiveness of self-healing systems are also analysed.

Chapter 3: This chapter offers a clear and detailed breakdown of the methods used to achieve the study's objectives, showing how each step aligns with the broader research goals. The methodology is thoughtfully structured into three interconnected phases, each designed to address key research questions.

Chapter 4: This chapter examines how concrete interacts with its chemical environment and microbial activity through two main components. The first explores how different chemical elements affect pH levels and overall properties, using pH monitoring and composition analysis to understand the impact of carbonation and environmental factors on concrete durability. The second looks at how concrete properties influence bacterial activity and calcium carbonate production, focusing on how chemical composition, moisture, and physical conditions support concrete's self-healing ability.

Chapter 5: This chapter explores how calcium carbonate and calcium alginate microcapsules can be incorporated into concrete, assessing their impact on the material's properties and their potential as nutrient carriers for microbial self-healing. It examines how these microcapsules affect concrete's mechanical performance and evaluates their ability to release nutrients effectively when cracks form.

Chapter 6: This chapter examines how well the self-healing system repairs concrete cracks caused by mechanical loading. The experiments focus on evaluating its performance, identifying where calcium carbonate ($CaCO_3$) forms, and finding ways to improve the process. Visual inspection and image analysis are used to track crack closure, assess the effectiveness of microbial-induced calcium carbonate precipitation (MICP), and determine whether healing happens mainly on the surface or deeper within the concrete.

Chapter 7: This chapter synthesizes the key findings of the research, summarizing the conclusions derived from the studies conducted in this thesis. Additionally, it outlines recommendations for future research to further investigate the potential of bio-based self-healing concrete, particularly when incubated in soil.

2 Chapter 2: literature review

2.1 Introduction

Underground concrete structures are frequently constructed to keep water out, but they are vulnerable to moisture penetration and leaks, which can occur due to cracking or poor construction. Even if water does not completely penetrate the structure, it can cause difficulties like reinforcement corrosion in monolithic structures like foundations. To check and fix concrete cracks, human interaction is necessary, but engineers may find it difficult to reach damaged locations for repair work in some circumstances due to their location and/or environmental conditions (Chandra and Ravitheja, 2019). Underground structural members, walls of tanks carrying extremely hazardous waste, and nuclear waste disposal facilities are all examples of the previously mentioned scenario (Wu et al., 2012a). Furthermore, in other circumstances, such as with tunnel linings, water transport can cause erosion of the surrounding soil, causing load pathways through the structure. However, the application of self-healing materials is certainly a cutting-edge and creative concern for the civil engineering industry's long-term sustainability. For a standard extended period, the need for unexpected maintenance and repair can be eliminated. As a result of adopting construction materials with self-healing qualities, better and more sustainable civil infrastructure is created (Van der Zwaag, 2007). Fibres (Homma et al., 2009a), microorganisms ('Bacteria-based self-healing concrete', 2011), and capsules containing healing agents (Li et al., 1998) are all part of the self-healing technology now in use. The first two procedures aim to reduce the crack width within the concrete, but the third seeks to immediately bind or fill the crack by breaking a repair agent capsule. Although these technologies have enhanced concrete's self-healing capabilities to varying degrees, they have certain drawbacks, such as the time required for fibre-reinforced self-healing technology and the toxicity of the repair agents (Wang *et al.*, 2018a). Additionally, sometimes dead microorganisms produce holes in the concrete, lowering the overall strength of the building. However, the technology of self-healing has many challenges, not least those of producing and storing large numbers of spores or senescent cells within the concrete mass for indeterminate periods of time, which means that a practical and resilient biological self-healing technology for concrete remains out of reach at present. However, little study has been done to far on the impact of the soil environment on portions of concrete structures such as foundations, retaining walls, bridge piers, and tunnels. Chemicals, organic compounds, and microorganisms in natural soil and manufactured aggregates contribute to concrete exposure conditions and may have a substantial impact on the effectiveness of autogenous and autonomous concrete crack healing (Hamza *et al.*, 2020). For example, the existing bacteria in soil can give services that can be harnessed to produce the self-healing process for underground structures, reducing the influence on the mechanical characteristics of the concrete owing to the space taken up by the additives. According to Bulletins (1977) in soil systems, microorganisms account for 70% to 85% of the biological component, however, a thorough grasp of their metabolic rate is required to accurately predict how microbes would behave under various conditions (Epelde *et al.*, 2008). A single kilogramme of soil at the surface contains between 10^9 and 10^{12}organisms (Umar et al., 2016). According to DeJong *et al.*, (2014) and his team, a gram of soil may contain 10^{12} bacteria, while a single gram of badly graded soil can have over 10^6 microorganisms. Yargicoglu and Reddy (2015) reported that in a gram of soil roughly 10^9 cells. Microorganisms, particularly bacteria, have been related to the creation of carbonate minerals in studies, and they also play an essential role in carbon cycling (Hamdan *et al.*, 2011). Our research project distinguishes itself by utilizing naturally occurring bacteria from soil and introducing nutrient

supplementation in concrete, creating a unique research gap with significant potential for innovative advancements in sustainable construction practices. By harnessing the inherent self-healing properties and environmental adaptability of soil-derived bacteria, we aim to develop sustainable self-healing technologies. However, two primary challenges must be addressed: the leaching of high Ph from the concrete matrix and the impact of electrical conductivity (salt) on bacterial viability. The leaching of high pH from concrete, influenced by its alkaline nature, may affect the survival and effectiveness of bacteria. Understanding the dynamics of pH leaching and its implications for bacterial activity is crucial for optimizing the self-healing process. Additionally, the presence of salts in concrete, contributing to electrical conductivity, can negatively impact bacterial viability by affecting osmotic balance and metabolic processes. Evaluating the compatibility of soil-derived bacteria with different salt levels in concrete is vital. Identifying bacterial strains tolerant to elevated electrical conductivity or developing strategies to mitigate its detrimental effects is a critical area requiring further research. To unlock the full potential of our approach, addressing the challenges associated with high pH leaching and electrical conductivity is necessary. Through dedicated study and investigation, encompassing optimization of encapsulation techniques, strain selection, and tailored nutrient supplementation, we can propel the advancement of self-healing technologies, enhancing the durability and sustainability of concrete structure.

2.2 Types and Causes of Cracks in Concrete Structures

Concrete's tensile strength is typically weak, often accounting for less than 10% of its compressive strength. Due to this inherent weakness in the tension zone, cracks can form due to inevitable tensile stresses. Cracking is common and almost unavoidable in concrete structures. Applied stresses combined with exposure to severe environments are typically the primary cause of cracks in concrete (Lee et al., 2016). Several factors contribute to the formation of surface cracks in concrete structures. These include tensile stresses, excessive heat, excess moisture, drying shrinkage, freeze-thaw cycles, and inadequate curing practices. Moreover, chlorides and carbon dioxide can penetrate concrete during early hydration, exacerbating damage through cracking and accelerating the degradation process (Achal *et al.*, 2013). Cracks can either be superficial, affecting only the concrete's appearance, or they may severely compromise the structure's integrity and reduce its service life. The significance of cracks depends on the type of crack and the structure's function. For example, cracks that might be acceptable in residential buildings are not suitable for water-retaining or nuclear structures (Lee et al., 2016). In most cases, concrete cracks do not lead to immediate structural failure but can degrade performance, increasing maintenance and repair costs (Biondini and Frangopol, 2016). Cracks can be divided into two major categories based on the timing of their occurrence: those that develop before concrete hardens and those that appear after hardening. Below is a diagram illustrating the various types of cracks that can occur in concrete structures. These cracks are divided into two main categories: those that form before the concrete hardens and those that develop after hardening.

2.2.1 Cracks Before Hardening

Cracks that form before concrete hardens are primarily due to factors associated with construction processes. These include construction movements, subgrade settlement, and issues such as timber swelling or weak formwork, all of which can destabilize the concrete and lead to cracking during the setting phase as showing in figure2 adopted and modified from *TR22 Non-structural cracks in concrete.* (2010). A notable example is plastic shrinkage cracks, which

arise when there is rapid moisture loss from the surface during hydration. This loss of moisture generates tensile stresses, especially on the surface, causing cracks before the concrete achieves significant strength. Research indicates that plastic shrinkage cracks are more likely in conditions of elevated temperatures, low humidity, and strong winds, where evaporation surpasses the rate of bleeding water rising to the surface (Kovler and Roussel, 2011). Implementing proper curing techniques and environmental control can effectively reduce the occurrence of these cracks by slowing down moisture loss and promoting uniform hydration (Kosmatka et al., 2003). Cracks appearing before the concrete hardens are caused by construction-related factors, such as movements during construction, subgrade settlement, and insufficient formwork strength. These factors can compromise the stability of the fresh concrete, resulting in premature cracks. For example, subgrade movement, often driven by timber swelling or uneven soil conditions, can cause settlement cracks, particularly in thick slabs. One of the most common early-age cracks is plastic shrinkage cracking, which happens when excessive moisture evaporates from the surface of the concrete during the early hydration process. This moisture loss creates tensile stresses on the surface of the concrete before it gains enough strength to withstand these forces, leading to cracks. According to Altoubat. (2001) such cracks are particularly prevalent in hot, dry, or windy environments where the evaporation rate outpaces the movement of bleeding water to the surface. These conditions disrupt moisture balance within the concrete, causing the surface to shrink rapidly while deeper layers retain more moisture. Plastic shrinkage cracks typically develop within hours of concrete placement as rapid moisture loss leads to capillary stresses, which the young concrete cannot yet resist. The severity of cracking is closely linked to environmental factors like temperature, wind speed, and relative humidity, all of which can speed up evaporation. Preventive measures, such as using windbreaks, shading, or controlled water misting, have been shown to significantly reduce the risk of plastic shrinkage cracking (Bentur and Mitchell, 2008). In addition, research by Banthia (2006) highlights that the composition of the concrete mix itself plays a crucial role in the susceptibility to plastic shrinkage cracks. High water-cement ratios, large aggregate surface areas, and the absence of shrinkage-reducing admixtures can increase the likelihood of cracking. The use of fibres, such as polypropylene or glass fibres, has been explored as a method to mitigate this issue, as they help distribute tensile stresses more evenly across the concrete, thereby reducing localized cracking (Soroushian and Bayasi, 1991). Alongside proper curing practices, such as applying curing compounds, damp burlap, or polyethylene sheets, adopting best practices during the mixing and placing of concrete is essential to reduce the risk of plastic shrinkage cracks. New advancements in concrete technology, including self-healing materials and shrinkage-reducing admixtures, have shown promise in controlling early-age cracks by enhancing moisture retention and minimizing capillary stresses (De Belie and Wang, 2016).

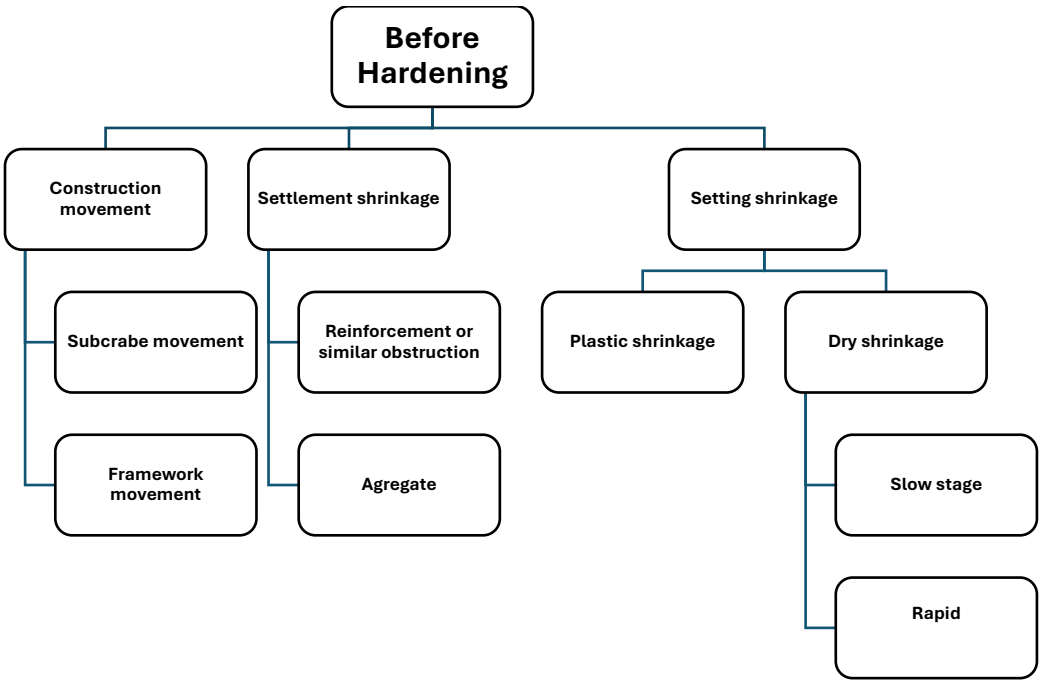

Figure 2: Causes of cracks before hardening adopted form (TR22 Non-structural cracks in concrete 2010)

2.2.2 Cracks After Hardening

Cracks that form after the hardening of concrete can be classified into six main categories: chemical cracks, physical cracks, thermal cracks, cracks related to structural design, stress concentration cracks, and cracks resulting from accidental overload (Larosche, 2009). Figure 3 adopted form *TR22 Non-structural cracks in concrete,* (2010) illustrated each category is associated with specific mechanisms and external conditions affecting the concrete's structural integrity. Chemical cracks are typically caused by internal reactions within the concrete. A well-known example is the alkali-silica reaction (ASR), where alkalis in the cement react with reactive silica in the aggregates, forming an expansive gel. This expansion creates internal stresses, which lead to cracking. Other chemical-induced cracks may result from carbonation, sulphate attack, or chloride-induced corrosion in reinforced concrete (Neville, 1995a). Physical cracks usually develop due to shrinkage processes, such as drying or plastic shrinkage. These occur due to moisture loss from the concrete, particularly in its initial stages. Factors like inadequate curing or environmental influences, including wind or temperature changes, can result in surface or internal cracks (Mehta, and Title, 2006). Thermal cracks arise primarily due to temperature changes within the concrete. During hydration, especially in large concrete elements, heat is produced, leading to thermal gradients between the interior and exterior. This temperature difference causes expansion and contraction, creating tensile stresses that exceed the concrete's strength, resulting in cracks (Title, 1974). In colder climates, thermal cracking can also occur due to frost action when water inside the concrete freezes and expands, producing internal stresses (Cope *et al.*, 2002). Cracks related to structural design are typically due to errors or oversights during the design phase, such as insufficient reinforcement, poor detailing, or underestimating loads. When concrete is inadequately reinforced or design assumptions do not match real-world loading conditions, cracks can form, often in areas with high stress concentrations, like beam-column connections or corners of slabs (Mosley, and Hulse, 1999). Stress concentration cracks occur in areas with localized high stresses, often due to external loads, sharp corners, or openings. These areas experience high tensile stresses, which lead to cracking. Effective reinforcement and detailing are critical to minimizing these

cracks (Chandra and Berntsson, 2002). Lastly, accidental overload cracks are the result of unexpected external forces or loads, such as earthquakes, vehicle collisions, or construction mishaps. These cracks are often unpredictable and can significantly compromise the structure's integrity if the loads exceed the design limits (Larosche, 2009). Recognizing the causes and mechanisms behind cracks in hardened concrete is essential for preventing them during the design and construction phases, as well as for developing strategies for repair after cracking occurs. Proper design, material selection, and careful monitoring during construction can help reduce the occurrence of cracks, thus improving the durability and performance of concrete structures.

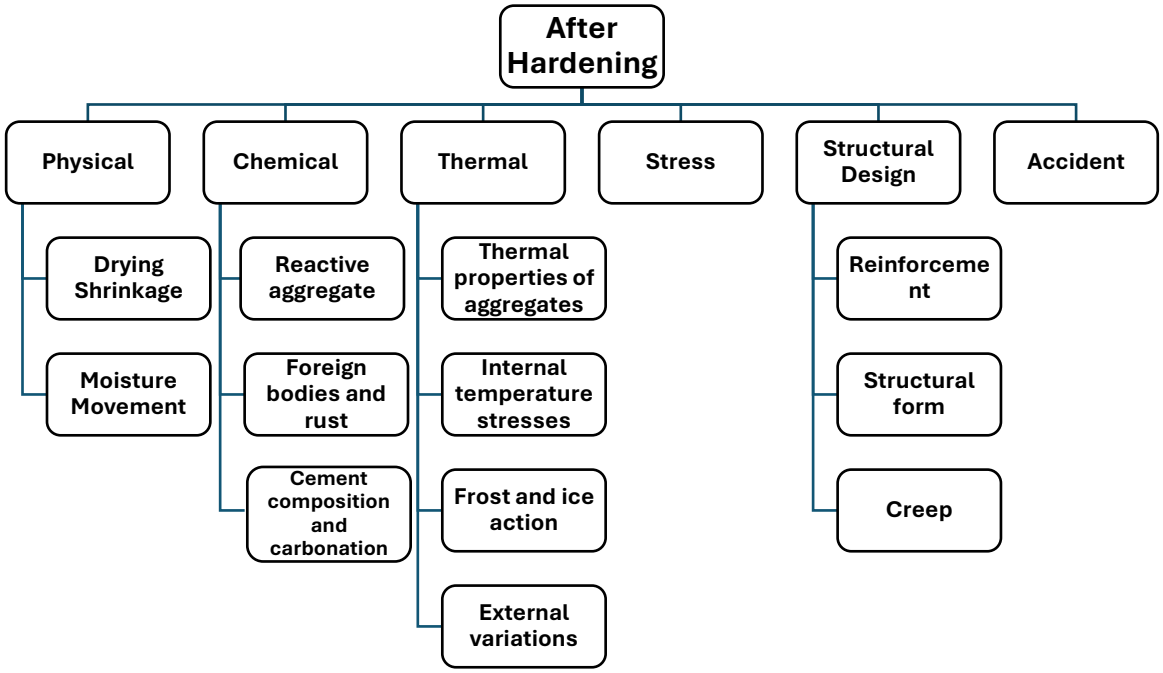

Figure 3: Types of cracks after hardening adopted form (TR22 Non-structural cracks in concrete. 2010)

2.3 Effect of Cracks on Corrosion of Reinforcement Steel

The presence of cracks in concrete significantly accelerates the corrosion of embedded steel reinforcement by allowing harmful agents like chlorides, carbon dioxide, and moisture to penetrate the concrete matrix. This penetration creates an environment that favours the onset and progression of steel corrosion, especially in chloride-rich settings. Studies have consistently shown that cracks serve as pathways for these corrosive agents, compromising the durability of reinforced concrete structures. Several factors influence the extent to which cracks affect corrosion, including the water-to-binder ratio, the type of binder used, the overall quality of the concrete, and the depth of cover over the steel reinforcement. Research by Jaffer and Hansson (2009) highlighted the importance of crack width, noting that cracks wider than 0.4 mm significantly increase corrosion rates. This is because wider cracks allow more oxygen, chlorides, and moisture to reach the steel reinforcement, especially in marine environments where chloride-induced corrosion is a major concern. Similarly, Arya and Ofori-Darko (1996) found that an increase in crack frequency correlates with higher corrosion rates, although the impact of cracks can vary based on the type of binder used. Their study showed that binders incorporating supplementary cementitious materials, such as fly ash or ground granulated blast-furnace slag (GGBS), may offer some resistance to the effects of cracking due to reduced

concrete permeability. However, these binders do not fully eliminate the risks posed by cracks, particularly when crack widths exceed the critical threshold for chloride penetration.

In contrast, Mohammed *et al.* (2001) provided a different view, arguing that while cracks can accelerate the initiation of corrosion, they may not necessarily affect the long-term progression of the corrosion process. According to Beeby, the key factor in corrosion progression is the availability of oxygen and moisture at the steel surface, rather than the crack width itself. Beeby's research suggests that the corrosion process may slow down after the initial stages if the surrounding concrete remains intact enough to resist further chloride penetration.

2.4 Importance of Controlling Cracks in Concrete Structures

Completely eliminating cracks in concrete is extremely challenging due to a variety of factors such as poor material selection, inadequate reinforcement, or exposure to harsh environmental conditions. Despite advances in construction techniques and materials that can reduce the likelihood of cracking, it remains impossible to prevent cracks altogether. Cracks in concrete raise significant concerns regarding both serviceability and structural durability, primarily because they allow water infiltration and accelerate the corrosion of steel reinforcement (Neville, 1995b). This issue is particularly severe in environments rich in chlorides or where concrete is exposed to carbon dioxide, both of which can penetrate cracks and compromise the protective properties of reinforced concrete structures.

In its natural alkaline state, concrete has a pH level above 12.5, which promotes the formation of a passive oxide layer on the surface of steel reinforcement. This passive layer acts as a protective barrier, shielding the steel from external corrosive agents (Poursaee *et al.*, 2016). However, the effectiveness of this protective film is diminished when cracks in the concrete matrix allow chlorides, carbon dioxide, or moisture to infiltrate. Chloride ions, commonly found in marine environments or de-icing salts, are particularly aggressive and can cause the breakdown of the passive layer. Likewise, carbon dioxide reacts with the alkaline components of concrete in a process called carbonation, which lowers the pH and further weakens the protective layer around the steel (Broomfield, 2023). As the steel begins to corrode, rust forms, expanding up to six times the volume of the original steel. This expansion creates internal tensile stresses in the concrete, which can exceed the tensile strength of the material, leading to spalling and additional cracking. This, in turn, accelerates corrosion and structural degradation (Park *et al.*, 2012). Extensive research has examined the relationship between crack width and corrosion rates, showing that wider cracks lead to faster corrosion initiation and progression, especially in the initial stages of exposure (Arya and Ofori-Darko, 1996). Cracks wider than 0.3–0.4 mm are often considered critical, as they significantly increase the ingress of chlorides and moisture, thereby reducing the durability of the structure (Fang *et al.*, 2017).However, even small cracks or microcracks, which may seem inconsequential at first, can still serve as pathways for corrosive agents, emphasizing the importance of effective crack control (Mohammed *et al.*, 2001).

Implementing robust crack control measures is essential not only for maintaining the aesthetics and functionality of concrete structures but also for preventing serious long-term structural damage. These measures include proactive design strategies, such as optimizing concrete mixes, ensuring proper reinforcement, and using supplementary cementitious materials to lower permeability. Maintenance strategies are equally important and may involve routine inspections, applying surface sealants, and carrying out targeted repairs to prevent cracks from widening or allowing corrosive agents to penetrate (‘Control of cracking in concrete

structures', 2001). In environments with high exposure to aggressive elements, additional protective measures, such as cathodic protection systems and corrosion inhibitors, may be necessary to mitigate the effects of cracks on the longevity of the concrete structure (Materials et al.,1996).

While it is impossible to completely prevent cracks in concrete, controlling their formation and progression is vital for ensuring the serviceability and longevity of reinforced concrete structures. Cracks, regardless of size, pose a serious threat to structural integrity by enabling the corrosion of steel reinforcement. Therefore, the implementation of effective crack control and maintenance strategies is essential to mitigate these risks and extend the lifespan of concrete structures. Continued research is needed to further develop these strategies and deepen our understanding of the interactions between crack development, concrete composition, and environmental conditions.

2.5 Concrete classification of self-healing

Self-healing concrete refers to the process of recovery (from cracking and detrition) motivated without external diagnosis or interference of the human. In specific terms, there are two types of self-healing approaches: autogenous healing and autonomous healing. Autogenous healing arises organically from the cementation's material, i.e., the additional hydration of unhydrated cement in concrete, whereas autonomous healing necessitates the use of a trigger. The major reasons for autogenous and autonomous concrete healing are the incorporation and activation of healing agents. Healing agents can be injected directly, through a vascular system, or after encapsulation. CA, bacteria, and micro- or macro-encapsulated agents, such as polymers, minerals, and other micro- or macro-encapsulated agents, are some of the recognised healing agents that have recently been introduced in the use of cementitious composites (Hermawan *et al.*, 2021). Numerous ways have been developed for the incorporation of self-healing agents in concrete. Crystalline admixtures (CA) are added directly or as fewer fillers, cement, or aggregates, with typically 0.8–4.5% of the weight of the cement. Bacteria-based healing induces either direct addition of whole bacteria or encapsulation thereof to enhance viability, accounting for the type of bacteria, dosage (10^3–10^{10} cfu/ml) nutrient availability as well as compatibility with other low bioactive materials. The concrete is designed without altering the concrete design, with key mixed in as microencapsulated healing agents (Hermawan *et al.*, 2021). Figure 4 redrawn from Meharie et al. (2017) shows an overview of the self-healing approaches.

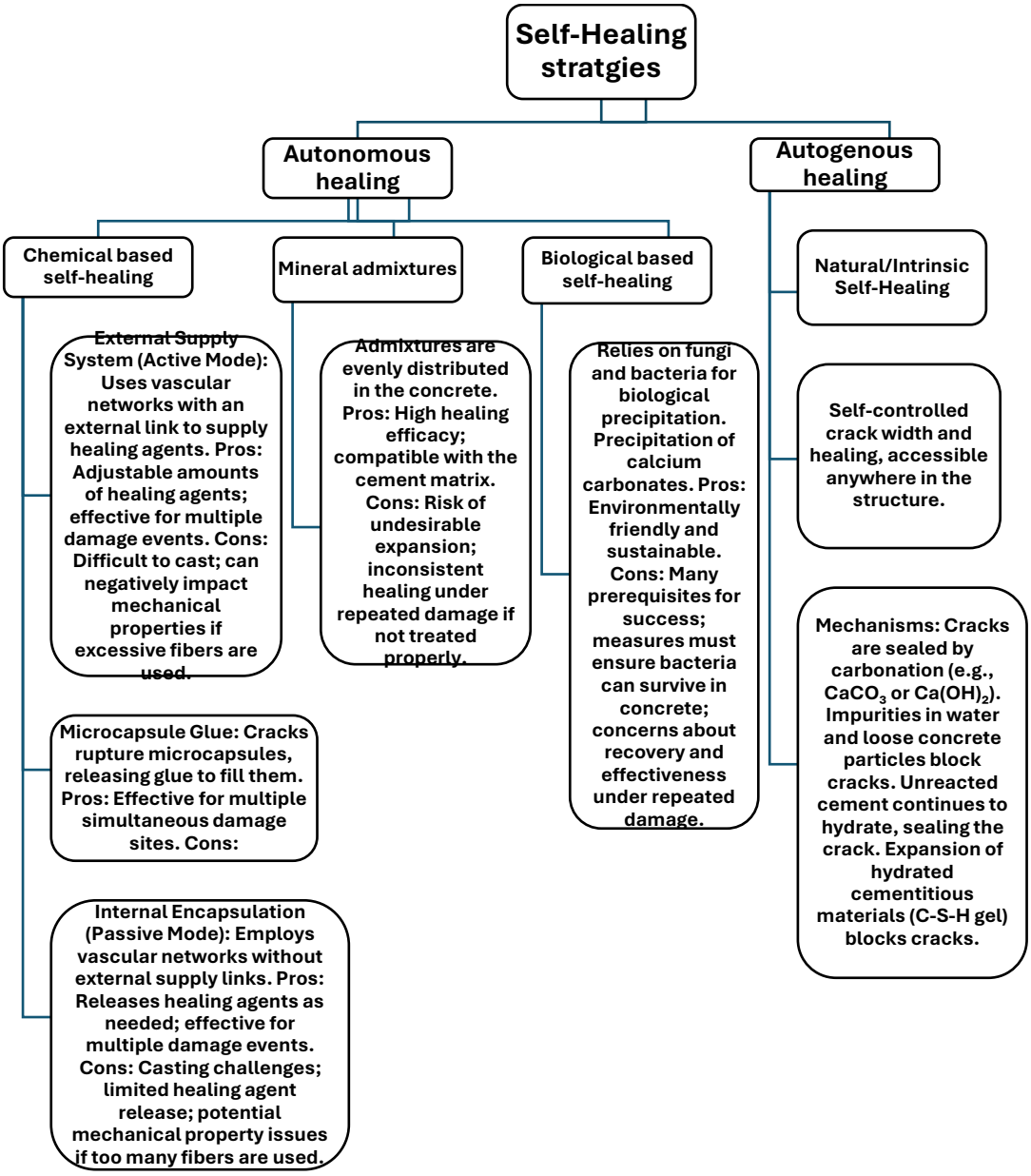

Figure 4: An overview of the self-healing approaches adopted (Meharie et al. 2017).

The following sections provided a detailed examination of the two primary approaches to self-healing in concrete: autonomous and autogenous healing. Autonomous healing involves the use of external agents, such as encapsulated chemicals or bacteria, which activate to repair cracks and prevent further deterioration. In contrast, autogenous healing leverages concrete's inherent ability to heal itself through natural processes, including hydration and carbonation. These sections will discuss the mechanisms, benefits, challenges, and practical applications of each approach, highlighting their potential to enhance the durability and service life of concrete structures.

2.5.1 Autogenous self-healing

The main phenomena determining partial or entire self-closure of cracks and implicitly, partial recovery of initial durability and physical–mechanical performances of composites are autogenously healing of cementations materials. One of the key reasons for the significant life extension of historical structures and buildings (Ghosh, 2009). Furthermore, autogenous self-

healing is defined as a material's ability to repair internal damage without the need for external intervention (Rajczakowska *et al.*, 2019). In addition, mineral additives, fibres, nanofillers, and healing agents can improve the efficiency of autogenous healing,(Zhang *et al.*, 2016). The impacts of material expansion, continual hydration of the cement, the production of calcium carbonate, and the influence of filling with small particles are the four main processes of autogenous self-healing (Van Tittelboom, *et al.*, 2012). Chemical process processes in autogenous self-healing concrete include:

- Unhydrated cement grains continue to hydrate. Lauer and Slate (1957) in their work, autogenous healing was owing to continuous hydration, which bridged cracks with the formation of hydration products.
- Small particles bridging between crack surfaces caused matrix swelling and blockage.
- Calcium carbonate crystals (CaCO3) precipitate on the crack faces as a direct result of chemical interactions between calcium ions Ca2+ (found in the concrete matrix) and carbonate ions CO3 2 accessible in the water or carbon dioxide. Figure 5, adapted from Schmets (2007), illustrates several key mechanisms contributing to autogenous healing in cementitious materials. These include: (a) the formation of calcium carbonate ($CaCO_3$) through the carbonation of calcium hydroxide [$Ca(OH)_2$], (b) the settlement and consolidation of loose cement particles within the crack, (c) the presence and movement of water facilitating continued hydration, (d) the delayed hydration of previously unhydrated cement particles, and (e) the volumetric expansion of the hydrated cementitious matrix. Collectively, these processes contribute to the closure of cracks and the restoration of structural integrity in cement-based systems.

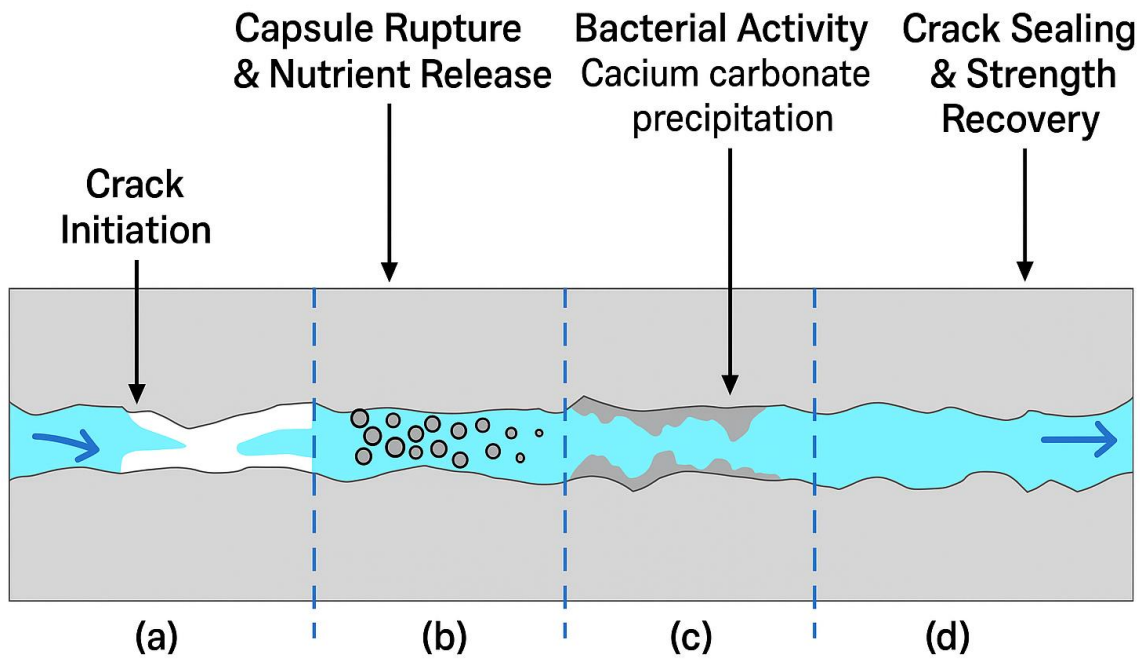

Figure 5: The formation of caco3 from ca(oH)2, b) the settlement of loose cement particles, c) the presence of water, d) the late hydration of unhydrated cement particles and excessive expansion of hydrated cementitious matrix are all mechanisms for autogenous healing adopted from Schmets. (2007).

The ability of concrete to heal itself depends heavily on the presence of water and unhydrated cement. For early-age concrete to undergo effective healing, both water and anhydrous phases need to be present at the damaged areas. Similarly, carbonation reactions, which play a key role in sealing cracks, require portlandite, water, and carbon dioxide. In typical carbonation processes, CO_2 enters the concrete through surface defects caused by wear and degradation. As portlandite is consumed during carbonation, the pH of the cement matrix decreases. This reduction in pH can increase the likelihood of reinforcement corrosion and further weaken the material. Managing the chemical environment within the concrete is therefore crucial to improving its self-healing ability and maintaining its durability over time (Muntean et al., 2011). Even though the effects of autogenous self-healing have been studied for many years, the findings of the research into the components of reaction products created by the autogenous self-healing process are inconsistent. In cracks in high-performance concrete, some freshly produced portlandite and ettringite were identified by Jacobsen and Sellevold (1996). After the cracked samples were treated in water, freshly generated C-S-H in the cracks. They concluded that continued hydration of unhydrated cement clinker promoted autogenous self-healing. Qian *et al.* (2009) discovered CaCO3 in fractures throughout their examinations. CO3 2- ions seep into cracks through the crack mouth when CO2 in the air dissolves in water. When the concentrations of Ca2+ and CO3 2- ions reach a supersaturating level, CaCO3 precipitates. Moreover, since the concentration of CO3 2- near by the crack mouth is higher than that inside the cracks, CaCO3 tends to precipitate near by the crack mouth. Figure 6, adapted and modified from Rooij et al. (2013), illustrates the mechanisms involved in autogenous healing cement grain hydration. Mineral admixtures, fibres, and nanofillers can all significantly increase the performance of autogenous healing.

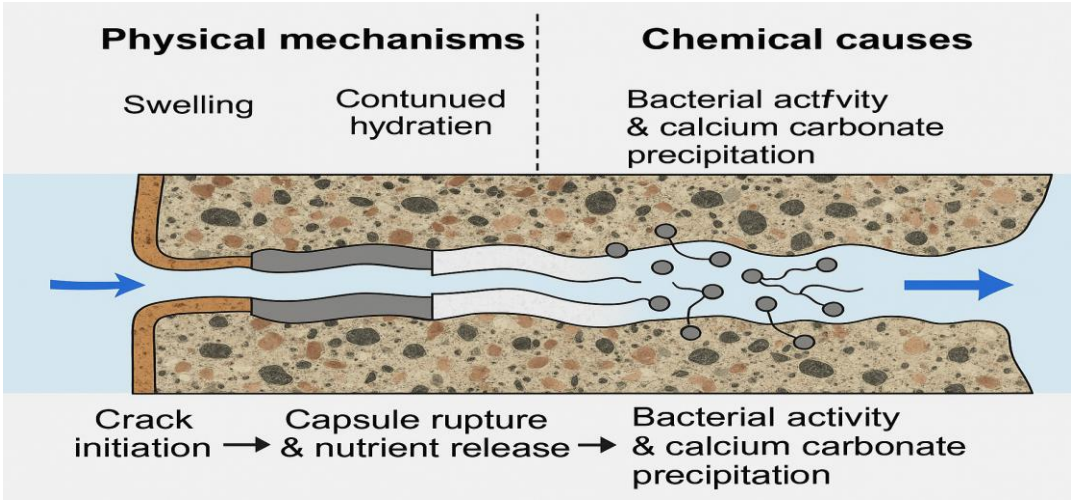

Figure 6: Mechanisms of autogenous self-healing concrete modified from (Rooij et al., 2013)

2.5.1.1 Autogenous healing technique based on adding mineral admixture.

According to the findings of Van Tittelboom, *et al.* (2012) blast furnace slag and fly ash react slower than cement, leaving more unreacted binder material inside the hardened matrix to induce fracture healing by additional hydration. Slag and fly ash, on the other hand, consume calcium hydroxide during their reactions, lowering the risk of calcium carbonate production. They said that cement replacement by blast furnace or fly ash did not seem to improve crystal

precipitation and from their experiment smaller cracks can be closed more completely and faster compared to larger cracks. Researchers use a variety of methods to evaluate the self-healing ability of cementation materials. Van Tittelboom, *et al.* (2012) studied self-healing using blast furnace slag or fly ash in mortars submerged in water and a three-point flexion test. Schlangen et al. (2006) investigated the influence of crack age on the creation of cracks (mouth opening of 50 um) in concrete specimens at the ages of 20, 48, and 72 hours after moulding. A three-point flexion test was used to determine the creation of cracks as well as the self-healing ability of the material. The degree of self-healing varied with the concrete composition (Jacobsen and Homain, 1995a). The use of fly ash improves the self-healing capability of concrete (Zhang et al., 2014). While Sahmaran and Erdem (2013) examined the effectiveness of 0 percent, 35 percent, and 55 percent fly ash replacement ratios. Termkhajornkit *et al.* (2009) used 0 percent, 15%, 25%, and 50% were utilised as percentages. They discovered that as the percentage of fly ash in the mixture increased, similarly increased the healing ability. Other researchers employed replacement percentages of 55 and 70 percent, or even 85 percent, in their studies. They did not explore the influence on the possibility of autogenous crack healing because they employed the binder ingredients within strain hardening fibre reinforced cementation composites to limit the crack width. To make their strain hardening fibre reinforced cementations material more ecologically friendly, they substituted some of the cement with blast furnace slag by Qian *et al.* (2009). The impact of this replacement on long-term hydration was not investigated. Up to date, Zhou *et al.*, (2011) were the only researchers that compared the efficacy of blast furnace slag and fly ash substitution on autogenous healing improvement. They concluded that increasing the amount of slag or fly ash added to concrete improved its self-healing capabilities. Since blast furnace slag and fly ash react more slowly than Portland clinker, the amount of unreacted binder available is longer. However, it is reasonable to hypothesize on how long the slag and fly ash systems will be capable of self-healing. This is related to the hydration time of blast furnace slag and fly ash. There are two factors, according to Termkhajornkit *et al.* (2009) first, the accessible space for the hydration products; second, the key components for the self-healing process, unreacted binder, and Ca (OH)2. Within the first 140 hours of contact with water, increasing the proportion of blast furnace slag appears to have negligible effect on cumulative heat production and hence crack healing efficiency ((Van Tittelboom, *et al.*, 2012). Sahmaran and Erdem, (2013) reported that class c fly ash is more recommended than class f fly ash, as the latter could accelerate the degradation of unloaded concrete or self-healing concrete during freeze-thew cycles. Blast furnace slag improves fly ash in terms of enhancing concrete's self-healing ability, which is presumably due to the higher pH value of the pore solution and greater Cao content of the slag, which favours calcite precipitation (Sahmaran and Erdem, 2013). Hung and Su (2018) reported that blended ground-granulated blast furnace slag and fly ash contribute to a better self-healing rate of strain-hardening cementations composites than fly ash alone. Furthermore, Maddalena and Gardner, (2021) said that by replacing (SF, GGBS, and FA) with Portland cement in various percentages, autogenous self-healing can be promoted through various mechanisms. This supplementary material promoted the self-healing technique by consuming calcium hydroxide (portlandite) to form more (C-S-H) and reduce the potential for carbonation. However, alternative materials like as FA, GGBS, and SF have been utilised to replace cement, there have been few studies that have employed self-healing concrete to make subterranean structures more durable. The advantage of employing these ingredients is that it may make concrete denser, reduce permeability, and improve workability. In addition, the amount of cement consumed would be lowered.

2.5.1.2 Self- healing technique based on crystalline admixture.

Concrete's mechanical properties and/or durability may be affected as a result of cracks. Cracks can autogenously heal under certain conditions, according to a few studies. This is in addition to the typical passive repair with deliberate external intervention. The presence of water is favourable to the healing of underground concrete structures since it is needed for chemical reactions of the healing additives. In terms of precipitated CaCO3 or freshly produced CSH (Calcium Silicate Hydrate), the presence of water is needed for healing to occur. Mineral additives, for example, can be mixed into concrete, and when cracking develops, water from the subsurface environment can seep into the cracks, generating a physical-chemical reaction of the elements inside at the exposed crack surfaces where water is available. The new products, CaCO3 and/or CSH, will fill in the cracks, narrowing them until they are completely closed. As a result, a mineral self–healing method has been presented, which takes advantage of the surrounding environment and the possible healing capacity of mineral components in concrete (Jiang *et al.*, 2014). Based on the underlying healing mechanisms, such as permeation-crystallization, expansion induced by crystalline effects, and pozzolanic reactions, the additives used to promote autogenous healing in concrete can be broadly classified into three categories. Mineral additives that facilitate permeation-crystallization enhance the supply of carbonate ions (CO_3^{2-}) and accelerate the migration of reactive ions, particularly calcium (Ca^{2+}), within the cementitious matrix. As water infiltrates the cracks, these ions leach out and crystallize, leading to the formation of calcium carbonate ($CaCO_3$), which effectively fills the cracks. In some cases, the newly formed compounds are expansively voluminous, contributing to crack closure through mechanical filling. Alternatively, pozzolanic reactions between mineral additives and calcium hydroxide generate additional hydration products that precipitate within the cracks, further enhancing the self-healing capacity of the material (Jiang *et al.*, 2014). Crystalline admixture (CA) also known as cementations capillary crystalline water proofing materials. Calcium aluminate (CA) has demonstrated the ability to fully heal cracks up to 0.4 mm in width, outperforming other self-healing approaches such as shape memory materials, bacterial agents, and microcapsule-based systems. The healing products formed by CA are highly compatible with the cementitious matrix, contributing to effective crack closure. In addition to promoting self-healing, CA enhances the overall structural performance by improving both strength and impermeability, partly through its influence on matrix porosity. According to Coppola and Crotti (2018), specimens incorporating CA exhibited mechanical strength increases of approximately 7–10% compared to conventional cement-based specimens.

Some studies have utilized commercial crystalline admixtures with undisclosed compositions, while others have employed alkali-activated materials—such as sodium hydroxide, sodium silicate, sodium carbonate, and metakaolin—as alternative crystalline admixtures to promote self-healing in cementitious systems (Oliveira *et al.*, 2021). They went on to say that crystalline admixtures (CAs), is also known as permeability-reducing admixtures, are commercial compounds used in low concentrations in cement-based materials to increase concrete durability or promote autogenously fracture healing. Furthermore, crystalline additives are mostly water-soluble additives that improve concrete properties in a fresh and hardened state. Consequently, crystalline additives lead to sustainable development and an increase in the service life of concrete structures. Typically, their effects on concrete properties in the plastic stage include increased workability, improved permeability, setting time, or finish ability; on the other hand, when the concrete hardens, chemical admixtures contribute to improving durability, increasing compressive and flexural strength at all ages, reducing shrinkage phenomena, or decreasing permeability of concrete. Chemical admixtures also act as agents

which allow the manufacture and construction of special concrete types such as self-healing concrete, high-strength concrete, and self-consolidating concrete (Gojević *et al.*, 2021). However, the American concrete institute (ACI) writes in their report crystalline additives are one type of permeability reducing admixture. ACI divides permeability reducing additives into two parts. That reduces water permeability in no-hydrostatic conditions and under hydrostatic conditions. In a category that reduces water permeability at no-hydrostatic conditions falls typical hydrophobic products. Admixtures that can function under hydrostatic conditions include crystalline admixtures. Some of these additives have a lot of benefits like reducing drying shrinkage, minimizing chloride ion penetration to the surface, and improved frost resistance and autogenous healing properties (Violetta and Yuers, 2015).

Furthermore, ACI Committee has reported that there is a better adoption of self-healing properties in self-healing concrete when there is an addition of crystalline admixture (CA) is also known as permeability reducer admixtures. Crystalline admixture materials react quickly with water and are used as hydrophilic materials. Calcium silicate hydrate (CSH) density is further enhanced which resists water penetration. In the presence of water, matrix components react with tricalcium silicate (C3S). Sisomphon and Koenders (2013) analysed the recovery of mechanical properties of strain-hardening cementations composites containing CA (1.5% by weight of cementations materials) and reported hardly any benefit produced by the admixtures when compared with control specimens. As well as he investigated the potential self-healing of cracks by employing calcium sufflaminate-based expensive and crystalline additives and found out calcium carbonate was the main healing agent has been named. Copuroglu and Koenders (2013) reportedthat the deflection deformation of specimens mixed with CA and CSA was about 1.5 times that of CA specimens when the specimens were cured for 28 days. Copuroglu and Koenders, (2012) said that only specimens mixed with CA and CSA could heal entirely within 28 days when cracks were 0.3~0.4 mm. Moreover, when the healing time was seven days, the crack closure rate of the specimen mixed with CA and CSA was 3 times that of the CA specimen. (Park et al., (2018) that the specimens mixed with CA, CSA, and basic magnesium carbonate (MgCO3·Mg (OH)2·5H2O) could completely heal the cracks with a width of 0.295 mm after five days of healing, and the seepage stopped completely.

2.5.1.3 Self-healing concrete containing fibres

Types of fibre reinforced cementitious composites (FRCCs) were tested in the lab to see how well they might self-heal in terms of watertightness and mechanical properties (Nishiwaki *et al.*, 2012). Nevertheless, fibber reinforced cementations composites (FRCCs) offer the best chance of achieving self-healing in concrete in practice. FRCCs are now widely used in real-world applications, with good outcomes. Durability and cost efficiency are assured because no unique components are needed. By manipulating the crack width and the rate of CaCO3 precipitation, ubiquitous reinforcing fibres in the cement matrix can be employed to improve self-healing (Nishiwaki *et al.*, 2014). PVA, PE, PP, steel, and carbon fibres are the most used fibres in self-concrete. Glass fibre, natural fibres, and other synthetic fibres can be also used as self-healing materials (Snoeck and de Belie, 2015). However, fibber Materials Used in Self-Healing Investigations: The distribution is illustrated in Figure 7, following an approach inspired by the work of Cuenca and Ferrara (2017). The difficulty of ensuring the healing agent's durability is overcome because the healing process does not involve the Fiber's reaction. Reinforcement fibres containing high-polarity synthetic composites (e.g., PVA) have a high potential for self-healing precipitation surrounding the crack-bridging fibres (Nishiwaki *et al.*, 2012). The ability of

concrete with fibres, particularly ECC, to self-heal has been extensively researched. According to Yang *et al.* (2009) self-healing behaviour of ECC with 4.5 percent PVA fibres might occur in cracks less than 150 m in width, while crack widths less than 50 m were favoured. After self-healing, the broken ECC's resonance frequency was regained by 76–100%, and its stiffness also showed a noticeable rebound. The tensile strain capacity of pre-damaged specimens that are purposely subjected to tensile strain of up to 3% can be totally recovered following self-healing (Yang *et al.*, 2009). Carbon fibre can improve ECC's self-healing capabilities and increasing fibre content within a particular range can speed up the recovery of flexural strength, deflection, and electrical resistance. Investigation that is done by Nishiwaki *et al.*, (2012) during a tensile loading test, cracks were generated in the FRCC (fibber reinforced cementations composites) specimens, which were then immersed in static water for self-healing. Water permeability and reloading tests revealed that FRCCs with synthetic fibre and cracks with widths within a specified range (0.1 mm) have good self-healing capacities in terms of watertightness. The synthetic fibre (polyvinyl alcohol (PVA)) and hybrid fibre reinforcing (polyethylene (PE), and steel code (SC)) series showed a significant recovery ratio due to their strong polarity. When the residual elongation remains below 2 mm, self-healing concrete incorporating a hybrid fibre system of polyethylene (PE) and steel cord has been shown to recover over 100% of its original tensile strength. This indicates that the tensile strength after healing can exceed both the initial unloading stress and the tensile strength recorded during the first loading cycle (Homma and Nishiwaki, 2009b). Moreover, concrete composites utilizing PE and steel cord fibres exhibit excellent recovery in mechanical properties and watertightness, even for cracks up to 0.7 mm in width (Nishiwaki *et al.*, 2012). Similarly, Kan *et al.* (2010) reported that engineered cementitious composites (ECC) reinforced with polyvinyl alcohol (PVA) fibres achieved over 90% recovery of resonant frequency following 10 water/air curing cycles, despite an imposed strain of 2.0%. Water-based curing was identified as the most effective method for promoting self-healing. Additionally, Hung, Su and Hung (2017) observed that increased humidity enhances the recovery of both resonant frequency and tensile stiffness in damaged concrete specimens, further highlighting the significance of environmental moisture in facilitating self-healing mechanisms.

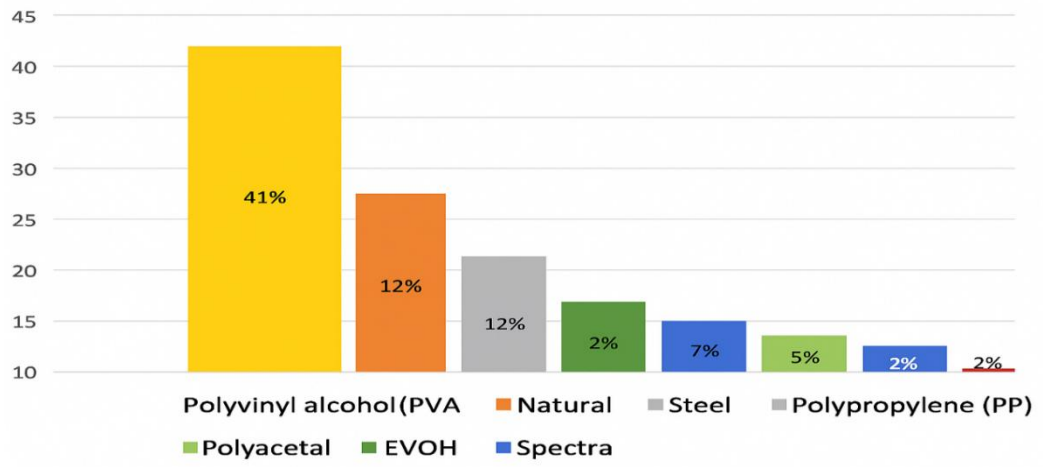

Figure 7: Fibre Materials distribution Used in Self-Healing Investigations: Adopted from (Cuenca and Ferrara, 2017)

2.5.1.4 Self-healing concrete technique based on nanofibers

As concrete has a low cost, high compressive strength, and wide adaptability, it becomes the most extensively used material in infrastructure construction. However, concrete's mechanical properties, such as toughness, tensile strength, and impact resistance, are all exceedingly weak due to its quasi-brittle nature. Meanwhile, the obvious discreteness of raw materials and the complexity of environmental conditions have led to the concrete structural reliability being full of challenges when in use. Because of its nature, concrete is inclined to crack and thus fail when subjected to actions such as load, temperature, and humidity. To improve the reliability of infrastructure, researchers have tried to endow the materials with smart capacities such as self-sensing, self-healing and self-adjusting abilities for the monitoring and repair of potential defects (Wang *et al.*, 2018b). According to Lee et al. (2007) powder concrete (RPC) has been widely used in bridges, buildings, tunnels, maintenance and reinforcement fields because of its excellent mechanical properties, high durability, and thermal deformability. However, the RPC, when in use, tends to generate many microcracks due to its own defects, which in turn causes the occurrence of macroscopic cracks, eventually leading to concrete failure (Van Tittelboom and de Belie, 2013a). For general ground-based concrete structures, methods such as grouting, spraying, and patching can repair cracks in concrete. However, these passive repair methods are no longer practical for concrete structures in special environments such as nuclear power plants and underground construction. As a result, self-healing concrete has a potential attraction (Dry, 1994a). Fibres, microorganisms, and capsules containing repairing agents are all part of the current self-healing technology. Fibber and microorganism's procedures try to reduce the crack width within the concrete, while the capsules aim to directly bond or fill the crack by breaking a repair agent capsule (Sun, Yu and Ge, 2011). Conversely, compared to traditional self-healing technology, the use of nanofillers can improve the concrete spatial network structure and control the morphology of hydration products at the micro scale. Furthermore, many studies have shown that nanomaterials, due to their unique structure and exceptional characteristics, have a tremendous potential to change cementation composites in a variety of ways (Guadagno *et al.*, 2019). The ability to use nanomaterials to make self-healing composites such self-healing epoxy nanocomposites, nanocomposite elastomers, epoxidized natural rubber, and so on has been proven (Nie *et al.*, 2019). Unfortunately, there is currently a lack of research on concrete composites using nanofillers. In conclude, three methods have been identified to explain how nanofillers improve concrete self-healing. To begin with, nanofillers operate as nucleation sites for hydration products in pore solution, facilitating more hydration. Second, nanofillers improve the three-dimensional network structure of the cement matrix, resulting in more fine cracks and dispersing the crack propagation direction (H. Liu *et al.*, 2017). Finally, active nanofillers with pozzolanic reactivity, such as nano-SiO2 and nano-SiO2 coated nano-TiO2, can react with Ca (OH)2 to produce extra calcium silicate hydration, enhancing specimen compactness (Zhang et al., 2016). The impact of nanofillers on the mechanical performance and durability of concrete have been studied. Nanofillers have a good enhancing impact in most circumstances, showing that they could be useful in self-healing concrete (Palla *et al.*, 2017). According to Siad *et al.* (2018) under a four-point loading test, the maximum crack width in ECC containing 0.25 percent and 0.5 percent carbon nanotubes (CNTs) was 50 μm, which was lower than the control sample (70 um). Furthermore, higher CNT (carbon nanotubes) content resulted in faster and better flexural strength and deflection recovery, stronger electrical resistivity recovery, and more cracks with smaller crack widths. Wang *et al.* (2018b) found that incorporating nano-SiO2, nano-TiO2, or nano-ZrO2 into reactive powder concrete improved its self-healing capabilities (RPC). Under secondary loadings, the nanofillers decreased and even eliminated the Kaiser effect of RPC, showing that the internal

cracks had healed to some extent. In terms of RPC self-healing performance, nano-SiO2 is the most effective of the three nanofillers. Furthermore, water curing has been discovered as a critical aspect in the development of self-healing concrete using nanofillers. When RPC containing 3 percent nano-SiO2 was healed in water, the self-healing coefficients of compressive and flexural strengths were 39.4 percent and 33.7 percent greater, respectively, than the control sample (Wang *et al.*, 2018b).

2.5.2 Autonomous self-healing concrete

Autonomous self-healing concrete is an advanced material capable of repairing internal cracks and damage by activating embedded chemical or biological agents. This innovative concrete type, studied by Wu et al. (2012b), initiates a self-repair process when these agents, integrated within the concrete or applied externally, detect structural damage. A key feature of this material is its ability to restore structural strength without requiring external human intervention, enhancing the durability and lifespan of concrete infrastructures. Self-healing mechanisms are driven by the inclusion of specific agents or additives in the concrete, delivered through various forms such as spherical or cylindrical capsules or complex tubular systems (De Belie and Wang, 2016). The agents are released when cracks form, enabling a repair process that reduces maintenance costs and increases the service life of structures exposed to challenging environmental conditions. (Van Tittelboom and de Belie, 2013b) emphasize the importance of both the design and the delivery mechanisms for these agents, this can be achieved either through the incorporation of capsules or via vascular networks, as illustrated in Figure 8, adapted from Van Tittelboom and de Belie. (2013b) . In biological self-healing processes, crack repair is often facilitated by microorganisms, such as bacteria, which precipitate calcium carbonate ($CaCO_3$) or other compounds, effectively sealing the cracks. (Al-Thawadi, 2011) demonstrated how bacteria can induce $CaCO_3$ precipitation within cracks, restoring the material's integrity through microbial-induced carbonate precipitation (MICP), an area of enormous potential for autonomous self-healing concrete.

Chemical methods for self-healing can be categorized as passive or active. Passive systems involve the encapsulation of healing agents within capsules, which break when cracks form, releasing their contents to repair the damage. Active systems, on the other hand, use more advanced methods like vascular networks that continuously or periodically deliver repair agents through channels embedded within the concrete (Toohey *et al.*, 2007). These systems are particularly useful in handling complex or widespread cracks by ensuring a constant supply of healing agents. Several innovative approaches have been developed to enhance concrete's autonomous healing abilities. One such method involves super absorbent polymers (SAPs), which swell and release water into cracks, encouraging the formation of healing products like $CaCO_3$. Another promising method is MICP, in which bacteria embedded in the concrete generate $CaCO_3$ in response to moisture and nutrients, sealing cracks effectively. Textile-reinforced concrete, incorporating flexible textile elements, also supports the healing process by providing a durable framework for the agents to act upon (De Rooij *et al.*, 2013). These various methods highlight the evolving landscape of self-healing concrete technologies, aiming to improve both the efficiency and longevity of concrete structures, particularly those exposed to harsh conditions. Autonomous healing systems, by incorporating biological and chemical agents, not only address crack formation but also contribute to the overall resilience of construction materials.

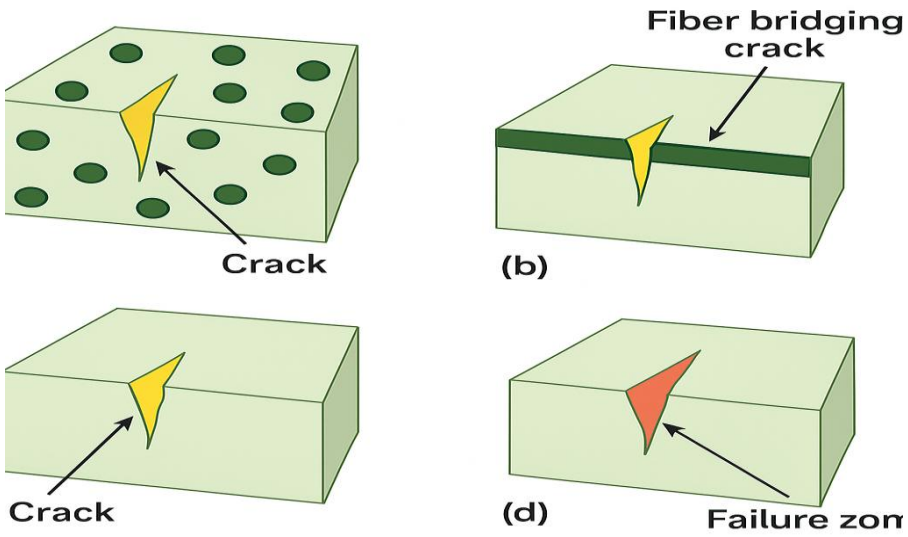

Figure 8: b) Fiber bridging crack. (d) Failure zone adopted from (Van Tittelboom and de Belie. 2013b)

2.5.2.1 Bacteria-based self-healing concrete

The idea behind bacteria-based self-healing is to use bacteria to encourage calcium carbonate precipitation in cracks. In the 1990s, Gollapudi *et al.* (1995) proposed that cracks can be repaired by using microorganisms to cause the precipitation of calcium carbonate (CaCO3). Calcium carbonate precipitation can be induced by a variety of metabolic pathways, including the hydrolysis of urea and the oxidation of organic acids.

- Urea hydrolysis (ureolysis) with ureolytic bacteria (Hommel *et al.*, 2016); this reaction occurs in the presence of urease-positive microorganisms:

  $CO(NH_2) + 2H_2O + Ca^{2+} + Cell 2NH^{4+} + Cell - CaCO_3, with NH^{4+}$ as by product.

- Using cyanobacteria algae for photosynthesis (Baumgartner *et al.*, no date)

  $2HCO_3 + Ca^2 + CH_2O + CaCO_3 + O_2$ as by product.

- Sulphate reduction by sulphate-reducing bacteria (Paul, Wronkiewicz and Mormile, 2017);

$SO^4 2 + 2[CH_2O] + OH + Ca^2 + CaCO_3 + CO_2 + 2H_2O + HS$ with CO_2 and HS as by product.

- Using nitrate-reducing bacteria for denitrification (nitrate reduction) (Erşan, de Belie and Boon, 2015): When the reaction is complete, $CH_2COO^- + 2.6H^+ + 1.6NO_3^- \rightarrow 2CO_2 + 0.8N_2 + 2.8H_2O$ is produced, with CO_2 +N as by-products; when the reaction is incomplete, $Ca^{2+} + CO_2(aq) + 2OHCaCO_3(s) + H_2O$ is produced, with NO and N_2O as by-products.

- Using myxobacteria for ammonification (González-Muñoz *et al.*, 2010):

$$HCO_3^- + H_2O \rightarrow (CH_2O) + O_2 + OH^- \quad (1)$$

$$HCO^- + H_2O \rightarrow (CH_2O) + O_2 + OH^- \quad (2)$$

$$HCO_3^- + OH^- \rightarrow CO_3^{2-} + H_2O \quad (3)$$

$$Ca^{2+} + CO_3^{2-} \rightarrow CaCO_3 \qquad (4)$$

- NH3 is produced as a by-product. Anaerobic oxidation: $CH_4 + SO_4^{2-} + Ca^{2+} \rightarrow CaCO_3 + H_2S + H_2O$; methane oxidation employing methanogens (Reeburgh, 2007) . $CH_4 + 2O_2 \rightarrow Co_2 + 2H_2O$ (aerobic oxidation), withH_2S as a by-product of both anaerobic and aerobic processes.

Table 1 lists the benefits and drawbacks of several $CaCO_3$ precipitation metabolic processes. Figure 9 schematically illustrates ureolytic carbonate precipitation on bacterial cell walls, adapted with modifications from de Muynck, et al. (2010). The calcium ions in the solution are attracted to the negatively charged bacterial cell walls, for starters. Urease in bacteria dissolves urea into inorganic carbon and ammonium. CaCO3 precipitates on the bacteria's cell wall when the local calcium ions become oversaturated, eventually encasing the entire cell.

Table 1: The CaCO3 precipitation metabolic processes

Metabolic Pathway	Benefits	Drawbacks
Hydrolysis of Urea	- Rapid carbonate production - Catalyzed by urease	- Excessive ammonium production
Oxidation of Organic Compounds	- Lower environmental impact - CO_2 reacts with portlandite	- Carbonate production is slower
Nitrate (NO_3^-) Reduction	- Effective in low-oxygen conditions - Lower environmental impact	- Lower $CaCO_3$ precipitation compared to urea hydrolysis

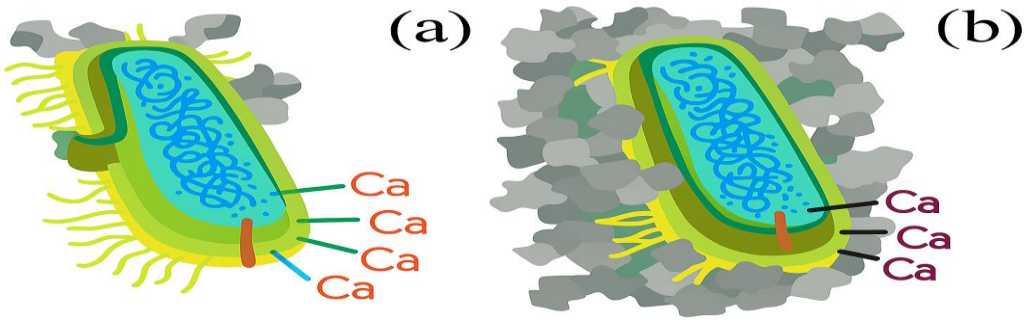

Figure 9: (a) the entire cell becomes encapsulated; (b) the imprints of bacterial cells involved in carbonate precipitation adopted with modifications from (De Muynck, et al., 2010).

Bacteria can be used to heal concrete cracks by precipitating minerals using the mechanism described above ($CaCO_3$). However, MICP concrete techniques are divided into two major categories: self-healing concrete and surface coatings. To fill cracks, bio concrete is made by incorporating suitable microorganisms and nutrients into the concrete matrix (Song *et al.*, 2014). The process by which microorganisms inside the matrix, primarily bacteria, generate precipitates to mend gaps and enhance structural performance is known as self-healing (Lee and Park, 2018b). Group University of Derby by Souid *et al.*, (2019) explored the effect of soil incubation to see if the self-healing process can be activated in underground condition. In compared to traditional incubation environment (water). And they found out from their experiment the effectiveness of bio-concrete in particular constructions, such as tunnels and deep foundations, where concrete pieces are exposed to the elements of the ground conditions. Another study by the same group of Derby examined the impact of soil pH on industrially recognised classifications of exposure, ranging from minimal danger of chemical attack (neutral pH & 7) to extremely elevated risk of chemical attack (pH & 4.5) (Esaker *et al.*, 2021). Nevertheless, most bacteria find it difficult to survive in such a strong alkaline environment, as the pH inside concrete is typically about pH 11–13 (Tang and Xu, 2021). Study by Witkor, (2011) bacterial spores were only observed to remain viable for up to two months after being applied to the concrete matrix as a result, it is not a long-term solution. Encapsulation of bacterial spores and nutrients in a variety of materials, such as hydrogel, glass capillaries, and melamine-based microcapsules, has been attempted to extend the lifespan of bacteria (Zhang *et al.*, 2021). Furthermore, the crack widths that can be healed are restricted, with the biggest cracks healed measuring less than 1 mm in diameter (Wang *et al.*, 2014). Moreover, the inclusion of healing chemicals reduces the mechanical strength of concrete (Wang *et al.*, 2014). To begin, the concrete matrix is inoculated with dormant yet alive microorganisms. During the curing process, the nutrients are either added into the concrete at the same time Van Tittelboom *et al.* (2010) supplied by a nutrition solution (Achal et al., 2010). Water entering newly formed cracks will activate the dormant bacteria, which will eventually seal the cracks through the process of $CaCO_3$ precipitation induced by metabolism. (Gadd and Dyer, 2017b) stated that surface coatings might thus be a potential technique to extending concrete durability to overcome this problem. Coatings, in comparison to remedial treatments, may be considered of as a preventative strategy that can be utilised before any cracks appear and can act as a barrier to keep liquids and gases out (Gadd and Dyer, 2017b). Research demonstrates that a urease-positive fungus can deposit calcium carbonate precipitation (MICP) creating a think calcium carbonate coating on Portland cement and fly ash (Zhao *et al.*, 2022). Yet, a deeper study is needed about the surface coating and bacteria's application to improve the self-healing.

Both bacteria, nutrients, and carbon or nitrogen sources are necessary to perform self-healing of concrete using microbial technology. To survive dry, barren, and alkaline concrete, it is also critical to choose the right bacteria and calcium/nitrogen sources (Zhang *et al.*, 2020). Regrettably, several studies have revealed that the concentration of the cementation materials (calcium ion, dissolved organic carbon), geometric compatibility, pH, temperature, and the availability of nucleation sites are the main factors that influence microbially induced calcite precipitation techniques (Dhami et al., 2013b). In addition, other environmental parameters that influence the performance of calcite precipitate, include bacterial concentration, soil type, the particle size of the soil sample, and bacterial solution viscosity (Amarakoon and Kawasaki, 2016).

2.5.2.1.1 Effect of pH

The presence of a significant amount of Ca (OH)2 in the concrete pores makes determining the influence of pH on bacteria activity in concrete critical. Because of the ingress of water from the external environment, the concrete microenvironment is highly alkaline, with pH values as high as 13, while the pH of a concrete crack mouth is predicted to be between 9 and 11, owing to the ingress of water (Wu *et al.*, 2019). Additionally, environmental concerns arise from the release of ions such as aluminium, calcium, chromium, magnesium, sodium, potassium, and zinc into the surrounding water, as well as an increase in the pH of the water due to concrete leaching. It is indeed common for fresh water to become toxic when it highly becomes alkali (Law and Evans, 2013 a) optical density value of the bacterial solution normally decreases with increasing pH for the entire test time, as shown in Fig 10a. When the pH of the growth media was 7–9, the lag phase lasted about 4 hours. The lag phase rose to 5.5 h, 10 h, and 10.5 h, respectively, as the pH was elevated to 10, 11, and 12 (Wu *et al.*, 2019). When the pH was 7 to 8, the propagation rate (slope of the tangent line of the graph) was almost the same, but it fell when the pH was 9 to 12. In all cultures, no further growth was detected after 21 hours. Figure 10 b that adopted from Wu *et al.* (2019) illustrates urea decomposition by bacteria under various pH values. Though, the pH of the concrete pore solution is in the range 13- 14 due to the alkalinity provided by the dissolved sodium and potassium oxides present in Portland cement. Yet, pH on the concrete surface has a variety of values as concrete is a heterogeneous and porous material with different components (Femenias et al., 2017). With the variety of pH at the surface or with distance from the surface of concrete, the precipitation of CaCO3 can be possible. Researchers E. Liu *et al.* (2017) and Müller *et al.* (2018) were the first who introduced the imaging technique of a pH variety on the concrete surface. Nevertheless, the techniques employed in their study have not gained widespread acceptance among other researchers due to the absence of defined pH ranges, the use of non-standard solutions, and a lack of focus on scale formation on concrete surfaces. Figure 11 present the findings of the investigation conducted by E. Liu et al. (2017), adapted from their original work.

For microbial ureases, the ideal pH is typically near neutral. When utilising S. pasteurii, Stocks-Fischer et al., (1999a) found an ideal pH of 8, whereas other researchers using the same S. pasteurii reported different optimal pH values, e.g., Dupraz *et al.* (2009) reported a pH value of 8.7–9.5.Fujita *et al.* (2004) recorded a pH of 9.1, and a pH of 9.5 was also reported by Ferris *et al.* (2004). The pH of the environment normally rises during urea hydrolysis due to the microbially driven calcite precipitation process, which helps to buffer the overall increase in pH value. Several factors affect the concentration of hydroxyl ions leached from concrete, including cement type, structural shape, surface area to volume ratio, carbonation, and water flow (Law and Evans, 2013).

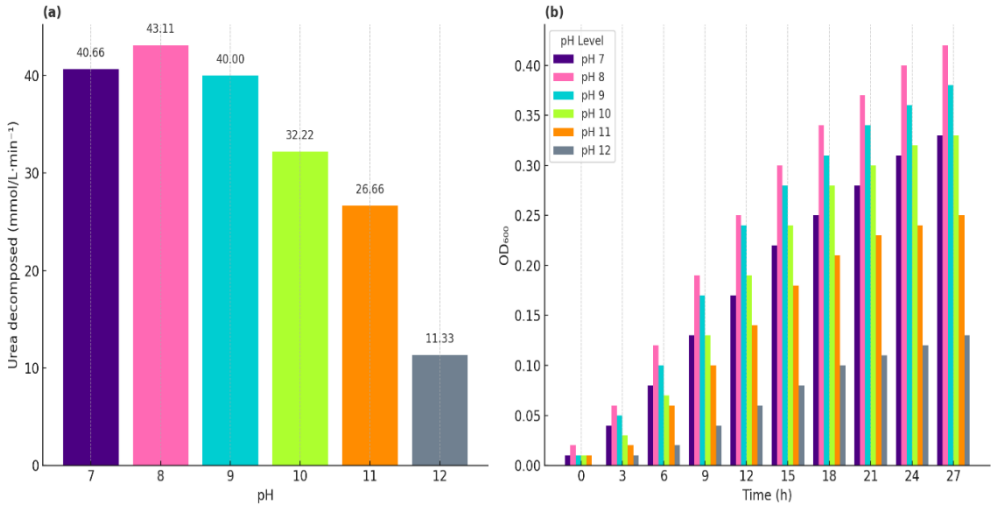

Figure 10: At different pH levels, bacterial growth and urease activity adopted from (Wu et al., 2019).

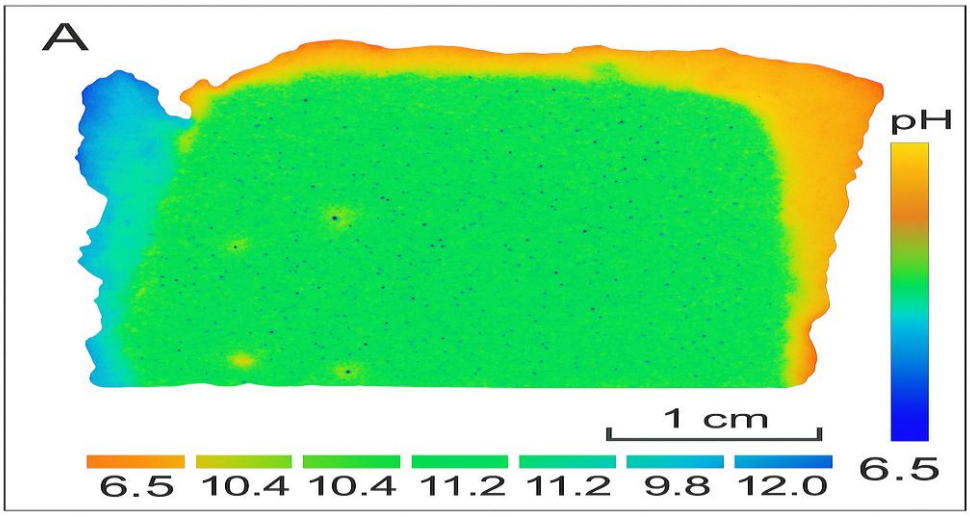

Figure 11: The variety of pH at concrete surface adopted from original work of (Liu et al. 2017).

2.5.2.1.2 Effect of Calcium ions

Calcium leaching can be a matter of concern for the long-term durability of concrete constructions. It increases the porosity of the surface layers, which has a negative impact on the material's resistance to mechanical loads (Bangert *et al.*, 2003). Nevertheless, microorganism that precipitates carbonate generates urease, which catalyses urea hydrolysis and produces carbonate and ammonium ions consequently. CaCO3 can occur in the presence of Ca2+ due to the precipitation interaction between calcium and carbonate ions. The productivity of biogenic CaCO3, which is the fundamental crack healing material in the bacteria-based healing method, is directly determined by bacterial urease activity (Wu *et al.*, 2019). Furthermore, when it comes to the precipitation of CaCO3, the concentration of calcium ions has a significant impact on the precipitation activity. On the one side, calcium ions are required to produce CaCO3. On the other side, calcium ions can impact ureolytic activity in bacteria. Bacteria are toxic to excessive calcium ions because they only require a small amount to regulate their life activities (Wang *et al.*, 2017). Low Ca2+ and urea concentrations (0–0.9 mol/L and 0–0.75 mol/L, respectively) have insignificant effect on bacterial growth but have a substantial impact on urease activity. As a result, the effects of calcium ions and urea

concentrations on enzyme activity (0.9 mol/L and 0.75 mol/L, respectively) were determined (Wu *et al.*, 2019). Bacterial growth at varying calcium ion concentrations, as reported by Wu *et al.* (2019), is depicted in Figure 12.

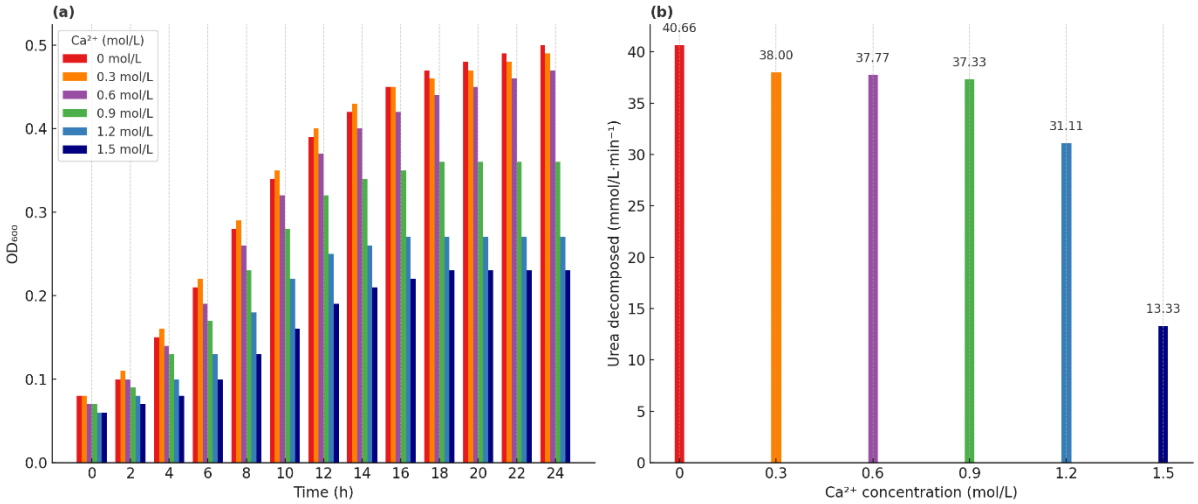

Figure 12: Bacterial growth and urease activity at various Ca2+ concentrations adopted from (Wu et al., 2019)

2.5.2.1.3 Impact of nutrients availability

The bioavailability of nutrients is a crucial factor in Microbially Induced Calcium Carbonate Precipitation (MICP), as nutrients are vital for bacterial growth and activity. These nutrients serve as the primary source of dissolved inorganic carbon, which precipitates as calcium carbonate ($CaCO_3$) during the MICP process. To develop an effective microbial self-healing concrete where nutrients are used both economically and efficiently during the crack healing process, it is important to optimize the initial nutrient content of the concrete (Kardogan *et al.*, 2021). Additionally, in MICP, the type of nutrients required varies according to the specific microbial metabolism driving the process. Therefore, the nutrient composition for several types of microbial self-healing concrete should be optimized individually based on the proposed metabolic pathway and the associated nutrients (Kardogan *et al.*, 2021). The precise number of chemical precursors (nutrients required for MICP) needed in the mix design of microbial self-healing concrete is still uncertain. Most studies have primarily focused on selecting suitable bacteria and testing their application at a bench scale to explore the potential of the concept, often neglecting the role of nutrients. While demonstrating the feasibility of microbial-induced self-healing, these studies used an excess of nutrients to avoid any limitations or deficiencies during the MICP and self-healing processes. In these experiments, nutrients were either provided within carriers or capsules or added directly as concrete admixtures. However, there is currently no available information on the bioavailability of these supplied nutrients for MICP, and the optimal nutrient content for microbial self-healing concrete mix design remains undetermined. Several types of nutrients can influence the mechanical properties of concrete, as demonstrated in a study by Son et al. (2022), which involved compressive strength testing of mortar specimens at 7, 14, 28, and 56 days. The inclusion of bacteria and nutrients was found to affect the hydration kinetics and hydration products, leading to noticeable changes in the specimens' compressive strength. The lowest compressive strength was observed in specimens that contained the culture medium without co-cultured bacteria at the 7-day mark. Additionally, specimens with pure yeast extract showed the lowest compressive strength, while the compressive strength of other types of specimens was higher than both groups.

2.5.2.1.4 Capsules based on self-healing concrete.

One of the most common methods for getting healing chemicals into the concrete matrix is encapsulation. Encapsulation is the process of encapsulating droplets or solids in an inert shell to protect them from unwanted and undesirable external reactions (Wu et al., 2012c). Due to its benefit of responding directly to the damaged region, the use of encapsulated healing agents for self-healing concrete has gained a lot of interest in research. This is due to the microcapsules breaking during the creation of concrete cracks, permitting healing chemicals to be released into the cracks via capillary action, assisting in the sealing of the concrete gaps. Because it measures the effectiveness of crack-repair processes, the choice of a healing agent is an essential part of this procedure (Milla et al., 2017). Furthermore, ensuring that microcapsules are distributed evenly throughout the concrete matrix is critical to the application's success (Milla et al., 2017).

The effectiveness of microencapsulation can be measured in terms of the microcapsules' effects on concrete properties. In this situation, the microcapsules should have no negative impact on the concrete's properties (Kanellopoulos et al., 2016). Another principal factor to consider is the survival of microcapsules during the concrete production process. The microcapsules are subjected to external forces from aggregates during industrial concrete production (Al-Tabbaa et al., 2016). To ensure the viability of the stored healing agents, the microcapsules must remain intact throughout the concrete manufacturing process. Additionally, when it comes to microcapsule breaking in response to cracks, it's critical that the microcapsules truly break at crack locations to release the healing chemicals. Furthermore, the impact of microcapsules and stored compounds on cement hydration must be considered. Finally, microcapsules should not have a significant impact on the workability of fresh concrete (van Tittelboom and de Belie, 2013b). However, for example, the encapsulation of the bacteria has a high chance of surviving inside the concrete matrix, there are various challenges to overcome once bacteria are introduced. Elevated temperatures, a lack of oxygen during concrete production, high alkalinity of the concrete matrix (ranging from 12 to 13), concrete mixing, and cement hydration are just some of the challenges (Gupta et al., 2017b). Due to the general harsh conditions inside the concrete matrix, it is preferable to encapsulate bacteria in a protective carrier before introducing them into the matrix (Wang, Soens, *et al.*, 2014). To protect the bacteria from this harsh environment, researchers used a variety of encapsulation techniques, including diatomaceous earth, expanded clay aggregate, melamine-based microcapsules, and hydrogels (Gupta et al., 2017b). Suitable carriers must meet three conditions to achieve high performance of self-healing concrete employing carriers: Biocompatible carriers should be used. Carriers should not have a negative impact on the concrete's mechanical properties. Carriers should be robust enough to withstand the concrete mixing process, but not too strong because they must fracture when cracks in the concrete matrix begin to appear (Lee and Park, 2018b).

In general, adding healing agent microcapsules and capsules to concrete has a negative impact on its mechanical properties. This is because many chemical and polymer materials form weak bonds in the concrete matrix. Furthermore, when the healing agent capsules are released, cylindrical or spherical voids remain in the structure, potentially weakening the concrete's tensile and compressive strength (van Tittelboom and de Belie, 2013b). In general, spherical capsules outperform cylindrical capsules in terms of impact on concrete mechanical properties because their shape reduces stress concentration in the void left after the capsule is released (van Tittelboom and de Belie, 2013b). According to their size, capsules are divided into

microcapsules and macrocapsules. The self-healing technique is represented in Figure 13 was adapted and modified from White *et al.* (2001).

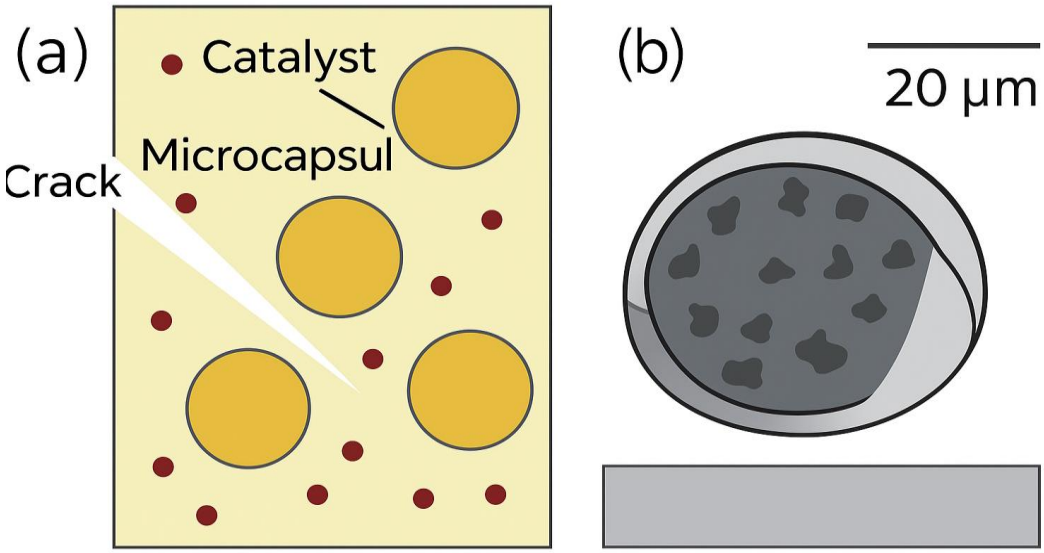

Figure 13: The capsule technology's healing concept is as follows: (a) cracks appear in the matrix. (b) An ESEM image shows a ruptured microcapsule adopted from (White et al. 2001).

2.5.2.1.4.1 Microencapsulation

Inspired by the ground-breaking work of White *et al.* (2001), microencapsulation has remained a popular technology for producing autonomous self-healing components for cementitious systems. Microcapsules were directly embedded in the matrix in this mechanism, and when fractures formed, they attracted propagating cracks, rupturing, and releasing the core into the crack volume (White *et al.*, 2001). The released substance would then react with a distributed catalyst in the matrix, causing the crack to heal. Microcapsule-based concrete healing has been proven several times as a proof of concept (Souradeep and Kua, 2016a). Yet, in situ polymerization, interfacial polymerization, pickering emulsion templating, mini-emulsion polymerization, solvent evaporation/solvent extraction, sol-gel reaction, and miscellaneous are only a few of the microencapsulation techniques covered by Zhu et al. (2015) Other microcapsule fabrication techniques include the interfacial self-healing process (Yang *et al.*, 2011). Complex coacervation, as described by Xu and Yao (2014), along with extrusion spherization and hollow tube extrusion techniques (Hilloulin *et al.*, 2015), have also been employed for microcapsule fabrication. Additionally, Lv *et al.* (2016) demonstrated that the agitation rate during synthesis plays a critical role in controlling the average diameter and size distribution of the resulting microcapsules. The self-healing agent determines the self-healing mechanisms of microcapsules. Polymerization triggered by the catalyst, which ties the fracture sides together, is one of methyl methacrylate monomer's self-healing mechanisms (Yang *et al.*, 2011). Ring opening metathesis polymerization is used to repair cracks in dicyclopentadiene (Gilford *et al.*, 2014). When epoxy resin is released from microcapsules, it reacts with the matrix material's pre-mixed thinner and hardener to generate healing products, which are subsequently used to repair cracks. When sodium silicate is utilized as a healing agent, it reacts with the calcium hydroxide in cement, resulting in C–S–H gels that can be used to fill fractures

(Hilloulin *et al.*, 2016). As a result, larger microcapsules embedded in concrete have a higher negative impact on the mechanical properties of the concrete than smaller microcapsules. The larger microcapsules create greater voids. An experimental investigation was conducted using varying quantities of microcapsules, as illustrated in the redrawn Figure 14, adapted from Dong *et al.*, (2017). When comparing the compressive strength of the same number of microcapsules of varied sizes, it was discovered that the bigger microcapsules had a greater loss in compressive strength than the smaller microcapsules. Soens, *et al.*, (2014) investigated melamine-based microcapsules with a diameter of 2 to 5 μm and varying percentages of microcapsules (from 1% to 5%), and discovered that as the quantity of microcapsules increased, the compressive strength decreased drastically. On the other hand, Pelletier *et al.* (2011) embedded polyurethane microcapsules (2 percent by volume, with microcapsule sizes ranging from 40 to 800 μm) into concrete and found no reduction in the concrete's compressive strength. The number of microcapsules is a significant aspect when it comes to the impact on the concrete's mechanical properties. Several parameters influence self-healing efficiency, including microcapsule size (Kosarli *et al.*, 2019), microcapsule content (Dong *et al.*, 2017), crack width (Dong *et al.*, 2017), preload level (Li *et al.*, 2013), healing age, and curing temperature. According to Dong *et al.*, (2017) self-healing effectiveness increased as the microcapsule content (2 percent, 4 percent, 6 percent, 8 percent) and size (132 μm, 180 μm, 230 μm) increased. Nonetheless, these "next-generation" microencapsulation suites can make microcapsule-based self-healing cementitious systems more widely adopted in practise. The first large-scale application of microcapsules in reinforced concrete panels has already taken the initial steps toward that target (Davies *et al.*, 2018). A retaining wall panel was built using 8% cement microcapsules by volume and was subjected to damage. Crack healing was then tracked over a six-month period using a variety of in-situ and laboratory measurements. The field trials proved that scaling the capsules was feasible and that full-scale healing performance could be achieved over a lengthy period (Davies *et al.*, 2018).

The effectiveness of the microcapsule approach for self-healing has been intensively investigated, and it is primarily dependent on the healing agent inside. The principles to obtaining self-healing capabilities using capsule technology are how to keep capsules alive during the mixing process, how to release the healing chemical, and how to trigger the healing mechanism. Phanyawong *et al.* (2017) created gelatine/acacia gum microcapsules that can change their mechanical behaviour from a rubbery soft state to a glassy stiff state when wet and dried conditions. This change in properties allows microcapsules to survive the wet cement mixing process and rupture properly when cracks appear in the dry composite, releasing the encapsulated sodium silicate solution. The microcapsules are also resilient at high temperatures of up to 190 degrees Celsius or in strong alkaline solutions that mimic the pH of concrete. The releasing behaviour of microcapsules in a simulated concrete pore solution was investigated by Dong *et al.* (2015). The findings of the experiments show that the release of the corrosion inhibitor covered in polystyrene resin rose over time and decreased as the pH value decreased, and that the wall thickness of the microcapsules successfully controlled the release. More research is needed to optimise the use of microcapsules, particularly in terms of microcapsule size and microcapsule volume incorporated into the concrete. This research should try to improve self-healing concrete's ability to retain and release an appropriate amount of chemical when it cracks, as well as to reduce the effects of these microcapsules on the mechanical properties of concrete, particularly compressive strength.

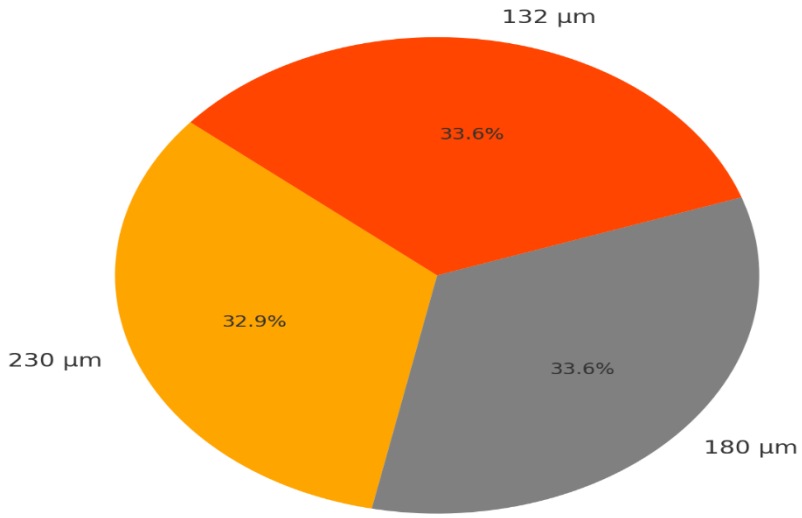

Figure 14: Mortar compressive strength with varying microcapsule contents reproduced from (Dong et al., 2017).

2.5.2.1.4.2 Macrocapsules

Dry offered polypropylene and glass fibres with mono- or multicomponent methyl methacrylate cores for concrete crack healing in one of the early types of research utilising macro-encapsulation. Macrocapsules are larger than microcapsules (>1 mm) and can hold a greater number of therapeutic ingredients. Macrocapsules, such as borosilicate glass or ceramic capsules cut from a long tube, are commercially available, or the capsules can be made using an extruder and an extrusion technique (Anglani et al., 2020). Glass capsules may reduce concrete durability by causing an undesired alkali-silica reaction (ASR) (de Belie *et al.*, 2018a), whereas polymeric capsules may cause premature curing of an entrapped ingredient such as PU (Gruyaert *et al.*, 2016a). Ceramic capsules (van Tittelboom *et al.*, 2015a) and cementitious capsules Anglani et al., (2020) have been successfully demonstrated to eliminate these limitations. Spherical macro-capsules, hollow tubes (glass tubes, ceramic tubes, polymeric tubes, etc.) and porous carriers such as LWA are the most often used macro-capsule containers (Zhang *et al.*, 2020). Other factors, such as capsule parameters (diameter, thickness, and length), play a significant role in the self-healing scenario since the capsule must be able to break when a crack propagates (Hermawan *et al.*, 2021). Macro-capsules are typically a few millimetres in diameter. Unhydrated minerals on the crack surface and those released from capsules will participate in the rehydration reaction to achieve self-healing when expansive powder minerals such as CaO, MgO, and bentonite are used as healing agents (Zhang *et al.*, 2020). The crack will be bridged by hydration products such as Ca (OH)2, Mg (OH)2, C–S–H, and alumino-silicate hydrates. The carbonization of reactive hydrating products will then help to heal the cracks (Qureshi et al., 2016). The important challenge is to activate capsules' healing abilities to achieve concrete self-healing. A mechanical trigger, such as the puncture of cracks, release the self-healing agent from capsules.

When an embedded EVA pipe (3.4 mm outer diameter and 2.0 mm inner diameter) is fractured, it selectively melts due to an increase in its resistance and releases the healing agent (epoxy resin) in the crack, then fractures with a width of up to 2.5 mm are healed according to (Nishiwaki *et al.*, 2006) Though, due to lower processing temperatures and the ability to

integrate extrusion, filling, and sealing processes, polymeric capsules may well be easier to produce. The sizes of cylindrical capsules range from 0.8 to 5 mm to ensure that the capillary attractive force of the crack and the gravitational force on the fluid mass are enough to overcome the cylindrical capsules' capillary resistive force and the negative pressure forces caused by the sealed ends (Gruyaert *et al.*, 2016b). A study by Xiong *et al.* (2015) created a novel capsule based self-healing system by using chloride ions as a trigger. Theses capsules are made of a silver alginate hydrogel and disintegrate when exposed to chloride ions, releasing the active core materials. Van Tittelboom *et al.* (2011) demonstrated the recovery of strength and stiffness of specimens after numerous loading cycles by embedding two couples of tubular capsules into cement mortar, each containing a healing agent and a combination of accelerator and water. During the first loading cycle, more than half of the original strength and stiffness recovery was attained. Diep and Thao, (2011) found that in the first and second healing cycles, the reinforced beam embedded with glass tubes containing isocyanate prepolymer recovered 88 percent and 85 percent of normalised stiffness, respectively. Stiffness is restored to up to 70% and 99 percent for columns and slabs, respectively. Sun et al., (2011) suggested that a self-healing system may be created by inserting hollow glass fibres holding a healing agent into concrete. according to simulation results, when the crack width was kept below 0.3 mm, the strength recovery rate reached 50%. Van Tittelboom *et al.* (2012) investigated concrete beams with ceramic tubes embedded in them, each of which was protected by mortar bars and held either a polyurethane prepolymer or a mixture of accelerator and water. Strength and stiffness restored to more than 80% of their former levels because of autonomous self-healing. Furthermore, the self-healing cracks with polyurethane regained the same strength and stiffness as cracks manually repaired with high strength epoxy resin. Cracks were sealed and chloride infiltration was prevented by adding glass tubes-encapsulated polyurethane to cement mortar. Although the proportion was slightly lower than manual crack healing, this autonomous healing procedure was able to close crack widths of 100 μm and 300 μm for chloride penetration in 67 percent and 33 percent of cases, respectively (Maes et al., 2014). Guadagno et al. (2019) created concentric glass macrocapsules containing expanding minerals (outer capsule) and water (inner capsule) that could close enormous fractures in cement mortar (approximately 400 μm). Nevertheless, the aspect ratio of capsules and the viscosity of encapsulated healing agents both influence the release of healing agents. Short tubes are superior to long tubes for achieving self-healing, owing to the high attractive forces inside long tubes (van Tittelboom *et al.*, 2015b). The low viscosity of the precursor is essential for successful crack sealing. The healing agent, a polymer precursor with super low viscosity, has a global strain capacity of 50 to 100 percent, beyond which the sealing action is disturbed. When the polymer debones from the crack walls as the crack opens, the failure mode occurs. The rupture of closed foam cells is the failure mode for foaming precursors (Feiteira et al., 2016).

2.5.2.1.5 Encapsulation Techniques for Chemical Agents

A diverse range of encapsulated materials, including lightweight aggregates, ceramic tubes, glass tubes, and polymers, has been utilized in the development of self-healing concrete, with polymeric microcapsules being particularly prevalent in this context (Souradeep and Kua, 2016b). In self-healing systems employing microencapsulation, these microcapsules are integrated within the concrete matrix. Upon the occurrence of cracks, the microcapsules rupture, thereby releasing the stored healing agents into the fissures. The movement of the healing agents along the cracks is significantly influenced by capillary action (Wu, Johannesson, *et al.*, 2012). The advantages of using microcapsules include their ease of application and uniform dispersion within the concrete, which allows them to effectively respond to fractures at

various locations within the material. However, the interfacial bond between the concrete matrix and the microcapsules is critical for the successful operation of the self-healing mechanism, as it must not adversely affect the desired properties of the concrete. To facilitate effective rupture of the microcapsules upon crack initiation, it is essential that the strength of the microcapsule wall is lower than the bond strength (Wu, Johannesson, *et al.*, 2012). Lv *et al.* (2016) conducted a successful innovative study at Shenzhen University, utilizing organic microcapsules in concrete, which yielded promising results. However, the integration of microcapsules in the development of self-healing concrete encounters three significant challenges, compounded by issues of reduced compatibility with concrete resulting from weak bonding between the cement matrix and microcapsules, as well as a limited self-healing effect. The first challenge involves ensuring that the healing agent efficiently solidifies upon reaching the designated location. The second challenge pertains to the need for the healing agent contained within the microcapsule to exhibit low viscosity and good fluidity to facilitate effective release. The third challenge addresses the fundamental performance requirements of the microcapsules within the concrete: they must possess sufficient strength to withstand mechanical forces during concrete production while simultaneously being weak enough to rupture in response to cracking, thereby releasing the healing agent (Lv *et al.*, 2016). In the context of autogenous healing of concrete, microcapsules serve as crucial components. A study by Dong *et al.* (2015) those larger microcapsules produced superior results compared to smaller ones in concrete specimens. This improvement can be attributed to the increased likelihood of microcapsule rupture associated with larger particle size and higher concentration. However, it is essential to consider that an increase in particle size and concentration may adversely affect the mechanical properties of concrete. Additionally, the age of the healing process plays a significant role in the efficacy of the healing mechanism, and factors such as curing temperature must also be considered.

2.5.2.1.6 The influence of microcapsules size and geometry of microcapsules on concrete properties and bio-concrete techniques

The incorporation of healing agent microcapsules and capsules exerts a detrimental effect on the mechanical properties of concrete. This adverse impact arises from the introduction of various chemical materials and polymers that tend to form weak bonds within the concrete matrix. Furthermore, upon the release of the healing agent capsules, cylindrical or spherical voids are left within the structure, which can compromise the tensile and compressive strength of the concrete (Van Tittelboom and De Belie, 2013). Spherical capsules are typically more advantageous than cylindrical capsules concerning their influence on the mechanical properties of concrete. The spherical shape reduces stress concentration throughout the voids left by the released capsules, thereby minimizing potential weaknesses in the concrete matrix (Van Tittelboom and De Belie, 2013). Consequently, larger microcapsules embedded in concrete tend to have a more pronounced negative effect on mechanical properties compared to smaller microcapsules, as the former create larger voids. An experimental study conducted by (Dong *et al.*, no date) examined the effects of varying sizes and amounts of microcapsules. The findings indicated that, for the same quantity of microcapsules, larger microcapsules resulted in a greater reduction in compressive strength compared to their smaller counterparts. Similarly, (Wang, *et al.*, 2014) utilized melamine-based microcapsules with diameters ranging from 2 to 5 μm at different concentrations (from 1% to 5%) and observed a significant decline in compressive strength correlating with the increased number of microcapsules. Conversely, Pelletier et al. embedded polyurethane microcapsules (2% by volume, with sizes ranging from 40 μm to 800 μm) into concrete and reported no loss in compressive strength (Pelletier *et al.*,

2010; Maes et al., 2014). Therefore, the quantity of microcapsules is a critical factor influencing the mechanical properties of concrete.

2.5.2.1.7 Release efficiency of the healing agent from microcapsules.

The deployment and release of microcapsules within the concrete matrix are anticipated to occur upon fracturing of the microcapsules. Regarding capsule shape, spherical capsules are more effective in enhancing and controlling the release of healing agents compared to cylindrical capsules (Tittelboom et al., 2013; Souradeep and Kua, 2016b). The superiority of spherical capsules can be attributed to their uniform shape, which mitigates the suction effects encountered at the closed ends of cylindrical capsules, thereby facilitating a more efficient release of healing agents. However, the enhanced release of healing agents from spherical capsules can pose challenges if not properly regulated, as it may lead to the rapid depletion of the healing agent. For instance, Dong *et al.* (2013) utilized epoxy as a healing agent within spherical capsules and observed that it only effectively healed a limited number of cracks due to the swift exhaustion of the material. The viscosity of encapsulated healing agents is another critical factor influencing the control of their release and deployment upon crack formation in concrete. Viscosity is a fundamental parameter in selecting appropriate healing agents, as it directly impacts the mobility of the healing agents (Wu, Johannesson and Geiker, 2012d). Healing agents with high viscosity may not be fully released to the crack sites from the capsules, while those with excessively low viscosity may leak out through the cracks that require repair (Souradeep and Kua, 2016b). Furthermore, Tittelboom et al. (2013) noted that if the viscosity of healing agents is excessively low, the agents may become lost due to absorption by the surrounding concrete matrix or leakage through cracks. Dry (1994a) recommended that the viscosity of suitable healing agents should fall within the range of 100 to 500 centipoise (cps). Cyanoacrylate adhesive has been employed as a healing agent for repairing cracks in cementitious materials, despite its extremely low viscosity. This adhesive has demonstrated significant potential for healing techniques that leverage capillary action due to its extremely low viscosity, typically around five centipoises (Joseph *et al.*, 2010). Various healing agents, including cyanoacrylate and epoxy resins, have been tested and evaluated based on their curing periods, viscosities, and mechanical bonding capabilities within concrete. Cyanoacrylates (superglues) are particularly favoured as healing agents due to their lower viscosity compared to epoxy resins, enabling them to effectively infiltrate and repair finer cracks (Joseph *et al.*, 2010). Additionally, Joseph *et al.* (2010) conducted simulations and modelling of capillary flow of water in prismatic cementitious specimens, further contributing to the understanding of these healing mechanisms.

2.5.2.2 Vascular based self-healing technic

Self-healing technologies have been shown to be effective for polymer, composite, and metallic materials, with healing mechanisms classified as intrinsic, (micro)capsule-based, and vascular systems as shown in figure 15 adopted from (Blaiszik *et al.*, 2010). In concrete, the vascular healing concept uses a biomimetic approach to self-healing. The human cardiovascular system, which distributes blood throughout the body, and the plant vascular tissue system, which transports food, water, and nutrients via xylem and phloem networks, are both examples of vascular network systems. Concrete vascular networks can provide liquid healing chemicals to damaged areas in a comparable manner. There is no theoretical limit to the amount of damaged material that can be repaired when this healing substance is supplied from an external source (De Belie *et al.*, 2018b). One-channel (1D), two-channels (2D), and three-channels (3D) vascular networks exist in concrete. However, the healing agent can be injected into 1D channels from either one or both ends of the concrete surface. (Jacobsen' et al., 1995b) presented the vascular approach to heal concrete cracks for the first time in 1994. They discovered no loss of strength but an increase in permeability and flexural toughness when hollow glass fibres carrying liquid methyl methacrylate were placed within concrete. Furthermore, a vascular system in their experiment, as the healing agent can be externally pressurised, and the supply of the agent can be properly controlled. The system is illustrated in Figure 16, derived from (Selvarajoo *et al.*, 2020).

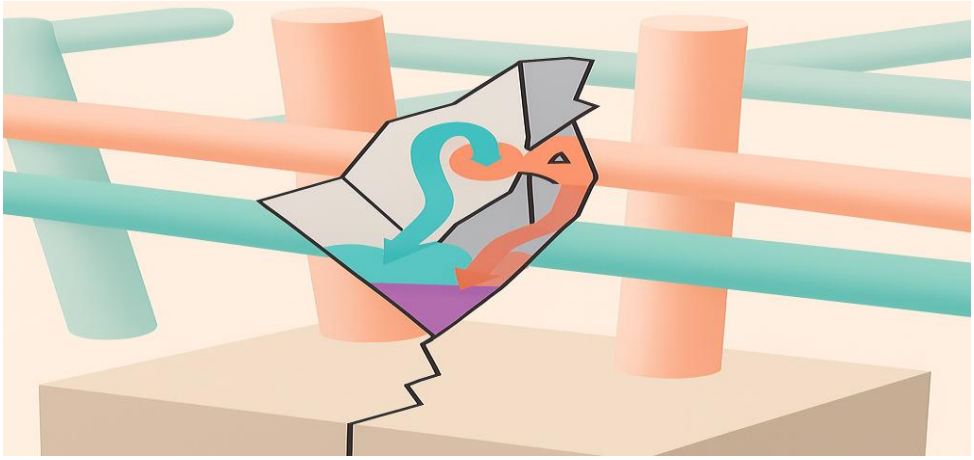

Figure 15: Vascular is examples of self-healing techniques derived from (Blaiszik et al., 2010)

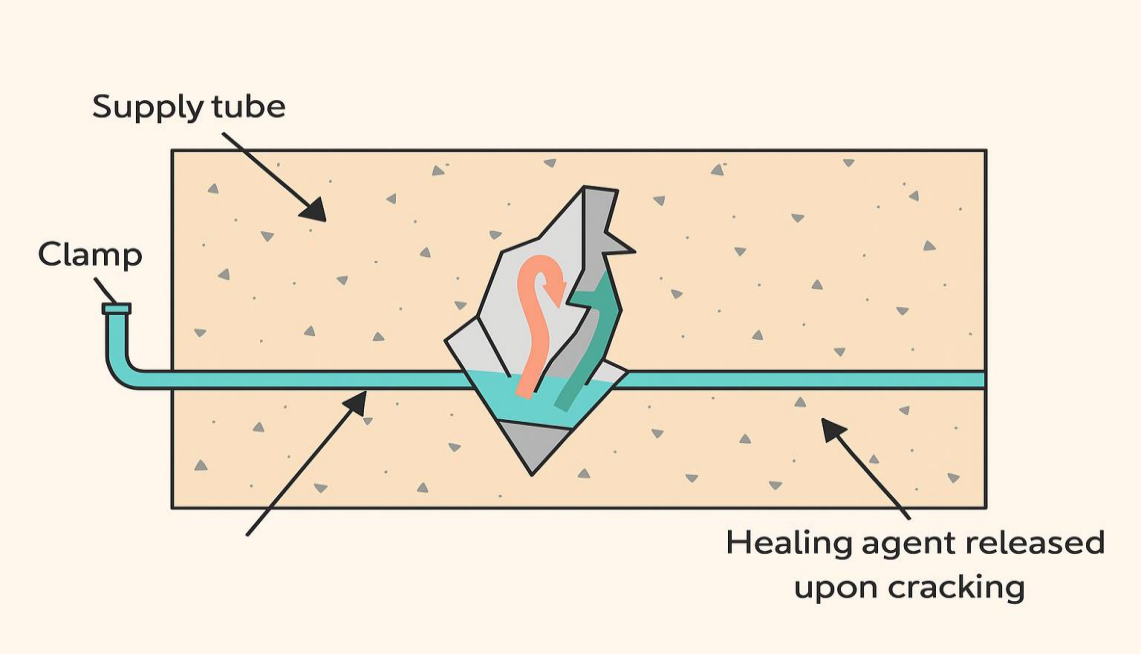

Figure 16: The generic vascular healing system adopted from (Selvarajoo et al., 2020).

A study by Joseph *et al.* (2015) created a vascular network of 1D channels in reinforced mortar beams and used cyanoacrylate-filled glass tubes. However, during the first and second loading cycles, the response of primary and secondary healing occurred. In addition, a larger stiffens of initial healing response was observed when the reinforcing percentage was increased and loading rate was reduced. All methods for creating vascular channels either by casting breakable tubes into cementitious matrix or by embedding the tubular into cementitious matrix (Joseph *et al.*, 2015) or flexible polymer tubes (Minnebo *et al.*, 2017), or embedding 3D printed vascular (Pareek *et al.*, 2014). Capillary forces play a significant role for delivering the healing agent into cracks. Most of methods that of delivery system depends on capillary forces. However, other researchers have expended vascular network to increase healing agent flow and delivery (Minnebo *et al.*, 2017). Research by Pareek *et al.* (2017) for example, used canal networks to create vascular systems in concrete buildings. Steel bars with a flat surface are pre-embedded into the concrete matrix during the casting process to obtain this. The embedded steel bars are pulled out once the concrete has hardened for one day. As a result, inside the concrete matrix, a canal is formed. When these canals are linked together, they form a network. Senot *et al.* (2012) are also looking at the possibility of installing a vascular system in concrete constructions. The pores inside the porous concrete have a high degree of connectedness, with pore sizes in the millimetre range. The canal networks presented are like those proposed by Pareek et al. This technology may distribute liquid healing agents to cracks when any component of the porous concrete network is crossed by cracks (Pareek *et al.*, 2017). Several different vascular network components have been prototyped utilising 3D printing. The printed polylactide material may be used to create tubular channels, although the lengths are usually limited by the size of the 3D printer. Minnebo *et al.* (2017) constructed a 3D vascular network distribution component that allowed one intake to be linked to several channels implanted in the concrete. Davies *et al.* (2018) developed a 3D joint that allowed a crossing matrix of tubes to be removed, leaving a 2D linked vascular network. Figure 17 shows an example of a 2D vascular

network implanted within a 600 mm square slab with a healing agent applied and the figure reconstructed from (Senot *et al.*, 2012). Novel way by Li *et al.* (2019) for creating complicated 3D interior hollow tunnels using polyvinyl alcohol 3D printing (PVA). Using computed tomography (CT) and X-ray diffraction, the behaviour of 3D printed PVA structures in cement pastes was examined (XRD) as showing in figure 18 that reproduced and modified from (Li et al., 2019) . The feasibility of incorporating a vascular network into concrete has been proved several times (Dry, 1994b) The vascular network concept's adaptability might make it the best answer for conquering the most severe issues of preventing water infiltration and cracking in concrete. However, developing massive concrete structures with vascular network systems that may commence healing without human involvement remains a problem. More study on healing agents, their storage, delivery systems, and ways for remotely stimulating vascular networks is required before this can be performed (Gardner *et al.*, 2018).

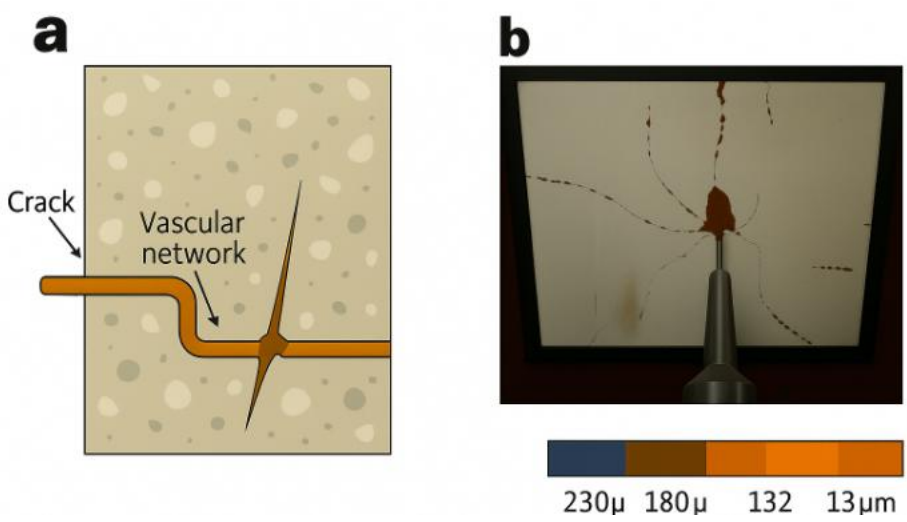

Figure 17: The creation of vascular systems, "porous concrete. (b) In a 600 mm square concrete slab, a 2D vascular network releases sodium silicate reconstructed from (Senot et al., 2012)

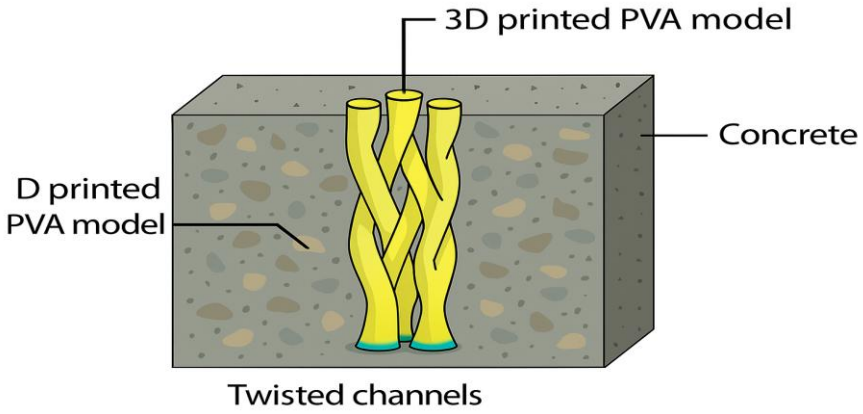

Figure 18: 3D printed PVA model with two twisted channels adopted from (Li et al., 2019)

2.5.2.2.1 Shape memory alloys based self-healing

Shape memory alloys (SMAs) are a class of active materials that possess the remarkable ability to return to their original shape upon heating, even after being subjected to significant stress (Janke *et al.*, 2005). These materials exhibit two distinct transformation phases: martensite (M), which forms at lower temperatures, and austenite (A), which forms at higher temperatures. The shape change in SMAs is driven by shear lattice distortions as the temperature varies, a phenomenon known as martensitic transformation (Janke *et al.*, 2005). When a SMA is deformed (loaded) while in the twinned martensitic phase, which is an orientation generated by a combination of self-accommodated martensitic variations, at a temperature below the austenitic start point, SME occurs (As). When the alloy temperature rises over the austenitic finish temperature (Af), the SMA will revert to the parent austenitic phase and restore its original shape. Figure 19 inspired from Janke *et al.* (2005) helps to understand and visualise these transition processes. However, both experimental and simulation-based studies indicate that the incorporation of shape memory alloy (SMA) technology significantly enhances fracture healing in concrete structures. Upon heating, the pre-installed SMA wires are capable of rapidly closing and filling fractures after the removal of external loading, demonstrating their potential to mitigate emergency damage in concrete (Kuang and Ou, 2008). This healing ability stems from the super elastic properties of SMAs, which allow them to return to their original shape even after substantial deformation. When applied to concrete, this characteristic offers a novel solution for self-repair in structural applications. In the proposed self-repairing system, SMA wires and brittle fibres embedded with adhesives are introduced into the concrete during its fabrication. This system leverages both the super elasticity of SMAs and the adhesive's ability to bond and repair cracks, creating an intelligent, self-healing material. As shown in Figure 20 adopted from (Kuang and Ou, 2008), the brittle fibres are connected to a vessel via rubber tubing, which stores the mending adhesive. When cracks develop, the fibres facilitate the delivery of the adhesive to the damaged regions, ensuring a consistent supply of material for efficient crack repair. Additionally, the adhesive can be replenished or recovered through the connected vessel system, allowing for repeated healing cycles without manual intervention. This approach to embedding SMAs and adhesive-carrying fibres into concrete highlights the potential for developing advanced, smart materials that autonomously maintain structural integrity. By combining the mechanical advantages of SMAs with the self-repairing functionality of adhesive fibres, this technology offers significant advancements in prolonging the lifespan of concrete structures, particularly in environments subject to frequent or severe mechanical stress.

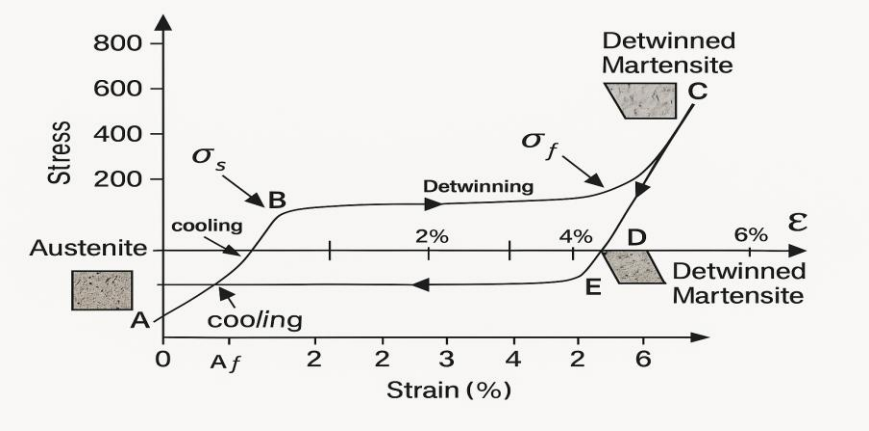

Figure 19: Stress-strain-temperature SME for a nickel-titanium shape memory alloy with uniaxial loading adopted from (Janke et al., 2005)

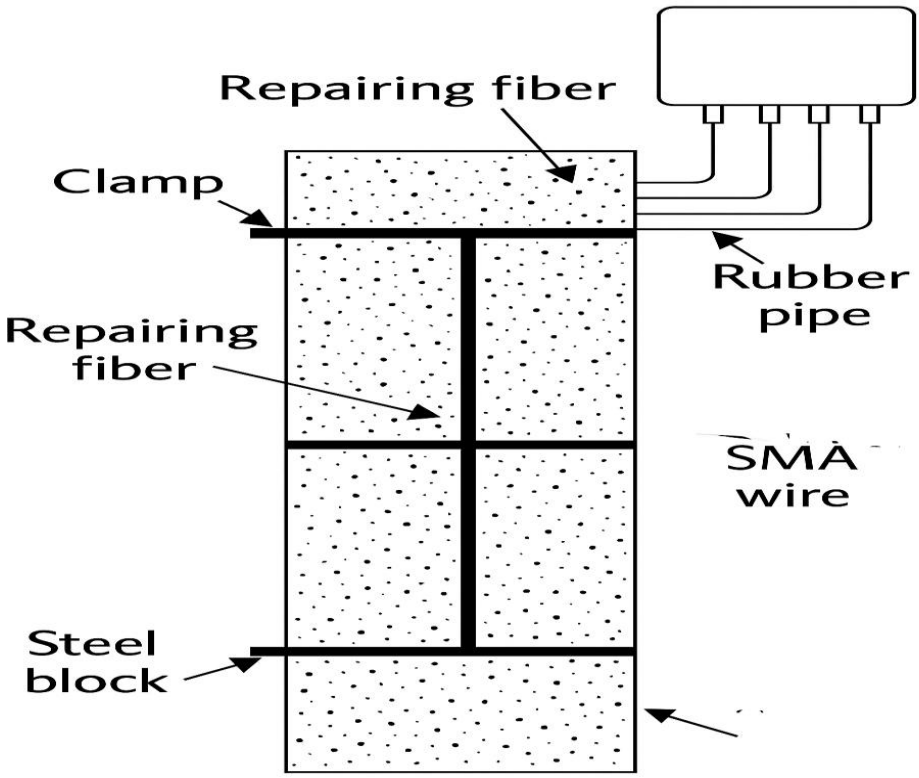

Figure 20: Self-repairing concrete with embedded SMA wires and adhesive-coated fibres adopted from (Kuang and Ou, 2008).

By implanting a shape memory polymer into a prismatic mortar specimen, Jefferson et al. took use of the SME characteristic and generated an axial shrinkage force of up to 34 MPa by thermally activating the polymers. Furthermore, heating the mortar using curing cycles ranging from four to eight days enhanced its overall strength by 25% The proposed design is illustrated in Figure 21, redrawn from Jefferson *et al.* (2010). After unloading the specimens, Kuang and Ou, (2008) observed that the concrete beams containing SMAs had a self-restoration potential, resulting in a nearly completed crack closure. Furthermore, the combined action of SMA and adhesive-containing fibres resulted in a significant improvement in crack healing. When these specimens were reloaded, new crack sectors appeared, but previously cracked sections remained closed (Kuang and Ou, 2008). SMA's pull-out resistance improves as its form changes before and after heat treatment. And certain parameters affecting pull-out resistance and crack closure have been investigated, such as shape, type, and size of SMA and showed a brief heat treatment reduced the length but increased the diameter of cold-drawn SMA fibre.

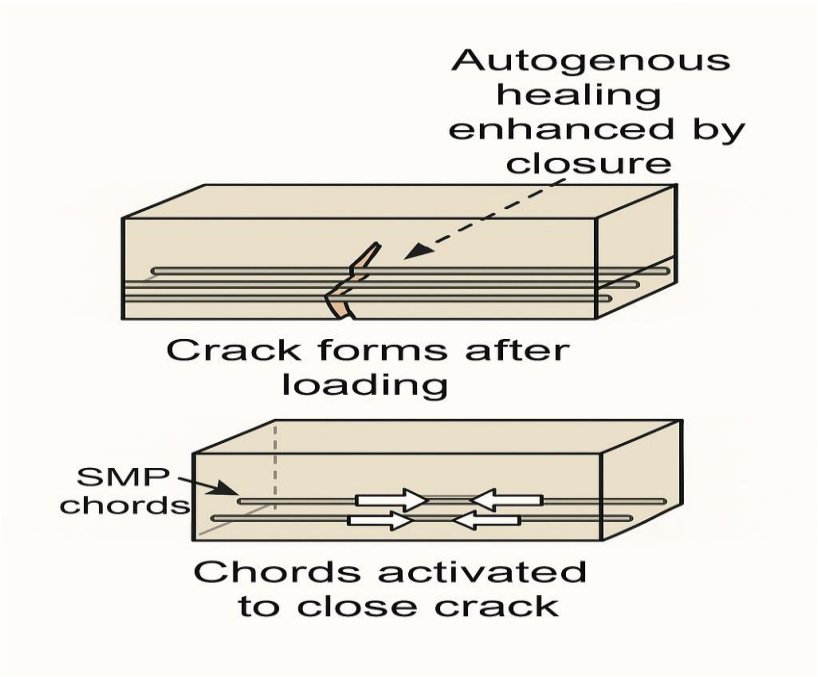

Figure 21: SMA cementitious composite adopted from (Jefferson et al., 2010)

2.6 Factors impact the chemical environment of concrete

Concrete's high pH and electrical conductivity make it a tough environment for bacteria to survive, which in turn limits its ability to self-heal and maintain long-term durability. While bacteria can generate calcium carbonate—a key component in self-healing—this process works best at a pH of 9 to 10 (Stocks-Fischer et al., 1999b). However, because concrete's surface pH varies, bacterial activity can be less effective, reducing its healing potential. This research explores how bacteria interact with cement-based materials and what influences the formation of calcium carbonate. It also considers factors like supplementary cementitious materials, carbonation, and fluid movement, which can change concrete's chemical environment. By finding ways to support bacterial activity in these conditions, this study aims to improve self-healing concrete technologies.

2.6.1 The impact of supplementary on chemical environment of concrete

As the need for concrete-based infrastructure continues to increase globally, the sustainability of Portland cement (PC) starts moving towards the spotlight. Most of the environmental problems connected to the production of PC are due to its high energy demand, which obviously also increases the CO2 emissions released during its manufacturing processes. Alternative binders to PC have been produced using a variety of waste and industrial by-product materials as substitutes to PC and, in this way, they reduce (to some extent) its carbon footprint. Collectively, these are the so-called supplementary cementitious materials (SCMs): these include pulverised fuel ash (PFA) and the ground granulated blast-furnace slag (GGBS), which are among the most widely used (Lothenbach et al., 2011). In a study by Cheng *et al.*, (2005a) that reviewed and evaluated the effect of GGBS replacement on the corrosion rate and flexural rigidity of reinforced concrete beams, it has been found that the replacement of cement with GGBS certainly inhibited corrosion to a certain extent and reduced the permeability. The addition of slag and continued loading had a certain effect on both the corrosion rate of the beams and the flexural rigidity. Moreover, SCMs can affect the pH levels because during the pozzolanic reaction, SCMs consume Ca $(OH)_2$, thereby reducing alkaline content. This causes the formation of calcium silicate, which absorbs alkali ions. This allows the alkaline content in concrete to decrease more and becomes another source for the formation of C-S-H gel (Fraay et al., 1989). Besides, SCMs such as notably the slag has a positive influence as they diminish the high alkalinity of cement concrete, they fill the micro pores and hardening the matrix, which reduces concrete porosity and permeability. Although SCMs can lower the pH of cement-based materials (CBM), which is needed for the hydration process protecting the passivating layer of the reinforcement from corrosion (Papadakis *et al.*, 2002), a pH decrease from its initial impact usually has a destructive effect on concrete. Thus, according to Cao *et al.* (1997) an increase in carbonation can decrease the consistence of paste mainly due to a decrease in the pH of the pore liquids, which makes the hydration products unstable. This stability, especially in the early hydration stages, could be expressed in aggressive nucleation of large ettringite crystals with weak bonding to the hydrated cement matrix, which weakens the concrete and damages it even at early ages and problematizes the concrete long-term durability. A further decrease in pH exacerbates this destructive impact usually leading to porous concrete with lower strength – certainly, not a desirable attribute for concrete engineers and designers. On the other hand, regulations that stipulate the replacement of cement by SCMs could help bio concrete technology as a pH reduction due to SCM substitution from cement creates a 'bacteria friendly

environment' for the colonisation process that is critical for the bio concrete functionality. Williams et al. (2017) determined that an extreme pH of 13.6 resulted in the greatest decline in viable cell concentration and the initial rate of ammonia production via urea hydrolysis.

2.6.2 The impact of carbonation

Carbonation is a chemical reaction that occurs between portlandite, which is present in hydrated cement, and carbon dioxide (CO_2). Carbon dioxide is found in the atmosphere at approximately 0.03% by volume of air. When CO_2 penetrates hardened concrete, it reacts with portlandite in the presence of moisture, forming calcium carbonate ($CaCO_3$). The rate of carbonation is primarily influenced by factors such as relative humidity, CO_2 concentration, penetration pressure, and the temperature of the environment in which the concrete is situated (Atiş, 2003). Additionally, steel reinforcement corrosion is a significant factor in the degradation of concrete (Basheer *et al.*, 1996). It is well established that steel reinforcement within concrete typically remains in a passive state, protected against corrosion by a thin iron oxide layer, which is maintained by the highly alkaline environment of the concrete's pore solution. Although carbonation does not directly cause concrete deterioration, it alters the pH of the pore solution (Mcpolin *et al.*, 2007). When the carbonation-induced acidification of the pore solution disrupts the passive layer on the steel reinforcement, corrosion of the steel is initiated. A study by (Pu *et al.*, 2012) found that the pH values of the pore solution predominantly decreased within the first 15 days of carbonation, with a nearly linear correlation between the pore solution pH and the carbonation period during this timeframe. The concentrations of Na^+ and K^+ in the pore solution dropped significantly within the first 3 days of carbonation, with minimal changes in the subsequent periods. Furthermore, the pH of the carbonated concrete's pore solution could be inferred from the suspension pH. However, a reduction in pH within the concrete's chemical environment and around its surface could create a conducive environment for bacterial activity. Despite this, the presence of carbon dioxide in the concrete will react with calcium hydroxide, which provides the essential calcium ions for the self-healing process. According to a study by Su *et al.*, (2024), the effectiveness of bacterial self-healing concrete is heavily reliant on the availability of Ca^{2+} ions.

2.6.3 The impact of flowing water

A substantial amount of concrete is utilized in the construction of structures located in marine environments, such as bridge supports and piers. Construction in these settings can raise environmental concerns, particularly due to the potential release of ions such as aluminium, calcium, chromium, magnesium, sodium, potassium, and zinc (composites and 2009, no date). Additionally, the pH value of concrete exposed to flowing water systems tends to decrease over time, as the continuous renewal of water leads to the removal of hydroxyl ions from the system (Law and Evans, no date b). Furthermore, this process can lead to a more acidic environment, which may affect the durability of the concrete. Furthermore, the leaching of essential ions like calcium and sodium from the concrete can compromise its structural integrity over time, highlighting the importance of considering water flow in the design of such structures (Law and Evans, no date b). In underground environments, distinct types of water flow—such as groundwater flow, seepage, and pore water flow—can significantly affect concrete structures. These water flows can lower the pH levels, which increases the risk of corrosion and compromises the structural integrity of underground concrete structures (Zhang et al., 2022). However, a flowing water system can also create favourable conditions for bacteria to thrive, as it alters the chemical environment on and around the concrete surface by lowering the pH, which can initially be as high as 13.50 in fresh concrete, a level intolerable to most soil bacteria.

Additionally, a flowing water system offers several benefits for bacterial self-healing concrete, such as supplying nutrients and oxygen, removing waste, activating, and maintaining bacterial activity, and enhancing the diffusion of ions, including carbonate ions produced by bacteria. This process promotes the formation of calcium carbonate crystals, which help fill cracks and restore the concrete's integrity.

2.7 Conclusion

This review explores a wide range of self-healing mechanisms in concrete, focusing on the causes of cracks and methods to repair them. It examines autogenous self-healing, crystalline self-healing, and the use of fibres and nanofibers to enhance crack repair. Autonomous self-healing approaches, such as bacteria-based self-healing, encapsulation techniques, and vascular networks, are also discussed for their potential in automatic crack repair. Additionally, the review looks at factors like cement type, flow systems, and the carbonation process, which play key roles in shaping the chemical environment that influences self-healing. Autogenous self-healing is driven by the natural hydration of unreacted cement particles, which helps partially close cracks. Crystalline self-healing, on the other hand, involves the growth of crystalline structures in the presence of water, effectively sealing cracks. Fibres and nanofibers are highlighted for their ability to bridge cracks, prevent them from growing further, and enhance the self-healing process. Bacteria-based self-healing is a particularly promising approach in autonomous systems. This method embeds bacteria in the concrete, which become active when moisture enters cracks, producing calcium carbonate ($CaCO_3$) to seal them. Encapsulation techniques store healing agents in microcapsules embedded in the concrete, releasing them upon crack formation to repair the damage. Vascular networks, which consist of pre-installed channels, provide a more advanced system for delivering healing agents to damaged areas. While current research demonstrates the potential of these methods, there are gaps in understanding how they work in real-world conditions, especially in underground structures. These environments bring unique challenges, such as limited access for maintenance and exposure to harsh chemicals and moisture. Existing studies primarily focus on introducing external bacteria into the concrete, often overlooking the potential of naturally occurring bacteria in the soil to support self-healing. A key gap in current research is the lack of focus on how native soil bacteria can enhance the self-healing process in concrete. Most studies have concentrated on introducing external bacteria into the concrete matrix, overlooking the potential of naturally occurring soil bacteria to naturally repair cracks. Additionally, the impact of the chemical environment—shaped by factors like the type of cement used—on the effectiveness of these mechanisms has not been fully explored. Flow systems, which help transport healing agents to cracks, and the carbonation process, where carbon dioxide reacts with the concrete matrix to alter its surface chemistry, are also areas that warrant further investigation. This study seeks to bridge this gap by examining how native soil bacteria can thrive under optimized conditions, such as an accelerated carbonation process and a flowing water system, to promote calcium carbonate production and improve crack repair. By leveraging naturally occurring soil bacteria, this research offers a more sustainable and cost-effective way to enhance self-healing in concrete. It fills a crucial gap in previous studies and aims to develop innovative, long-lasting materials specifically suited to the challenges of underground construction.

3 Chapter 3: Methodology and Materials

3.1 Methodology

This chapter provides a detailed explanation of the methods used to achieve the study's goals, highlighting how each step connects to the broader research objectives. The methodology is thoughtfully divided into three interconnected phases, each designed to address specific questions. The figure 22 shows the research methodology.

The first phase of this study explored the chemical environment inside concrete—both within the material and at its surface—and how it influenced bacterial activity. This was a key factor in microbial-induced calcium carbonate precipitation (MICP), which plays a vital role in self-healing concrete. To gain a better understanding, key chemical properties such as pH, electrical conductivity (EC), and calcium ion concentration were carefully measured in both the concrete and its surrounding environment. A major part of the research focused on how different factors—such as supplementary cementitious materials, flowing water, and accelerated carbonation—affected these chemical conditions over time. The aim was to determine whether these changes created a more (or less) favourable environment for bacterial growth and activity. Understanding these shifts was crucial for optimizing conditions that support MICP and improving concrete's ability to repair itself. To further investigate the conditions needed for bacteria to successfully induce calcium carbonate precipitation, an experiment was conducted to test bacterial activity across different pH levels. Bacterial cultures were exposed to pH values ranging from 7 to 12 to examine how alkalinity impacted their survival and function. Since concrete is naturally highly alkaline, this experiment helped identify the optimal pH range for bacteria to thrive and contribute effectively to self-healing. Additionally, another experiment was set up to simulate calcium carbonate precipitation under controlled conditions. A supersaturated calcium ion solution was prepared, and carbon dioxide was introduced to trigger calcium carbonate formation. This process mimicked natural mineralization in MICP, allowing for a detailed analysis of how calcium carbonate formed. By studying the rate of precipitation, crystal structure, and deposition patterns, the research provided a comparative view of microbial and non-microbial calcium carbonate formation, reinforcing the potential of bacteria in enhancing concrete's self-healing properties. The second phase of this study looked at how different nutrient carriers could boost the performance of self-healing concrete. Various carriers, like macro and microcapsules, were tested to see how well they delivered nutrients such as calcium lactate. The focus was on fine-tuning the size and composition of these capsules to make sure they positively impacted both the concrete's strength and its ability to heal itself. Concrete samples were prepared with different amounts of these capsules to assess their effect on compressive strength. By experimenting with various concentrations, the study aimed to find a balance between maintaining the concrete's structural integrity and enhancing its self-healing capabilities. This phase directly contributed to developing a reliable system for delivering nutrients that support bacterial activity, all while keeping the concrete strong and durable. The final phase of this study explored how self-healing concrete performed under different conditions. To simulate real damage, cracks were introduced into the concrete, allowing researchers to assess its ability to repair itself. This phase looked at how various factors influenced the healing process, including different percentages of supplementary cementitious materials, a flowing water system, accelerated carbonation, and exposure to different types of soil. To measure the effectiveness of the healing process, compressive strength tests tracked changes in structural performance over time, while water absorption

tests evaluated improvements in permeability. Light microscopy was used to observe how cracks gradually closed. At a more detailed level, scanning electron microscopy (SEM) provided insights into the microstructure of the healed concrete, and energy dispersive X-ray spectroscopy (EDS) helped analyse the chemical composition of the healing products.

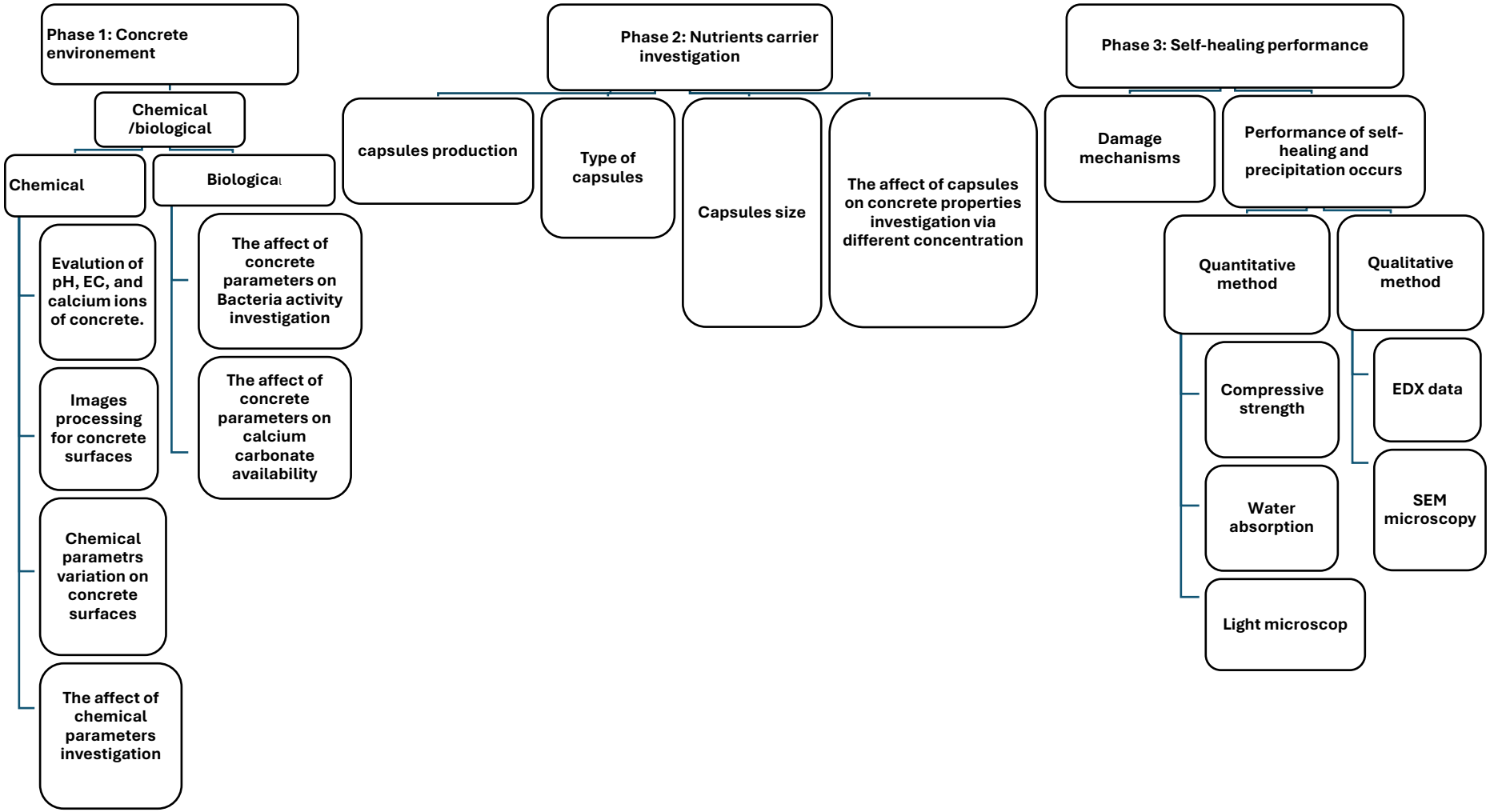

Figure 22: Research methodology

3.2 Overview of the Investigation

This study was carried out in three key phases, each focusing on a crucial aspect of self-healing concrete. Phase 1 explored the chemical and biological environment within concrete, investigating how factors like pH, electrical conductivity (EC), and calcium ion concentration influenced bacterial activity and calcium carbonate precipitation. Image processing techniques were used to analyses chemical variations on concrete surfaces, helping to understand how different conditions affected bacterial growth and the self-healing process. Phase 2 then shifted the focus to nutrient carriers, specifically calcium carbonate and calcium alginate microcapsules, looking at how they were produced, characterized, and integrated into the concrete mix. The study examined different capsule sizes, types, and concentrations to assess their impact on concrete properties such as compressive strength, aiming to find the best balance between structural integrity and self-healing performance. Finally, Phase 3 evaluated the effectiveness of the self-healing mechanism under varying concrete conditions, including different cement types and other factors influencing the concrete environment. This phase also examined damage mechanisms and calcium carbonate precipitation within cracked concrete. A combination of quantitative methods, such as compressive strength tests, water absorption measurements, and light microscopy, was employed to monitor crack closure, while qualitative techniques, including scanning electron microscopy (SEM) and energy-dispersive X-ray spectroscopy (EDS), were used to analyse the microstructure and chemical composition of the healing products. By systematically progressing through these stages, the research generated valuable insights into the mechanisms of microbial self-healing in concrete, contributing to the advancement of more durable and sustainable construction materials.

3.3 First phase (Concrete environment)

3.3.1 Evaluation pH, EC, and calcium ions release

This study aims to investigate the chemical environment surrounding immersed mortar, specifically assessing the implications for the survival of microorganisms on the concrete surface. To achieve this, we will utilize a comparative approach involving a plain mortar cube and additional cubes that incorporate fly ash. Previous research has indicated that a 10% concentration of fly ash can lead to a reduction in the initial pH of concrete subjected to standard curing conditions for both 3 and 28 days (Zeng *et al.*, 2022). Furthermore, the incorporation of fly ash may significantly diminish calcium ion leaching from the concrete matrix (Lun *et al.*, 2021).

Understanding these interactions is crucial, as the chemical environment at the concrete surface can influence microbial viability and activity. This investigation seeks to elucidate the effects of fly ash on pH, electrical conductivity (EC), and calcium ion release, along with how these parameters evolve over time and under varying scales of observation. This study explored the chemical environment surrounding immersed mortar, aiming to understand how it might influence the survival of microorganisms on the concrete surface. To do this, a comparative approach was taken, using both plain mortar cubes and cubes containing fly ash. Fly ash was chosen for its ability to modify key chemical properties of concrete, particularly pH, electrical conductivity (EC), and calcium ion leaching factors that play a role in microbial viability. Research by Zeng *et al.* (2022) has shown that replacing 10% of the cement with fly ash can lower the initial pH of concrete, creating a less extreme alkaline environment that may be more

suitable for microbial activity. Additionally, fly ash helps retain calcium ions, which are essential for microbial-induced calcium carbonate precipitation (MICP), while its slow pozzolanic reaction allows for a gradual shift in chemical conditions, making it easier to track these changes over time. Beyond these benefits, fly ash also improves concrete durability by refining its pore structure and reducing permeability, while promoting sustainability by repurposing industrial waste. Given its potential to optimize the concrete's chemical environment, understanding how fly ash interacts with these conditions was crucial. This study aimed to explore how fly ash influenced pH, EC, and calcium ion release, as well as how these factors changed over time and at different depths within the material.

To comprehensively assess these factors, two distinct treatment methodologies were employed.

- Water Replacement Treatment: In this setup, the water in two designated containers was regularly replaced with fresh tap water. This method was used to mimic real-world conditions where leachates are constantly diluted, helping to understand how this process affects the chemical composition of the surrounding environment over time.
- No Water Replacement Treatment: In contrast, the other two containers kept the same water for the entire experiment. This approach was used to observe how the chemical environment evolved in a stagnant system, where ion concentrations could gradually build up over time due to leaching, without the influence of dilution.

3.3.2 pH calibration study

The alkalinity of the pore solution in Portland cement is primarily attributed to the presence of dissolved sodium and potassium oxides, resulting in a pH range of 13 to 14. However, due to the heterogeneous and porous nature of concrete, pH levels at the concrete surface can exhibit significant variability (Femenias et al., 2017). Previous studies have employed imaging techniques to assess pH variations at concrete surfaces (Müller *et al.*, 2018) . Despite this, many researchers have refrained from adopting these methodologies due to limitations, including insufficient pH range specifications, reliance on proprietary solutions, and a lack of focus on micro-scale variations at the surfaces. The elevated pH levels are known to influence microbial activity in self-healing concrete systems (Amer Algaifi *et al.*, 2020b). This study examined the variability of pH on concrete surfaces to gain a better understanding of the conditions necessary for microbial survival. A unique calibration method was employed, involving the gradual addition of 0.5 ml of sodium hydroxide to carbonated water at specific intervals, combined with image analysis using ImageJ software. To measure pH levels, two indicators were tested: phenolphthalein and a universal indicator.

Phenolphthalein, commonly used to determine carbonation depth in concrete, changes colour depending on pH. On non-carbonated concrete surfaces, it shifted from dark purple to light purple as the pH decreased. In this study, sodium hydroxide was gradually added to increase the pH, and the resulting colour changes were recorded and analysed to match specific colours to corresponding pH levels. The universal indicator provided an alternative for tracking pH variations through its broad range of colour transitions. However, it presented challenges at higher pH levels, as pH values of 10, 11, and 12 all produced similar dark purple hues, making clear differentiation difficult. To enhance the accuracy of pH measurements, image processing techniques were also employed to analyse pH in solutions. By examining the relationship between RGB values and pH, building on findings from previous research by Beycioğlu et al. (2017) that indicated higher pH levels correlated with increased red values, this approach offered a more detailed and precise method for evaluating pH changes. These insights contributed to a deeper understanding of pH variability on concrete surfaces and its implications for microbial activity.

3.3.3 Image processing techniques

This study focuses on finding effective ways to measure pH levels on concrete surfaces by comparing two indicators—phenolphthalein and a universal indicator—to determine which works best. After this comparison, images of the concrete surfaces will be taken with a standard camera and analysed using ImageJ software. This approach introduces a creative way to monitor changes in pH and electrical conductivity (EC) on concrete surfaces. The main aim is to identify and understand the range of pH levels on concrete surfaces, offering valuable insights into the chemical conditions that impact microbial activity and self-healing processes. The process involves a few clear steps: capturing images of the surface, analysing them with ImageJ, and using the average RGB values from the images to estimate the corresponding pH levels. The workflow of the proposed image processing system is illustrated in Figure 23. Initially, images of the liquid or solid surfaces are captured and imported into the ImageJ software. The software processes these images, allowing for segmentation and quantification of the RGB colour components. The mean RGB values are then extracted, enabling the calculation of the percentage contributions of red, green, and blue components using the following equations:

$$Red\% = Rmean + Gmean + BmeanRmean \times 100 \quad (5)$$

$$Green\% = Gmean + Rmean + BmeanGmean \times 100 \quad (6)$$

$$Blue\% = Bmean + Rmean + GmeanBmean \times 100 \quad (7)$$

RGB represent the mean intensity values of the red, green, and blue colour channels, respectively. Once the contributions of each colour channel are calculated, regression analysis will be used to identify the relationship between the colour percentages and their corresponding pH values. This approach aims to develop a predictive model that links the observed colour changes to pH levels on concrete surfaces. By leveraging image processing techniques through ImageJ, the study offers a systematic and accurate method for determining pH values on concrete. This connection between RGB values and pH levels will provide a clearer understanding of the chemical environment at the concrete surface and offer insights into how it influences microbial activity and self-healing processes. The proposed method represents a step forward in pH detection, delivering a reliable and innovative tool for studying materials in civil engineering and paving the way for more advanced research in this area.

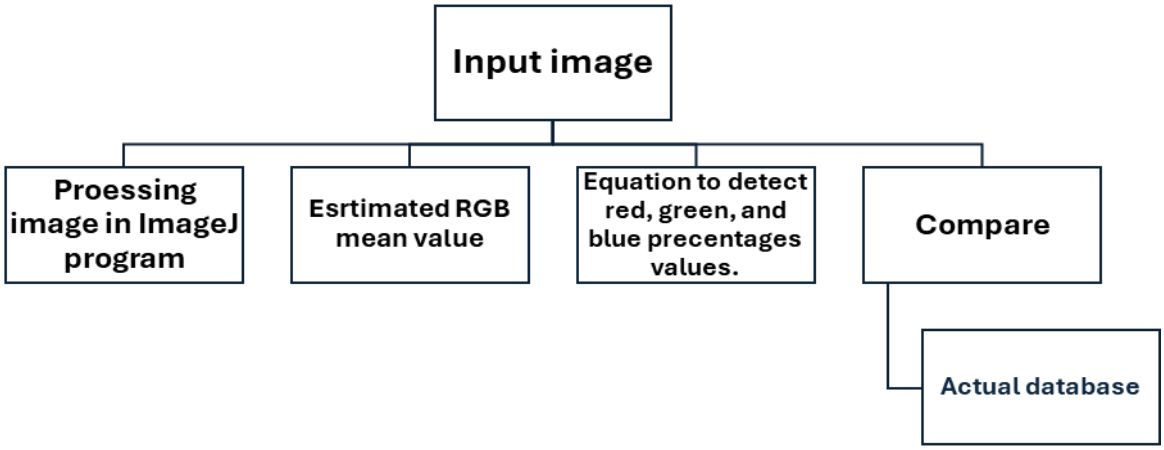

Figure 23: ImageJ technic

3.3.4 Variability of the Chemical Environment in Concrete Surfaces

Understanding how pH and electrical conductivity (EC) change on concrete surfaces is crucial for evaluating microbial growth and activity. In this study, phenolphthalein was used to indicate alkalinity, turning pink or purple at pH levels above 8.2, while a universal indicator provided a wider pH range with distinct colour changes, making it easier to visualize and measure surface pH. To analyse the data, images of the treated concrete surfaces were processed using ImageJ software to extract RGB colour values and link them to pH levels. Since pH affects ion movement and conductivity, EC was also estimated based on ion concentration. The results helped identify the ideal pH and EC conditions needed to support microbial activity, which plays a key role in self-healing, nutrient cycling, and pollutant breakdown. By combining colour indicators with image analysis, this study demonstrated a practical and accessible method for assessing concrete's chemical environment, paving the way for more durable and sustainable concrete structures.

3.3.5 Measuring Surface Chemical Parameters of Concrete Under Various Exposure Conditions

This study explored how different environmental factors affected pH levels at the surface of concrete. Factors such as carbonation, groundwater flow, and cracks were examined to understand how they influenced pH variations over time. Building on earlier findings, which showed that higher pH levels were linked to increased calcium ion concentrations and electrical conductivity, the research aimed to find the best way to track pH changes both at the surface and at different depths within the concrete. The experiments followed a structured approach, with adjustments made to factors like test duration and the shape of the concrete samples, whether cubes or beams. By investigating how these environmental conditions influenced pH distribution and related chemical reactions, the study provided valuable insights into the chemical environment of concrete under different conditions.

3.3.5.1 Carbonation

In this experiment, half of the mortar cubes were placed in carbonated water after three days of hydration to undergo carbonation, while the other half were submerged in tap water as a control group. The experiment ran for three days, during which pH levels were measured at set intervals (2, 6, 24, 48, and 72 hours) using a pH probe. Once the pH readings were recorded, phenolphthalein or a universal indicator was applied to the cube surfaces to observe any colour changes. These changes were then analysed using ImageJ software, focusing on the red colour channel percentage to track pH variations caused by carbonation. After completing these initial tests—measuring pH at both the surface and different depths—the results helped determine which indicator, phenolphthalein or the universal indicator, was more effective for further analysis.

3.3.5.2 Groundwater flow

In this part two studies were conducted which are:

- **Study 1: Initial Experiments with Water Replacement**

The first part of this research focused on understanding how different water flow conditions impact the pH levels at the surface of concrete. This experiment explored the chemical environment surrounding concrete and its implications for microbial activity. Factors like cement type, matrix size, and the water-cement ratio were considered to assess how ions leach from the concrete.

Three flow conditions were tested: no flow (control), slow flow, and fast flow. In the fast flow setup, water was replaced every two days, while for slow flow, water was replenished every seven days. In the no-flow condition, the water remained unchanged throughout the experiment. pH measurements were taken using a probe at the concrete surface and in the surrounding water. The water replacement rates were calculated based on the speed and distance of water movement to ensure the experiment accurately reflected the effects of different flow conditions. This phase provided valuable initial insights into how groundwater movement affects the chemical environment of concrete and its potential influence on microbial activity.

- **Study 2: Experiments Using a Hydraulic Bench**

Building on the initial experiments, a hydraulic bench was used to simulate more consistent and controlled water flow conditions. This advanced setup allowed for a continuous flow of water, providing precise control overflow rates and pressure to mimic real-world groundwater movement more closely.

In this study, pH levels were measured at both the concrete surface and in the surrounding water under steady flow conditions created by the hydraulic bench. This approach provided a clearer understanding of how constant water flow influences the leaching of ions and the chemical environment around the concrete. By comparing these results with those from the initial water replacement experiments, the study offered deeper insights into the relationship between water flow and microbial activity in concrete systems.

Together, these studies of this phase provide a more comprehensive understanding of how groundwater flow affects the chemical properties of concrete. This knowledge is essential for exploring strategies to enhance microbial activity in concrete, supporting innovations in self-healing and sustainable construction technologies.

3.3.6 Investigating Bacterial Activity and Microbial-Induced Calcite Precipitation (MICP) on Concrete Surfaces

This experiment aimed to explore the fundamental factors affecting bacterial growth and activity under controlled conditions before moving on to more complex environments like concrete and soil surfaces. The main goal was to understand how different environmental conditions influenced the ability of the selected bacteria to precipitate calcium carbonate ($CaCO_3$), a key process in microbial-induced calcite precipitation (MICP).

3.3.6.1 Investigation of Environmental Variables (pH).

After selecting the appropriate bacterial strains, the next phase of the experiment explored how different environmental factors—specifically pH affected bacterial growth and activity. These

conditions were carefully adjusted in controlled aqueous solutions to establish baseline data on how they influenced bacterial metabolism and the precipitation of calcium carbonate ($CaCO_3$). The focus then moved to examining these factors at the concrete surface, where additional challenges—such as surface interactions and changing chemical conditions—could influence bacterial behaviour. To better understand these effects, in situ pH measurements were taken to assess how these conditions impacted bacterial activity within the concrete matrix.

The decision to focus only on pH measurements was based on findings from both previous experiments in this study and existing literature, which showed that as pH levels increased, electrical conductivity and calcium ion concentration also rose. This made pH a reliable indicator for tracking changes in the chemical environment.

3.3.6.1.1 Experiment procedure

This study aimed to investigate the activity of *Bacillus pasturii* in response to different pH conditions, utilizing the ImageJ program for analysis and quantification of bacterial growth and metabolic activity. Understanding the optimal pH conditions for *Bacillus subtilis* is crucial, as pH significantly influences microbial growth and metabolic processes (Tran, Lander and Prindle, 2024). The experiment involved preparing growth media with varying pH levels, specifically adjusted to 7, 8, 9, 10, 11, and 12 using hydrochloric acid (HCl) and sodium hydroxide (NaOH). *Bacillus subtilis* was cultured in these media, and samples were taken at different time intervals to assess bacterial activity. The samples were subjected to imaging using microscopy to capture the growth visually.

3.3.6.1.2 Image Analysis Using ImageJ

ImageJ, a widely utilized image processing software, was employed to analyse and quantify the microscopic images of the bacterial cultures. The following steps outline the methodology used for image analysis: ImageJ, a widely utilized image processing software, was employed to analyse and quantify microscopic images of *Bacillus subtilis* cultures at predetermined time points to monitor growth. The methodology involved several steps: first, the captured images were imported into ImageJ and converted to grayscale to enhance contrast, facilitating the identification of bacterial colonies (Ducre et al., 2016a). Next, a threshold was applied to distinguish between bacterial colonies and the background, a crucial step for accurate quantification that allows for the segmentation of individual colonies (Ducret et al., 2016b). Subsequently, ImageJ's measurement tools were utilized to quantify parameters such as colony area, number of colonies, and mean intensity, which serve as indicators of bacterial activity and growth in response to varying pH levels (Ducret et al., 2016a). Finally, the data obtained from the ImageJ analysis were compiled and subjected to statistical analysis to assess the effect of pH on *Bacillus subtilis* activity, providing comparative insights into the optimal growth conditions across different pH levels. ImageJ analysis indicated distinct patterns in bacterial activity correlating with the pH levels. An increase in metabolic activity was observed at pH levels ranging from 7 to 9, aligning with the optimal growth conditions for *Bacillus subtilis* (Gauvry *et al.*, 2021). In contrast, pH levels above 10 demonstrated a decline in bacterial activity, suggesting that the alkaline environment may adversely affect the organism's growth (Hoseini *et al.*, 2018).

3.3.6.2 Evaluation of $CaCO_3$ Availability

Finally, the experiment examined how much calcium carbonate ($CaCO_3$) had formed around the concrete surface. Understanding where $CaCO_3$ accumulated in relation to bacterial activity was

key to evaluating how effectively microbial processes worked in cementitious environments. To assess this, samples were taken from both the concrete surface and the surrounding solution to measure the amount of precipitated $CaCO_3$ and link these findings to bacterial growth patterns.

3.3.6.2.1 Experiment procedure

In this study, a culture of Bacillus subtilis was employed alongside a growth medium composed of urea and calcium chloride ($CaCl_2$) to serve as the calcium ion source. For pH adjustments, hydrochloric acid (HCl) and sodium hydroxide (NaOH) were utilized. The experimental arrangement included a pH meter, and six flasks situated within a shaking incubator, along with a filtration apparatus. The preparation of the bacterial culture commenced with the creation of the growth medium, which involved dissolving nutrient broth, urea, and ammonium chloride in distilled water at concentrations of 5 g/L, 10 g/L, and 1 g/L, respectively. This mixture underwent sterilization through autoclaving at 121 °C for a duration of 15 minutes. After sterilization, Bacillus subtilis was inoculated into the sterilized medium, which was subsequently incubated in a shaking incubator set to a temperature range of 30-37 °C and a shaking speed of 150-200 rpm. The sterilized growth medium was then distributed into several flasks. The pH of each flask was measured using a pH meter, and the levels were adjusted to 7, 8, 9, 10, 11, and 12 with HCl and NaOH. Finally, calcium chloride was added to each flask to achieve the target final concentration of calcium ions. In the subsequent phase of the experiment, an equal volume of the cultured Bacillus subtilis, representing 10% of the total volume in each flask, was introduced into the pH-adjusted flasks.

3.4 Second phase (Carrier investigation)

The primary aim of this phase was to explore the integration of calcium carbonate microcapsules, calcium alginate microcapsules, and calcium lactate powder into concrete to improve its durability. These additions were designed to act as nutrient carriers, supporting microbial self-healing by providing essential resources for bacteria to thrive and facilitate calcium carbonate precipitation. Since bacteria require nutrients to remain active and initiate self-healing when cracks form, calcium lactate was selected as an effective food source. It played a key role in promoting bacterial growth and calcium carbonate production, which naturally sealed cracks in the concrete. Additionally, these nutrients had the potential to attract naturally occurring soil bacteria, further enhancing the self-healing process. To achieve this, a structured experimental approach was used. Microcapsules of different sizes were first synthesized using established encapsulation techniques to ensure consistency in production and quality. Their size and structural integrity were then verified through scanning electron microscopy (SEM). Mortar specimens were prepared with different amounts of microcapsules and tested for compressive and tensile strength following ASTM and BS standards to determine their impact on mechanical performance.

3.4.1 Production of Microcapsules with Optimal Size

The size of microcapsules plays a crucial role in determining their effectiveness within concrete. Large microcapsules may negatively affect the mechanical properties of the concrete, while overly small microcapsules may not carry enough nutrients for microbial activity. Therefore, the first objective is to develop a methodology for producing microcapsules of suitable size for embedding in concrete. Factors such as the concentration of encapsulating agents and the microcapsule formation technique will be considered to ensure a balance between sufficient nutrient loading and minimal impact on the mechanical properties of the concrete matrix.

Studies such as those by, Wang *et al.* (2019 b) have shown that smaller microcapsules tend to be more efficient at self-healing without causing significant reductions in strength.

3.4.2 Procedure of calcium carbonate capsules

The preparation of calcium lactate microcapsules, which are designed to enhance the self-healing properties of concrete, requires specific materials and equipment: The successful encapsulation of calcium lactate microcapsules, designed to enhance the self-healing properties of concrete, relies on a specific set of materials and equipment. Calcium chloride ($CaCl_2$) serves as a critical source of calcium ions, which are essential for the precipitation of calcium carbonate during the encapsulation process, facilitating the chemical reactions necessary for microcapsule formation (H M Jonkers, 2010). Sodium carbonate (Na_2CO_3) acts as a source of carbonate ions, which react with calcium ions to promote the precipitation of calcium carbonate, a fundamental aspect of the encapsulation method. Calcium lactate is specifically intended for encapsulation to support self-healing mechanisms in concrete, as it enhances the healing process by supplying calcium ions upon dissolution, further promoting calcium carbonate precipitation and the overall self-healing capacity of the concrete matrix (Whiffin, 2007). Deionized water (DI water) is utilized in preparing various solutions necessary for the encapsulation procedure, ensuring that no contaminants interfere with the chemical reactions and maintaining the integrity of the encapsulation process. Additionally, beakers and measuring cylinders are essential laboratory tools for the accurate measurement and mixing of solutions, which is crucial for maintaining the appropriate concentrations and ratios of reactants to ensure consistency and reliability. Lastly, a magnetic stirrer and stirring bar are employed for effective mixing of the solutions, providing uniform agitation to achieve homogeneity in the reactant mixtures, vital for optimal encapsulation outcomes. This selection of materials and equipment is integral to the successful encapsulation of calcium lactate microcapsules, significantly contributing to the effectiveness of self-healing concrete technology.

3.4.3 Procedure of calcium alginate capsules

In the encapsulation process of calcium lactate microcapsules intended for enhancing the self-healing properties of concrete, a variety of materials and equipment are essential. Sodium alginate powder, typically used at a concentration of 0.5% w/v, serves as the primary polymer matrix for encapsulation, providing a biodegradable and biocompatible medium that allows for the controlled release of nutrients Additionally, (Harbottle *et al.*, 2013) demonstrated that a concentration of 2.88% w/v sodium alginate and 3.09% w/v calcium chloride effectively supports a large population of *Sporosarcina pasteurii* bacteria, maintaining their viability on new slurry surfaces for several weeks. However, this project does not involve bacterial encapsulation but focuses instead on nutrient encapsulation, utilizing native soil bacteria and aiming to produce smaller capsule sizes. Nevertheless, understanding the mechanisms of bacterial calcium carbonate precipitation under varying environmental conditions remains an area requiring further investigation.

3.4.4 Optimization of Alginate Concentration and Microcapsule Quantity

A critical objective of this research is to identify the optimal concentrations of alginate and the appropriate number of microcapsules to be embedded in concrete. The study will investigate various concentrations of alginate in the microcapsule formulation, specifically focusing on 3% and 5%, while also testing different quantities of microcapsules in concrete specimens. This

approach aims to establish a balance between maximizing self-healing capacity and maintaining satisfactory mechanical properties. Previous studies have demonstrated that elevated concentrations of encapsulating materials can negatively impact compressive strength, whereas insufficient microcapsule quantities may lead to inadequate nutrient release necessary for microbial activity (H M Jonkers, no date). The experimental design will encompass multiple mix designs with varying microcapsule concentrations, accompanied by compressive and tensile strength tests and evaluations of healing efficiency.

3.4.5 Impact on Concrete Properties

An essential part of the research is understanding how the addition of these microcapsules affects the overall properties of the concrete. Compressive strength, tensile strength, and durability under various environmental conditions will be evaluated. Previous studies have shown that while the addition of microcapsules can lead to an improvement in crack healing, it can also negatively affect the mechanical strength of the material if not optimized (Belleghem *et al.*, no date). This study will provide insights into how different types of microcapsules—specifically calcium alginate, calcium carbonate, and calcium lactate—affect the performance of concrete and whether their inclusion can be justified based on the self-healing benefits they provide.

3.5 Third phase (Self-healing performance)

The final phase of this study explored how well self-healing concrete performed and how long it remained effective under different conditions. To simulate real damage, cracks were introduced into the concrete, allowing researchers to assess its ability to repair itself. To track these changes over time, various tests were carried out. Compressive strength tests measured how the concrete's structural performance evolved, while water absorption tests helped determine improvements in permeability. Light microscopy was used to observe how cracks gradually closed, providing a visual record of the healing process. For a more detailed analysis, scanning electron microscopy (SEM) provided insights into the microstructure of the healed concrete, while energy dispersive X-ray spectroscopy (EDS) examined the chemical composition of the healing products. By combining these methods, the study offered a comprehensive understanding of how the self-healing process worked and how the healing agents helped restore the material's strength and durability.

3.5.1 Three-points bending test

Concrete prisms from each specified group will be subjected to three-point bending tests using an Avery Dennison testing machine to assess the specimens' flexural behaviour. The testing process will proceed at a precisely controlled loading rate of 0.01 mm/s, allowing a gradual force application that facilitates accurate identification of crack initiation and growth. The test will conclude as soon as visible cracking is observed, marking the specimen's failure point under flexural stress. The three-point bending test is a standard method for evaluating fracture characteristics in concrete, as it provides critical data on tensile strength and the inherent brittleness of the material ('Test Method for Flexural Strength of Concrete (Using Simple Beam with Third-Point Loading)', 2018). The schematic representation in Figure 24 illustrates the three-point bending test procedure.

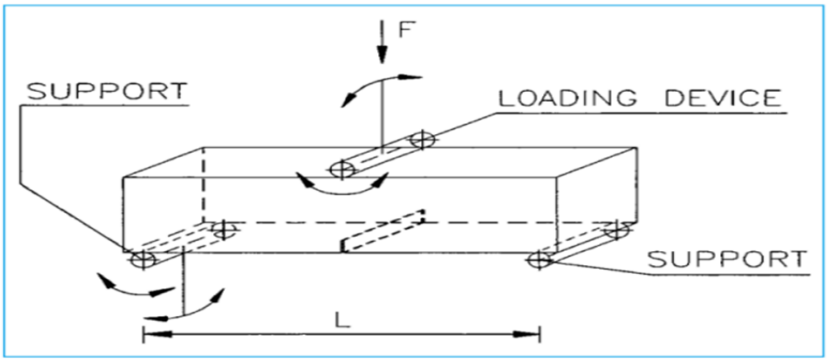

Figure 24: The load on the prism specimen and the position of the supports adopted from ('Test Method for Flexural Strength of Concrete (Using Simple Beam with Third-Point Loading)', 2018)

3.5.2 Water absorption test

Capillary rise frequently occurs over the service life of cement-based materials (CBMs). In environments where groundwater contains harmful agents like chloride ions, sulphates, and carbon dioxide, capillary action can transport these aggressive elements, leading to degradation of the CBM matrix and potential corrosion of embedded reinforcing steel (Belleghem *et al.*,1991). The water absorption test, a non-invasive approach, assesses CBMs' impermeability by measuring water tightness before and after crack formation (Martys and Ferraris, 1997). Capillary action, influenced by surface tension variations across interfaces, is central to this process (Hartland, 2004). For testing preparation, cracked mortar specimens are routinely dried in a controlled environment using an oven set to a stable temperature of 100°C. This drying process extends over a period of at least one week, with the weight of each specimen carefully monitored until variations are reduced to within 0.2%, signifying consistent moisture content. This step is essential for achieving uniform testing conditions and ensuring accuracy and reproducibility in the results. In numerous studies employing similar procedures, an epoxy resin is meticulously applied to the sides of each mortar prism, providing a waterproof barrier that prevents moisture movement during testing. By sealing the lateral surfaces with epoxy, only a small area around the crack on the bottom surface remains exposed. This selective exposure allows for focused assessments of crack healing or material behaviour, thereby improving the accuracy of test results by restricting the area of interaction to the designated crack region.

3.5.3 Visual inspection

Visual inspection is a fundamental method for evaluating self-healing in concrete, as it allows for direct assessment of crack closure and qualitative observations of the healing process over time. This non-destructive technique is often employed to monitor the progression of self-healing, particularly in cracks that are relatively shallow and visible on the concrete surface. Observations typically include assessing changes in crack width, identifying any deposit formation within the crack, and noting the extent of closure across the affected area. The efficacy of visual inspection has been highlighted by researchers such as Dhir and Jones, (1999), who observed the formation of calcite deposits within cracks, providing evidence of autogenous healing in concrete. Moreover, visual inspection offers a straightforward and low-cost approach for routine monitoring and is particularly effective when combined with photographic documentation to track healing progress over specific intervals. When coupled with digital image analysis techniques, visual inspection can provide semi-quantitative data on

crack reduction, enhancing the reliability of visual assessments (Cuenca *et al.*, no date). Visual inspection remains a widely adopted method in self-healing studies due to its simplicity and effectiveness in initial and routine evaluations of crack closure and healing material formation.

3.5.4 MICP formation on the surface.

X-Ray Diffraction (XRD) and Scanning Electron Microscopy (SEM) are selected as primary analytical techniques for characterizing and identifying crystalline phases in cementitious materials as shown in Figure 25. XRD is employed to determine the crystalline structure and phase composition of materials by analysing the diffraction patterns generated when X-rays interact with the crystal lattice, enabling the identification of distinct mineral phases and providing insights into the material's crystallography (Stutzman, Feng and Bullard, 2016). Meanwhile, SEM offers high-resolution imaging of surface morphology and microstructural features, allowing for a detailed examination of particle shapes, surface texture, and elemental distribution when coupled with Energy Dispersive X-ray Spectroscopy (EDS) (Goldstein *et al.*, 2017). This complementary approach facilitates a comprehensive analysis, with XRD providing quantitative phase identification and SEM revealing the microstructural characteristics critical to understanding the material's durability and reactivity in various environments (Goldstein *et al.*, 2017). Together, these methods are integral to a thorough evaluation of crystalline formations in cement-based materials, aiding in assessing their impact on long-term performance.

Figure 25: Scanning electron microscopy and energy dispersive X-ray (SEM-EDX)

3.6 Materials

3.6.1 An overview

The following sections provide an overview of the materials used in this study, explaining their composition and role in the self-healing process. In certain phases of the research, supplementary cementitious materials like fly ash (FA) and ground granulated blast-furnace slag (GGBS) were included to explore how they influence the chemical environment of the mortar. The impact of these materials will be discussed in more detail in the relevant sections.

3.6.2 Cement

In the preliminary phase of this research, Blue Circle Cement was utilized, classified as Ordinary Portland Cement (Type I Portland Cement) and widely available in the UK. This cement conforms to the quality assurance standards set forth in EN 197-1:2000, specifically meeting the designation BS EN 197-1:2000 CEM II/A-LL 32.5R. The selection of this type of cement is noteworthy due to its common use in construction and its proven performance characteristics. In addition, the Ground Granulated Blast Furnace Slag (GGBS) cement used in this study was obtained from the Hanson HEIDELBERG CEMENT GROUP in the UK. This material complies with the rigorous standards of BS EN 196-2, which outline the testing methods and specifications for cement, ensuring its appropriateness for high-performance applications. Moreover, the Fly Ash utilized in this research, identified as 450-N, meets the normal fineness (N) category requirements as per BS EN 450-1. This fly ash was sourced from the Conserv Ltd group, based in Middlesbrough, North Yorkshire, UK. The incorporation of fly ash enhances the workability and durability of the concrete while promoting sustainability by leveraging industrial by-products. The combination of Ordinary Portland Cement, GGBS, and Fly Ash establishes a robust foundation for investigating their synergistic impacts on concrete properties, especially regarding self-healing capabilities and the improvement of mechanical performance.

3.6.3 Sand

The fine aggregate employed in the production of cement mortar is comprised of sand, which has a maximum particle size of 2 mm and a specific gravity of 2.63. This commercially available sand was sourced from Travis Perkins, a well-regarded supplier within the UK construction sector. In the context of cementitious composites, the inclusion of sand plays several vital roles that enhance the material's overall performance. Firstly, sand enhances the compaction of the mortar mix, which is critical for minimizing voids and increasing the density of the final product. A denser mix not only improves the mechanical properties of the mortar but also reduces permeability, thereby enhancing durability (Neville, 1995b). Secondly, the incorporation of sand significantly increases the bond strength between the mortar and the adhered substrates or reinforcement materials. The irregular surface texture of sand particles offers a larger area for adhesion, facilitating stronger interfacial bonding. This aspect is particularly crucial in applications where structural integrity and load-bearing capacity are of utmost importance. Moreover, the use of sand in cement mortar contributes to achieving a superior casting finish. The fine grain size of the sand enables a smoother surface finish, which is not only visually appealing but also functional, especially in architectural applications where aesthetic considerations are significant. The judicious selection of sand as a fine aggregate is therefore essential for optimizing the performance characteristics of cementitious composites, enhancing their mechanical strength, bond efficiency, and overall quality.

3.6.4 Carrier (capsules)

In Phase 2 of this study, different nutrient carriers were explored to improve nutrient delivery, with a focus on calcium lactate powder, calcium alginate capsules, and a new approach using calcium carbonate capsules in various sizes. Calcium lactate powder is an accessible source of calcium ions, which play a crucial role in enhancing the self-healing capabilities of concrete. Its direct incorporation into the mortar mix can significantly improve the material's performance, particularly regarding compressive strength and overall durability (H M Jonkers, 2010). The soluble nature of calcium lactate enables it to dissociate readily, contributing to the healing process upon exposure to moisture and facilitating calcium carbonate formation

through carbonation (Wang *et al.*, 2019b). Another approach to nutrient encapsulation is the use of calcium alginate capsules. These capsules, derived from alginic acid, offer a biodegradable and biocompatible method for the controlled release of nutrients. Their application in self-healing concrete has demonstrated enhanced healing efficiency by providing a nutrient reservoir that can gradually release its contents when cracks develop (Reda and Chidiac, 2022). Encapsulating nutrients within calcium alginate ensures a targeted healing process, as it protects the nutrients from premature dissolution prior to their necessity. The introduction of calcium carbonate capsules, particularly with varying sizes, represents a significant innovation in nutrient delivery systems for self-healing concrete. The size of these capsules plays a vital role in determining their dissolution rates and the subsequent release of calcium ions, which in turn affects the self-healing potential of the concrete. Smaller capsules may dissolve rapidly, offering a quick supply of nutrients, while larger capsules can provide a more extended release, supporting sustained healing over time (Tziviloglou *et al.*, 2016). Therefore, optimizing capsule size is essential for maximizing the effectiveness of the self-healing mechanism.

3.6.5 Bacteria selection

For this study, Bacillus subtilis and Sporosarcina pasteurii (formerly Bacillus pasteurii) were chosen because of their well-known ability to produce calcium carbonate, which helps improve concrete durability and self-healing properties. Figure 26 shows six flasks in an incubator with cultivated bacteria. These bacteria are naturally found in soil and are particularly resilient, making them suitable for surviving in the harsh, high-alkaline environment of concrete. Bacillus subtilis is a widely distributed bacterium capable of forming spores, allowing it to endure extreme conditions. Sporosarcina pasteurii, on the other hand, is highly efficient in calcium carbonate precipitation due to its strong urease activity. This enzyme breaks down urea, increasing the pH of the surrounding environment and encouraging calcium carbonate to form—an essential process for sealing cracks in concrete. As part of Phase 1, experiments were conducted to test how well these bacteria survived and performed in controlled conditions. The focus was on understanding how pH levels affected their ability to produce calcium carbonate, both in direct bacterial cultures and in a separate experiment that examined calcium carbonate formation in solution at different pH values. These tests provided valuable insights into the ideal conditions for microbial mineralization, helping to refine the approach for integrating bacteria into self-healing concrete systems. Bacillus subtilis, a gram-positive bacterium, is notable for its resilience and capability to form endospores, allowing it to endure harsh conditions, including the alkaline environment typical of concrete. When integrated into the concrete matrix, B. subtilis engages in metabolic processes that lead to the precipitation of calcium carbonate ($CaCO_3$), effectively filling cracks and voids (Wang *et al.*, no date b). The formation of $CaCO_3$ not only seals these imperfections but also enhances the overall mechanical strength of the concrete. The effectiveness of these bacteria in enhancing self-healing capabilities is also significantly influenced by environmental factors, especially pH levels. The pH of the concrete environment plays a critical role in determining bacterial activity and metabolic functions. Generally, both B. subtilis and B. pasteurii thrive within an optimal pH range of 7 to 9, which aligns with the alkaline conditions found in concrete (Zeigler and Perkins, 2021). Lower pH levels can negatively impact the viability and metabolic processes of these bacteria, leading to decreased effectiveness in facilitating calcite precipitation. On the other hand, excessively high pH levels can also hinder bacterial activity due to heightened alkalinity, creating an unfavourable environment for metabolic functions (Shrestha *et al.*, 2022).

Figure 26: six flasks and shaking incubator

4 Chapter 4: Investigate the chemical environment of concrete at and around its surface (Phase 1)

4.1 Overview

The initial phase of this investigation is divided into two distinct components aimed at understanding the interactions between concrete, its chemical environment, and microbial activity. The first component focuses on examining the chemical environment of concrete, both within the surrounding solution and on its surface, elucidating how various chemical constituents influence pH levels and overall chemical properties. Through systematic pH monitoring and chemical composition analysis, this part seeks to provide insights into how carbonation and other environmental factors affect concrete integrity. The second component delves into microbiological aspects, specifically investigating how concrete parameters impact bacterial activity and the productivity of calcium carbonate in relation to concrete cracking. This segment explores how variations in concrete's chemical composition, moisture levels, and physical characteristics influence microbial growth and metabolic activity, aiming to identify mechanisms through which bacteria contribute to the self-healing properties of concrete. Furthermore, the study emphasizes understanding bacterial precipitation at the concrete/soil interface, assessing conditions conducive to bacterial survival and the formation of biominerals necessary for self-healing. Key factors influencing microbially induced calcite precipitation (MICP) include cementitious agent concentrations, pH, salinity, temperature, and environmental conditions such as soil type and particle size. This research is significant for advancing self-healing mechanisms and the durability of underground structures while contributing to a broader understanding of soil chemistry and biology in built environments. The findings are relevant to interdisciplinary fields, including contaminated land remediation, soil quality enhancement, and environmental sustainability initiatives.

4.2 Chemical investigation

4.2.1 Chemical investigation on concrete solution

4.2.1.1 Impact of Water Replacement on pH, Electrical Conductivity, and Calcium Ions in Concrete solution

4.2.1.1.1 Method and materials

As part of the preparation process, mortar cubes of 40*40*40 mm were prepared as showing in fig 27. In this experiment, there was only one mix that was used and in term of preventing contact with the external environment, the cubes were stored in sealed containers without being exposed to air as. It was determined that the pH concentration in the containers collected was within the range of the pH probe, which was used to analyse it as seen in figure 27. The cubes in the experiment were made small due to the experiment's requirements. However, the aim is also to study the chemical surroundings of concrete surfaces in solution on a small scale. All cubes are made with the same ratio of water to binder (w/b) that is set at 0.50 for all cubes, while the ratio of cement to sand is set at 1:3 for all cubes. Using Hanson Sulphate Resistant cement (CEMIII/A+SR). After that, the six cubes were divided into two groups, which were tested for a period of 14 weeks and were measured on a weekly basis. Numerous test methods have been developed to investigate the effect of leachate on groundwater flow. The

impact of concrete leaching into groundwater and soil is investigated using three methods previously(Chai, Onitsuk and Hayashi, 2009).

- Test of batch contact - mixing of solid masses with groundwater in a batch.
- Leaching test in a tank - solid mass submerged in groundwater for a period.
- Test of column percolation of leachate into soil based on seepage of water containing leachate.

Considering a solid mass submerged in water, tank leaching tests can investigate concrete leaching. The precision of tank leaching tests has been shown to be reliable, and they are reproducible(Hohberg *et al.*, 2000). Additionally, there are static and dynamic tank leaching tests. A static leaching test determines how different intrinsic properties affect leaching. Dynamic leaching tests determine whether changing environmental conditions affect leaching. However, in this experiment tap water was employed as groundwater (GW). The two type methods of leaching test were selected based on the interest of investigating the concrete chemical environment, at what rate can GW effect it and those methods are:

a. Replacing water test, this was intended to be a simple leaching test method that was intended to be cost effective without losing the same results as those of a traditional tank test. The method works in an open system, such as a continuous flow of water column or pipe, by replacing the water every week and taking a reading before each new water replacement.

b. A non-replacement water test is a conventional method of testing concrete by placing the cubes into a plastic container filled with water and taking a measurement of the parameters each week.

4.2.1.2 Impact of 15-25% Fly Ash on pH, Electrical Conductivity, and Calcium Ion Levels in Concrete Solutions

4.2.1.2.1 Materials and method

Fly ash (FA), supplementary cementitious materials, was supplied by Conserve, a UK manufacturer and distributor of lime mortar and building conservation materials. The FA is quality assured in accordance with BS EN 450-1 2005 and Portland cement in accordance with BS EN196-1 [13]. Table 2 shows the chemical composition components of Portland cement and fly ash.

Table 2: The chemical composition component for Portland cement and Fly ash

Portland cement (PC)		**Fly ash (FA)**	
Oxide	%	Oxide	%
SiO_2	20.69	SiO_2	59.04
Al_2O_3	3.80	Al_2O_3	34.08
CaO	62.99	CaO	2.0
Fe_2O_3	2.12	Fe_2O_3	0.22
MgO	2.62	MgO	0.05

K_2O	0.55	K_2O	0.43
Na2O	0.13	Na2O	1.26
SO_3	3.10	Loss on ignition	0.63

4.2.1.2.2 Preparation of cubes

This was achieved by placing the cubes in a container filled with tap water. This container was then sealed up to prevent the cubes from getting in contact with the external environment and water evaporation. As for the cubes size, the cubes have the following dimensions: 40*40*40 mm. A small size was prepared for this study based on the experimental requirements. and designed according to BSEN procedures (British Standards Institution, no date). This study investigates the variations in key parameters, including pH, electrical conductivity, and calcium ion concentration, around the concrete surface in solution, examining their changes over time and at different scales. The water-to-binder (w/b) ratio was maintained at 0.50 for all mortar cubes, while the cement-to-sand ratio was fixed at 1:3. The nine cubes were categorized into three groups, prepared using Hanson Sulphate Resisting Cement (CEM III/A + SR), sand, and tap water, as previously outlined. To encompass a wide range of conditions, different types of cementitious matrices with various binder compositions were utilized. The specific dosages of these binders are detailed in Table 3. The study incorporated nine different mortar cube formulations, incorporating a range of cements and supplementary materials, including fly ash (FA), to assess their influence on the investigated parameters. A ten-week period was used to test the cubes of mortar that were placed in containers containing tap water. They were given weekly tests for ten weeks. As can be seen from the figure 28, three devices were used in this experiment to determine pH, conductivity as well as calcium ions. Here is an example of a SensION+ EC5 Portable Conductivity that can be used to measure conductivity. It also has a Jenway Benchtop pH Meter 3510 for measuring pH, and a Perkin Elmer Analyzer 400 for determining calcium ions content as shown in figure 28.

Table 3: Materials proportion

Ingredients (g)	**Mixture**		
	Control mix	**Fly ash 15%**	**Fly ash 25%**
Cement	45	38.25	33.75
Sand	135	135	135
Fly ash	-	6.75	11.25
Water	22.5	22.5	22.5

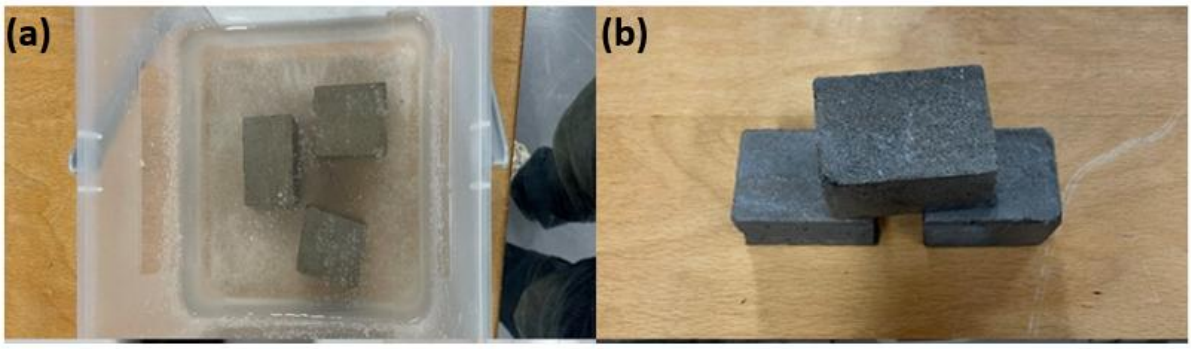

Figure 27: (a) Cubes placed inside a container. (b) Cube dimensions.

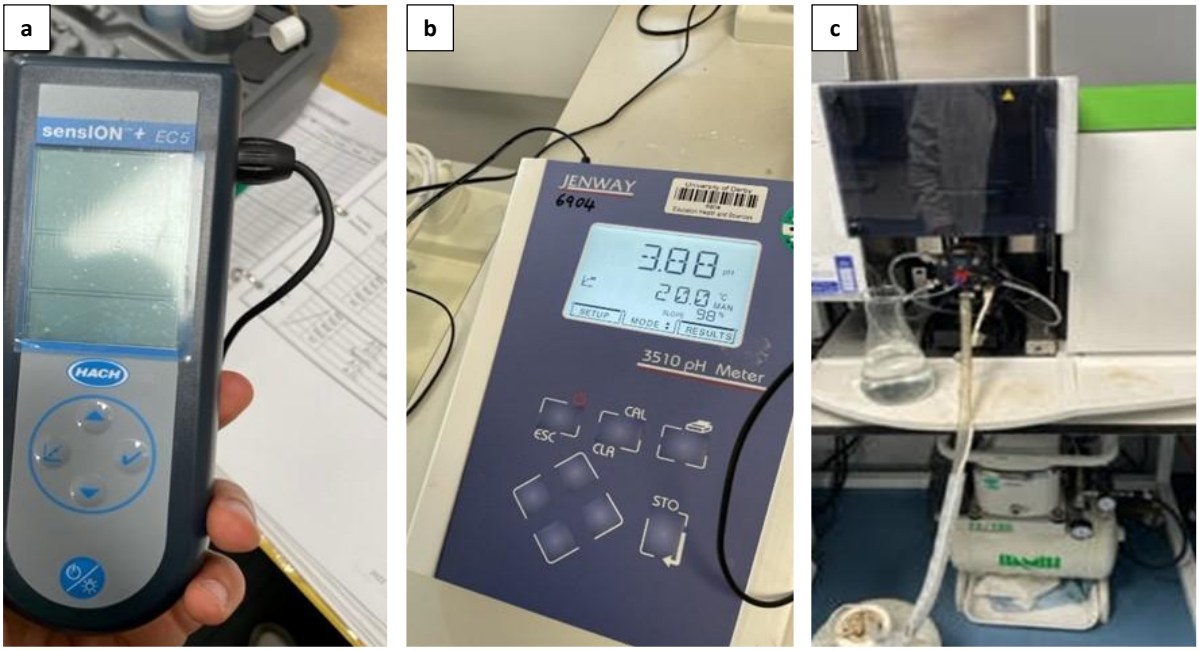

Figure 28: a) SensION+ EC5 Portable Conductivity to measure conductivity and salinity. b) Jenway Benchtop pH Meter 3510 to measure pH.c) Perkin Elmer Analyzer 400 to measure calcium content.

4.2.1.3 Effect of 35% GGBS and Fly Ash Replacement on Concrete solution Environment

4.2.1.3.1 Materials and Methods

4.2.1.3.2 Specimen preparation and crack creation

According to BS EN 196-1 standards, plain mortar specimens (control), along with mortar specimens incorporating fly ash (FA) and ground granulated blast-furnace slag (GGBS), were prepared for this study. The GGBS cement used was sourced from the Hanson Heidelberg Cement Group in the UK and complies with BS EN 196-2 standards. Additionally, the fly ash utilized, categorized as 450-N with standard fineness (N), meets the specifications of BS EN 450-1 and was provided by Conserv Ltd, located in Middlesbrough, North Yorkshire, UK. Table 4 provides a detailed overview of the chemical compositions of Portland cement, GGBS cement, and FA cement. In this study, supplementary cementitious materials were incorporated at a replacement level of 35% by weight with Portland cement for both fly ash and GGBS.

Table 4: Chemical properties of Portland cement, GGBS cement, and FA cement

Properties%	Portland cement%	GGBS cement%	FA cement%
SiO_2	23.7	32.77	45 to 51
CaO	57.27	40.83	1 to 5
MgO	3.85	6.91	1 to 4
Fe_2O_3	4.83	0.57	7 to 11
Al_2O_3	4.51	14.33	27 to 32
SO_3	2.73	0.28	0.3 to 1.3
Na_2O	-	-	0.8 to 1.7
K_2O	0.37	-	1 to 5
Cl	0.0068	0.00	0.05 to 0.1
TiO_2	-	0.63	0.8 to 1.1
Loss in ignition	7.24	-	-

To prepare the mortar samples, a mixture of Hanson Sulphate Resisting Cement (CEM III/A + SR) and CEM II, combined with sand and tap water, was formulated following the proportions outlined in Table 5. A water-to-cement ratio of 0.6 was maintained for all mixtures. Prismatic specimens with dimensions of 40 x 40 x 160 mm were cast. To mitigate the risk of complete failure under loading, a fibre mesh reinforcement was centrally placed within each specimen during casting. After an initial setting period of 24 hours, the mortar prisms were demoulded and cured by immersion in water for 28 days, after which mechanical testing commenced. Throughout the curing period, pH measurements were systematically recorded using the Jenway Benchtop pH Meter 3510 to observe any chemical environment shifts, particularly due to the incorporation of supplementary materials. These measurements provided insight into the alkalinity maintained within the matrix and highlighted the influence of supplementary cementitious materials on pH stability over time. Typically, samples incorporating fly ash (FA) and ground granulated blast-furnace slag (GGBS) demonstrated pH variability, which could influence the reactivity and hydration processes within the matrix, potentially affecting durability and mechanical properties over the long term. The pH changes associated with the supplementary materials demonstrated the potential for variability in the cement matrix, underscoring the need for ongoing pH monitoring in studies assessing the self-healing capacity of mortar mixes with added FA and GGBS.

Table 5: Mortar specimen proportions

Ingredient (Kg/m^3)	MC	MF	MG
Cement	418	271.7	271.7
Fly ash	-	146.3	-
GGBS	-	-	146.3
Sand	1254	1254	1254
Water	250	250	250

4.2.1.4 Effect of 50 % GGBS and Fly Ash Replacement on Concrete Solution Environment

4.2.1.4.1 Materials and methods

4.2.1.4.2 Specimen preparation

The methodology and materials applied in this experiment closely mirror those of the previous study, with the primary modification being an increase in the replacement percentage of supplementary cementitious materials. In this experiment, the replacement level of ground granulated blast-furnace slag (GGBS) and fly ash (FA) was elevated to 50%, compared to the previous 35%. This adjustment was made to examine the impact of a higher dosage of supplementary materials on the concrete's chemical environment and physical properties, as increased replacement levels can significantly influence concrete's alkalinity, hydration rate, and long-term durability. Higher substitution levels of GGBS and FA are often associated with reduced calcium hydroxide content and a potentially denser microstructure due to enhanced pozzolanic reactions (Mehta et al., 2006). However, these changes may also introduce variations in the pH stability of the matrix and impact the mechanical properties over extended curing periods. The methodology, including sample preparation, curing conditions, and testing protocols, remained consistent with the previous experimental design to ensure comparability across both replacement levels, enabling a clearer assessment of the effects associated specifically with the increase in supplementary material dosage.

4.2.1.5 Impact of Carbonation on the pH Value of Concrete solution

The initial inquiry aimed to evaluate the influence of carbonation on the concrete solution The experimental procedure involved employing Portland cement (conforming to BSEN 196-1) and GGBS cement (meeting BSEN 196-2 standards) sourced from HANSON HEIDELBERG CEMENT GROUP in the UK. The chemical compositions of these cement types like previous experiments. To facilitate appropriate CO2 diffusion and sample creation, a water-to-cement ratio of 0.3 was selected during the preparation phase. The resulting mixture was compacted into prisms measuring 40mm × 40mm × 160mm. Following compaction, the load was applied and sustained for 30 seconds. These prisms were subsequently divided into two categories. Specifically, three prisms were submerged in containers containing standard water conditions, while the remaining three prisms were situated within containers holding carbonated water. Likewise, an additional set of six mortar specimens, incorporating replacement with GGBS cement, were subjected to a parallel experimental regimen. This regimen closely mirrored the earlier curing methods. In this manner, three specimens cured in a normal water environment. The remaining trio underwent curing within containers filled with carbonated water. This systematic and methodical approach was meticulously developed to enable a thorough and exhaustive exploration of the ramifications of carbonation on bio-concrete technology. A pivotal ingredient in the experimentation. After a 24-hour setting period, the mortar prisms were extracted from their moulds and submerged in water for 28 days. Following this curing phase, the specimens underwent comprehensive testing. Throughout the curing period, pH levels were ascertained employing the Jenway Benchtop pH Meter 3510. Once the curing regimen was completed, the specimens were extracted from the water and allowed to air-dry at ambient temperatures, preparing them for crack initiation through conventional mechanical testing. To ensure that each sample was accommodated within these small containers, the samples were placed inside containers with a capacity of five litters. To maintain consistency, each container was rinsed with either normal water or carbonated water for 1 litter. Following that, all

containers were securely sealed and kept at a constant room temperature of 20°C to prevent CO2 escaping or entering.

4.2.1.5.1 Test methods

The objective of this investigation was to determine the influence of carbonation on the solution surrounding concrete. The initial methodology involved systematically monitoring pH levels within the solution encompassing the concrete prisms, which were immersed in both carbonated water and standard water environments. This observation was maintained over a predetermined time frame to assess the effects of carbonation on the solution's properties.

4.2.1.6 Solution pH Monitoring and Analysis

In this study, the pH values of the surrounding solution were continuously monitored to evaluate the extent of carbonation affecting mortar prisms. The experimental procedure involved immersing the prisms in both carbonated water and normal water. Throughout the experiment, pH measurements were taken at regular intervals and meticulously documented. Notably, the prisms exposed to carbonated water for a specified duration were subsequently immersed in normal water to facilitate the hydration process. This sequential immersion aimed to maintain the desired conditions for hydration in the carbonated samples. The primary objective of the study was to observe and analyse changes in pH over time, specifically investigating the impact of carbonation on the acidity or alkalinity of the solution. Calibration of the pH meter probe (Jenway Benchtop) was an essential procedure to ensure accuracy and precision in measuring the pH of the pore solution. By calibrating the pH meter, potential measurement errors and biases were minimized, thereby enhancing the reliability of the recorded pH values. The monitoring process involved measuring the solution surrounding the prisms using the calibrated pH meter at specific intervals throughout the four-day experimental duration, specifically at 30 minutes, 2 hours, and 4 days. By comparing the pH values obtained from the carbonated and normal water environments, a comprehensive evaluation of the impact of carbonation on the solution's pH could be achieved. The recorded pH values were analysed to examine any observed variations or trends, thereby inferring the progression and magnitude of carbonation over time. The comparative analysis of pH changes between the carbonated and normal water environments facilitated a clear differentiation of the effects associated with the carbonation process. By employing rigorous pH monitoring techniques and ensuring accurate calibration of the measurement instrument, this study aimed to provide reliable data regarding the extent of carbonation effects on the surrounding solution.

4.2.1.7 pH Value Calibration Using ImageJ Software

4.2.1.7.1 Material and Method

4.2.1.7.2 Materials

The experimental setup involved the following materials and equipment:

- 150 ml of carbonated water.
- Sodium hydroxide solution with a concentration of 1M.
- Universal indicator and phenolphthalein solutions for visual pH determination.
- Two light sources to ensure imaging without reflections or shadows.
- White paper as a neutral background.
- Extech 110 pH probe meter, with a measurement range of 0 to 14, pH accuracy of ±0.01, and a temperature range from 23°F to 194°F.
- Burette, initially set to 50 ml, for precise solution addition.

- RICOH digital camera (model 3842) with a 2.7-inch-wide LCD screen, 16-megapixel CMOS sensor, mounted vertically above the solution at a distance of 20 cm to capture images.
- Image analysis was conducted using the ImageJ software, which was employed to evaluate the images captured during the experiment. Specifically, ImageJ was used to quantify the red percentage values for the phenolphthalein indicator and the red, green, and blue (RGB) percentage values for the universal indicator. These RGB values represent the intensity of red, green, and blue colours, allowing for the detection of pH changes by measuring the reflected light from the solution. This method facilitated precise tracking of pH shifts through colour intensity analysis.

4.2.1.7.3 Method

In this study, sodium hydroxide was added incrementally in 0.5 ml steps of a 1M solution, with thorough stirring to achieve uniform pH and consistent colour distribution throughout the solution. This experiment aims to develop a system capable of detecting pH values and pH fluctuations through colour change, achieved by isolating each RGB value from captured images. A technical diagram of the experimental setup is presented in Figure 29. The setup employed dual light sources to uniformly illuminate the solution, enhancing colour reflectance, and images were subsequently captured with a camera to analyse RGB values. Two indicators, phenolphthalein and a universal indicator, were used to visualize pH changes through colour variation. Phenolphthalein, which shifts to pink under basic conditions, enabled the calculation of red percentage values via Equation 5. In contrast, the universal indicator, which produces a spectrum of colours based on pH level, required a more complex approach. For example, at pH 8, the universal indicator imparts a blue hue to the solution, necessitating the application of three separate equations to determine the red, blue, and green colour percentages, thereby establishing the relationship between pH values and specific colour intensities. This method proposes a technique for detecting pH variations at concrete surfaces by observing colour changes associated with pH-sensitive indicators. Through applying phenolphthalein to assess basic conditions (noted by a pink hue) and the universal indicator to cover a wider pH range, the experiment demonstrates a colorimetric approach to precise pH measurement on concrete surfaces.

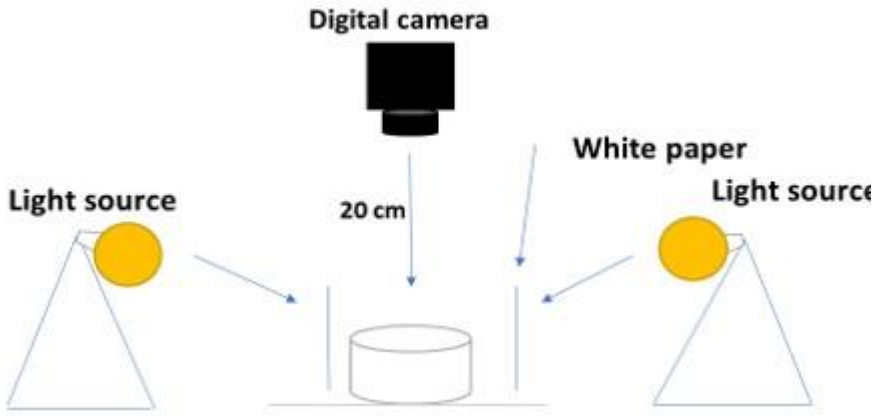

Figure 29: Experimental Setup Diagram

4.2.1.8 Application of Phenolphthalein Solution and Universal Indicator on Concrete Surfaces

In this experiment, the behaviour of phenolphthalein solution and universal indicator on the concrete surface was examined to observe their effectiveness in visually identifying pH variations. Both indicators are widely used for detecting pH due to their colorimetric responses to different pH levels, though each provides distinct insights based on their respective colour-change mechanisms. Phenolphthalein solution was applied to the concrete surface to identify basic conditions. As a pH-sensitive indicator, phenolphthalein remains colourless in acidic and neutral environments but shifts to a pink or magenta hue at pH values above 8.2, thereby offering a clear visual indication of alkaline conditions typical of fresh or uncarbonated concrete. This colour change is particularly useful for identifying areas of the concrete that may be at a higher risk for carbonation, as carbonation generally reduces surface alkalinity (Alonso *et al.*, 2006). On the other hand, the universal indicator, which provides a wider colour spectrum covering pH values from 1 to 14, was applied to observe a broader range of pH changes on the concrete surface. The universal indicator transitions through a series of colours—ranging from red in acidic conditions, through green at neutral pH, to blue and violet in more basic environments—making it suitable for assessing concrete surfaces that have undergone varying levels of carbonation or exposure to environmental conditions that reduce alkalinity. For example, areas of concrete with lower pH (due to carbonation or exposure to acidic environments) could be readily identified by the shift in colour to yellow or orange, while less-carbonated, more alkaline regions would appear in the green or blue spectrum. This comparative study of phenolphthalein and universal indicator allows for a nuanced understanding of pH distribution on concrete surfaces. By utilizing both indicators, the experiment demonstrates a method for identifying areas of potential degradation and provides insights into the degree of carbonation in concrete structures.

4.2.2 Chemical investigation on the surface

Concrete's heterogeneous nature creates diverse chemical environments within its structure, often resulting in localized variations in chemical activity and ion distribution. This study's main objective is to examine how these environmental factors affect pH, electrical conductivity (EC), and calcium ion concentrations on the concrete surface, with a particular focus on pH as a core variable. Prior research has indicated a correlation between pH levels, EC, and calcium ion concentration, where elevated pH values are associated with higher EC and calcium ion levels (Neville, 1995b). By concentrating on pH, this investigation aims to clarify the interactions driving ionic behaviour and mineral precipitation on concrete surfaces. Additionally, it will explore whether calcium carbonate and other mineral precipitation occurs directly at the concrete surface, providing a nuanced understanding of cementitious surface chemistry. Insights from this study hold valuable implications for self-healing concrete, where microbial or chemical precipitation can enhance durability and lower permeability by sealing micro-cracks and pores (Wang *et al.*, 2014). With systematic measurement and analysis, this research seeks to build foundational knowledge of pH-driven chemical processes on concrete surfaces in varied environments, advancing sustainable concrete technology.

4.2.2.1 The effect of supplementary materials on concrete surface

This study explores the impact of different replacement percentages of supplementary cementitious materials, specifically ground granulated blast furnace slag (GGBS) and fly ash, in place of Portland cement within concrete mixtures. Replacement rates were systematically adjusted, beginning at 15% and increasing through 25%, 35%, and 50%, to assess how these

materials affect both the chemical and mechanical properties of concrete. Known for their pozzolanic and latent hydraulic qualities, GGBS and fly ash are valued for enhancing concrete's durability and sustainability by reducing the necessary cement volume, thus lowering the associated CO_2 emissions in cement production (Shi et al., 2019; Juenger & Siddique, 2015). This investigation examines the effects of these materials at different substitution levels, focusing on changes in pH, electrical conductivity, and calcium ion concentration within the concrete environment. Additionally, it aims to evaluate how varying levels of supplementary materials might support conditions favourable for bacterial activity in self-healing concrete, contributing to a deeper understanding of the optimal rates for promoting self-repair in concrete structures over time.

4.2.2.1.1 Method

This study measured carbonation levels across various mortar surfaces over a 28-day period to examine the influence of different cement types on the mortar's surface pH. Four distinct mortar samples were prepared: plain mortar, mortar with Ground Granulated Blast Furnace Slag (GGBS), and mortar with Fly Ash (FA) replacements. Each surface was subjected to phenolphthalein spray to observe colorimetric shifts, with darker purple hues indicating higher pH values as identified in previous research. This colour-based pH indication, aligned with empirical data, established that an increase in pH value corresponds to a darker shade of purple. Further, ImageJ software was employed for quantitative image analysis to evaluate pH, using RGB values from images of the mortar surfaces. The percentage of red values (%Red) was calculated using equation 5.

The primary objective of this research is to evaluate the potential role of indigenous soil bacteria in enhancing the self-healing capacity of concrete, alongside investigating the influence and efficacy of supplementary materials in bio-concrete applications. Comparisons of pH levels among various mortar types—including those with supplementary materials—revealed that replacements with GGBS and FA resulted in a noticeable decrease in pH over time, suggesting alterations in the chemical environment of the concrete. These changes hold significant implications for bio-concrete performance, as pH variations can affect microbial activity and, consequently, the self-healing capacity of the concrete system.

4.2.2.2 The effect of flowing water on chemical environments of concrete surface

4.2.2.2.1 Materials and Methods

4.2.2.2.1.1 Specimen preparation and crack creation

In accordance with BS EN 196-1 guidelines, various mortar specimens were prepared for this study, incorporating nutrient additives across three cement types: Portland cement, fly ash (FA) mortar, and ground granulated blast-furnace slag (GGBS) mortar. The GGBS cement, sourced from Hanson Heidelberg Cement Group in the UK, conformed to BS EN 196-2 standards, while the FA 450-N, provided by Conserv Ltd Group (Middlesbrough, North Yorkshire), met the normal fineness (N) category requirements specified in BS EN 450-1. The chemical composition of Portland cement, GGBS cement, and FA cement aligns with prior studies within this research.

For mortar sample production, a mix was carefully prepared with Hanson Sulphate Resisting Cement (CEM III/A +SR), sand, and tap water. A consistent water-to-cement ratio of 0.6 was maintained across all mixtures. Prismatic specimens measuring 40 x 40 x 160 mm were cast, and after 24 hours, the prisms were demoulded.

The primary aim of this study was to evaluate the impact of water flow on the prismatic specimens by comparing exposure to flowing water with immersion in stagnant water. This comparison was designed to determine the influence of flowing water on the efficacy of bio-concrete technology. Nine prisms were subjected to flowing water, while another nine were immersed in stagnant water, with both groups undergoing a 28-day curing period. During this time, pH was measured in solution using a Jenway Benchtop pH Meter 3510 as shown in figure 30, and a pH indicator solution was applied to the specimen surfaces. To further analyse the surface characteristics of selected samples, four groups were examined: the Control 0% group, FA mortar, and GGBS mortar. Phenolphthalein, a pH indicator solution, was used to assess carbonation levels in the prisms. A lack of colour change or faint pink shade (pH 9) indicated complete carbonation, while a pink to dark pink coloration (pH > 9) indicated incomplete carbonation. This phenolphthalein method detects carbonation by observing colour shifts in an acid-base indicator solution when applied to concrete surfaces, with the colour intensity linked to the pH of the surrounding environment.

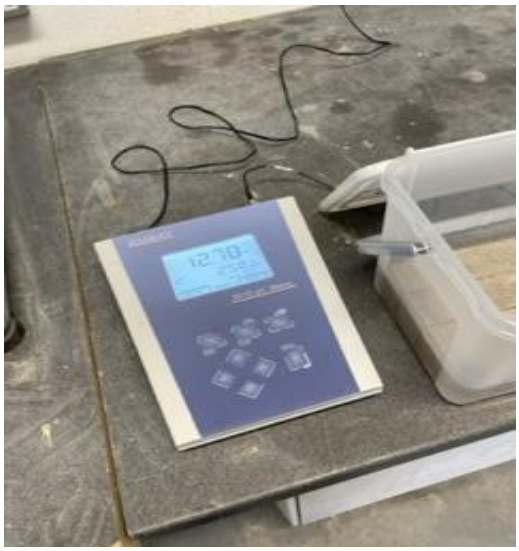

Figure 30: Jenway Benchtop pH Meter 3510

- **Flowing water exposure**

For the flowing water test, a digital hydraulic bench was used, carefully calibrated to maintain a steady flow rate of 17.7 litres per minute and a working pressure of 0.295 litres. Nine prisms were arranged vertically on the bench with equal spacing between them. Over the 28-day testing period, the prisms were fully submerged in tap water, which was replaced daily to ensure consistent conditions. At the end of the exposure period, the prisms were removed from the flowing water to allow cracks to form. Figure 31 shows the hydraulic bench, while Figure 32 provides a schematic of the experimental setup.

Figure 31: Digital hydraulic bench and the prisms inside it

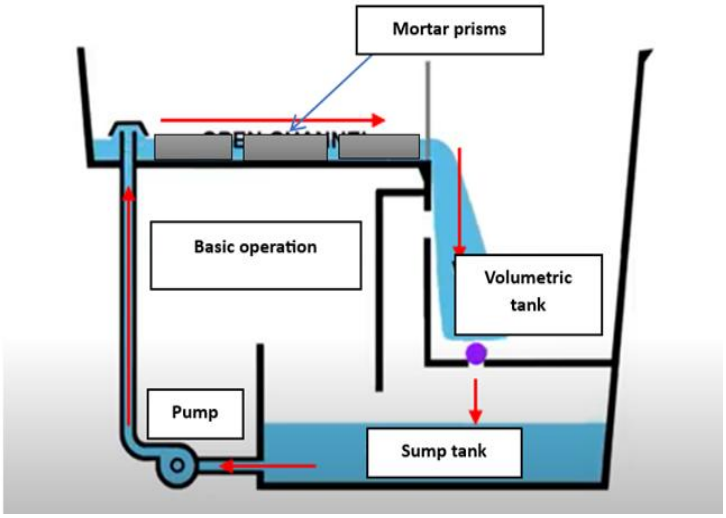

Figure 32: The diagram of the flowing water exposure experiment.

- **Stagnant water**

Three identical 5-liter plastic containers were employed in this study. Each container was filled with tap water up to a 1-liter volume, sufficient to ensure complete submersion of the prisms. Nine mortar prisms, uniform in size and composition, were evenly distributed among the three containers, as illustrated in Figure 33. A calibrated pH probe was used to monitor the solution's pH throughout the 28-day immersion period.

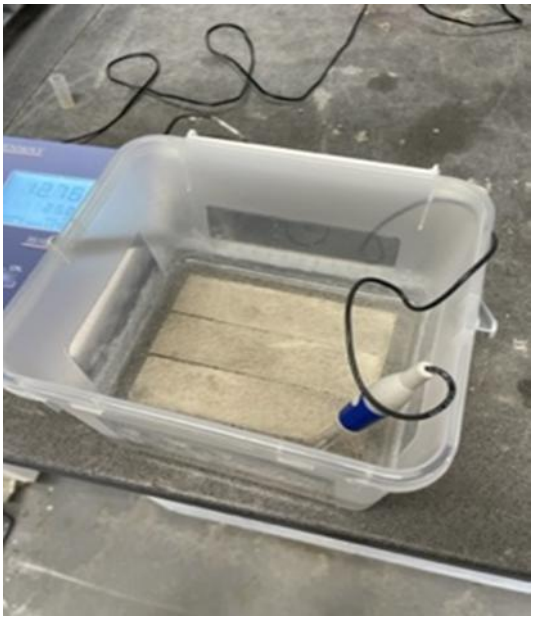

Figure 33: Prisms inside the containers

4.2.2.3 The effect of carbonation on concrete surface

4.2.2.3.1 Materials and methods

4.2.2.3.1.1 Specimen preparation and crack creation

The study investigation focused on assessing the effects of carbonation on both the concrete solution and its surface. Portland cement, adhering to BS EN 196-1 standards, and GGBS cement, meeting BS EN 196-2 requirements, were utilized, both sourced from Hanson Heidelberg Cement Group in the UK. To ensure effective CO_2 diffusion and consistent sample preparation, a water-to-cement ratio of 0.3 was selected. The resulting mixture was cast into prisms measuring 40 mm × 40 mm × 160 mm, compacted, and subjected to a sustained load for 30 seconds. Following this process, the prisms were divided into two categories. Three prisms were submerged in containers with standard water conditions, while the remaining three were placed in containers containing carbonated water. Similarly, an additional set of six mortar specimens, incorporating GGBS cement as a partial replacement, was subjected to an identical experimental procedure. In this set, three specimens were cured in a standard water environment, while the other three were cured in containers filled with carbonated water. This systematic approach was designed to thoroughly investigate the effects of carbonation on bio-concrete technology, with carbonation serving as a central variable in the experimental setup. A consistent water-to-cement ratio of 0.3 was maintained across all mixtures. Prismatic specimens, measuring 40 mm × 40 mm × 160 mm, were meticulously cast. To prevent complete structural failure, fibre mesh was strategically embedded in the centre of each specimen during the casting process. After a 24-hour setting period, the mortar prisms were demoulded and submerged in water for 28 days for curing. During the curing phase, pH levels were monitored using a Jenway Benchtop pH Meter 3510. Upon completion of the curing regimen, the specimens were removed from the water and allowed to air-dry at ambient temperatures, preparing them for crack initiation through conventional mechanical testing.

4.3 Microbiology investigation

4.3.1 The Influence of pH on Bacterial Activity

This study aimed to investigate the activity of Bacillus pasturii across a controlled range of pH conditions, using ImageJ software for detailed quantification and analysis. Bacillus pasturii exhibits notable metabolic flexibility across diverse environments, but pH has a substantial impact on its growth, cellular processes, and metabolic rates. Identifying the specific pH range that optimally supports bacterial activity is therefore essential, particularly for applications in biotechnology, such as bioremediation and biomineralization, where regulated microbial growth is beneficial. To carry out the experiment, growth media were prepared and adjusted to various pH levels, specifically targeting values from 7 to 12. Using hydrochloric acid (HCl) and sodium hydroxide (NaOH), these pH levels were carefully set and maintained to create stable conditions in the media. Each pH value served as a distinct treatment condition to evaluate the adaptability and activity profile of Bacillus pasturii in response to increasing alkalinity. ImageJ software was applied to these images, systematically measuring bacterial growth rates, colony numbers, and any morphological changes with high precision. Expected findings from this study should clarify the ideal pH range for Bacillus pasturii growth and activity, informing how to optimize conditions for enhanced bacterial performance in various practical applications. The results may also shed light on bacterial adaptability to pH changes, with broader implications for microbial ecology and industrial microbiology.

4.3.2 Influence of pH Variation on MICP Production in Aqueous Solution (Controlled Experimental Study)

4.3.2.1 Materials needed and Experiment set

In this experiment, a culture of Bacillus subtilis was used alongside a growth medium containing urea and calcium chloride ($CaCl_2$) as the calcium ion source. Hydrochloric acid (HCl) and sodium hydroxide (NaOH) were utilized to achieve precise pH adjustments. The experimental setup comprised a pH meter, six flasks placed in a temperature-controlled shaking incubator. Figure 34 shows the pH meter used in the experiment.

The preparation of the bacterial culture commenced with formulating the growth medium by dissolving nutrient broth, urea, and ammonium chloride in distilled water, at respective concentrations of 5 g/L, 10 g/L, and 1 g/L. This solution was then sterilized via autoclaving at 121 °C for 15 minutes. Following sterilization, Bacillus subtilis was inoculated into the medium, which was subsequently incubated under controlled conditions in a shaking incubator at a temperature range of 30-37 °C and a shaking speed of 150-200 rpm. After incubation, the sterile growth medium was aliquoted into individual flasks. Using a pH meter, the pH of each flask was measured and adjusted to target values of 7, 8, 9, 10, 11, and 12 by adding HCl or NaOH, as illustrated in Figure 35. Calcium chloride was subsequently added to each flask to achieve the intended calcium ion concentration. In the subsequent phase, an equal volume of cultured Bacillus subtilis, comprising 10% of each flask's total volume, was introduced to the pH-adjusted flasks. These flasks were then returned to the shaking incubator, set to the same conditions of 30-37 °C and 150-200 rpm, and incubated for a period of 7 days, as shown in Figure 36.

Figure 34: pH meter

Figure 36: Flasks with different pH value

Figure 35: Six flasks and shaking incubator.

4.4 Results and discussion

4.4.1 Chemical investigation on concrete solution

4.4.1.1 Impact of Water Replacement on pH, Electrical Conductivity, and Calcium Ions in Concrete solution

In the context of cement paste, a porous material, it is assumed that the pore solution and the surrounding hydration products maintain thermodynamic equilibrium. When concrete is submerged in pure water, the chemical potential gradient between the pore solution and the external surface of the concrete element induces ion diffusion out of the material. This leads to changes in the pore solution's chemical composition, potentially disrupting the equilibrium of the system and causing the dissolution of specific hydration phases, as noted by previous research Nielsen *et al.* (2019a) . Figure 37 compares the pH levels in same-sized concrete cubes under two conditions: with and without periodic water replacement. The findings indicate that the pH in non-replaced water consistently exceeds that of replaced water, as water in the replacement system is refreshed weekly. This behaviour is also evident in Figure 37, which shows that alkalis are initially leached rapidly from the inner core due to their matrix bonds. A similar conclusion on calcium ion leaching in concrete was reported by (Nielsen *et al.*, 2019a). In this study, both systems initially exhibited an increase in pH within the first three days following ion leaching. However, on the fourth day, after water replacement, the pH of the replacement system dropped as hydroxyl ions were removed. Conversely, in the non-replacement system, pH values continued to increase weekly, until a slight drop was observed at the end of the tenth week. This decrease could be attributed to carbonation of the water during the measurement. Concrete inherently has a high pH value, but this diminishes over time as the material ages. Due to its high alkalinity, concrete is chemically more reactive than many other materials. When exposed to substances with a lower pH, the alkalis in concrete react, reducing its pH and thus its strength. Fresh concrete is highly reactive with acidic substances, such that even atmospheric carbon dioxide begins to neutralize its alkalis, a process known as carbonation.

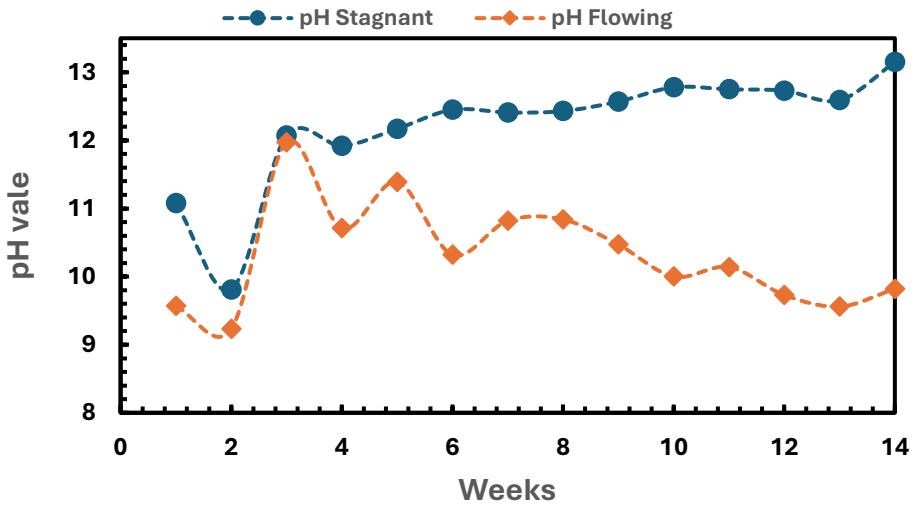

Figure 37: pH results under different water conditions.

As shown in Figure 38, the results of the electrical conductivity (EC) test reveal distinct differences between the EC values of the replacement and non-replacement systems. A comparison between these values demonstrates that the EC in the non-replacement system is consistently higher than in the replacement system. This difference is attributed to the ongoing removal of ions in each measurement, which is not replenished in the non-replacement system. An important observation regarding EC values was noted: during the initial three days of the experiment, prior to the initiation of the replacement system, the EC values for both systems were at their highest recorded levels. However, following the initiation of water replacement on the fourth day, a consistent decline in EC was observed with each subsequent measurement, corresponding to the removal of ions from the replacement system.

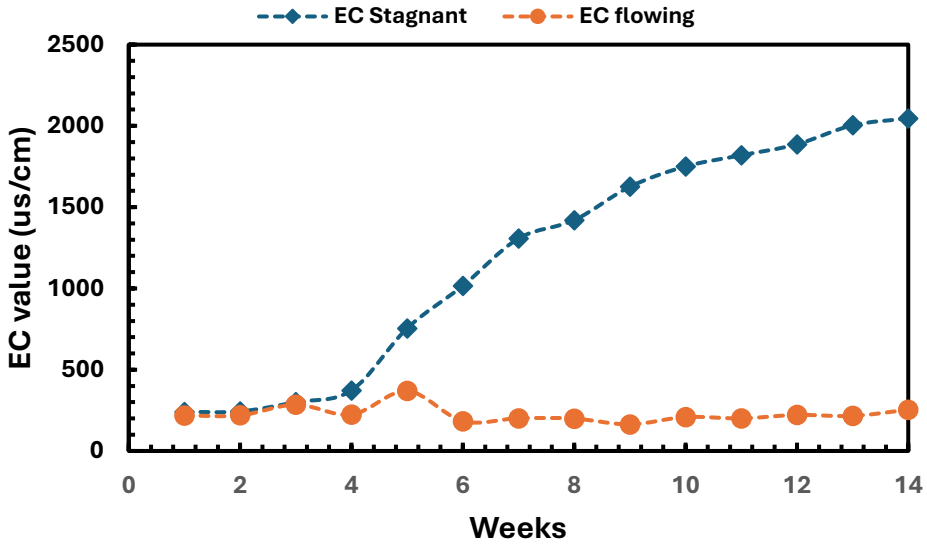

Figure 38: Electrical conductivity results for two water conditions

In designing a robust leaching test, it is essential to consider environmental conditions. However, this is often challenging in practice, as leaching tests commonly use accelerated processes in laboratory settings. It is crucial that such acceleration does not alter the fundamental leaching mechanisms. Notably, significant differences in calcium ion leaching were observed between none-replacement and replacement water systems. Over the experiment's duration, the non-replacement system exhibited substantially higher levels of calcium ion leaching compared to the replacement system. This outcome is anticipated, as the periodic water refreshment in the replacement system facilitated ion removal. Moreover, water replacement introduces notable alterations to the chemical environment at the concrete surface due to dynamic interaction with the flowing water. The figure 39 shows how calcium ion concentration (mmol/L) changes over 14 weeks in stagnant and flowing water conditions. In stagnant water, calcium levels fluctuate at first but then rise sharply after week 6, surpassing 100 mmol/L by week 14, likely due to reduced ion movement and accumulation. In contrast, the flowing water condition sees a slower, steadier increase with lower overall calcium levels, suggesting that continuous water movement prevents excessive buildup. This comparison highlights the impact of water flow on calcium retention—stagnant water encourages accumulation, while flowing water disperses it. These insights are particularly relevant for self-healing concrete, where calcium carbonate precipitation plays a key role in crack repair, and water movement directly affects the process.

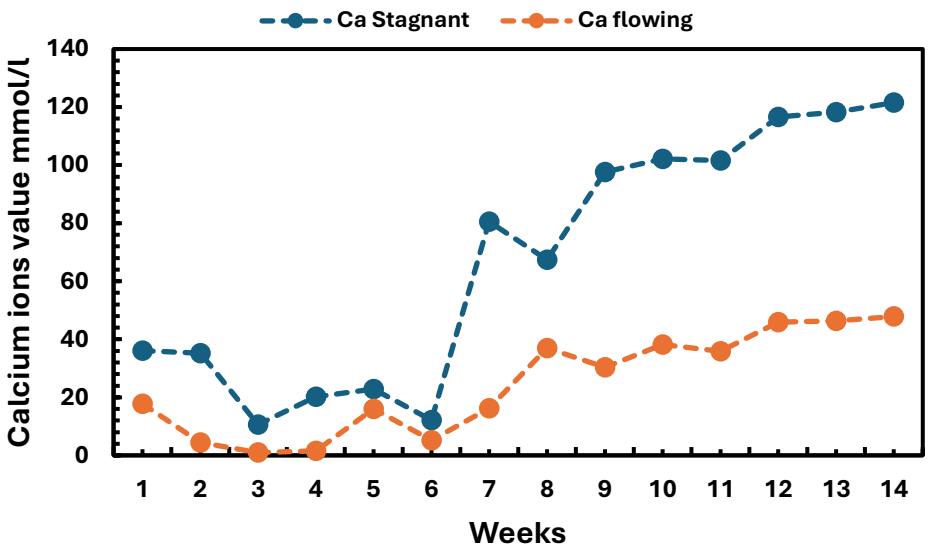

Figure 39: Calcium ions result under different water conditions

4.4.1.2 Impact of 15-25% Fly Ash on pH, Electrical Conductivity, and Calcium Ion Levels in Concrete Solutions

Figure 40 presents three measurements: group pH1 represents plain mortar; group pH2 contains 15% fly ash (FA) as a partial replacement for Portland cement; and group pH3 includes 25% FA. After 28 days of standard curing, the pH of group pH2 is nearly equivalent to that of the control (pH1), indicating that a 15% FA replacement does not significantly affect the material's alkalinity. The only notable pH difference between these groups appeared in the second week, after which both groups displayed a linear trend, likely due to the high proportion of vitreous components and the limited replacement percentage. In contrast, group pH3, which contains a higher amount of FA, exhibited consistently lower pH values compared to groups pH1 and pH2. This difference can be attributed to FA's pozzolanic nature, which facilitates the consumption of calcium hydroxide (CH) crystals during secondary hydration, producing calcium-silicate-hydrate (C-S-H) gels and other by-products. Given the weakly alkaline nature of C-S-H gels and the reduction in CH, the basicity of the concrete further decreases. Analysis indicates that pH discrepancies within group pH3 are considerably lower than those observed in groups pH1 and pH2. This study concludes that adding FA alters the distribution of hydration products within the concrete matrix, resulting in a redistribution of alkalinity. The lower pH in group pH3, as compared to other groups, is due to FA's prolonged reaction period following the hydration process, which reduces the amount of portlandite in the cement matrix. Consequently, the pH of the pore solution decreases, particularly after portlandite is depleted. As FA reactions proceed more slowly than those in conventional cement, the pH values of both FA-containing groups (pH2 and pH3) declined in the second week, from 12.26 to 11.30 for the 15% FA replacement and from 12.12 to 11.29 for the 25% replacement. This trend aligns with findings from similar research, such as that of Nielsen *et al.* (2019b), which also observed accelerated pH reduction with increasing FA content and hydration time. Additionally, another study by Nielsen *et al.* (2019a) reported that increasing FA content and hydration time reduced pH from above 11 to below 10, which facilitated microbial growth—a beneficial outcome for bio-concrete applications. Increased FA substitution in cement correlates with lower pH and enhanced bacterial activity, indicating that a higher FA content could support bio-concrete processes by creating a more favourable environment for microbial activity.

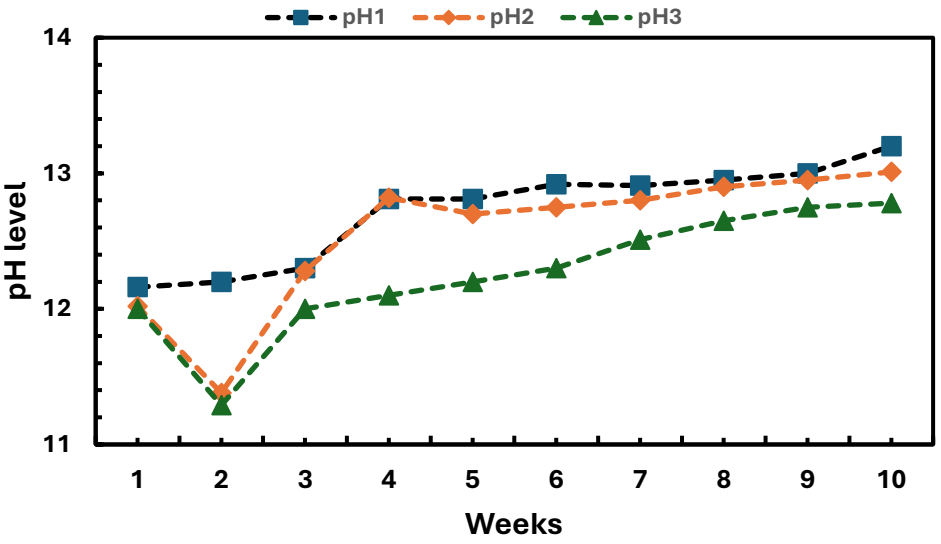

Figure 40: pH results with different type of cement

Salinity, defined as the concentration of all dissolved salts in an alkaline solution, contributes to a solution's electrical conductivity (EC), or its ability to conduct electric current. This parameter remains under-researched regarding its influence on conductivity and salinity in alkaline environments, particularly in bacterial concrete technology, resulting in a limited body of literature in this area. The electrical conductivity of concrete serves as an indirect measure of its salinity, with salinity influencing concrete durability and bacterial growth on its surface. In an ion-containing solution (such as one with dissolved salts), EC increases in response to the presence of ions. In the absence of salts, however, EC remains low, indicating poor conductivity. Factors such as cement type, concrete porosity, and water flow over the concrete surface further influence salt dynamics at the concrete interface. Figure 41 presents three sets of EC measurements: EC1 represents plain mortar; EC2 represents a 15% fly ash (FA) replacement of Portland cement; and EC3 represents a 25% FA replacement. Results indicate an increase in EC for group EC1, while group EC2, with 15% FA, exhibited the highest EC values, and group EC3, with 25% FA, showed the lowest. Significant differences in EC values were observed across all mixes. The lower ion presence in group EC3 is consistent with literature suggesting that high FA content reduces concrete porosity, thus limiting ion movement through the concrete matrix and into the solution. From the eighth week onward, EC values across all mixes began to decline, with group EC3 recording the lowest EC value throughout the measurement period. These findings align with those of Ch Madhavi and Annamalai (2016), who reported that conductivity and salinity increase with rising pH levels. A notable shift in EC values was observed in all groups from the first to the seventh week, underscoring the impact of FA content and curing time on the ionic conductivity of concrete.

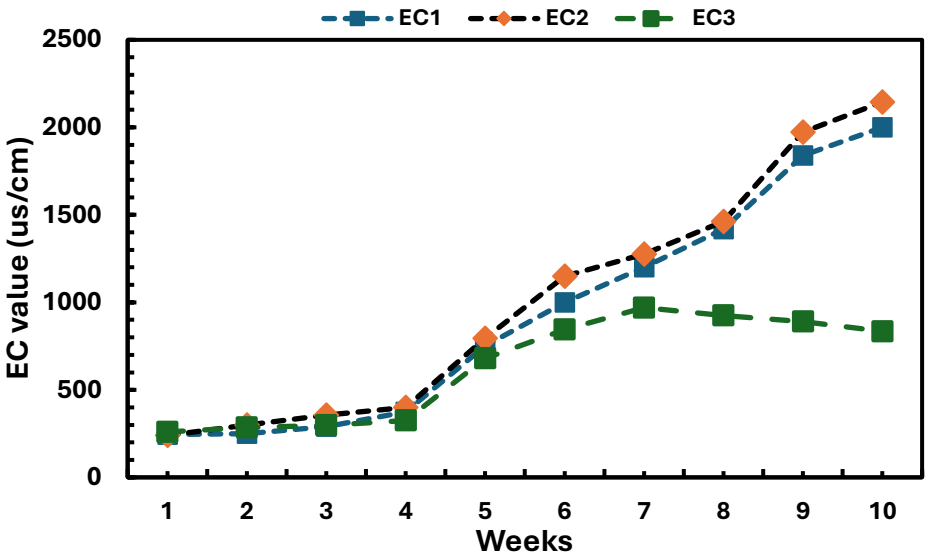

Figure 41: Electrical conductivity results of different types of cement

Figure 42 shows the results of calcium ion concentration measurements for three groups of mortar samples over a 10-week period. The first group, C1, is plain mortar with no-fly ash (FA); the second group, C2, contains Portland cement with 15% FA replacement; and the third group, C3, includes Portland cement with 25% FA replacement. Because the calcium ion concentrations were very high, they couldn't be measured directly using the Perkin Elmer device. To address this, the samples were diluted in volumetric flasks to obtain accurate readings. The results clearly demonstrate the effect of FA content on calcium ion leaching. As shown in figure below, higher FA replacement levels resulted in lower calcium ion concentrations. For example, the concentration in C2 (15% FA) was higher than in C3 (25% FA). During the initial stages of leaching, C1 (0% FA) had much higher calcium ion leaching compared to the samples with FA. This lower concentration in C3 can be explained by the way FA reduces the porosity of the concrete. With lower porosity, it becomes harder for calcium ions to migrate from the interior to the surface. This highlights how using FA, especially at higher levels, helps reduce calcium ion leaching and contributes to the durability of the material. Extensive research supports the role of supplementary materials in reducing concrete porosity. For example, Cheng *et al.* (2013) found that mineral admixtures decreased calcium hydroxide content and refined pore structures through pozzolanic reactions, thus enhancing compressive strength and durability of cement-based materials. His observations further noted that specimens with mineral admixtures demonstrated reduced porosity, contributing to improved durability. While reduced porosity leads to higher compressive strength, the availability of calcium ions in the leachate is critical for bio-concrete applications. Lower calcium ion release can impact the effectiveness of bacterial self-healing processes, as calcium ions play a key role in supporting microbial activity essential to bio-concrete technology.

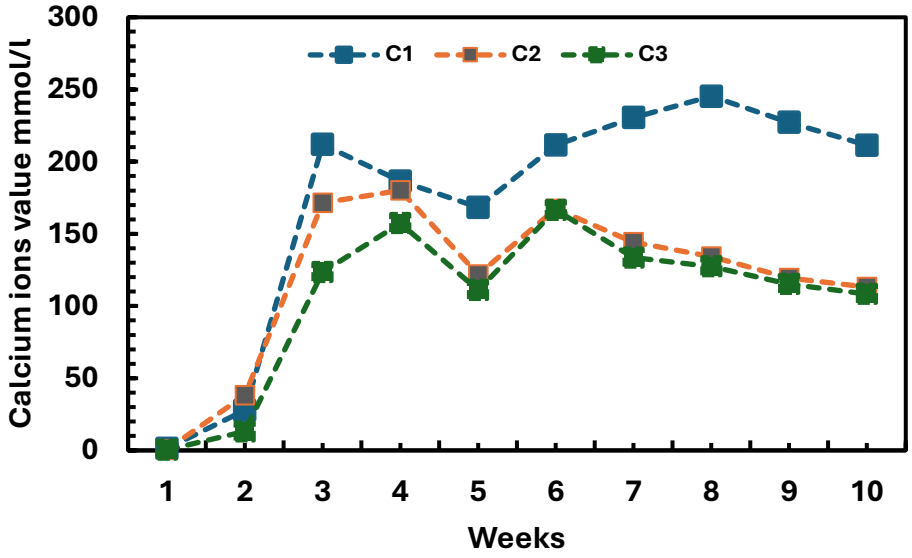

Figure 42: Calcium ions results

4.4.1.3 Effect of 35% GGBS and Fly Ash Replacement on Concrete solution Environment

The pH values of pore water (solution) were both calculated and measured, with results summarized in Figure 43. Analysis of the data reveals a subtle yet notable difference in pH values across samples, particularly in cases where supplementary materials were used at a 35% replacement level. The pH in these samples was significantly lower than that of the pore solution in plain mortar containing only Portland cement, indicating that supplementary materials notably influence the pH values of the pore solution. These pH variations are consistent and closely tied to changes in hydroxide ion (OH^-) concentration, with measurable differences apparent across varying ages of the solution and degrees of substitution. It is important to note that pH values are measured on a logarithmic scale, suggesting a nonlinear relationship between pH levels and their corresponding systemic changes. As (Ortolan, Mancio and Tutikian, 2016) noted, a shift in pH units, such as from 13.6 to 12.6 (observed at 28 days in a 10% silica fume mix), reflects a tenfold reduction in OH^- ion concentration compared to reference specimens. Furthermore, the incorporation of fly ash (FA) in concrete has been associated with maintaining a slightly alkaline pH in the pore solution. This effect arises from the interaction between calcium hydroxide (a by-product of cement hydration) and silica in FA, which react to form calcium silicate hydrate (C-S-H) gel. This C-S-H gel formation has been observed to enhance the alkalinity of the pore solution. Similarly, ground granulated blast furnace slag (GGBFS) also contributes alkaline properties to the pore solution by reacting with calcium hydroxide to produce additional C-S-H gel, thereby increasing solution alkalinity. The extent to which supplementary materials impact pH is influenced by variables such as the material's composition and fineness, types of cementitious materials used, and the water-to-cement ratio. Additionally, factors including carbonation and exposure to external chemicals can further affect the pore solution pH in concrete, introducing additional variability to the system's alkalinity.

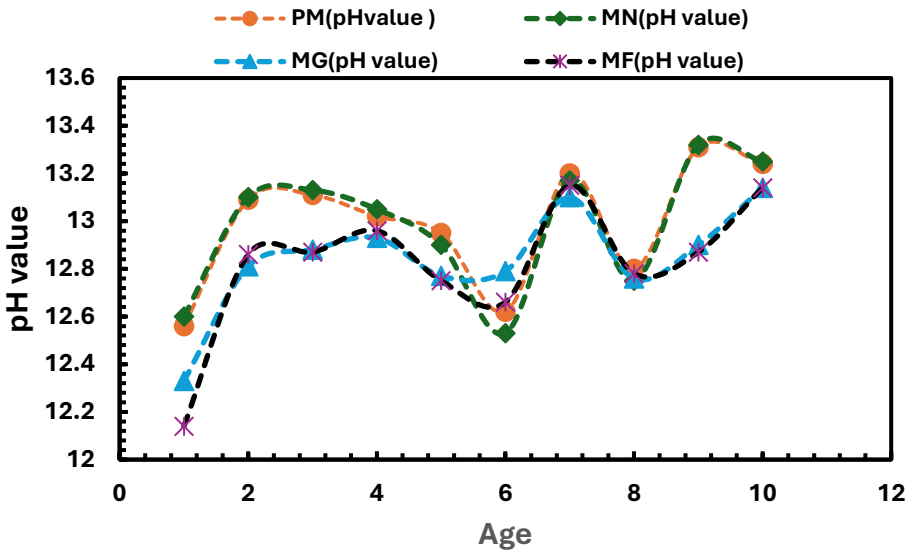

Figure 43: pH results %35 replacement of cement

4.4.1.4 Effect of 50% GGBS and Fly Ash Replacement on Concrete solution Environment

The pH values of the pore water were computed and measured, with the summarized results presented in Figure 44. An analysis of the data indicates a slight disparity in the pH values obtained from the pore solution measurements. Notably, samples with a 50% replacement of supplementary materials exhibited a significant decrease in pH values compared to those observed in the pore solution of plain mortar, which contains only Portland cement. This observation suggests a notable influence of supplementary materials on the pH levels. The consistent variations in pH can be attributed to significant fluctuations in hydroxide ion (OH^-) concentrations, which depend on both the age of the solution and the degree of substitution. It is essential to highlight that pH values adhere to a logarithmic scale, indicating a nonlinear relationship between the measured pH values and the corresponding changes within the system. Ground granulated blast-furnace slag (GGBFS) contributes alkaline properties to the concrete pore solution, facilitating the generation of additional calcium silicate hydrate (C-S-H) gel through its reaction with calcium hydroxide, thereby enhancing the solution's alkalinity. However, it is important to recognize that the specific effects of supplementary materials on pH may vary based on factors such as material composition, fineness, types of cementitious substances utilized, and the water-to-cement ratio. Additionally, external factors, including carbonation and the presence of various chemicals, can further influence the pH of the concrete pore solution. To evaluate the impact of different cement types on mortar surfaces, carbonation levels on various surfaces were assessed over a 28-day period. This investigation underscores the complex interplay of factors that affect the pH and chemical environment of concrete, highlighting the importance of understanding these dynamics in concrete technology.

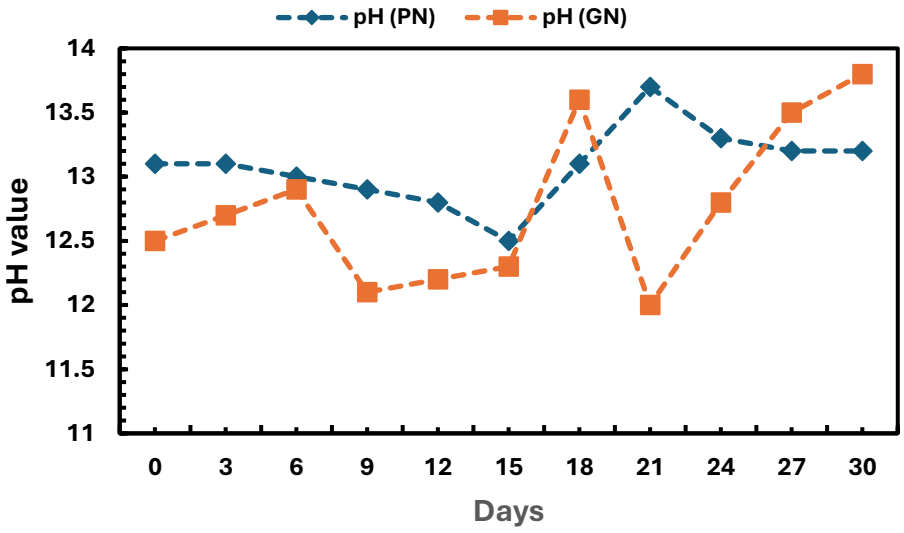

Figure 44: pH results for different type of cement

4.4.1.5 Impact of Carbonation on the pH Value of Concrete solution

This study examined two types of mortar specimens: plain mortar (PM), made without any additional materials, and mortar with ground granulated blast-furnace slag (GGBS) as a partial replacement for Portland cement, referred to as PG. The pH levels of the samples were measured after 7 days of water curing in both normal water and carbonated water. The results are shown in Figure 45, Figure 46, and Table 6. The specimens immersed in carbonated water underwent an additional hydration phase involving immersion in regular water for three days. For samples cured solely in normal water, the pH values differed slightly between PM and PG. Specifically, the plain mortar displayed higher pH values than the GGBS-replaced mortar. After two hours of curing in normal water, the PM samples exhibited high alkalinity, with pH values between 12.60 and 12.35. Conversely, at two hours in carbonated water, the pH values of PM and PG samples measured 6.44 and 6.39, respectively. The increased calcite content in PG samples (as demonstrated in Fig. 47) may have acted as a buffer within the carbonated water environment. Notably, the pH values of both PM and PG samples cured in normal water were consistently higher than those cured in carbonated water. However, according to the hydration mechanisms of cementitious materials, the pH of the pore solution experiences a rapid increase when in contact with water.

Within the first 24 hours, a substantial increase in pH levels was noted, particularly in specimens submerged in carbonated water. This increases likely results from the depletion of dissolved gases due to carbonation, subsequently neutralizing the carbonated water's acidity. In general, carbonation in concrete occurs as atmospheric carbon dioxide permeates the porous concrete matrix, where it reacts with calcium hydroxide ($Ca(OH)_2$) to form calcium carbonate ($CaCO_3$) (Gadd & Dyer, 2017). This interaction also promotes the transformation of calcium hydroxide into calcium carbonate, leading to slight volumetric shrinkage (Dhami et al., 2013). Elevated carbon dioxide concentrations in the carbonated water, introduced directly into containers, triggered a reaction with calcium hydroxide within the concrete, consequently reducing pH levels. This pH reduction could create a favourable environment for bacterial growth; however, this reaction also diminishes the available calcium ions, which are essential for bio-concrete applications. To mitigate the depletion of calcium ions, two strategies can be

considered: utilizing groundwater with a high calcium content or supplementing calcium directly within the concrete mixture.

Numerous studies have explored the intricate mechanisms underlying the formation of calcium carbonate-based materials (CBM) under conditions of carbon dioxide (CO_2) exposure and low pH, such as that found in carbonated water. This complex reaction has drawn considerable interest due to its multi-faceted properties (Chandra & Ravitheja, 2019). When used as a curing agent, carbonated water has been shown to reduce both the pH of the curing solution and the concrete surface. However, this decrease in pH results in a concurrent reduction in calcium release from the concrete, a factor crucial for bio-concrete technology. Furthermore, curing in carbonated water has shown a tendency to enhance porosity within the matrix. These findings underscore the significant effects of carbonated water on pH reduction, surface properties, and its potential to increase porosity during the curing process.

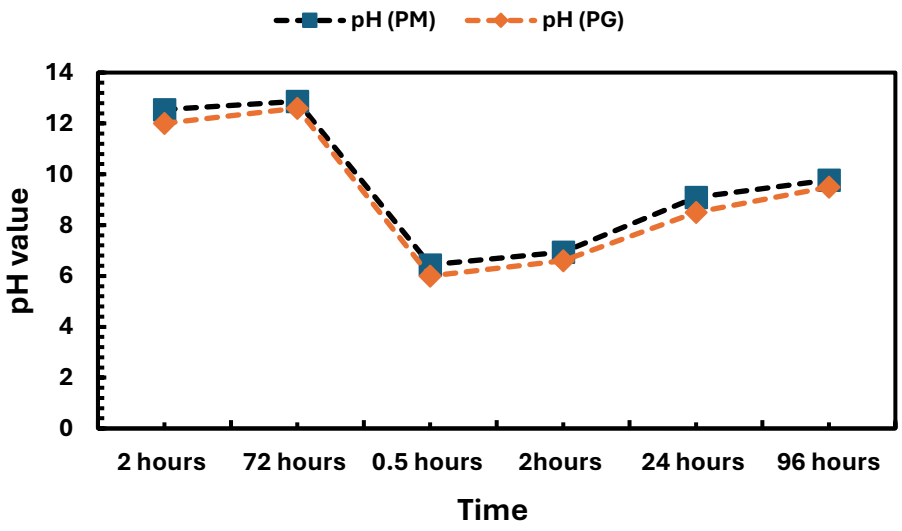

Figure 45: pH value Plain mortar and GGBS cement replacement immersed in carbonated water.

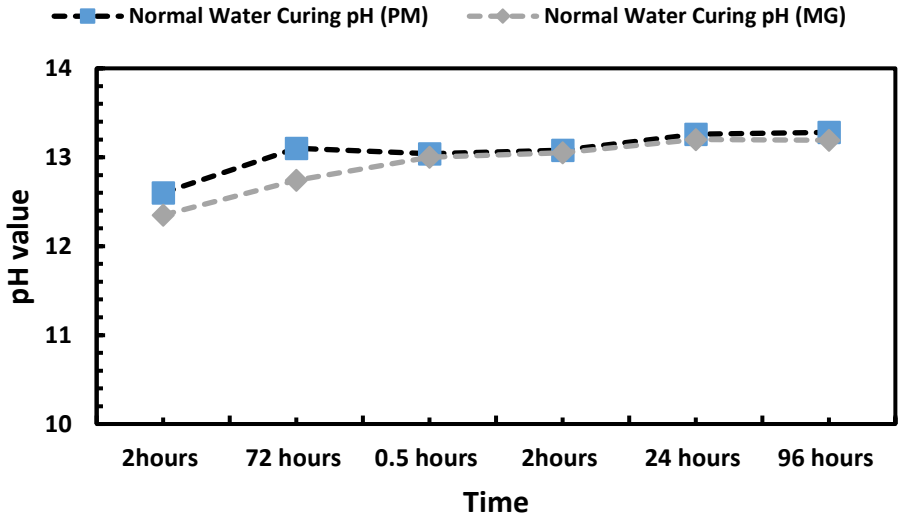

Figure 46: pH for plain mortar and GGBS cement replacement immersed in normal water.

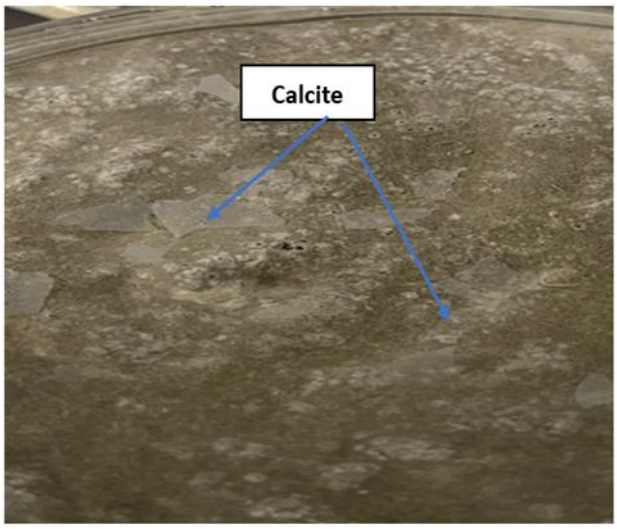

Figure 47: Calcite on the surface of GGBS mortar

Table 6: The results of the pH for all mixes

Time	Normal Water Curing pH (PM)	Carbonated Curing pH (PM)	Normal Water Curing pH (MG)	Carbonated Curing pH (MG)
2hours	12.60	12.55	12.2	12.3
72 hours	13.10	12.87	12.50	12.4
0.5 hour	13.04	6.44	12.70	5.8
2 hours	13.08	6.94	12.9	6
24 hours	13.26	9.10	12.97	8.5
96 hours	13.28	9.78	13	9

4.4.2 Chemical investigation on the surface

4.4.2.1 pH Value Calibration Using ImageJ Software

The images in figure 48 and table 7 illustrate how pH levels relate to the percentage of red coloration (Red%). The pH was first measured using a pH probe, and then the red intensity in the samples was analysed using ImageJ software after applying a phenolphthalein solution. Phenolphthalein is a pH indicator that changes colour depending on the pH level but remains colourless when the pH is below 8. For the tested samples (images 1 to 5), the pH ranged from 5 to 7.80, gradually increasing with each addition of NaOH. When the pH reached 8.44, the solution turned a light purple, and as the pH continued to rise, the colour deepened to a darker purple. These changes were both visually observed and measured. The Red% data from ImageJ was not detailed enough to provide reliable measurements for pH values between 5.00 and 7.80. However, it became more reliable for pH values between 8.44 and 12.63. By analysing the RGB values of the images in ImageJ, the proportion of red in the solution was measured and linked to the corresponding pH levels. As the pH increased, the solution gradually darkened. This colour change was then used to create a graph in Excel, illustrating the relationship

between pH and Red%. Figure 49 and the accompanying table clearly show a strong connection between pH levels and red colour intensity.

 *image 1(pH 5)*	 *image 2 (pH 5.59)*	 *image 3 (pH 6.65)*
 *image 4 (pH 7.13)*	 *image 5 (pH 7.80)*	 *image 6 (pH 8.44)*
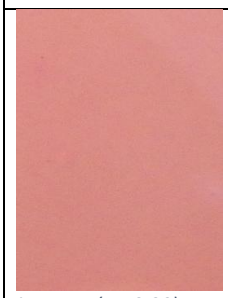 *image 7 (pH 9.20)*	 *image 8 (pH 10)*	 *image 9 (pH 10.55)*
 *image 10 (pH 11.15)*	 *image 11 (pH 11.70)*	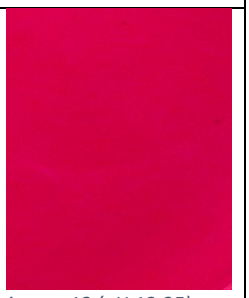 *image 12 (pH 12.25)*
	 *image 13 (pH 12.63)*	

Figure 48: pH value

Table 7: pH value and Red %

Image	pH	Red %
1	5.00	40.4
2	5.59	40.7
3	6.65	40.8
4	7.10	41.0
5	7.80	40.7
6	8.44	37.8
7	9.20	44.2
8	10.00	64.2
9	10.50	69.6
10	11.10	72.9
11	11.70	74.2
12	12.20	75.1
13	12.60	75.1

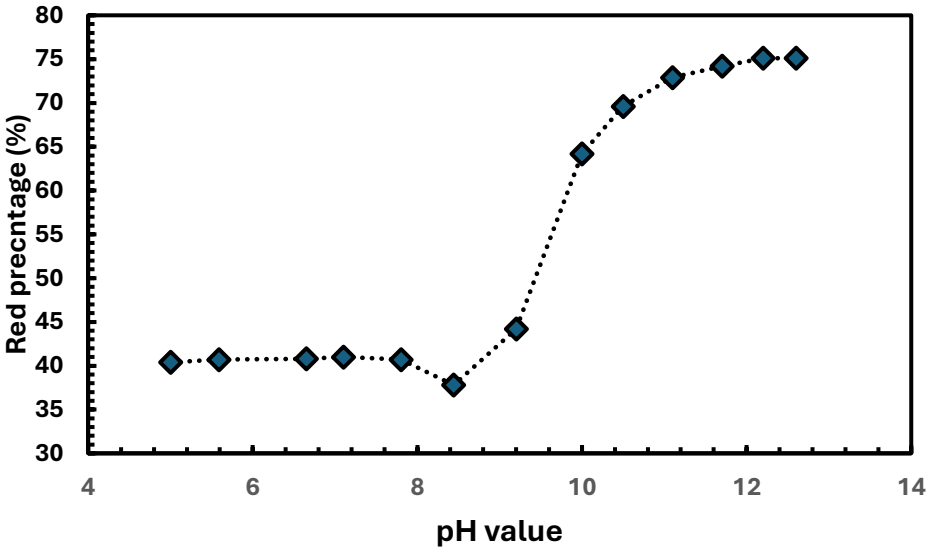

Figure 49: The relationship between Red % and pH value

The universal indicator covers a much broader pH range and shows more distinct colour transitions compared to phenolphthalein, as shown in Figure 50 and table 8. While phenolphthalein only changes from colourless to light or dark purple within a narrower pH range of approximately 8 to 14, the universal indicator provides clearer distinctions across a wider range. The images below illustrate the gradual colour changes that occurred with each addition of sodium hydroxide. With the universal indicator, even the first image, which represents carbonated water as the starting point, shows a visible pH change through a colour shift. Each step from pH 5 to 10 resulted in a distinct colour change, making it easy to differentiate between levels. However, at pH values above 10, the colour remained stable, as seen in images 10, 11, and 12. These images were analysed using ImageJ software to measure the percentages of red and blue in the solution. The colour transitions closely followed changes in pH, and Equations 6 and 7 were used to quantify this relationship. In images 1 to 3, the blue percentage fluctuated slightly due to a lower average blue intensity. However, from images 4 to 12, a clear pattern emerged: as the pH increased, so did the blue percentage, highlighting a strong correlation between pH and colour intensity. In contrast, the red and green percentages did not follow a

clear pattern with pH changes. Both started at higher values but gradually decreased as the solution's colour shifted to purple. For example, in images 1 to 5, the red and green values were initially high but dropped as the pH increased, reflecting the visible transition to a purple hue. Figure 51 illustrates the relationship between pH values and the red, green, and blue percentage values.

Figure 50: pH value with different image colour

Table 8: RGB percentage value and pH value

Image	pH	B%	R%	G%
1	5.00	9.92	60.00	29.00
2	5.54	8.66	55.00	36.00
3	6.57	8.45	53.00	38.00
4	7.25	9.05	51.00	39.00
5	7.90	10.33	49.00	39.98
6	8.60	12.90	46.50	40.50
7	9.25	28.30	34.00	37.40
8	9.50	34.48	32.00	33.00
9	9.95	44.57	34.00	24.80
10	10.35	45.06	36.00	18.50
11	11.40	48.70	37.00	13.40
12	12.40	48.20	38.00	14.00

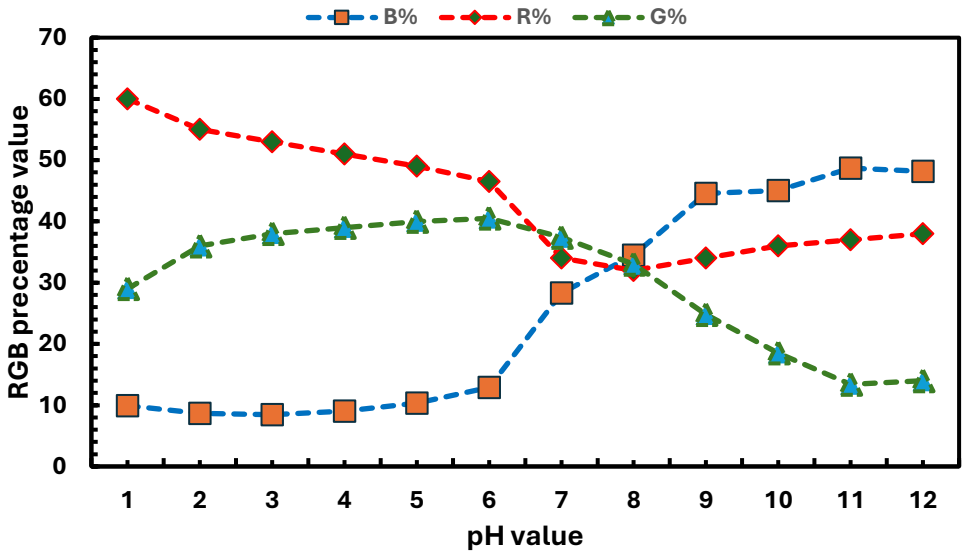

Figure 51: The relationship between red, blue and green % with pH values

4.4.2.2 Application of Phenolphthalein Solution and Universal Indicator on Concrete Surfaces

Figure 52 shows how the prisms reacted to phenolphthalein and a universal indicator, revealing different patterns of colour change based on pH levels. The prism treated with phenolphthalein consistently turned pink, with darker shades indicating higher pH levels and lighter shades reflecting lower pH values. Since phenolphthalein only changes colour at pH levels above 8 (Sandaruwan *et al.*, 2024), it provides a simple and effective way to detect pH changes in an alkaline environment. On the other hand, the prism treated with a universal indicator displayed a more complex colour pattern, with multiple shades appearing across its surface. This variation suggests that different pH levels exist within the concrete matrix, which could be useful for applications like self-healing concrete, where localized pH differences may support microbial activity essential for calcium carbonate precipitation. However, the universal indicator's multi-coloured response can be somewhat ambiguous, making it difficult to visually pinpoint precise pH values without further analysis. These results highlight the advantages of both indicators: phenolphthalein offers a clear and straightforward response in high-pH environments, while the universal indicator provides a more detailed pH map across the concrete surface, though with less visual clarity.

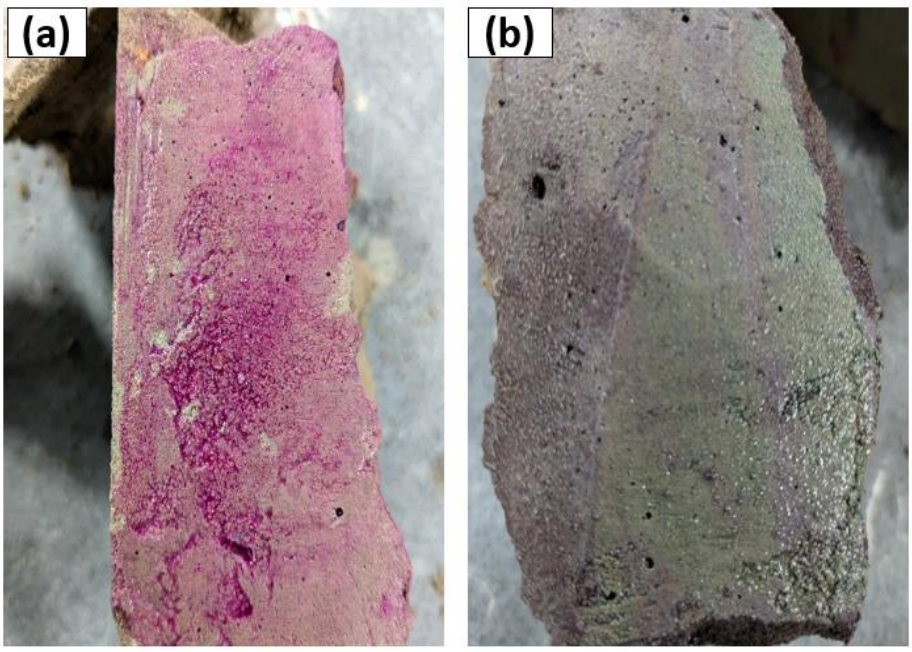

Figure 52: (a) Phenolphthalein indicator on mortar surface. (b) Universal indicator on mortar surface

4.4.2.3 The effect of supplementary materials on concrete surface

This phase utilized various types of cement, including ground granulated blast furnace slag (GGBS) and fly ash, as partial replacements for Portland cement at replacement levels ranging from 15% to 50%. Each percentage had a distinct impact on the concrete surface. Analysis of the data from the figures reveals slight variations in pH values derived from pore solution measurements. A notable correlation was observed between darker purple shades and higher pH values, with darker coloration appearing in both plain mortar and plain mortar with nutrient additives. Further evaluation of pH values was conducted using the ImageJ software, following the methodology described by Li et al. (1998). The specimen surface images were analysed for

their RGB values using ImageJ software. The percentage of the red component was determined using Equation (5), with the results summarized in Tables 9 and 10.

Previous pH measurements using a probe showed that adding fly ash affected the pH levels of the samples. The results suggest that supplementary cementitious materials (SCMs), especially fly ash used to replace part of the Portland cement, increased surface carbonation, as seen in Figure 54. Mortar cubes with 25% fly ash replacement showed the most carbonation, while those without any fly ash had no carbonation at all. It's worth mentioning that these cubes were freshly made, and the phenolphthalein solution was applied after about 20 weeks, giving their surfaces a light pink colour—an indication of carbonation. On the other hand, Figure 55 shows that samples with 35% supplementary material replacement had a noticeable drop in pH compared to the plain mortar, which only contained Portland cement. This highlights how SCMs can influence the pH of the pore solution, largely due to changes in hydroxide ion (OH^-) concentration. These changes depend on both the age of the mix and how much cement has been replaced. Since pH is measured on a logarithmic scale, even small changes can have a big impact, making the relationship between pH and the system's behaviour nonlinear. Ground granulated blast-furnace slag (GGBS), for example, boosts the alkalinity of the pore solution by reacting with calcium hydroxide to form more calcium-silicate-hydrate (C-S-H) gel, which helps maintain higher pH levels. However, the exact effect of these supplementary materials on pH can vary depending on factors like their composition, fineness, the type of cement used, and the water-to-cement ratio. External factors, such as carbonation and exposure to chemicals, can also play a role in altering the pH of the concrete's pore solution.

Table 9: The results of red percentage value

Images	Red %
Image 1(FA %25)	36.7
Image 2 (FA %15)	37.2
Image 3 (Plain)	39.8

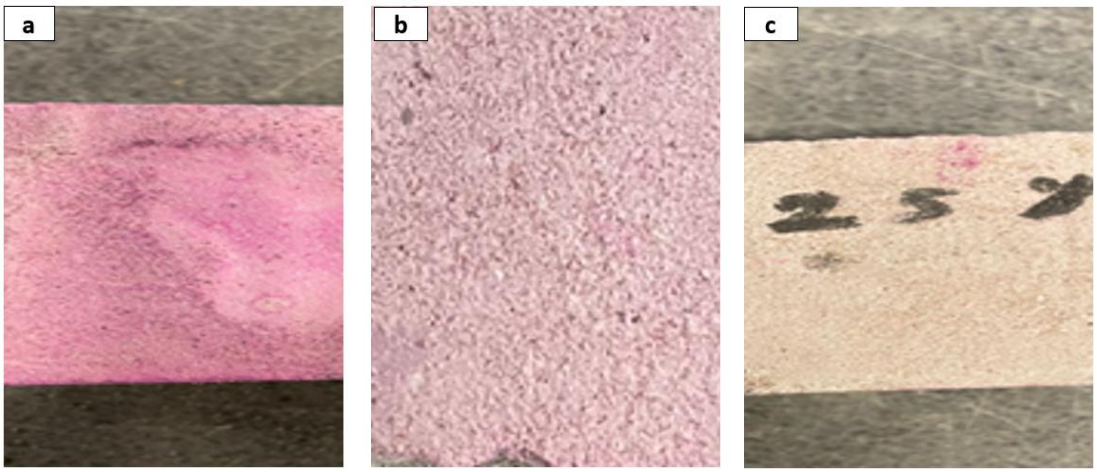

Figure 53: (a) Plain mortar. (b) Mortar with 15% fly ash replacement by weight of cement. (c) Mortar with 25% fly ash replacement by weight of cement.

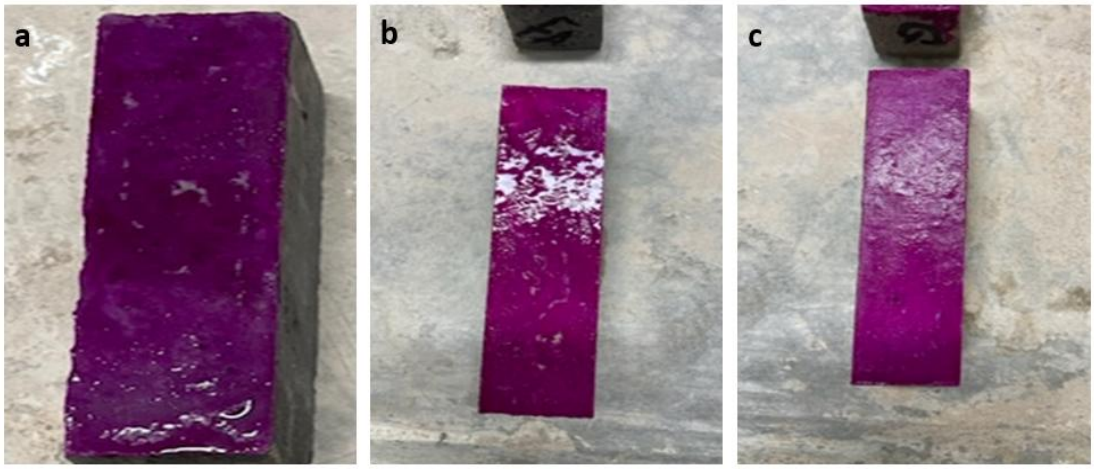

Figure 54: a) Plain mortar specimens sprayed with a Phenolphthalein indicator. (b) Mortar specimens containing 35% ground granulated blast-furnace slag (GGBS) replacement, sprayed with a Phenolphthalein indicator. (c) Mortar specimens containing 35% fly ash replacement, sprayed with a Phenolphthalein indicator.

Table 10: The results of Red % value

Images	Red %
Image 1(FA)	41
Image 2 (GGBS)	66
Image 3 (Plain)	98

4.4.2.4 The effect of flowing water on chemical environments of concrete surface

This study explored three types of mortar samples: plain mortar, mortar with ground granulated blast-furnace slag (GGBS) as a partial replacement, and mortar with fly ash (FA) as a replacement. To measure the carbonation depth on the surface of these samples, phenolphthalein spray was applied—a common technique for detecting carbonation in cement-based materials (Papadakis *et al.*, 1991). The main aim was to understand how the combination of water flow and supplementary materials affects carbonation behaviour, and whether these conditions could create an environment that supports soil bacteria, potentially paving the way for bio-concrete technologies in underground concrete structures. The results, shown in Figure 55, highlight how different water conditions impact carbonation in the mortar samples. One key observation was that samples kept in stagnant water consistently had higher pH levels compared to those exposed to flowing water. This difference comes down to the setup of the hydraulic bench, where the water in contact with the flowing samples was refreshed daily, simulating more dynamic conditions. Early in the experiment, the flowing water caused a faster leaching of alkalis from the inner core of the mortar due to its interaction with the bonding matrix. This leaching led to a noticeable drop in pH levels in the samples exposed to flowing water, a trend that aligns with earlier studies showing how water flow can affect the durability and chemical stability of concrete (Wang *et al.*, 2019). The images clearly illustrate this process,

showing how the combination of water exposure and the mortar composition affects the depth of carbonation. These findings provide valuable insights into how mortar behaves under different environmental conditions, particularly in relation to bio-concrete applications. Understanding the role of water flow in changing the chemical environment of concrete is essential for improving self-healing and bio-enhanced concrete technologies, especially for underground structures where moisture conditions can vary significantly

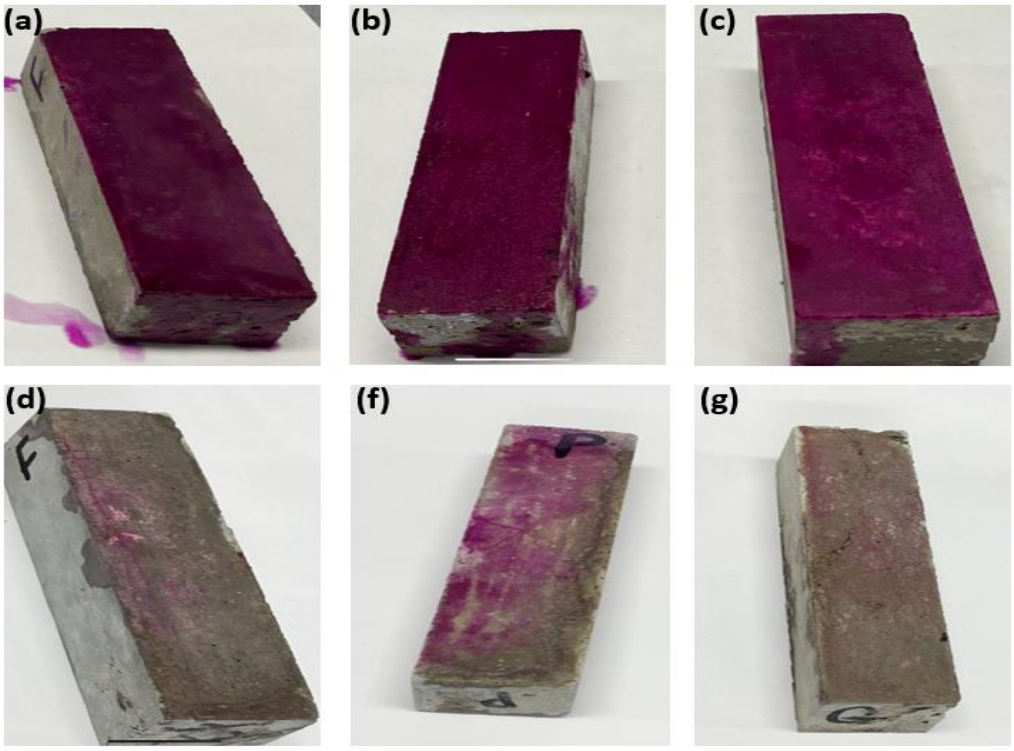

Figure 55: (a), (b), and (c) represent prisms composed of different types of cement exposed to a non-flowing water system, while (d), (f), and (g) depict prisms with varying cement types subjected to a flowing water system.

4.4.2.5 The effect of carbonation on concrete surface

Figures 56, 57, and 58 show how carbonation affected the surfaces of two different mortar mixes, tested after curing for 7 days. Phenolphthalein solution was used as an indicator to visualize the carbonation process. In these images, the non-carbonated areas appear purple, with lighter shades indicating lower pH levels, while darker shades represent areas with higher alkalinity. There were clear differences in colour intensity and brightness between samples cured in carbonated water and those cured in regular water, reflecting how carbonation progressed under different conditions. It's well-documented that carbonation can reduce the alkalinity of concrete, which in turn can affect its long-term durability and strength these observations align with the findings of Papadakis *et al.* (1991). In this study, when the samples were cured in regular water, no carbonation was detected at any curing stage. This was likely because the containers were tightly sealed, limiting the exposure to atmospheric carbon dioxide (CO_2), and because regular water contains only a minimal amount of CO_2. However, when carbonated water was used for curing, a thin layer of calcium carbonate formed on the surfaces of both mixes. This highlights the role of carbonated water in speeding up the carbonation process, leading to the formation of calcium carbonate and a noticeable drop in pH levels. These findings are in line with previous studies showing that higher CO_2 concentrations can accelerate carbonation reactions, which in turn alter the chemical

environment inside the concrete by reducing alkalinity (Silva-Castro *et al.*, 2015). The chemical environment within the mortar changed significantly due to carbonation. The drop in pH suggests a shift toward more acidic conditions, which can impact the material's durability over time. Lower pH levels in carbonated areas indicate more acidic conditions, which can compromise the protective layer around steel reinforcements in concrete, increasing the risk of corrosion. Interestingly, both Portland cement and GGBS-based mortars responded similarly to carbonation when cured in carbonated water. This suggests that, under the conditions of this study, the type of cement used did not have a major impact on how quickly or extensively carbonation occurred. This aligns with existing research showing that while supplementary materials like GGBS can affect carbonation, other factors such as curing conditions and environmental exposure play a significant role (Ahmad *et al.*, 2022).

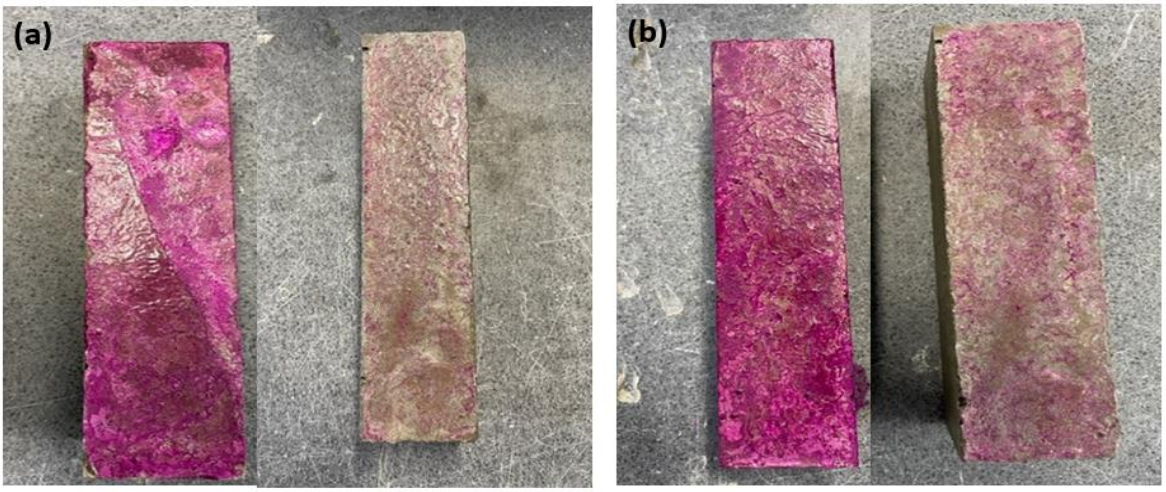

Figure 56: (a) Plain mortar exposure acceleration carbonation process after 30. (b) Plain mortar exposure acceleration carbonation process after 2 hours.

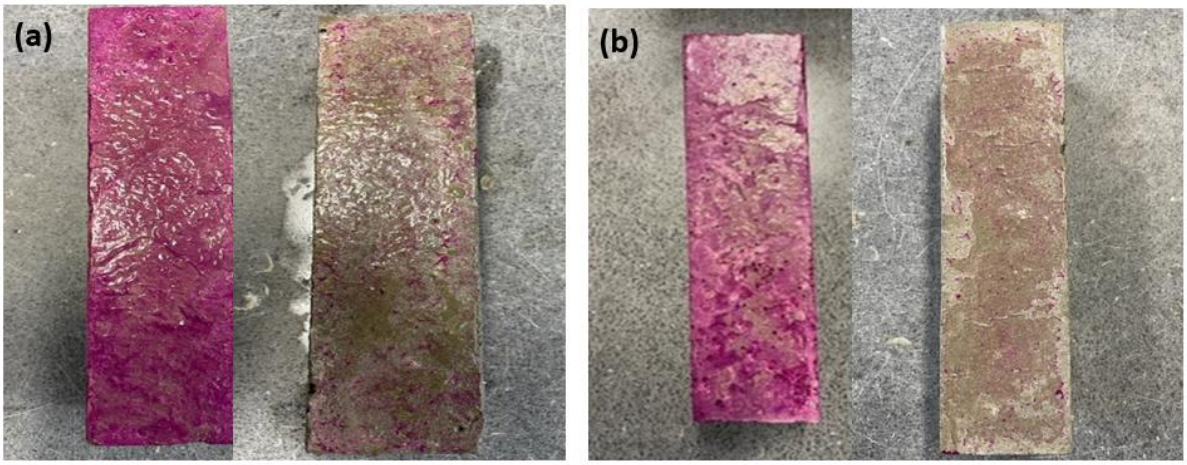

Figure 57: (a) Mortar with 35% ground granulated blast-furnace slag (GGBS) replacement subjected to an accelerated carbonation process for 30 minutes. (b) Mortar with 35% ground granulated blast-furnace slag (GGBS) replacement subjected to an accelerated carbonation process for 2 hours.

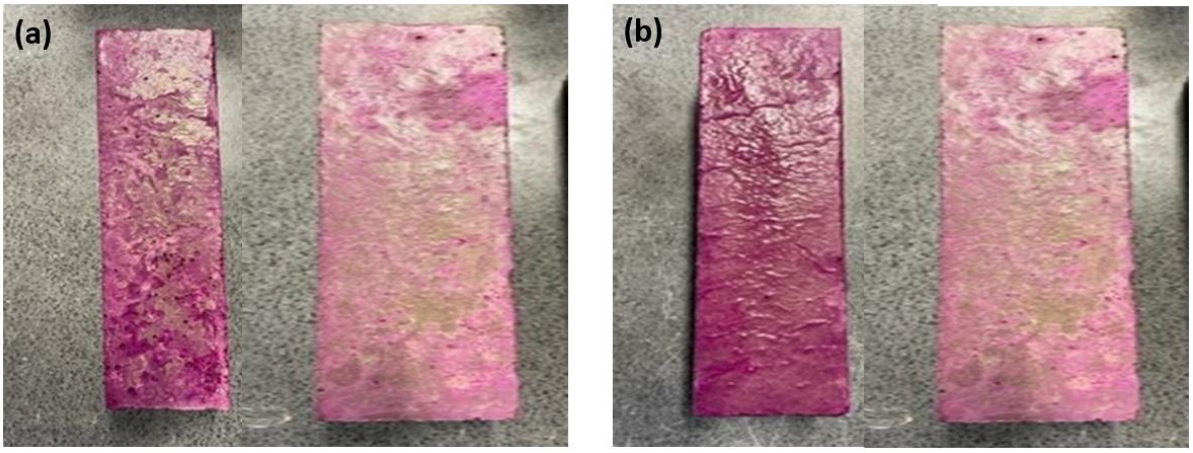

Figure 58: (a) Plain mortar subjected to an accelerated carbonation process for 4 days. (b) Mortar with 35% ground granulated blast-furnace slag (GGBS) replacement subjected to an accelerated carbonation process for 4 days.

4.4.3 Microbiology investigation

4.4.3.1 The Influence of pH on Bacterial Activity

Bacteria are highly sensitive to the pH of their environment, as it directly affects their ability to function and survive. The pH influences everything from how well their enzymes work to the stability of their cell membranes and how effectively they can absorb nutrients. Research shows that most bacteria thrive in a slightly acidic to neutral pH, typically between 6.5 and 7.5. Within this range, their metabolic processes and growth are at their best. However, if the pH moves outside this sweet spot, it can either boost or limit their activity, depending on the specific bacterial species (Luan *et al.*, 2023). Figures 59 and 60 show how bacterial activity changes under different pH conditions. The images in Figure 59 were taken using a microscope, but it was challenging to clearly identify bacterial activity due to the limited clarity of the images. While it was possible to observe bacterial viability under the microscope, additional analysis was carried out using ImageJ software, as shown in Figure 60, to provide clearer insights. This study highlights how even small changes in pH can significantly affect bacterial growth and activity. At lower pH levels, bacteria appeared to thrive, with higher density and more even distribution. This was especially clear in the pH 7 images, where bacterial activity was more concentrated and consistent. However, as the pH increased to 8, bacterial activity started to decline. While clusters of bacteria were still visible, they became larger and more spread out, suggesting that the environment was becoming less favourable. This drop-in activity could be due to enzymes not working as effectively or disruptions in the balance of ions within the bacterial cells. These results emphasize how sensitive bacteria are to changes in pH and how important it is to create the right conditions for their growth and activity (Puchkov, 2016). As the pH continued to rise, bacterial activity dropped further. At pH 9, the number of bacteria was noticeably lower, and their distribution was less uniform, suggesting the bacteria were under stress. By pH 10, growth was clearly restricted, with only sparse and scattered clusters remaining. This was likely due to the enzymes struggling to function and nutrients becoming harder for the bacteria to access. At pH 11, only a few isolated clusters were visible, showing that the high pH was causing severe stress and making it difficult for bacteria to survive (Razmi *et al.*, 2023). By pH 12, bacterial activity had almost completely stopped, as the extreme environment disrupted their ability to function and maintain their cell membranes.

These results show just how sensitive bacteria are to pH changes. As the pH moves further away from neutral, their ability to grow and survive becomes increasingly limited, reinforcing the importance of maintaining the right conditions for bacterial activity.

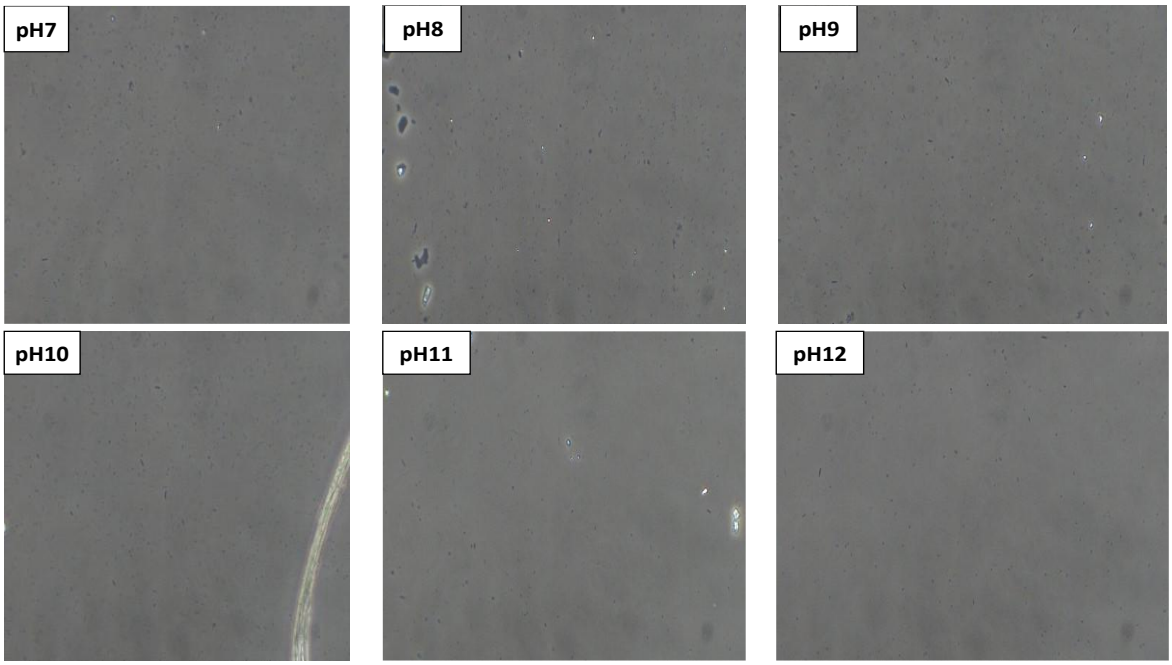

Figure 59: Images of bacteria activity was taken by microscopy.

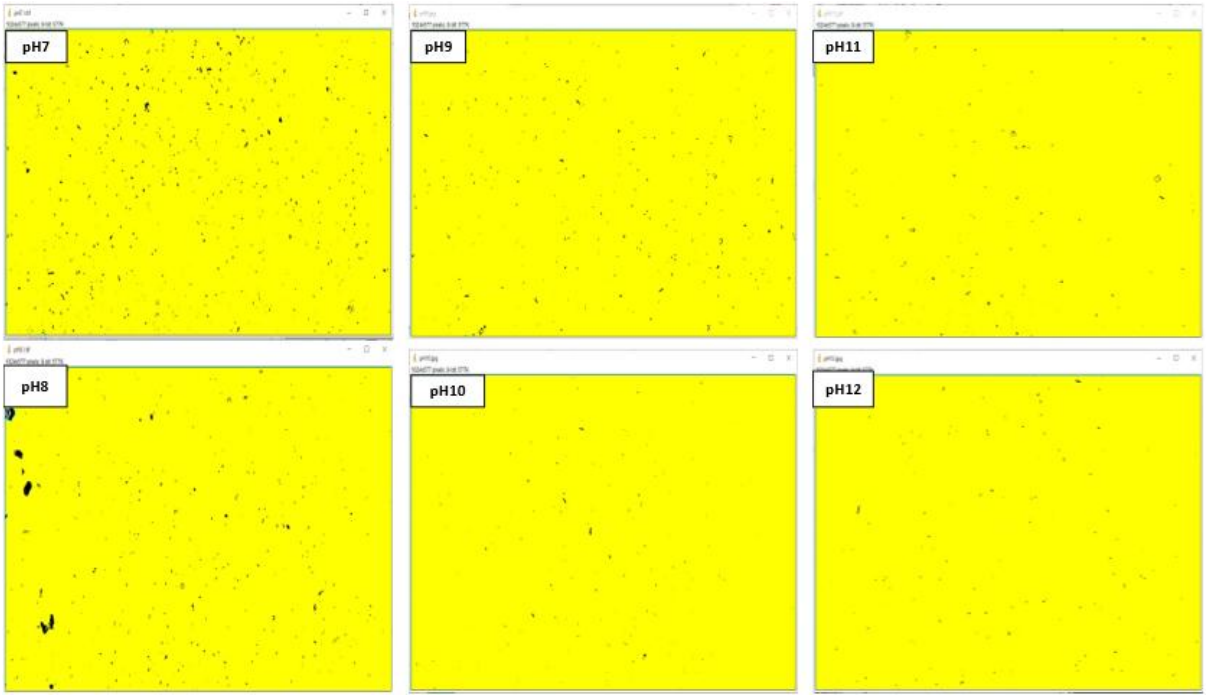

Figure 60: Theses images analysis by ImageJ program

4.4.3.2 Influence of pH Variation on MICP Production in Aqueous Solution (Controlled Experimental Study)

This experiment examined the study's findings, including how pH levels were tracked throughout the process, the crystal formations that were observed, and the analysis of images captured using microscopy techniques. It also included a detailed discussion to further interpret and understand these results.

4.4.3.2.1 pH measurements

Over the six-day measurement period in this study, pH levels were carefully monitored to better understand the conditions that support calcium carbonate crystal formation, as shown in Figure 61 and Table 11. Tracking these changes provided valuable insights into the optimal environment for calcium carbonate precipitation and crystallization. These variations were largely driven by the metabolic activity of *Bacillus subtilis* and the chemical reactions occurring in the surrounding medium. At higher pH levels of 11 and 12, there was a noticeable drop in pH after the first day. This is likely because high pH levels enhance urease enzyme activity, speeding up the breakdown of urea (Matczuk and Siczek, 2021). Initially, the pH may rise slightly as ammonia (NH3) and carbon dioxide (CO2) are produced during the reaction. However, when CO2 reacts with water, it forms carbonic acid (H2CO3), which releases hydrogen ions (H+) and lowers the pH (Doyle et al., 2023). Additionally, at such high pH levels, bacteria may struggle to maintain their metabolic activity due to reduced buffering capacity, leading to further pH fluctuations over time. In contrast, pH levels of 9 and 10 showed a gradual decrease over time. These pH levels are optimal for urease activity, allowing steady urea hydrolysis and consistent production of ammonia and CO2. As Sibhat *et al.*, (2024) explain, ammonia helps maintain a stable pH, but as CO2 forms carbonic acid, a slight drop occurs. Calcium carbonate, which forms during the process, acts as a natural buffer, keeping the pH relatively steady as the system reaches equilibrium. At lower pH levels, such as 7 and 8, the trend was reversed, with pH levels increasing after one day. This is because urease activity is slower at these levels, leading to slower urea hydrolysis. As the reaction progresses, ammonia is released, causing the pH to rise. A similar observation was made in a study by Moraes *et al.* (2017). Additionally, the medium's initial buffering capacity at these lower pH levels is weaker, so the accumulation of ammonia has a more noticeable impact (Yamanaka, 2003). *Bacillus subtilis* also tends to perform better in this pH range, producing by-products that further raise the pH (Park et al., 2022). As a result, at pH levels of 7 and 8, the slower breakdown of urea and reduced buffering capacity allow for a noticeable increase in pH over time.

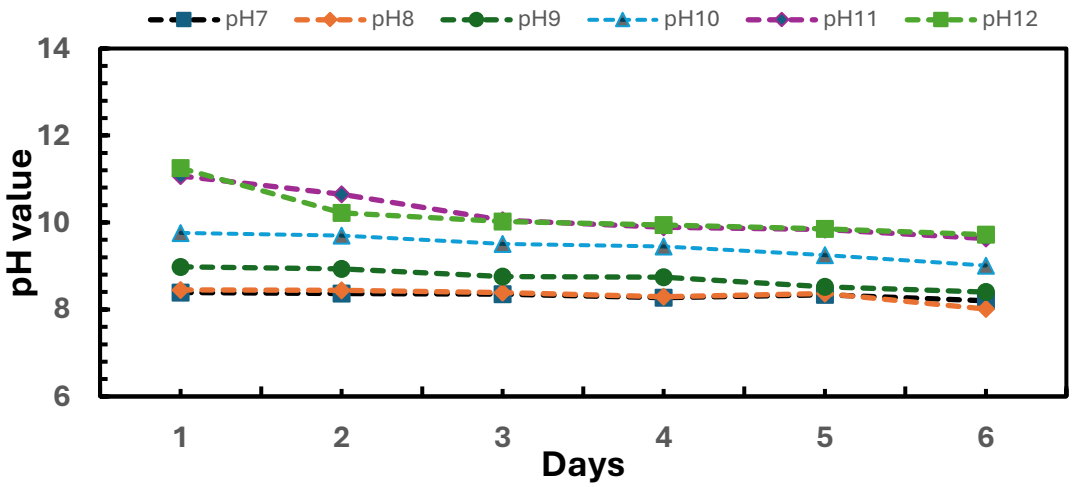

Figure 61: pH results

Table 11: pH results

pH	day 1	day2	day3	day4	day5	day6
pH7	8.39	8.37	8.35	8.27	8.34	8.2
pH8	8.45	8.44	8.39	8.29	8.37	8.01
pH9	8.98	8.93	8.76	8.74	8.52	8.4
pH10	9.76	9.7	9.51	9.45	9.25	9.01
pH11	11.07	10.65	10.05	9.89	9.84	9.63
pH12	11.25	10.22	10.02	9.94	9.85	9.72

4.4.3.2.2 Formation CaCO3 in flasks

Flasks with varying pH levels, as shown in Figure 62—(a) pH 7, (b) pH 8, (c) pH 9, (d) pH 10, (f) pH 11, and (g) pH 12—demonstrated how pH significantly influences the rate of calcium carbonate ($CaCO_3$) precipitation. At pH 7, there was minimal formation of $CaCO_3$. The solution remained mostly clear with very little sediment at the bottom, indicating that only a small amount of precipitation had occurred. This limited $CaCO_3$ formation is likely due to the low activity of urease enzymes at near-neutral pH, resulting in fewer carbonate ions available to react with calcium and form $CaCO_3$. When the pH increased to 8, there was a slight uptick in $CaCO_3$ precipitation. Some sedimentation became visible, suggesting that more crystals were forming. Although urease activity was still relatively low at this pH, it was slightly higher than at pH 7, leading to more urea being broken down and, consequently, more carbonate ions available for precipitation. At pH 9, a significant jump in $CaCO_3$ formation was observed. The solution contained a noticeable amount of sediment, reflecting a much higher density of $CaCO_3$ crystals. This increase is largely due to the urease enzymes performing at their optimal activity level at this pH, which boosts urea hydrolysis and increases the availability of carbonate ions. The trend continued at pH 10, where the flasks showed even more pronounced $CaCO_3$ precipitation. The sediment at the bottom was substantial, indicating a strong and sustained precipitation process. Urease activity remained high, supporting efficient urea breakdown and an accelerated rate of $CaCO_3$ crystal formation. At even higher pH levels—pH 11 and 12—the flasks showed a significant buildup of $CaCO_3$ sediment. The high pH levels supported rapid urea hydrolysis and a large production of carbonate ions, further speeding up $CaCO_3$ formation. While extremely alkaline conditions can eventually inhibit bacterial activity, in the short term, they led to a noticeable increase in $CaCO_3$ precipitation. In addition to the biological activity, the high alkalinity also promoted direct chemical precipitation of $CaCO_3$ due to the increased saturation of carbonate ions in the solution. The overall chemical process driving this precipitation can be summarized in the following reactions:

$$Ca^{2+} + CO_3^{2-} \rightarrow CaCO_3 \quad (8)$$

The hydrolysis of urea also produces ammonia and carbonate ions, which elevate local pH levels further. At such high pH levels, the increased concentration of carbonate ions can lead to the precipitation of CaCO3 directly without any significant bacterial involvement. CaCO3 precipitation may occur via bacterial cells, but chemical precipitation can also occur at elevated pH levels independent of bacteria. A study by (Stocks-Fischer et al., 1999b) demonstrate that chemical precipitation can occur without microbial activity, especially in highly alkaline environments. The considerable CaCO3 precipitation observed at pH 11 and 12 is most likely driven predominantly by chemical reactions. While some urease activity,

potentially from Bacillus subtilis, may still contribute to the precipitation process, the extreme pH levels primarily facilitate precipitation through chemical mechanisms. This analysis highlights the crucial role of pH in regulating urease activity and subsequent CaCO3 precipitation, identifying pH levels 9 and 10 as the most favourable for optimal crystal formation.

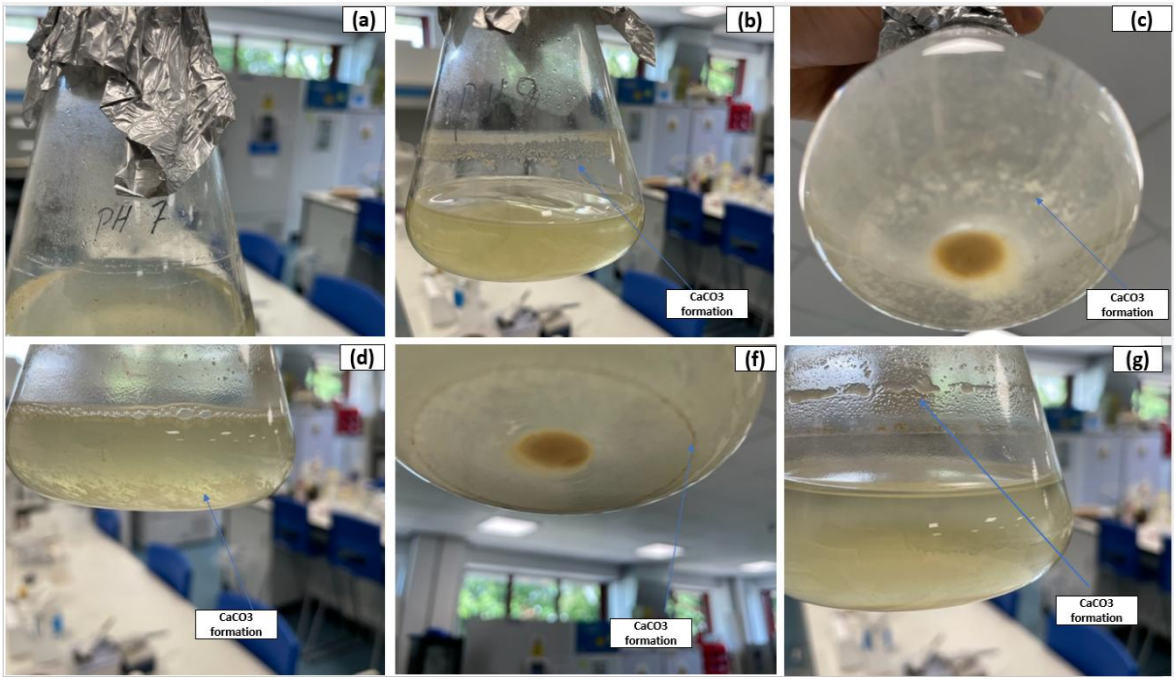

Figure 62: Formation of calcium carbonate ($CaCO_3$) in flasks subjected to varying pH levels (a) pH 7, (b) pH 8, (c) pH 9, (d) pH 10, (f) pH 11, and (g) pH 12.

4.4.3.2.3 Keyence microscopy analysis

The analysis of calcium carbonate (CaCO3) precipitation at various pH levels, as shown in Figure 63, highlights the impact of pH on CaCO3 formation. At pH 7, very few CaCO3 crystals are observed, due to low urease activity which results in minimal urea hydrolysis, reduced ammonia production, and therefore fewer carbonate ions for CaCO3 precipitation. Similarly, at pH 8, only slightly more crystals are present compared to pH 7. Although urease activity is still low, it is somewhat higher than at pH 7, leading to a slight increase in urea hydrolysis and CaCO3 formation. The crystals at this pH are small and dispersed. This finding aligns with the study by (Stocks-Fischer et al., 1999b), which indicated that calcite precipitation is influenced by pH, as urease enzyme activity is specific to certain pH values optimal for urea hydrolysis. Many researchers have reported that the optimal pH for urease is 8.0, above which its activity decreases. At pH 9, there is a significant increase in the number of CaCO3 crystals. Urease activity is optimal at this pH, leading to higher rates of urea hydrolysis and ammonia production, which in turn increases the availability of carbonate ions for CaCO3 formation. The crystals formed are larger and more numerous than those at pH 7 and 8. This trend continues at pH 10, with even larger and more abundant crystals. Urease activity remains optimal, facilitating effective urea hydrolysis. The images show a higher density of crystals, indicating robust CaCO3 precipitation. Other studies also emphasize the importance of high pH for ammonia production via urea hydrolysis. Aerobic bacteria release CO2 through cell respiration, increasing pH due to ammonia production (Ng *et al.*, 2012) . If the pH is too low, carbonate tends to dissolve rather

than precipitate (Lowenthal et al., 1976) . Most calcite precipitation occurs under alkaline conditions between pH 8.7 and 9.5 (Stocks-Fischer et al., 1999b).

At pH 11 and 12, there is a marked increase in both the size and number of CaCO3 crystals. Urease activity is very high at these pH levels, leading to rapid urea hydrolysis and significant ammonia and carbonate ion production. However, such high pH levels may begin to inhibit bacterial activity, although the immediate effect remains a high rate of CaCO3 formation. (Stocks-Fischer et al.,1999b) compared the efficiency of microbially induced CaCO3 precipitation with chemically induced precipitation at pH 9.0, confirming that 98% of initial Ca2+ concentrations were precipitated microbially, compared to only 35% and 54% chemically in water and medium, respectively. This difference occurs because bacterial cells provide nucleation sites for CaCO3 precipitation and create an alkaline environment conducive to further calcite growth (Stocks-Fischer et al., 1999b). In this study, pH levels of 9 and 10 exhibit the most efficient CaCO3 precipitation, striking a balance between high urease activity and stable bacterial metabolic function. Although pH levels of 11 and 12 initially show significant crystal formation, the extremely high pH might affect the chemical reactions involved. In contrast, pH levels of 7 and 8, marked by lower urease activity, lead to fewer and smaller CaCO3 crystals. This analysis highlights the crucial role of pH in regulating urease activity and subsequent CaCO3 precipitation, identifying pH levels of 9 and 10 as the most favourable for optimal crystal formation.

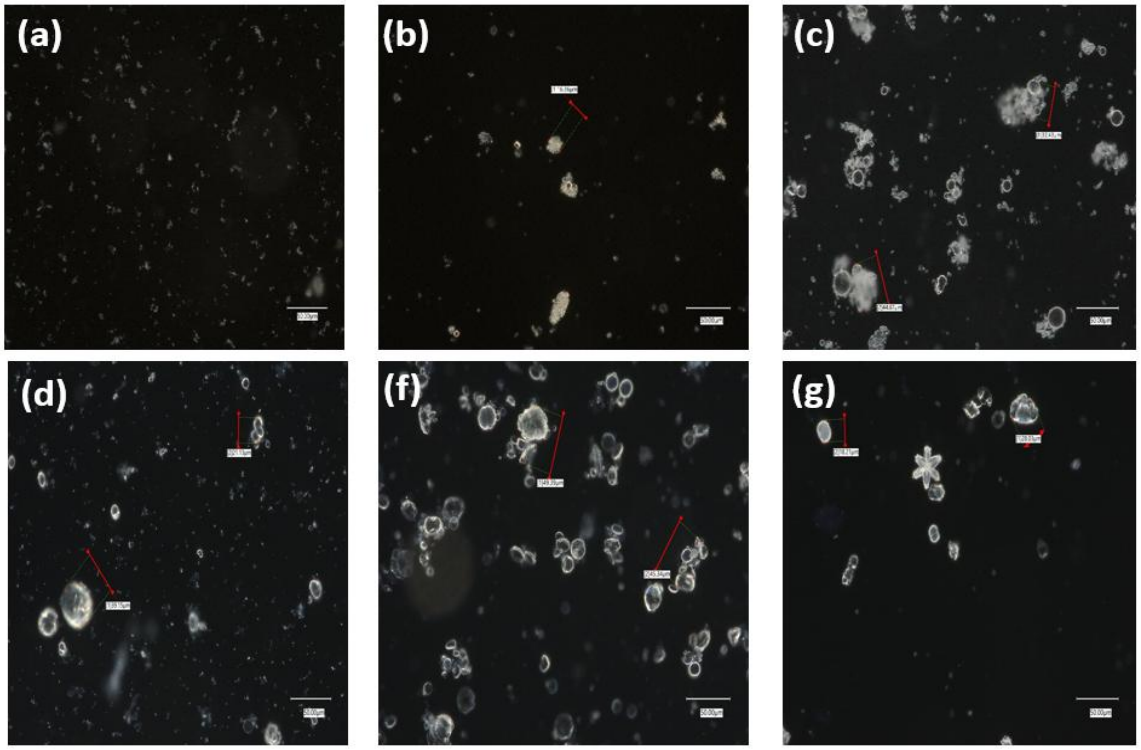

Figure 63: (a) At pH 7, minimal crystal formation was observed. (b) At pH 8, moderate crystal formation was detected. (c) At pH 9, significant crystal formation was evident. (d) At pH 10, advanced crystal formation was observed. (f) At pH 11, substantial crystal formation was noted. (g) At pH 11, complex crystal structures were identified.

4.4.3.2.4 Scanning Electron Microscopy (SEM) and Energy-Dispersive X-ray Spectroscopy (EDX) analysis.

Figure 64 showcases Scanning Electron Microscopy (SEM) images, while Figure 65 presents the corresponding Energy-Dispersive X-ray Spectroscopy (EDX) spectra for samples exposed to a

range of pH levels: (a) pH 7, (b) pH 8, (c) pH 9, (d) pH 10, (f) pH 11, and (g) pH 12. Together, the SEM and EDX analyses highlight how both the surface structure and chemical composition of the materials change progressively with increasing pH. At pH 7, the material's surface appears smooth and uniform, suggesting little to no crystal formation or surface modification. This lack of significant precipitation is typical under near-neutral pH conditions, where the environment does not favour crystal growth (Huang *et al.*, 2010). However, by pH 9, noticeable changes begin to appear, with the surface developing a granular and textured look. This indicates a shift in the material's microstructure, likely due to increased alkalinity promoting the nucleation and growth of crystalline phases (Rodriguez-Navarro *et al.*, 2003). As the pH continues to rise, particularly at pH 9 and 10, the surface becomes even more textured, evolving from granular patterns to well-defined hexagonal shapes. These changes suggest the formation of new crystalline phases—likely calcium carbonate polymorphs like vaterite or aragonite—or the clustering of materials on the surface (Pu *et al.*, 2012). The elevated pH appears to influence how quickly and in what form these crystals develop, leading to more complex and structured surface patterns.

The EDX spectra in Figure 65 provide further details on the chemical composition of these precipitates at different pH levels. At higher pH levels, subtle shifts are observed in the peaks corresponding to carbon (C), sodium (Na), and chlorine (Cl). While these elements are consistently present across all samples, their distribution seems to change with pH, reflecting alterations in the surface chemistry and precipitation processes. Interestingly, no calcium (Ca) peaks were detected at pH 7 and 8, suggesting either the absence of calcium carbonate or its presence in quantities too small for EDX detection in the sampled regions. This observation aligns with the smooth surface morphology and implies limited calcium-based precipitation under lower pH conditions. By pH 9 and 10, the granular textures observed in SEM images likely result from the formation of calcium carbonate polymorphs or other secondary phases that were not present at lower pH. At the highest pH levels, pH 11 and 12, significant crystallization becomes evident. The SEM images reveal well-defined crystalline structures, while the EDX spectra confirm the presence of key elements—calcium (Ca), carbon (C), and oxygen (O)—associated with calcium carbonate polymorphs like calcite and aragonite. The highly alkaline environment at these pH levels not only accelerates precipitation but also influences the size, shape, and stability of the resulting crystals (Pu *et al.*, 2012).

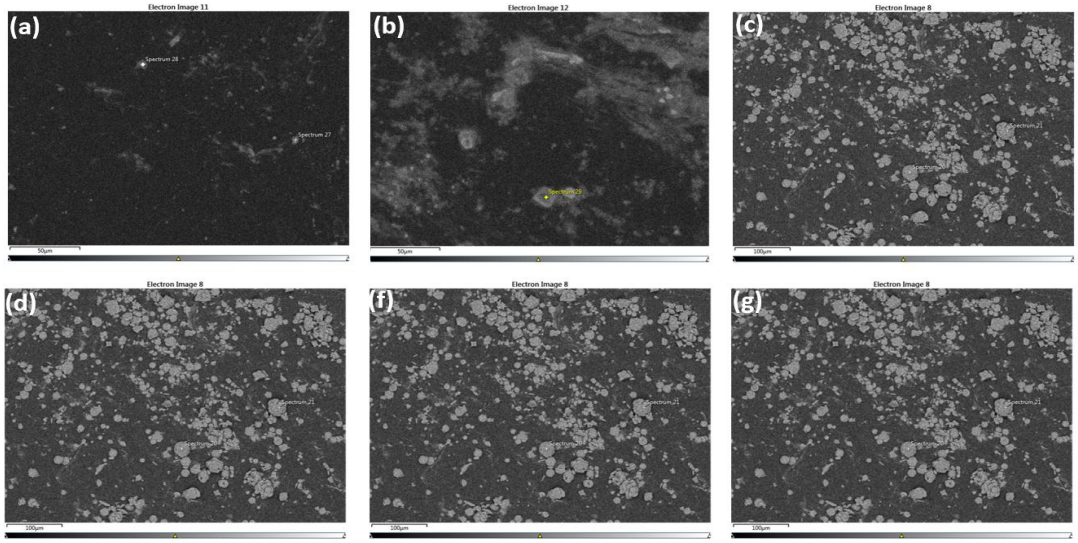

Figure 64: Results of Scanning Electron Microscopy (SEM) analysis of the white precipitated product at varying pH levels (a) pH 7, (b) pH 8, (c) pH 9, (d) pH 10, (f) pH 11, and (g) pH 12.

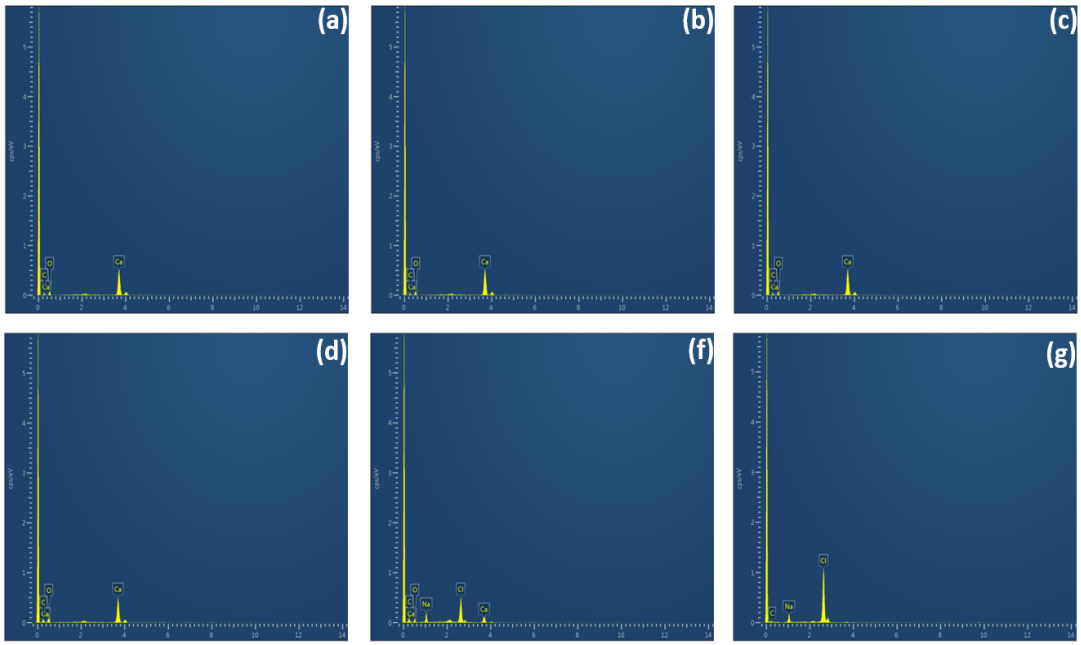

Figure 65: Results of Energy-Dispersive X-ray Spectroscopy (EDX) analysis of the white precipitated product across varying pH levels (a) pH 7, (b) pH 8, (c) pH 9, (d) pH 10, (f) pH 11, and (g) pH 12.

4.5 Conclusion

This study's research and development phase involved numerous comprehensive experiments aimed at investigating the chemical environment within concrete and examining how bacterial activity contributes to concrete cracking, ultimately supporting the progress of self-healing concrete technology. It is noted that bacteria may also be present during various stages of concrete production, such as mixing. However, this study specifically concentrates on the internal chemical environment of concrete and the ways in which certain factors—such as cement type, water flow, and carbonation processes—can influence this environment.

While there is potential to create a chemical setting within concrete that promotes bacterial activity, this study does not seek to replicate the full, realistic lifecycle of concrete. Instead, its goal is to clarify the chemical interactions at play without mirroring actual conditions precisely. The experiments and analyses conducted throughout this study have led to the following findings:

- The inclusion of supplementary materials in concrete has notable effects on its chemical properties. Additives such as fly ash and ground granulated blast-furnace slag (GGBS) can alter the pH and chemical composition of the surrounding environment. While these materials impact the concrete's chemical setting, they must be present in sufficient quantities to support bacterial activity that facilitates self-healing. Therefore, the proportions of these additives should be selected carefully to balance their chemical impact with the need to maintain the concrete's mechanical strength and durability.
- This study introduced a pH measurement technique using colorimetric indicators, specifically phenolphthalein and a universal indicator. The method involved calibrating pH levels with a pH probe and photographing the colour variations at different pH levels. The resulting images were analysed with ImageJ software to determine RGB (red, green, blue) values corresponding to each colour change. A linear correlation was found between pH and the red percentage when phenolphthalein was used, and between pH and the blue percentage when using the universal indicator. While initial blue values

with the universal indicator showed some variability, red and green values lacked consistent correlation with pH. These findings provide a basis for choosing the most suitable indicator for measuring both surface and solution pH in future research.

- When both phenolphthalein and a universal indicator were applied to the concrete surface, phenolphthalein emerged as a more practical and efficient pH indicator. Phenolphthalein produced a single, consistent colour change across the surface, allowing for a straightforward interpretation of the pH level. Conversely, the universal indicator displayed multiple colours simultaneously, reflecting its broad range of pH sensitivity but making it difficult to determine an exact pH value. The presence of mixed hues created inconsistencies and ambiguities, complicating accurate readings. This comparison highlights phenolphthalein's advantage in delivering a clear and dependable colour response, making it the preferred choice for surface pH evaluation in concrete applications where ease of interpretation is essential for precise analysis.
- The research underscored that adding supplementary materials, particularly GGBS, can accelerate the carbonation process in concrete. The interaction between GGBS and the concrete matrix leads to shifts in the chemical composition, facilitating a more effective reaction with carbon dioxide. Additionally, water flow technology was found to play an important role in modifying the concrete's chemical environment. Variations in flow rates affect the rate of carbonation, with higher flow rates generally inducing more substantial chemical changes. The combination of supplementary materials and controlled water flow can enhance carbonation, lowering pH levels and potentially influencing the material's durability.
- The concrete environment's pH level is crucial for supporting bacterial activity and enabling calcium carbonate production. The study demonstrated that optimal calcium carbonate formation occurs at pH levels of around 9 to 10, aligning with the conditions that favour efficient bacterial activity. Although some formation was observed at higher pH levels, specifically 11 and 12, these results were attributed to chemical rather than biological processes. Lower pH levels, particularly those near 7 to 8, were associated with minimal calcium carbonate production due to the reduced effectiveness of urea hydrolysis, which operates optimally in a more alkaline setting. This finding highlights the importance of maintaining an appropriate pH to sustain the bacterial processes necessary for self-healing concrete.

5 Chapter 5: Investigation of optimally sized microcapsules and their impact on concrete properties (Phase 2).

5.1 Overview

The main goal of this phase is to explore the incorporation of calcium carbonate and calcium alginate microcapsules into concrete, examining their effects on the material's properties and their potential as nutrient carriers for microbial self-healing systems. The research specifically evaluates how these encapsulated systems influence the mechanical performance of concrete and their ability to release nutrients effectively when cracks occur. This general approach to nutrient delivery in self-healing concrete aims to improve both the mechanical performance and the sustainability of concrete structures, ensuring greater durability and longevity. By analysing different nutrient carriers, this study seeks to identify the most effective methods for enhancing self-healing capabilities and promoting the long-term resilience of concrete in real-world applications.

5.2 Fabrication of Alginate Beds

Figures 66 and 67 illustrate the formation of microcapsules and the measurement of calcium alginate, respectively. The encapsulation of calcium lactate within sodium alginate microcapsules is a method specifically designed to enhance the self-healing properties of concrete. The process commences with the preparation of a 0.5% sodium alginate solution, achieved by dissolving 0.5 grams of sodium alginate in 100 millilitres of deionized water. Calcium lactate, at a concentration of 1–2% by weight of the alginate, is then added to ensure its incorporation within the microcapsules (Mousa *et al.*, 2021). To enable visual tracking, a small amount of Methylene Blue (0.01%) is mixed in, ensuring it does not affect the capsules' properties. Next, a calcium chloride solution (0.55–1.1 g of calcium chloride in 100 mL of deionized water) is prepared to act as the crosslinking agent. Using a syringe with a fine 30-gauge needle, droplets of the sodium alginate solution—containing calcium lactate and Methylene Blue—are gently introduced into the calcium chloride solution. These droplets immediately begin to gel, encapsulating the nutrients within the alginate matrix. The mixture is stirred lightly (50–100 rpm) for 10–30 minutes to ensure stable microcapsule formation. Once the crosslinking is complete, the capsules are filtered using a Buchner funnel and vacuum filtration system. They are washed thoroughly with deionized water (3–5 times) to remove any residual calcium chloride or unreacted substances. The cleaned microcapsules are then dried either by air for 24–48 hours or in an oven at 40–60°C for 12–24 hours, achieving the ideal moisture content. Finally, the size and uniformity of the microcapsules are examined under a microscope, ensuring they measure approximately 50 µm—an optimal size for integration into self-healing concrete (Meraz *et al.*, 2023). Maintaining the calcium lactate concentration within the alginate shell is vital for successful encapsulation while preserving the integrity of the gelation process (Zadeike *et al.*, 2024).

Figure 66: Stirrer for dissolving sodium alginate

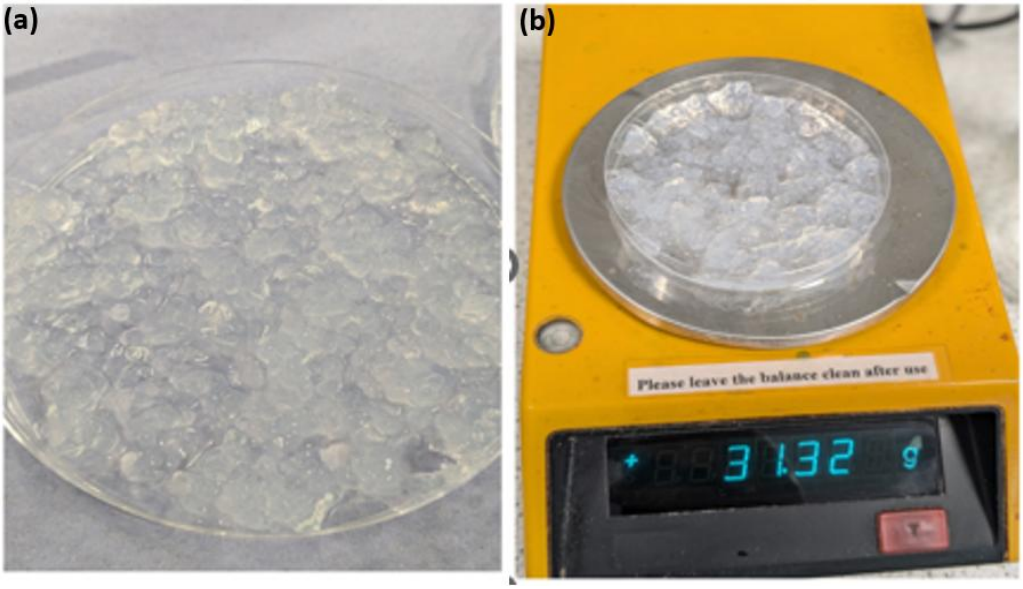

Figure 67: (a) Alginate capsules. (b) Weighing alginate capsules

5.3 Fabrication of calcium carbonate beds

Preparing microcapsules to encapsulate calcium lactate involves a series of well-planned steps to ensure they function effectively. The process begins by making a 0.1 M calcium chloride ($CaCl_2$) solution by dissolving 55.5 g of $CaCl_2$ in 5 litters of deionized water as showing in figure 69, providing the necessary calcium ions. At the same time, a sodium carbonate (Na_2CO_3) solution of the same concentration is prepared by dissolving 53 g of Na_2CO_3 in 5 litters of deionized water, which acts as the carbonate source for forming calcium carbonate. Next, 0.545 g of calcium lactate is added to the calcium chloride solution to serve as the nutrient for encapsulation, and the solution is stirred to mix it evenly. A small amount of methylene blue (0.32 g in 100 mL of deionized water) is then introduced to the mixture as a tracer to track the

capsules without affecting their performance. The sodium carbonate solution is added drop by drop into the calcium chloride-calcium lactate mixture at a steady pace of 1–2 drops per second. This controlled addition ensures the microcapsules grow uniformly and minimizes the formation of smaller, unwanted particles. Stirring is kept slow (100–200 rpm) to prevent high shear forces from damaging the developing capsules. The mixture is left to stir gently for 2–4 hours, allowing the capsules to grow and stabilize to an ideal size of about 50 µm. Once the capsules have formed, the solution is left to settle for 10–15 minutes before being filtered using a vacuum setup to collect them. The capsules are washed 3–5 times with deionized water to remove any leftover chemicals or byproducts, ensuring they are clean and ready for use. Finally, the capsules are dried, either by leaving them at room temperature for 24–48 hours or using an oven set to 40–60°C for 12–24 hours. This careful drying step ensures the capsules remain intact and ready for integration into self-healing concrete.

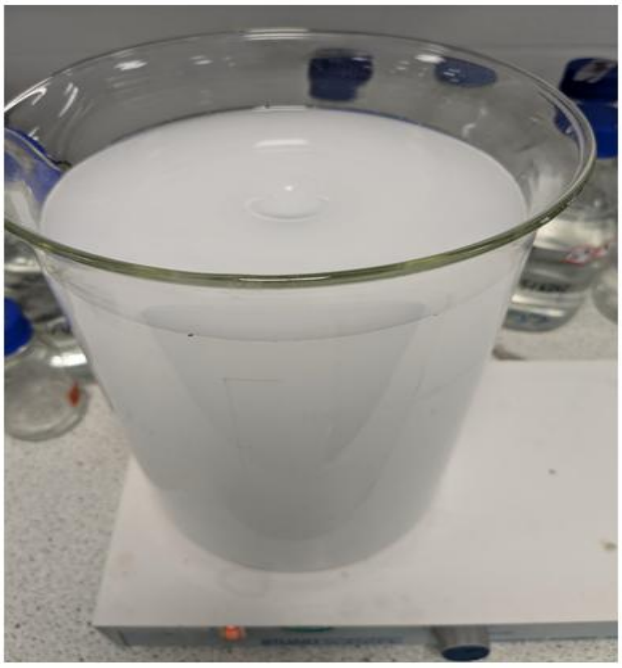

Figure 69: Ingredients and Proportions for Capsule Preparation

The image in figure 70 shows how calcium carbonate capsules can often look like powder because of their tiny particle size and the way they are processed and dispersed. On a microscopic level, these small particles tend to stick together, giving them a fine and indistinct appearance rather than looking like clearly defined capsules. This is especially noticeable because the capsules are designed with thin shells that break open when concrete cracks, releasing nutrients that activate bacteria and support the self-healing process. Calcium carbonate's natural properties also play a role in its powder-like appearance. Its low solubility, fine crystalline structure, and tendency to exist as micro- or nano-sized particles make it hard to distinguish from powder, even when encapsulation is done successfully. Additionally, calcium carbonate is often ground into ultra-fine particles to improve its performance as a filler in cement systems, which boosts its compatibility but further contributes to its powder-like appearance, even under a microscope. Encapsulating materials at such a fine scale comes with its own set of challenges. The tiny particles tend to clump together, the delicate shells of the capsules are prone to damage, and the mixing process can add extra stress, often making the

capsules look like powder. Despite this, the design ensures that the capsules break open when cracks form, releasing nutrients to activate bacteria and support the self-healing process. Tackling these challenges is key to refining the encapsulation process and making calcium carbonate even more effective in concrete and similar materials.

Figure 70: Calcium carbonate capsules

5.4 Effect of microcapsules on the mechanical properties of concrete

This study looks at how adding different types of capsules—calcium lactate powder, calcium alginate capsules, and calcium carbonate capsules—affects the strength and durability of concrete. The aim is to understand how these capsules, which carry healing agents or nutrients, influence the concrete's performance and ability to self-heal over time. The concrete samples were divided into four groups. The first group, the control mix, contained no capsules and served as a baseline for comparison. The second group included calcium lactate powder, which acts as a nutrient source to activate bacteria when cracks form. These bacteria consume the calcium lactate and produce calcium carbonate crystals, sealing the cracks naturally and restoring the structure. The third group used calcium alginate capsules, which protect the nutrients during the mixing process and release them in a controlled manner when cracks appear, ensuring effective self-healing. The fourth group incorporated calcium carbonate capsules, which directly help repair cracks by releasing calcium ions into the damaged areas, promoting the formation of calcium carbonate to close the cracks. Research have shown that smaller capsules generally have a lesser impact on the mechanical properties of concrete, as their size reduces interference with the material's internal structure (Wang *et al.*, no date c). By comparing these approaches, this study aims to improve capsule design for better concrete performance and durability. Capsules were added in varying amounts, ranging from 3% to 5% of the cement weight, to explore how different dosages affect the performance of the concrete as showing in table 12. To evaluate their impact, compressive strength tests were carried out at 7 and 28 days, providing insights into both the short-term and long-term effects.

Table 12: Concrete mix type and capsules

Mix Category	Type of Capsule Used	Capsule Dosage (% of Cement Weight)
Control Mix	None	0%
Calcium Lactate Powder	Calcium Lactate Powder	3% and 5%
Alginate Capsules	Calcium Alginate	3% and 5%
Carbonate Capsules	Calcium Carbonate	3% and 5%

5.4.1 The preparation of concrete specimens

To ensure consistency and accuracy, the mortar samples were prepared following standard lab practices. The mix used a water-to-cement ratio of 0.5 and a cement-to-sand ratio of 1:3, with ordinary Portland cement (OPC) as the binder. Four batches were created, each incorporating calcium lactate powder, alginate capsules, and calcium carbonate capsules at dosages of 0% (control) and 5% by the weight of cement as presented in Table 13. Careful measurement of these additives ensured the results would accurately reflect their impact on the mortar's performance. Water was gradually added to the mix, and all ingredients were blended in a concrete mixer for about 15 minutes, resulting in a uniform and well-mixed mortar. Before casting, the 100 mm × 100 mm × 100 mm moulds were prepared by applying a thin layer of oil to their inner surfaces to ensure easy removal of the hardened mortar later. The freshly mixed mortar was poured into the moulds in three layers, with each layer compacted on a vibrating table to remove trapped air and minimize voids. This process ensured the samples were dense and of high quality. After compaction, the moulds were placed in a curing tank filled with water kept at a consistent temperature of 20°C. This curing process followed standard procedures, promoting proper hydration of the cement. The mortar samples were cured for 7 and 28 days to assess their mechanical and durability properties at different stages. This approach provided clear insights into how the additives influenced the mortar's performance and long-term behaviour.

Table 13: Mix calculation

Mix Type	Cement (kg)	Sand (kg)	Water (kg)	Capsules (kg)	Total Weight (kg)
Control	4.725	14.175	2.3625	0.0000	21.2625
Calcium Carbonate Capsules	4.725	14.175	2.3625	0.23625	21.49875
Alginate Capsules	4.725	14.175	2.3625	0.23625	21.49875
Calcium Lactate Powder	4.725	14.175	2.3625	0.23625	21.49875

5.4.2 Concrete cubes' compressive strength test

The mortar cubes were cured in water maintained at a steady temperature of 20°C (±2°C) to ensure consistent cement hydration and proper strength development. Compressive strength tests were conducted on four cubes at 7 and 28 days using an Auto Max machine. This approach enabled the monitoring of strength development over time, providing valuable insights into the long-term performance and durability of the concrete. Figure 71 illustrates the

comprehensive process of compressive strength testing, including the procedure for testing cubes using the Auto Max machine.

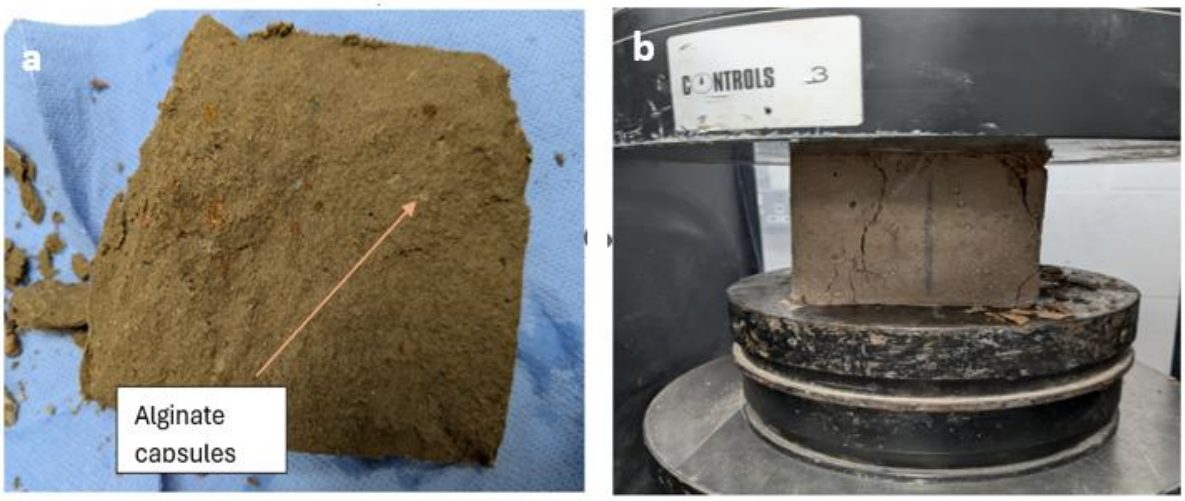

Figure 71: (a) Failed mortar sample. (b) Comprehensive strength set up

5.5 Results and discussion

5.5.1 Capsules beds

The main goal of developing different types of capsules is to understand how they affect self-healing concrete, particularly their influence on its mechanical properties. This phase also explores the effects of combining various capsule types, demonstrating how these combinations can enhance the performance of self-healing systems. By examining the link between capsule design and concrete behaviour, the study provides valuable insights into creating more efficient and sustainable self-healing concrete solutions. During the experiments, calcium alginate beads were observed to form almost instantly when a sodium alginate solution was added to calcium chloride ($CaCl_2$). Initially, the beads floated for a few seconds before gradually sinking, likely due to their increasing density over time. This observation aligns with findings from Bennacef *et al*. (2023), which showed that as sodium alginate reacts with calcium chloride, the density of the beads increases, influenced by the specific formulation of the solutions. The process for creating calcium carbonate capsules was different. These capsules formed through a reaction between sodium carbonate (Na_2CO_3) and calcium chloride ($CaCl_2$), resulting in the precipitation of calcium carbonate ($CaCO_3$) as a solid. These capsules play a vital role in self-healing concrete, acting as carriers for healing agents. When cracks appear, the capsules break open, releasing their contents to trigger a reaction that seals the cracks. This process improves the concrete's durability, helping it last longer and remain structurally sound. The performance of calcium carbonate capsules depends on factors such as the reaction time, the concentration of the chemicals used, and the environmental conditions during production. These factors influence the size, shape, and strength of the capsules, all of which are crucial for their role in self-healing concrete. Understanding these details allows researchers to optimize capsule production, making self-healing systems more reliable and effective. This study advances self-healing concrete technology by offering practical and sustainable solutions to extend the lifespan and resilience of infrastructure.

5.5.2 The measurement of capsules

The production of calcium carbonate and alginate capsules was successfully carried out and fine-tuned during the experiments. However, noticeable differences were observed in the sizes of the two capsule types. Alginate beads, produced during encapsulation, were expected to be highly symmetrical due to the well-documented gelation process, which typically ensures uniformity under controlled conditions (Tran *et al.*, 2024). To accurately measure their sizes, Keyence microscopy, a reliable tool for analysing shapes and dimensions, was used. The results presented in Figure 72, indicate the alginate capsules were significantly larger, with diameters ranging between 2755.850 µm and 2846.839 µm. In contrast, Figure 73 indicate that calcium carbonate capsules exhibited diameters ranging from 3.021 µm to 4.000 µm. This small particle size is a direct result of the controlled precipitation method employed during their synthesis, which effectively restricts crystal growth to the micrometre scale. This significant size difference is due to the different processes involved in their formation. Alginate capsules are created through ionic gelation, where calcium ions bond with sodium alginate to form stable and durable beads (Montanucci *et al.*, 2015). The larger size of the alginate capsules is consistent with the characteristics of their gelation process, while the smaller calcium carbonate capsules highlight the precision of the precipitation method. These findings emphasize the importance of tailoring production techniques to achieve specific capsule sizes, especially for applications like self-healing concrete, where the size of the capsules plays a critical role in their performance and effectiveness (Wang *et al.*, 2014c).

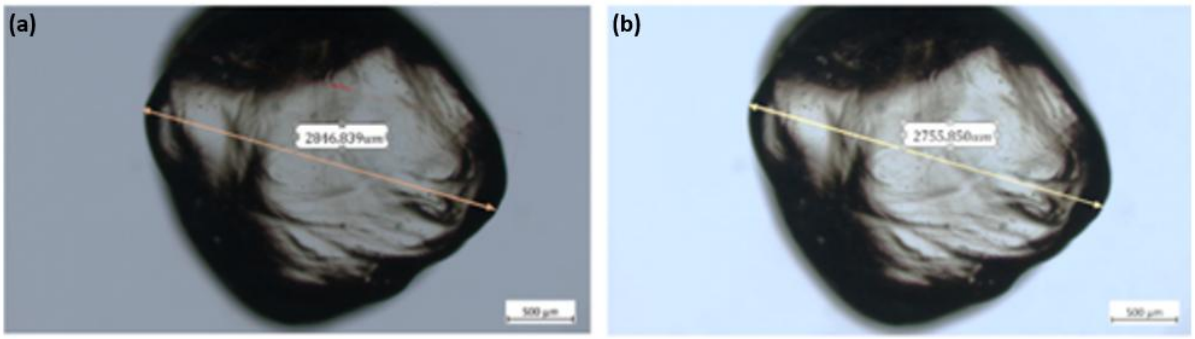

Figure 72: (a) Alginate capsules size 2846.839 um. (b) Alginate capsules size 2755.850 um

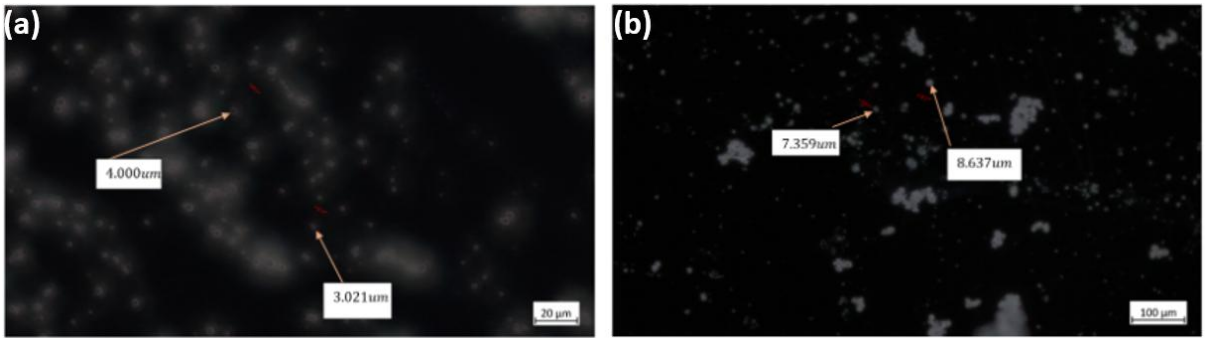

Figure 73: (a) Calcium carbonate capsules size 4 um. (b) Calcium carbonate capsules size 8.6 um

5.5.3 The influence of capsules on concrete properties

Figure 74 presents a comparative analysis of the compressive strength trends across all mortar mixes over time. This study identifies distinct patterns in the influence of calcium carbonate

capsules, calcium alginate capsules, and calcium lactate powder on the compressive strength of mortar samples, highlighting the interplay between structural performance and self-healing functionality. Notably, the control mix exhibited the highest compressive strength, attaining 9.65 MPa at 7 days and 33.30 MPa at 28 days. This superior performance is due to uninterrupted hydration and the formation of a consistent cement matrix, which allows for optimal strength development (Neville, 1995b). In comparison, mortar containing calcium carbonate capsules (3–4 µm in size) achieved 4.82 MPa at 7 days and 17.44 MPa at 28 days. These capsules acted as micro-fillers, reducing porosity and densifying the concrete matrix over time. However, the initial stages of strength development were disrupted due to uneven particle distribution and clumping (Duan *et al.*, 2023). Larger calcium alginate capsules, measuring 2755.850 µm to 2846.839 µm, showed the lowest compressive strength, recording approximately 3.8 MPa at 7 days and 16.0 MPa at 28 days. The significant reduction in strength is attributed to voids created by the large capsule size, which weakened the matrix and compromised load transfer (Wang *et al.*, no date b). Despite this, alginate capsules offer significant self-healing potential. They can encapsulate bacterial spores and nutrients, releasing them into cracks to promote calcium carbonate precipitation, which improves durability and seals cracks over time (H M Jonkers, 2010). Calcium lactate powder showed moderate results, with compressive strengths of 5.5 MPa at 7 days and 22.0 MPa at 28 days. Its fine particle size allowed it to spread evenly through the concrete, helping to reduce voids and acting as a nutrient source for bacterial activity. This activity supported the formation of calcium carbonate, which helped seal cracks and strengthen the concrete (Wiktor et al., 2011). However, its success depends on proper encapsulation to prevent premature hydration. The control mix demonstrated excellent strength, while calcium alginate and calcium lactate powder showed greater potential for durability and crack repair. Calcium carbonate capsules provided a well-balanced solution, offering moderate strength while improving matrix densification. The results highlight the importance of refining capsule size, dosage, and distribution to achieve both strength and durability.

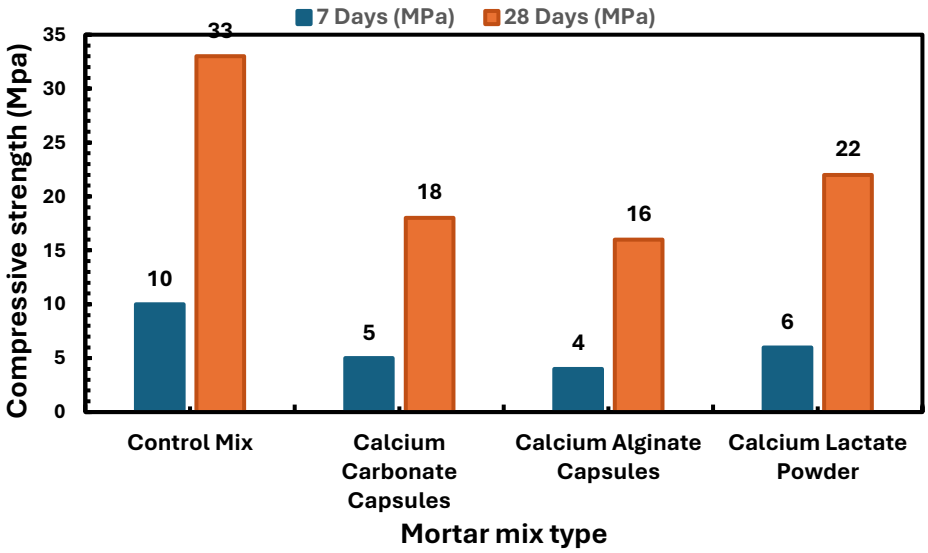

Figure 74: Compressive strength results capsules amount %5

The table 14 outlines how different capsule types affect compressive strength, variability, and reductions compared to the control mix at 7 and 28 days. The Control Mix (Series One), which did not include any capsules, showed the most consistent results with minimal variability, demonstrating reliable strength development over time. For Calcium Carbonate Capsules (Series Two), a small dosage of 0.031% resulted in only a minor drop in compressive strength—8.2% at 7 days and 9.1% at 28 days. These fine capsules caused minimal disruption to the cement structure, maintaining good overall performance. On the other hand, Calcium Alginate Capsules (Series Three), added at a higher volume of 0.078%, led to a significant reduction in compressive strength—39.8% at 7 days and 42.1% at 28 days. This reduction is mainly due to the voids created by their larger size. Despite this drawback, alginate capsules provide a valuable self-healing benefit, releasing bacteria and nutrients to repair cracks as they form. Calcium Lactate Powder Capsules (Series Four), included at 0.075%, caused a moderate reduction in compressive strength—19.7% at 7 days and 23.7% at 28 days. This mix strikes a practical balance, as it combines some loss in mechanical strength with the ability to promote microbial self-healing, contributing to improved long-term durability.

Table 14: Capsules at %5 addition influences the compressive strength

Series	Description	Cov (%) - 7 Days	Cov (%) - 28 Days	Volume and Quantity	Compressive Strength
Series One	Control Mix (No capsules)	2.6	3.1	-	No capsules added
Series Two	Calcium Carbonate Capsules (3 µm)	2.8	0.8	-	0.031% (approx. 2,200 capsules)
Series Three	Calcium Alginate Capsules (2.2 mm)	0.4	1.1	-	0.078% (approx. 5,500 capsules)
Series Four	Calcium Lactate Powder Capsules (fine size)	1.8	3.4	-	0.075% (approx. 3,400 capsules)

The figure 75 illustrates the compressive strength improvements achieved by reducing the capsule content from 5% to 3%. Reducing the capsule content from 5% to 3% had a clear positive effect on the compressive strength of all concrete mixes, helping to minimize the strength losses seen at higher dosages. The Control Mix, as expected, delivered the best performance, reaching 10 MPa at 7 days and 33 MPa at 28 days. This result reflects an uninterrupted hydration process and a consistent cement matrix, allowing the concrete to achieve its full-strength potential. For the Calcium Carbonate Capsules, the mix reached 7 MPa at 7 days and 22 MPa at 28 days, showing only a slight drop in strength compared to the control mix. This represents a noticeable improvement over the 5% dosage, where higher capsule content caused more significant disruptions to the matrix. At this lower dosage, calcium carbonate capsules act as fillers, helping to densify the cement matrix and partly offsetting early hydration delays. The Calcium Alginate Capsules mix experienced greater strength

reductions, with 6 MPa at 7 days and 20 MPa at 28 days. Although these values are lower than the control mix, they show a marked improvement over the results at 5% content, where early-age strength losses were nearly 40%. The larger capsule size (around 2.2 mm) creates voids in the cement matrix, weakening its structure. Despite this, alginate capsules remain beneficial because they release bacteria and nutrients into cracks, enabling self-healing through calcium carbonate formation over time (Jonkers, 2010). The Calcium Lactate Powder mix provided a more balanced performance, achieving 8 MPa at 7 days and 25 MPa at 28 days. Reducing the capsule content helped minimize the strength losses seen at 5% dosage, where the reductions were more pronounced. The powder disperses well within the cement matrix, reducing void formation while supporting microbial activity for self-healing. Its fine particle size delivers nutrients efficiently without significantly compromising the strength, making it a practical option for balancing performance and durability.

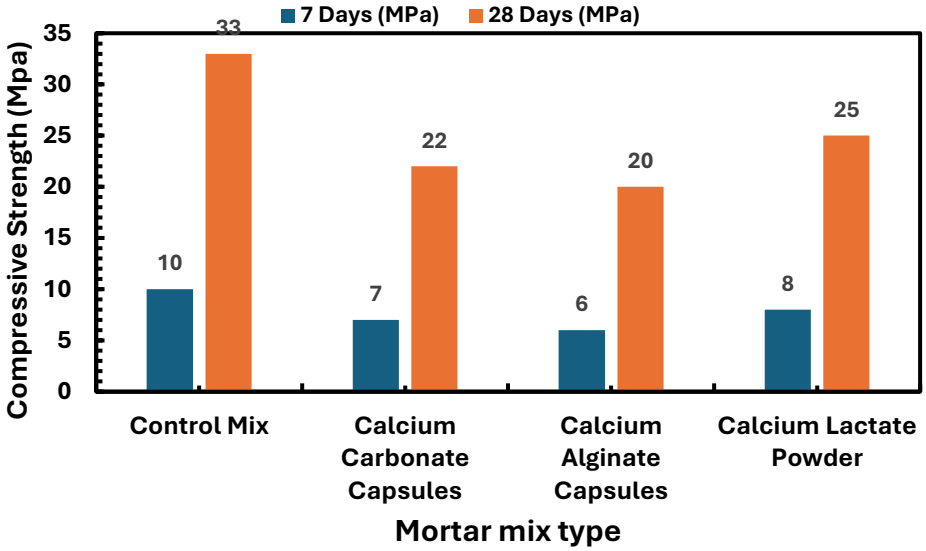

Figure 75: Compressive strength results capsules amount %3.

The findings in table 15 shows that Series One, the control mix without any capsules, provides a reliable baseline with the least variability (Cov %). This consistency is expected, as there are no additives to interfere with the hydration process, allowing the cement matrix to form uniformly. In Series Two, small calcium carbonate capsules (3 μm) were added at 0.018% volume, resulting in only slight variability. The fine capsules are evenly distributed throughout the cement matrix, causing minimal disruption to its structure or strength development. Series Three, which includes larger calcium alginate capsules (2.2 mm) at 0.048%, showed very low variability at 7 days. However, the larger capsule size created voids in the matrix, slightly hindering strength development as the concrete cured. Finally, Series Four, with calcium lactate powder capsules at 0.045%, struck a balance. The fine particles caused moderate variability but offered a trade-off between a small reduction in strength and the added benefit of self-healing through microbial activity. Reducing the capsule content to 3% improved compressive strength and reduced variability compared to higher dosages. These results highlight the importance of carefully managing the number of capsules to maintain both the performance and functionality of the concrete.

Table 15: Capsules at %3 addition influences the compressive strength

Mix Type	Description	7/28 Days Cov %	Capsule Details
Control Mix	No capsules, baseline mix	2.6 / 3.1	None
Calcium Carbonate	Fine capsules (~3 µm)	1.8 / 0.6	0.018%, ~1,300 capsules
Calcium Alginate	Large capsules (~2847 µm)	0.3 / 0.8	0.048%, ~3,300 capsules
Calcium Lactate	Fine powder capsules	1.2 / 2.3	0.045%, ~2,100 capsules

The amount of capsules added to concrete has a major impact on the balance between compressive strength and benefits like self-healing. Higher dosages, such as 5%, tend to cause greater reductions in strength because they create more voids and disrupt the concrete's internal structure. This happens when larger volumes of capsules interfere with the hydration process and weaken the bond between materials. For example, calcium alginate capsules are particularly prone to this at higher dosages due to their larger size (2846.839 um), which leads to significant void formation and noticeable strength loss, even though they enhance self-healing. In contrast, using lower dosages, such as 3%, can help reduce these strength losses. Smaller capsules, like calcium carbonate (3 µm) and calcium lactate powder, disperse more evenly in the cement mix, causing less disruption to the matrix. This allows the concrete to maintain more of its strength while still benefiting from self-healing capabilities. For instance, calcium lactate powder at 3% strikes a good balance, with only moderate strength reductions while contributing to long-term durability through microbial self-healing.

5.6 Conclusion

The phase explored how to optimize the size and type of capsules used in self-healing concrete to reduce their impact on compressive strength while maximizing their ability to heal cracks. We investigated the effects of calcium alginate capsules (~2847 µm), calcium carbonate capsules (~3 µm), and calcium lactate powder, and the results revealed key differences in their performance. Calcium alginate capsules, while highly effective for repairing larger cracks due to their ability to hold significant amounts of nutrients, had the greatest impact on compressive strength. At 7 days, concrete containing alginate capsules showed a 15–20% reduction in compressive strength, mainly because their larger size disrupted the matrix's homogeneity. In contrast, calcium carbonate capsules, much smaller at around 3 µm, had a much milder effect, with compressive strength reducing by just 5–7% at 7 days. Their small size allowed them to blend seamlessly into the concrete matrix, reducing porosity and increasing density. These capsules not only improved the structure but also supported efficient crack healing by gradually releasing nutrients for bacterial activity. Calcium lactate powder, the smallest of the three additives, had the least impact on compressive strength, causing only a 2–4% reduction at 7 days. However, its lack of encapsulation made it less effective for long-term healing, as nutrients could leach out or be consumed too quickly, leaving little for later crack repair. However, there were some challenges with using calcium lactate powder. Because it dissolves easily in water, it can start dissolving during the mixing process. Additionally, since concrete is a porous material, the dissolved calcium lactate can migrate out of the concrete before cracks even form. This could mean that the nutrients are no longer available to support bacterial activity within the concrete. Despite these challenges, this research takes advantage of naturally occurring bacteria in the soil around the concrete. As the calcium lactate moves out,

these bacteria can consume the nutrients and produce carbonate. This carbonate can then react with calcium ions released from the concrete, forming calcium carbonate to seal cracks and pores. This approach highlights a unique way of promoting self-healing by working with the natural environment surrounding the concrete. These results demonstrate the potential of smaller capsules, like calcium carbonate, to provide a better balance between preserving compressive strength and enabling effective self-healing. By refining the size and distribution of these capsules, we can overcome the limitations of larger systems like alginate capsules and improve the overall efficiency of self-healing concrete. This approach offers a promising path toward creating more durable and sustainable concrete solutions, with the added benefit of reduced maintenance and repair costs over time. In summary, reducing the capsule dosage to 3% helps mitigate the strength losses caused by their inclusion while retaining their self-healing benefits. Calcium carbonate and calcium lactate powders perform better at lower dosages, as they interfere less with the cement matrix. Although calcium alginate capsules cause larger strength reductions, their self-healing properties remain valuable for long-term durability. Optimizing the capsule content is therefore essential to achieving a balance between early-age strength and enhanced durability.

6 Chapter 6: Investigating the effectiveness of self-healing (Phase 3)

6.1 Overview

In the final phase of this research, the self-healing system's ability to repair cracks in concrete caused by mechanical loading was assessed. These experiments aimed to evaluate the system's performance, identify the locations of calcium carbonate ($CaCO_3$) formation, and determine opportunities for optimisation. Visual inspection and image processing techniques were employed to observe crack closure, assess the effectiveness of microbial-induced calcium carbonate precipitation (MICP), and ascertain whether healing occurred predominantly at the surface or deeper within the concrete. This phase also examined various factors influencing the performance of self-healing concrete. The effects of incorporating supplementary materials in different proportions were analysed to understand their impact on the healing process. The role of water flow systems was explored, focusing on the influence of water movement on the activation and distribution of healing agents. The effects of carbonation were studied to determine how this process interacts with the self-healing mechanism and alters the chemical environment of the concrete. Additionally, different types of soil were evaluated to investigate their contributions to self-healing, particularly in supporting microbial activity and nutrient supply. The study further explored the performance of various capsules as carriers for healing agents, assessing their effectiveness in nutrient delivery and promoting calcium carbonate precipitation. By addressing these factors, the research provided a comprehensive understanding of the variables affecting self-healing concrete and identified strategies for optimising its application. To gather robust evidence of $CaCO_3$ formation, Scanning Electron Microscopy (SEM) and Energy-Dispersive X-ray Spectroscopy (EDS) were utilised to examine the structure and composition of the precipitated material. These advanced analytical techniques offered valuable insights into the self-healing process. By integrating observation, analysis, and experimentation, this research contributed to a deeper understanding of self-healing concrete and its potential for practical use.

6.2 Assessing the Impact of 35% Supplementary Material Replacement on Self-Healing Concrete

Self-healing concrete offers several key benefits, including reducing material deterioration, extending the lifespan of infrastructure, and lowering the need for frequent and costly repairs. These benefits also support environmental sustainability by reducing material consumption, energy use, and emissions from material production and transportation. Additionally, self-healing concrete helps minimize traffic disruptions caused by maintenance and reconstruction, particularly in transportation infrastructure. This study explores whether using naturally occurring bacteria in soil delivers better results for bio-concrete compared to directly adding bacteria into the concrete mixture. It also addresses the challenges of maintaining bacterial activity within concrete and investigates how supplementary materials can improve the bio-concrete system by reducing the concrete's pH levels. To achieve this, the research subjected soil to fully saturated cycles and incubated cracked cement mortar specimens. The specimens included plain mortar as a control, mortar mixed with nutrients in naturally saturated soil, mortar with 35% fly ash (FA) replacement and nutrients, and mortar with 35% ground granulated blast furnace slag (GGBS) replacement and nutrients.

6.2.1 Materials and methods

6.2.1.1 Specimen preparation and crack creation

Following the guidelines of BS EN 196-1, several types of mortar specimens were prepared for this study, including plain mortar (Control), mortar combined with nutrients, mortar with fly ash (FA) and nutrients, and mortar with ground granulated blast-furnace slag (GGBS) and nutrients. The GGBS used in this research was supplied by Hanson Heidelberg Cement Group in the UK and meets the requirements of BS EN 196-2 standards. The fly ash (450-N), classified under the normal fineness (N) category as per BS EN 450-1, was provided by Conserv Ltd, based in Middlesbrough, North Yorkshire, UK. The chemical compositions of the Portland cement, GGBS, and FA used in the study are presented in Table 16, providing a clear understanding of the materials' properties and ensuring consistency with industry standards. Calcium lactate powder, a vital ingredient for promoting microbial-induced calcium carbonate precipitation (MICP), was sourced from Special Ingredients Ltd, UK. The selection and documentation of these materials were carried out with great care to ensure high quality and compatibility with the experimental objectives. This meticulous approach supports the study's aim of thoroughly investigating the self-healing properties of the mortar specimens while maintaining a focus on reliability and reproducibility. To prepare the mortar samples, a mixture was made using Hanson Sulphate Resisting Cement (CEM III/A + SR), CEM II, sand, tap water, and calcium lactate powder as a nutrient, based on the proportions outlined in Table 17. A water-to-cement ratio of 0.6 was maintained for all mixes. Prismatic specimens measuring 40x40x160 mm were cast, with fibre mesh placed at their centre during casting to prevent complete structural failure. After 24 hours, the specimens were removed from their moulds and cured in water for 28 days. Once the curing process was complete, the specimens were taken out of the water, air-dried at room temperature, and prepared for crack generation through mechanical testing. The cracks were induced using a three-point bending test, where the specimens were placed on two parallel supports positioned about two-thirds of their total length apart. Figure 76 illustrates how the central beam applied compression to the upper surface while crack initiation and propagation were tracked using Linear Variable Differential Transducers (LVDTs) attached to the underside of the specimens. The load was gradually applied at a rate of 0.001 mm/s until cracks began to form. To control crack development and prevent complete failure, the loading rate was deliberately reduced. The applied load ranged between 1.6 kN and 2.2 kN, creating cracks of different widths across the specimens. Once the load was removed, the cracks partially closed. Observations revealed crack widths ranging from 0.6 mm to 1.2 mm. To ensure consistent conditions across all testing environments, the cracks were carefully measured and classified.

Table 16: Chemical properties of Portland cement, GGBS cement, and FA cement

Properties%	**Portland cement%**	**GGBS cement%**	**FA cement%**
SiO_2	23.7	32.77	45 to 51
CaO	57.27	40.83	1 to 5
MgO	3.85	6.91	1 to 4
Fe_2O_3	4.83	0.57	7 to 11
Al_2O_3	4.51	14.33	27 to 32
SO_3	2.73	0.28	0.3 to 1.3
Na_2O	-	-	0.8 to 1.7
K_2O	0.37	-	1 to 5
Cl	0.0068	0.00	0.05 to 0.1
TiO_2	-	0.63	0.8 to 1.1
Loss in ignition	7.24	-	-

Table 17: Mortar specimen proportions

Ingredient	Control (MC)	With Nutrients (MN)	With Fly Ash (MF)	With GGBS (MG)
Cement	418	418	271.7	271.7
Fly Ash	-	-	146.3	-
GGBS	-	-	-	146.3
Sand	1250	1250	1250	1250
Water	250	250	250	250
Nutrients	-	10	10	10

Figure 76: Three-bending testing for generating the crack.

6.2.1.2 Incubation and soil analysis

This study investigated premium, high-quality soil with a free chemical composition and sub-rounded grain morphology, selected for its suitability in the experiments. A sieve test was conducted following the BS EN 933 standard to analyse the soil's Particle Size Distribution (PSD). Mortar specimens were prepared and categorized into four groups: PM (plain mortar), MN (mortar with nutrients), MF (mortar with nutrients and fly ash replacement), and MG (mortar with nutrients and GGBS replacement). All specimens were incubated in fully saturated soil for 28 days. Plain mortar served as the control group to examine the potential for natural remediation (autogenous healing) resulting from the ongoing hydration process in the mortar. The soil used in the study was sourced from natural fields near the University of Derby. A visual inspection classified it as a natural alluvial deposit, consisting of soft to firm, dark brown silty clay with slight sandy characteristics. This type of clay is known to naturally host a diverse range of bacterial species. After the specimens were cracked, they were carefully placed into plastic containers, as shown in Figure 77. Dry soil was added to each container in two layers: one layer beneath the specimens and another on top and between them. Each container held three specimens, and all incubations were conducted at room temperature, approximately 23°C. The cracked specimens were incubated in fully saturated soil cycles for 28 days, as shown in Figure 78. Before incubation, the soil was thoroughly saturated by raising the water level above the specimens to the soil surface. Any water lost through evaporation was replenished regularly to maintain a fully saturated environment throughout the incubation period.

Figure 77: Prisms covered with fully saturated soil inside the containers

1.2.2. Assessing the efficacy of repairing cracks.

After the curing process, the mortar specimens were carefully removed from the water and placed in a compression machine to generate controlled cracks. A three-point flexural test was used to create cracks of varying widths near the centre of each specimen. The specimens were supported on two parallel beams positioned about two-thirds of their length apart, while a central beam applied compression to the top surface. The load was gradually applied at a rate of 0.5 mm/s until cracks became visible. To ensure the cracks developed in a controlled manner without causing the specimens to fail completely, the load application rate was reduced. Once the cracks were formed, the specimens were removed from the machine, and the initial crack widths were measured. This process involved taking digital images of the specimens and analysing them using ImageJ software, which was modified to detect the size and location of the cracks. The study observed a range of crack widths, with an average size between 0.668 mm and 1.5 mm. This standardized process, based on the three-point flexural test, ensured consistent crack identification and evaluation across all samples. The main focus of this study was to explore the use of native soil bacteria in enhancing the self-healing ability of concrete. In addition, it examined how supplementary materials, such as ground granulated blast-furnace slag (GGBS) and fly ash (FA), influence the surface properties of concrete. These materials have the potential to improve the surface environment, which could enhance bacterial activity and promote self-healing. As a porous material, concrete's surface properties play a crucial role in its performance, particularly in self-healing applications. By incorporating GGBS and FA, the study aimed to assess how these materials alter the concrete's surface conditions, potentially creating an environment more favourable for bacterial activity. This research provides valuable

insights into optimizing concrete formulations to enhance self-healing properties and support sustainable construction practices

1.2.3. Results and discussion

At the end of the incubation period, the specimens were carefully retrieved from their fully saturated soil environment for analysis. To ensure accurate crack evaluation, they were thoroughly cleaned with water to remove any remaining soil particles. After cleaning, the specimens were immersed in water-filled containers for three hours to stabilise loose particles and allow for precise crack measurements following the self-healing process. To gain a deeper understanding of the materials involved in the healing process, Scanning Electron Microscopy (SEM) was used to capture detailed images of the crack surfaces, revealing the structure of the materials deposited during healing. To determine the chemical composition of these deposits, Energy-Dispersive X-ray Spectrometry (EDX) was performed, with the findings summarised in accompanying figures 78 and tables (18, 19, 20, and 21). EDX analysis confirmed the presence of calcium carbonate ($CaCO_3$) in certain specimens, particularly those containing ground granulated blast-furnace slag (GGBS) and nutrient-enhanced mortar. The GGBS samples exhibited a significantly higher presence of calcium carbonate compared to other specimens, supporting previous research that highlights GGBS's ability to promote calcium carbonate formation by modifying the environment to better support microbial activity (De Muynck et al., 2010a). Conversely, specimens containing fly ash replacements and plain mortar samples were found to be primarily composed of calcium hydroxide and ettringite (calcium sulphoaluminate). The formation of ettringite, observed in fly ash and plain mortar specimens, occurs through the reaction of sulphate compounds with calcium aluminate in the cement. This process reduces calcium hydroxide (CH) and tricalcium aluminate (C_3A) in the matrix, influencing the internal pressure caused by salt crystallisation within the mortar's pores. These findings align with established mechanisms described in previous studies (Chahal *et al.*, 2012) . In all specimens, EDX consistently detected silicon (Si) and oxygen (O), indicating the formation of calcium silicate hydrate (C–S–H). This compound, resulting from the continued hydration of cement particles, is essential for maintaining the strength and durability of the cement matrix (Kadapure *et al.*, 2019). The presence of C–S–H highlights the ongoing hydration process, which also contributes to self-healing. The results demonstrated that the type of supplementary material used significantly influenced the composition of the healing products. GGBS samples showed the highest levels of calcium carbonate, enhancing their ability to effectively seal cracks. In contrast, fly ash and plain mortar samples primarily contained calcium hydroxide and ettringite, which played a different role in the self-healing process. These findings emphasise the potential of GGBS as a superior material for enhancing self-healing performance, consistent with prior research by Tziviloglou *et al.* (2016). The effectiveness of the self-healing process was assessed by measuring crack widths using ImageJ software. The microstructure and composition of the healing materials were further analysed with SEM and EDX. The presence of calcium carbonate as the primary sealing material in GGBS-enhanced mortar confirmed its effectiveness, while other healing products, such as ettringite and C–S–H, were linked to the ongoing hydration of cement particles, validating the mechanisms of self-healing observed in this study.

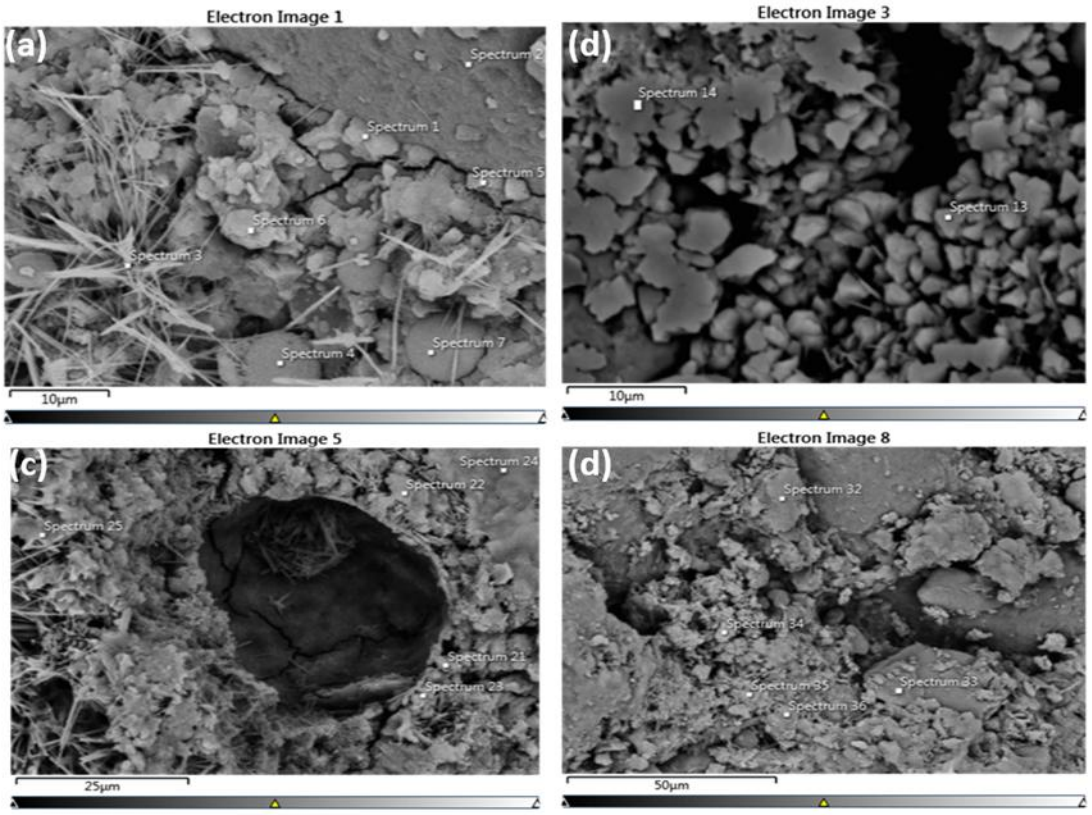

Figure 78: (a) SEM image taken from mortar containing 35% Fly ash, (b) SEM image taken from specimens containing 35% GGBS, (c) SEM image taken from specimens of plain mortar, (d) SEM image taken from specimens of mortar with only nutrients

Table 18: EDX date taken from specimens containing 35% fly ash.

Element	Spectrum 4
C	8.35
O	35.8
Mg	1.09
Al	14.31
Si	21.8
S	1.04
K	2.35
Ca	12.27
Ti	0.81
Fe	4.02
Total	100.0

Table 19: EDX data taken from specimens containing 35% GGBS.

Element	Spectrum 13
Carbon (C)	17.59
Oxygen (O)	56.03
Aluminium (Al)	-
Silicon (Si)	-
Calcium (Ca)	26.38
Total	100.0

Table 20: EDX data taken from specimens of plain mortar

Element	Spectrum 22
Carbon (C)	12.2
Oxygen (O)	37.48
Aluminium (Al)	1.94
Silicon (Si)	6.56
Sulphur (S)	-
Calcium (Ca)	38.27
Iron (Fe)	3.55
Total	100.0

Table 21: EDX data taken from specimens of mortar with only nutrients.

Element	Spectrum 34
Carbon (C)	15.93
Oxygen (O)	45.35
Magnesium (Mg)	1.07
Aluminium (Al)	1.82
Silicon (Si)	4.66
Potassium (K)	-
Calcium (Ca)	31.18
Iron (Fe)	-
Total	100.0

Based on the analysis of the spectra, it is apparent that chemical reactions differ from bacterial self-healing in concrete. Silicon (Si) is typically a sign of a chemical reaction, as it plays a crucial role in cement hydration. For example, Spectrum 4 (21.8% Si, 12.27% Ca) and Spectrum 34 (4.66% Si, 31.18% Ca) represent chemical reactions, with silicon playing an important role in both processes (Wiktor et al., 2011). Meanwhile, Spectrum 13 (26.38% Ca, 17.59% C, and 56.03% O with no Si) suggests bacterial self-healing, as the absence of silicon and elevated calcium and carbon suggest the formation of calcium carbonate (CaCO3), a product of bacterial activity (De Muynck et al., 2010a). Spectrum 22 (6.56% Si, 38.27% Ca) appears to show a mixed contribution, with low silicon levels indicating both chemical reactions and possible bacterial involvement. As a result of this understanding, silicon is indicated as a marker of chemical reactions, while the absence of silicon, in combination with a large amount of calcium and carbon, is indicative of bacterial self-healing.

6.3 Assessing the Impact of %50 Supplementary Material Replacement on Self-Healing Concrete

The approach used in this study is largely based on methods from previous research on bio-concrete technology, with a few key differences. One notable change is the inclusion of a water absorption test, as well as the exclusive use of ground granulated blast-furnace slag (GGBS) as the supplementary material, instead of fly ash. As in previous studies, this research involved plain mortar as a control and mortar mixed with nutrients, specifically calcium lactate powder, to encourage bacterial growth and promote microbial-induced calcium carbonate precipitation (MICP). However, in this study, only GGBS was added to the mortar mix to replace part of the cement. The goal was to lower the pH and create a better environment for bacterial activity. The specimens were incubated in naturally occurring soil under fully saturated conditions to

replicate real-world conditions, encouraging the bacteria to work without relying on laboratory-grown strains. The water absorption test was added to evaluate how well the specimens healed themselves by measuring how much water they absorbed after cracks formed. This modification, along with the use of only GGBS instead of fly ash, sets this study apart from earlier research but still follows the general approach of enhancing bio-concrete with bacterial activity and supplementary materials.

6.3.1 Setting up the incubation environment

In this study, two different incubation environments using saturated soil were explored to better understand how soil can influence the healing process in bio concrete. Soil types and compositions vary widely, including materials like gravel, sand, silt, and clay. Our research specifically focused on using saturated soil, as such conditions are common in real-world environments, particularly in areas with high annual rainfall, such as the UK. The initial soil assessment involved a visual inspection to classify it, identifying it as a natural alluvial clay with a soft to firm consistency. It was dark brown, predominantly silty with slight sandy components. This type of soil is known to naturally host a wide variety of bacteria, which could potentially aid in the self-healing process of concrete. The pH of the soil was found to be neutral, ranging between 6.5 and 7.5, as measured by a handheld pH testing device. Particle Size Distribution testing showed that the soil was largely made up of fine-grained material, with over 35% clay, while sand and gravel made up less than 7.4%. Given the low permeability of fine-grained soil, about 15% of medium-grained sand was added to slightly increase its permeability. In the study, two different environments were created for the cement mortar: one in water and the other in saturated sand soil. When cement mortar is immersed in water, it experiences direct contact with the water, allowing for the efficient transport of dissolved substances, including byproducts from the healing process. However, when the mortar is placed in saturated sand soil, the soil matrix creates a more complex environment. The sand particles form a network of interconnected pores that affect the transport of gases and liquids, which can influence bacterial activity and the movement of gases like carbon dioxide (CO_2) produced during healing. By studying the healing of cement mortar in both water and saturated sand soil, we can observe how these environmental factors impact the healing process. To prevent contamination between the control and bio-mortar specimens, each set was incubated in separate plastic boxes filled with saturated soil. Half of the specimens were incubated in saturated soil containing sub-rounded grains of sand with free chemicals. This type of soil, commonly found at construction sites, was carefully chosen for its mechanical and chemical properties, as detailed in previous studies (Engineering, 2011).

6.3.1.1 Preparing soil samples for SEM and EDX analysis.

SEM combined with EDX is a powerful technique used to examine the fine details of soil, allowing us to explore its surface features, elemental composition, and particle structure, as shown in Figure 79. Surface Morphology: SEM provides clear, high-resolution images that reveal the size, shape, and surface characteristics of soil particles. Microstructure Analysis: It also helps us understand the arrangement of soil aggregates, pore structures, and the way soil components are organized. Elemental Composition: With EDX, we can identify and measure the elements present in the soil. This technique detects the X-rays emitted when the sample is bombarded with electrons in the SEM, and it also maps how the elements are distributed within the sample, offering insight into the soil's elemental makeup and variation.

For this study, a soil sample was prepared to analyse its components. As shown in Figure 80, the sample was first dried and crushed before being prepared for scanning electron microscopy (SEM). To ensure proper adhesion for imaging, we applied carbon adhesive tape to a stud and gently sprinkled the dried clay sample onto the surface. Excess clay was carefully removed using a fan or pump, and the stud was coated with gold/platinum before being placed under the SEM for analysis ('Chapter 7 GUIDELINE SAMPLE PREPARATION', 2019). When preparing clay samples for X-ray Diffraction (XRD), The clay samples are carefully thinned to approximately 1–2 millimetres, and the surface intended for X-ray exposure is meticulously polished to ensure accurate analytical results. Without proper polishing, surface irregularities may introduce distortions that compromise the reliability of the data obtained ('Chapter 7 GUIDELINE SAMPLE PREPARATION', 2019) . SEM and EDX together are excellent tools for analysing soil. SEM's high-resolution imaging gives us a detailed look at the soil particles, including their size, shape, and surface features, while also helping to examine the soil's structure and how the elements are arranged. In this study, SEM and EDX were also used to examine the precipitated material (healing products), allowing us to investigate their crystalline structure and chemical composition. This technique is particularly useful for confirming the chemical makeup of the self-healing products, ensuring we understand how the concrete repairs itself.

Figure 79: Scanning electron microscopy and energy dispersive X-ray (SEM-EDX).

Figure 80: The soil, following the processes of drying and crashing.

6.3.1.2 Water absorption test

Capillary rise is a common occurrence during the life cycle of cement-based materials (CBMs). In environments where groundwater contains harmful substances like chloride ions, sulphates, and carbon dioxide, capillary action can carry these aggressive agents into the material. This transport of harmful elements through capillary rise leads to the degradation of the CBM matrix and the corrosion of the reinforcing steel bars embedded in it (Belleghem *et al.*, 2016). The water absorption test is a simple, non-destructive method used to assess how impermeable cement-based materials are, by measuring their ability to prevent water penetration both before and after cracks form (Martys et al., 1997). This process relies on capillary action, which happens due to differences in surface tension between the material and water (Hartland, 2004). In this study, cracked mortar prisms were first dried in an oven at 100°C for at least a week until their weight stabilized, with only a 0.2% change. To prevent water from soaking into the sides, epoxy resin was applied, leaving just a small, exposed area around the crack at the bottom of the prism, as shown in Figure 81. The weight of each specimen was recorded at the start of the test. The specimen was then placed on plastic strips in a tray with a slightly open lid to limit airflow, as shown in Figure 82. The tray was filled with distilled water, ensuring the specimen's face was submerged about 2 mm above the plastic strips. To measure how much water the specimens absorbed, an electronic balance, accurate to 0.01 grams, was used to weigh them before and after the incubation period, as shown in Figure 82. Before weighing, any surface moisture was wiped off with a damp cloth to ensure accurate measurements. Water uptake was measured at intervals of 30 minutes, 1 hour, 2 hours, 3 hours, and 24 hours. The process continued until the specimen reached a stable weight, referred to as W2. The percentage of water absorption was then calculated using the formula:

$$\text{Percentage of water absorption} = (W1 \times W2) / W1 \times 100 \quad (9)$$

Where W1 is the initial weight and W2 is the final weight after immersion in water, both in kilograms.

Figure 81: Mortar coating with epoxy

Figure 82: The sealed container and electric balance

6.3.1.3 Visual inspection and image analysis

The healing process of cracked concrete involves several methods, including natural self-repair through rehydration and compound precipitation, as well as external methods such as applying sealants or specialized materials. However, finding a simple formula to measure the rate of concrete healing is complex, as it depends on many factors, including the type of concrete, environmental conditions, and the specific healing methods used (Amran *et al.*, 2022a). These factors interact in different ways, making it difficult to establish a one-size-fits-all approach for determining healing rates across different situations. In this study, the healing progression of cracked concrete was monitored through visual inspections using a Nikon P-400R digital microscope. Images of the cracks were taken both before and after the incubation period, with key positions marked at regular intervals to track changes in the crack size over time. To ensure the results were accurate, ultrasonic cleaning was applied to remove any leftover soil particles that could affect the measurements. The reduction in crack size was measured using the Nikon microscope. The healing rate was calculated using the formula (Equation 10), which is based on the reduction in crack dimensions:

$$Healing\ rate = \frac{Initial\ crack\ width - Final\ crack\ widh}{Durtion\ of\ healing} \qquad (10)$$

This formula compares the size of the crack at the beginning and end of the healing period, providing a way to quantify how much healing has occurred over time. By using this approach, we can get a clearer picture of how different factors influence the healing process. In addition to examining natural healing, this study also looks at how supplementary materials can affect the effectiveness of bio-concrete technology. Three different concrete mixtures were tested, each placed in separate Petri dishes: one mixture containing 50% Ground Granulated Blast Furnace Slag (GGBS) with nutrients, one with mortar and nutrients, and one with plain mortar. The aim is to compare the performance of these different formulations in supporting bio-concrete technology and enhancing self-healing properties, providing insights into how the use of GGBS and nutrients can influence healing. By exploring both the natural healing abilities of concrete and the impact of supplementary materials, this research offers a comprehensive understanding of the factors that contribute to the durability and self-healing of bio concrete. The findings will help improve bio-concrete systems, guiding the development of more efficient, sustainable solutions for concrete repair and maintenance. Further studies will be necessary to

assess how these healing mechanisms perform over the long term in real-world conditions, especially in environments with varying stresses and environmental factors.

6.3.2 Results and discussion

6.3.2.1 Soil analysis

In this study, the microstructure of the soil was examined using Scanning Electron Microscopy (SEM) and Energy-Dispersive X-ray Spectroscopy (EDX). Figure 83 provides SEM images of the soil particles, offering a close-up view of their surface features. Figure 84 presents the EDX analysis, which was used to identify the elements present in the soil and their relative concentrations. EDX is a widely used technique for determining the elemental composition and chemical properties of materials, making it a valuable tool for analysing soil samples. The EDX results are displayed as a spectrum graph showing the elemental breakdown of the soil sample. The analysis revealed that silicon (Si) and oxygen (O) were the most dominant elements, confirming their major role in the composition of the soil particles. As summarized in Table 22, the key elements found in the soil included silica, oxygen, carbon, and calcium. In addition to the SEM-EDX analysis, a preliminary visual inspection and sieve test were performed to classify the soil. These assessments identified the soil as natural alluvial soil, with a texture that ranged from soft to firm. It was characterized as dark brown silty clay with minor sandy components, indicating a mixed granular composition influenced by natural deposition processes.

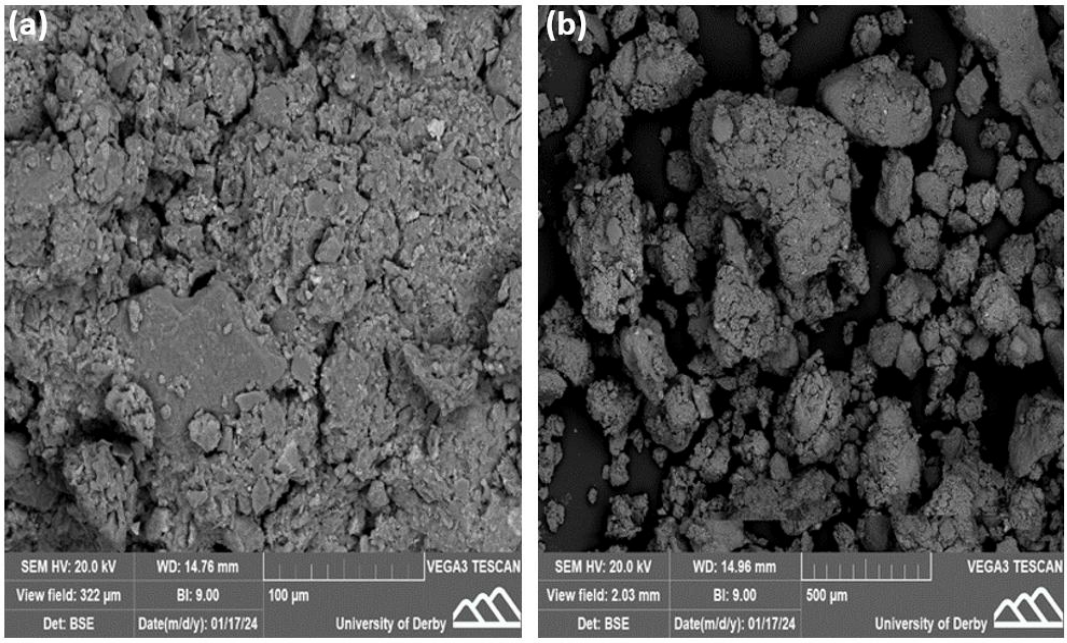

Figure 83: (a) Soil surfaces (b) soil particles

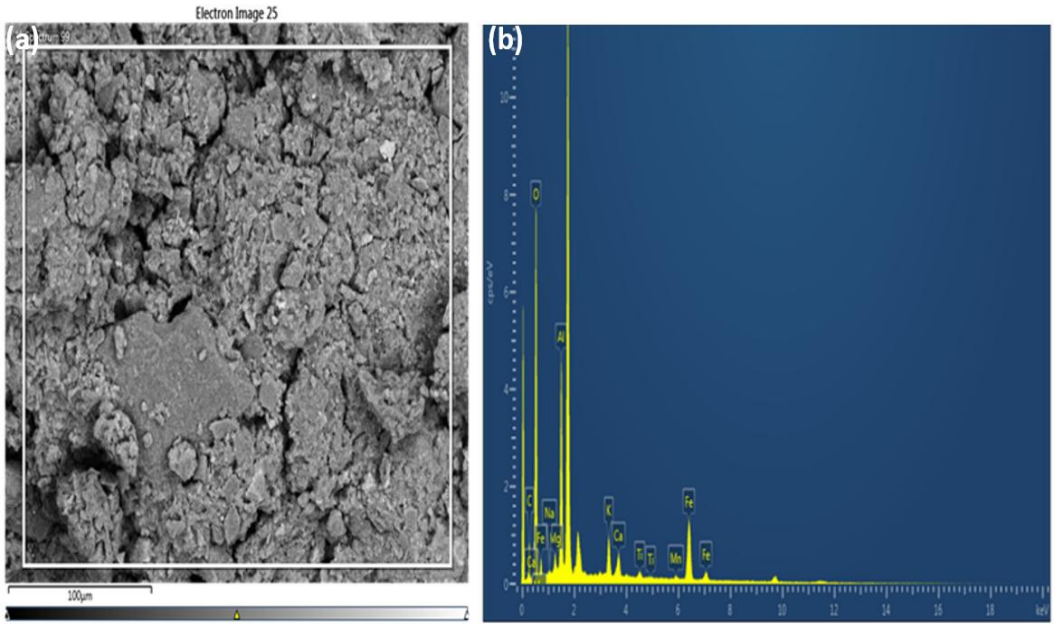

Figure 84: (a) Energy-Dispersive X-ray Spectroscopy (EDX) spectrum analysis. (b) Identified elements present in the EDX spectrum.

Table 22: EDX date of the soil sample

Element	%	Element	%	Element	%
C	30.45	Na	0.25	S	0.18
O	44.20	Mg	0.59	Cl	0.51
Al	3.47	Si	13.93	K	1.44
P	0.17	Ca	2.61	Fe	2.20
Ti	--	Mn	--	Total	100.00

6.3.2.2 Water absorption

The masses of the prisms were measured both before and after a 56-day incubation period in a fully saturated soil environment. During this phase, the prisms were exposed to different cement mixtures, including one containing 50% ground granulated blast furnace slag (GGBS) with added nutrients, and another made of Portland cement mortar supplemented with nutrients. Control mixtures of plain mortar and GGBS mortar, without any nutrient additives, were also evaluated. To ensure consistency, all prisms were initially oven-dried and then weighed in their saturated state after incubation. As shown in Figure 86, the results indicate a significant difference in water absorption levels after incubation. This effect is most pronounced in prisms containing GGBS with nutrient supplementation. In contrast, prisms made of plain mortar with nutrients exhibit a smaller change in water absorption compared to their GGBS counterparts. These findings align with existing research, which highlights the ability of GGBS to reduce water absorption due to its finer particle size and pozzolanic properties. Supporting this, a study by Almeida et al. (2018) concluded that GGBS cement reduces permeability, while another investigation by Hulagabali et al. (2018) demonstrated that GGBS decreases porosity and enhances compressive strength. However, figures 85 and 86 reinforces these observations, showing that GGBS mortar exhibits lower water absorption compared to plain mortar, even without nutrient additives. Moreover, prisms enriched with nutrients displayed improved crack healing and reduced water permeability after the incubation period. This effect was especially noticeable in prisms containing GGBS, underscoring the potential of bio-concrete technology in enhancing durability by effectively minimizing water intake. GGBS significantly reduces water absorption in prisms, particularly when combined with nutrients. On

the other hand, the limited changes observed in control prisms (without nutrients) before and after incubation suggest a minimal impact of the healing process in these cases.

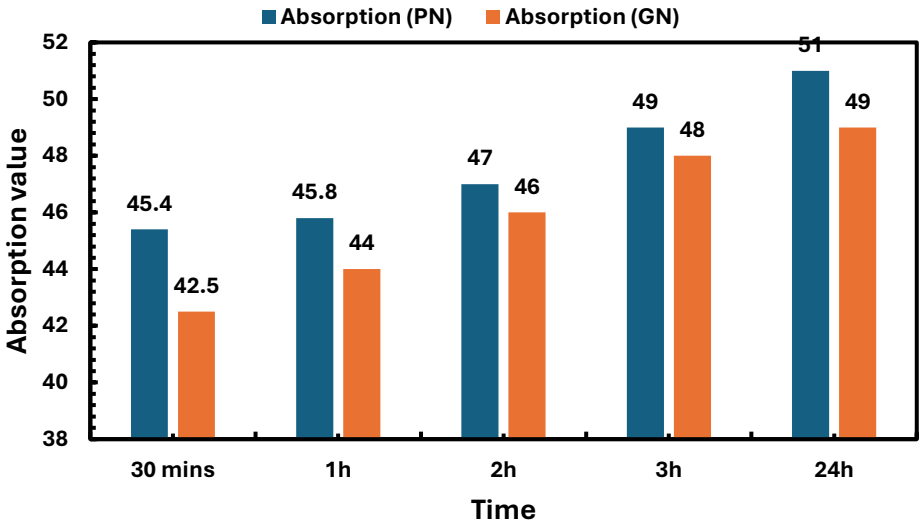

Figure 85: PN is a plain mortar with nutrients and GN is a GGBS mortar with nutrients.

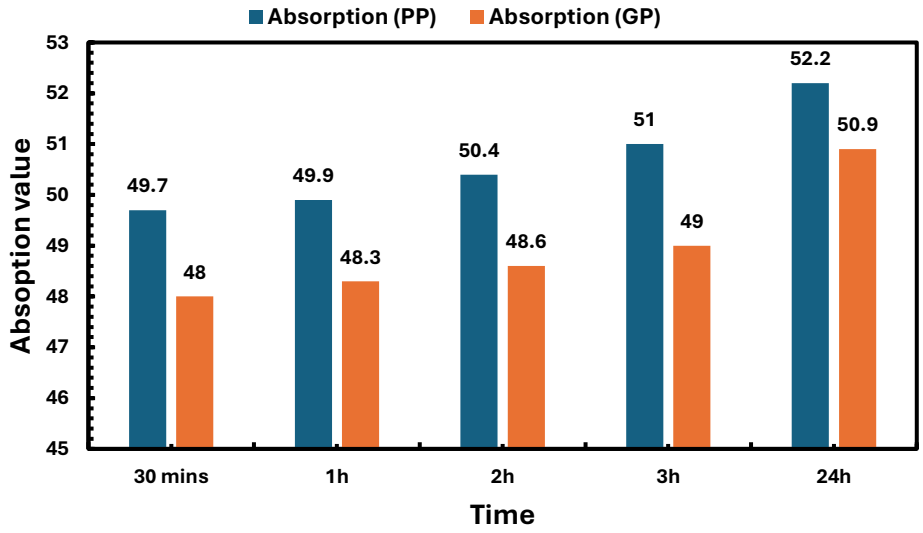

Figure 86: PP is a plain mortar, and GP is a GGBS mortar with no nutrients

6.3.2.3 Visual inspection and image analysis.

After the incubation phase, the samples were carefully retrieved from the soil environment, and detailed imaging was conducted to assess the effectiveness of crack sealing and quantify the healing ratio. Figures 87 and 88 provide a series of images illustrating the condition of cracks before and after incubation, highlighting varying degrees of closure, often marked by the presence of white precipitate material. The healing ratio was calculated using advanced image processing techniques applied to the crack areas. The results revealed a clear pattern: specimens containing GGBS and nutrients demonstrated significantly higher healing ratios compared to those made of plain mortar with nutrient supplementation. However, the precise mechanism driving this enhanced healing remains unclear. This raises questions about whether the improvement is due to the activity of indigenous soil bacteria or autogenous chemical reactions within the concrete. Supporting this, a study by Hamza *et al.* (2019) explored the

efficacy of bio-concrete technology using naturally occurring soil bacteria over a 100-day incubation period, achieving a notable healing ratio of up to 59.4%. Specimens without nutrient supplementation, such as plain mortar (PP) and GGBS mortar (GP), showed minimal evidence of healing on their crack surfaces after incubation in natural soil. In contrast, samples enriched with nutrients, particularly mortar with nutrients (PN) and GGBS mortar with nutrients (GN), exhibited the most substantial healing ratios. This observation is attributed to the metabolic activity of indigenous soil bacteria, which appears to be enhanced by the nutrient additives.

Figure 89 further supports these findings by illustrating the calculated healing rates. Specimens containing GGBS with nutrients (GN) exhibited the highest healing rate, followed by mortar with nutrients (PN). On the other hand, the control specimens (PP) and GGBS mixes without nutrients (GP) showed significantly lower healing rates, likely attributable to autogenous self-healing driven by chemical reactions. These findings align with the results of the absorption tests, highlighting the connection between water absorption behaviour and crack healing. The data suggest that the extent of crack healing has a significant impact on water absorption properties, which in turn influences the durability and overall performance of the concrete. This underscores the potential of nutrient-enriched GGBS mortars in advancing bio-concrete technology and improving the longevity of concrete structures.

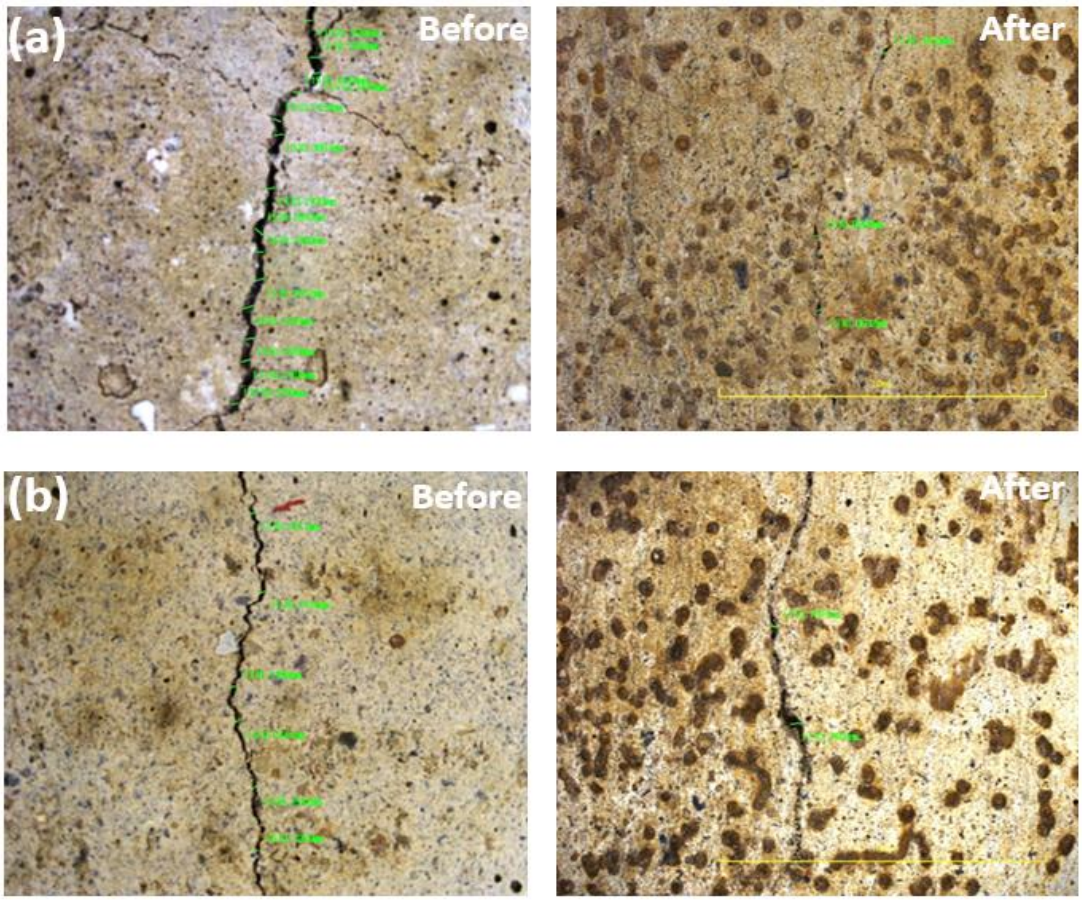

Figure 87: (a) Mortar containing 50% (GGBS) with added nutrients, before and after incubation. (b) Mortar containing 50% (GGBS) without nutrients before and after incubation.

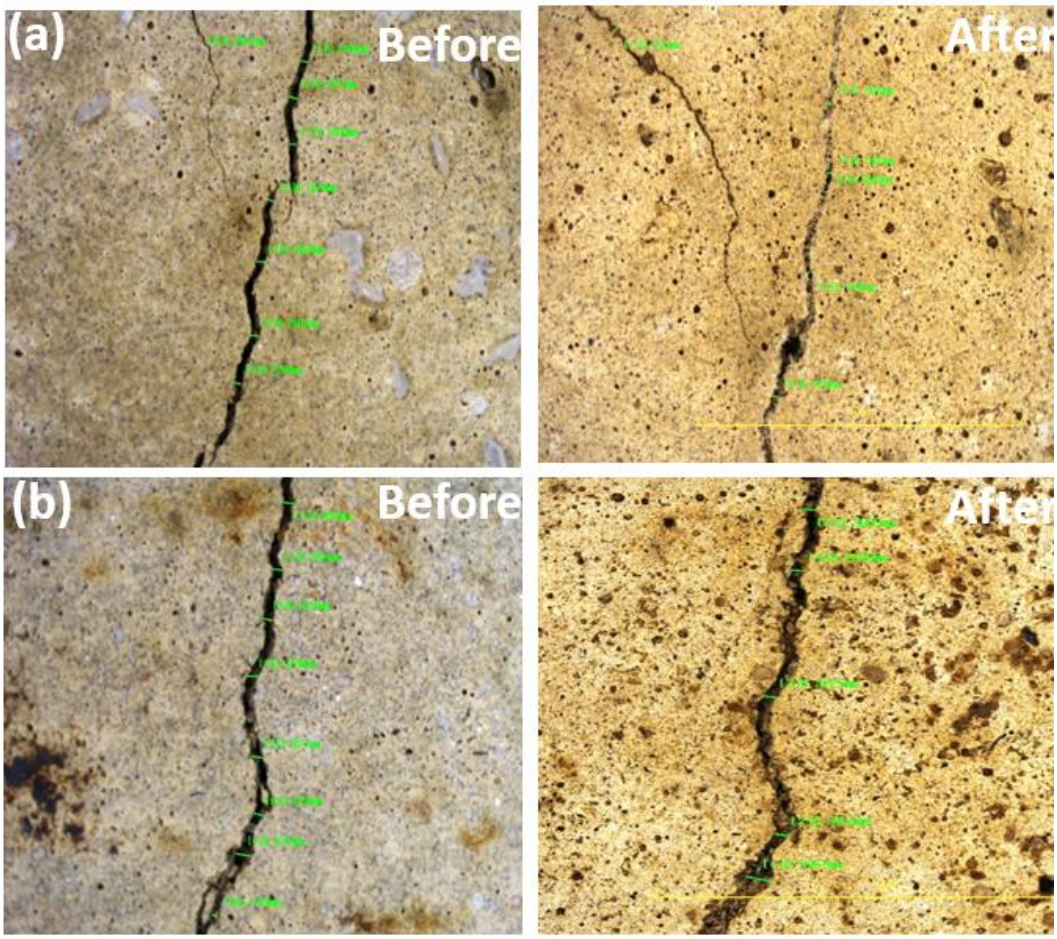

Figure 88 : (a) Plain mortar specimens with added nutrients before and after incubation. (b) Plain mortar specimens without nutrients before and after incubation.

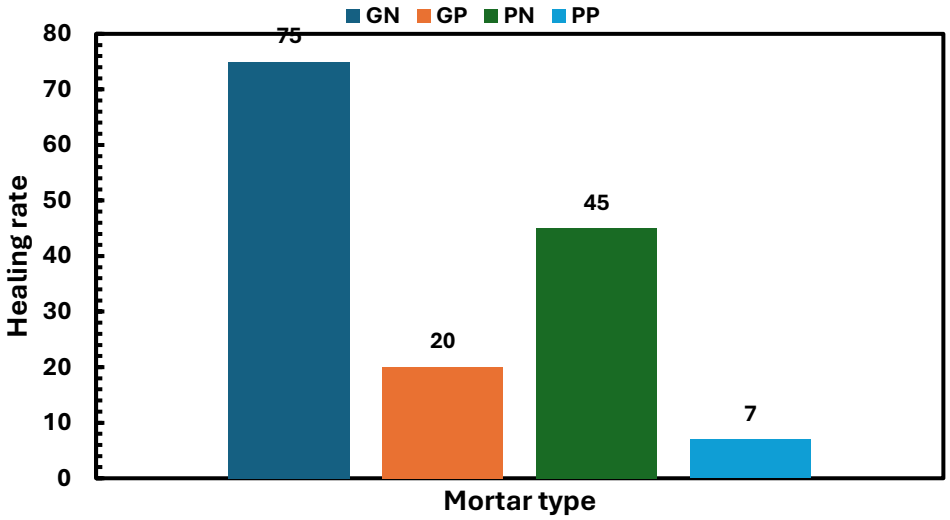

Figure 89: Healing rates of various mortar types.

6.3.2.4 Microstructural analysis of healing products

The investigation into the composition and characteristics of healing products involved a detailed analysis of the microstructure formed on the cracked surfaces of various specimens.

The analysis carried out using Scanning Electron Microscopy (SEM) shown in Figure 90 and Energy-Dispersive X-ray Spectroscopy (EDX) detailed in Tables 23, 24, 25, and 26, revealed that calcium carbonate crystals were the dominant microstructural feature, especially in mortar samples containing nutrients. The formation of these crystals was most noticeable in GGBS mortars enriched with nutrients. The results clearly show that adding nutrients, specifically calcium lactate powder, significantly improves the self-healing ability of all the tested specimens. In contrast, the control samples and GGBS mortars without added nutrients showed no signs of calcium carbonate formation on their crack surfaces. However, SEM and EDX analyses revealed significant formation of ettringite in these nutrient-free samples. Ettringite, a hydrated calcium aluminium sulfate hydroxide ($Ca_6Al_2(SO_4)_3(OH)_{12}{\cdot}26H_2O$), is typically formed through the reaction between sulfate ions and aluminate phases in cement. This compound naturally develops during the hydration process due to the inclusion of calcium sulfate in cement to regulate hydration (Hamdan et al., 2011). As suggested by Tittelboom et al. (1994), many biologically mediated chemical processes can now be harnessed to improve concrete healing. The findings of this study demonstrate that the chemical environment in plain concrete or mortar is often unsuitable for bacterial growth due to factors such as high pH and salinity, which can inhibit bacterial activity. However, the addition of supplementary materials like GGBS alters the chemical environment, creating conditions conducive to bacterial proliferation. This is supported by SEM and EDX analyses, which revealed calcium carbonate deposits within the cracks, indicative of bacterial activity and enhanced crack healing. The EDX analysis also identified the presence of silicate and oxygen, critical elements for the formation of calcium silicate hydrate (C–S–H). The ongoing hydration of cement particles leads to the formation of C–S–H, which plays a vital role in filling cracks and improving structural stability. While the SEM-EDX analysis was limited to specific microscopic regions, the study acknowledges that these regions may not fully represent the entire crack surface. Despite this limitation, the focus on these areas provided valuable insights into the microstructure and composition of the healing products. Additionally, complementary techniques, such as microscopic inspection and water absorption measurements (discussed in earlier sections), were integrated to offer a more comprehensive understanding of the self-healing mechanisms across all specimens. Together, these methods provided a holistic perspective, despite the inherent limitations of microscopic examination (Hamza *et al.*, 2021).

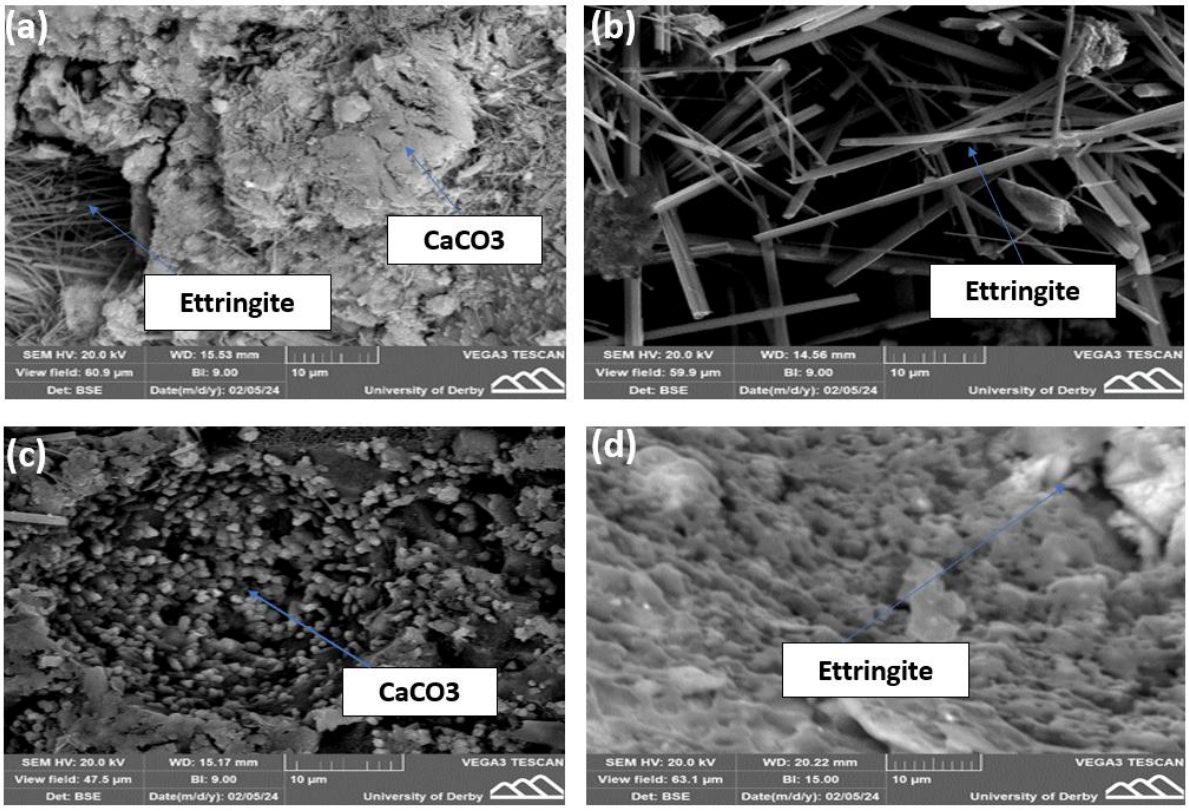

Figure 90: SEM analysis for (a) Mortar with nutrients incubation in soil environment. (b) %50 GGBS replacement with no nutrients in soil environment. (c) %50 GGBS replacement with nutrients incubation in soil environment. (d) Plain mortar incubation in soil environment

Table 23: Mortar with nutrients incubation in soil environment

Element	Percentage (%): Spectrum 14
Carbon (C)	3.42
Oxygen (O)	39.76
Aluminum (Al)	1.94
Sulfur (S)	4.57
Calcium (Ca)	50.32
Total Composition	100.00

Table 24: %50 GGBS replacement with nutrients incubation in soil environment

Element	Spectrum 26 (%)
C	6.96
O	29.60
Mg	0.88
Al	1.80
Si	6.87
Ca	53.90
Total	100.00

Table 25: Plain mortar incubation in soil environment

Element	Percentage (%): Spectrum 10
Carbon (C)	6.40
Oxygen (O)	40.55
Aluminum (Al)	4.52
Silicon (Si)	1.45
Sulfur (S)	7.44
Calcium (Ca)	38.20
Silver (Ag)	1.44
Total Composition	100.00

Table 26: %50 GGBS replacement with no nutrients in soil environment

Element	Percentage (%): Spectrum 24
Carbon (C)	8.64
Oxygen (O)	47.10
Magnesium (Mg)	8.07
Aluminum (Al)	4.26
Silicon (Si)	2.93
Sulfur (S)	4.65
Calcium (Ca)	23.33
Silver (Ag)	1.04
Total	100.00

6.4 Assessing the Impact of water flowing on Self-Healing Concrete

Understanding the impact of pH on bacterial activity within concrete is crucial due to the high presence of calcium hydroxide ($Ca(OH)_2$) in its pores. The interaction of water from the external environment creates a highly alkaline microenvironment, with pH levels often reaching 13. However, at the mouth of cracks, the pH is typically lower, between 9 and 11, due to water ingress (Wu et al., 2019). This high alkalinity also presents environmental concerns, as concrete structures have the potential to leach various ions—such as aluminium, calcium, chromium, magnesium, sodium, potassium, and zinc—into surrounding water bodies, thereby elevating the water's pH. The extent and rate of hydroxyl ion leaching are influenced by multiple factors, including the type of cement used, structural design, exposed surface area, degree of carbonation, and the dynamics of water flow across the concrete surface (David et al., 2013).

Calcium carbonate ($CaCO_3$) can form at different pH levels, either on the concrete surface or within cracks. For instance, Nielsen *et al.* (2019a) found that incorporating pozzolanic materials, such as fly ash, accelerates pH reductions in concrete. Similarly, (Cheng *et al.*, 2005b) observed that using ground granulated blast furnace slag (GGBS) lowers the pH from 11 to below 10. This reduction in pH creates a more favourable environment for bacterial activity, which plays a key role in bio-concrete's self-healing properties. Research by Nielsen *et al.* (2019a) further supports this, linking lower pH levels to increased bacterial activity, which enhances the effectiveness of the bio-concrete healing process. However, the production of cement contributes approximately 8% of global CO_2 emissions, making it a highly energy-intensive industry (Achternbosch *et al.*, 2011). This has led to a growing emphasis on using cement replacements, which not only reduce the carbon footprint but also repurpose waste materials that would otherwise go to landfills (Engineering, 2011). For example, fly ash has been shown to enhance concrete durability, improve resistance to sulfate attack and chloride penetration, and reduce leaching (Chalee *et al.*, 2009). Similarly, GGBS enhances sulfate resistance and maintains strength and durability (Pavía et al., 2008). Typically, GGBS replaces 30–85% of cement in mixtures, with 40–50% being the most common range. Fly ash is usually incorporated at levels of 6–35%, as outlined in British Standard EN 197-1 (*British Standards Institute, 2011. Bs En 197-1: 2011*). This study investigates the role of water flow in enhancing the self-healing capacity of bio-concrete, particularly in underground structures. While conventional methods of self-healing concrete are well-documented, the effects of dynamic water flow on the healing process remain unclear. Water flow introduces complex environmental factors that can influence nutrient distribution, bacterial activity, and the overall efficiency of crack healing. By exploring this dynamic interaction, the study aims to address a critical gap in understanding the impact of water flow on bio-concrete's performance. The findings will provide valuable insights into how water flow affects the self-healing mechanisms of bio-concrete, particularly in underground applications. This research seeks to optimize bio-concrete technology for sustainable infrastructure, ensuring its effectiveness under real-world conditions.

6.4.1 Materials and methods

The specimens were prepared, and cracks were introduced using well-established methods from previous studies to ensure consistency across all samples. For the flowing water test, a digital hydraulic bench was used to precisely control the water flow conditions. The bench was set to deliver a flow rate of 17.7 litters per minute at a working pressure of 0.295 litters. Nine mortar prisms were arranged vertically on the bench with equal spacing between them, as shown in Figure 91.

Throughout the 28-day experiment, the prisms were kept fully submerged in tap water, which was replaced daily to maintain consistent water quality and experimental conditions. After 28 days, the prisms were carefully removed from the water flow setup to allow for controlled crack formation. In addition, three identical plastic containers, each with a capacity of 5 litters, were prepared for further testing. To ensure the prisms were fully submerged, each container was filled with 1 litter of tap water. The nine mortar prisms, identical in size and composition, were evenly placed in the three containers, as illustrated in Figure 92. During the 28-day immersion period, the pH of the water was closely monitored using a calibrated pH probe to ensure stable and consistent conditions throughout the experiment.

Figure 91: Digital hydraulic bench with prisms positioned within the setup.

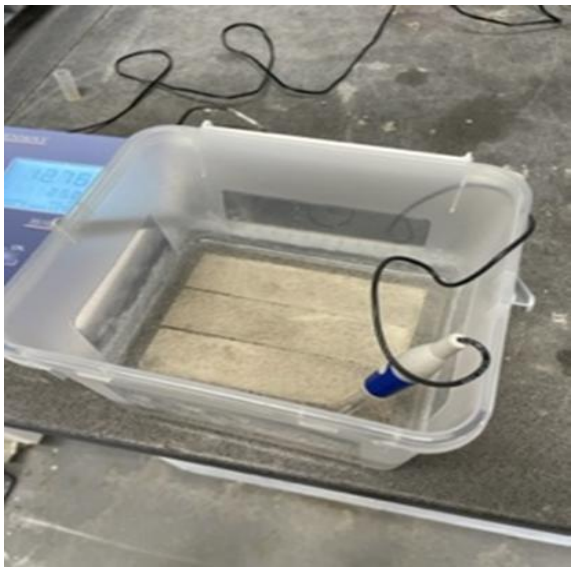

Figure 92: Prisms submerged within the experimental containers.

6.4.2 Incubation and soil analysis

In this study, natural soil was collected from the field and subjected to sieve analysis in accordance with the BS EN 933 standard to determine its Particle Size Distribution (PSD). The experimental setup involved preparing mortar specimens mixed with standard sand, which were divided into three groups: MN (mortar with nutrients), MF (mortar with nutrients and fly ash replacement), and MG (mortar with nutrients and GGBS replacement). These specimens were incubated in fully saturated soil for 28 days. To serve as a control, plain mortar with nutrients was also included to observe any natural healing (autogenous healing) that might occur through the continued hydration of the mortar or the activity of bacteria capable of thriving in the challenging chemical environment of concrete. After the mortar specimens developed cracks, they were carefully placed into plastic containers. Dry soil was then added, with sand layers placed below and above the specimens and an additional sand layer separating them. Each container held three specimens, and the incubation was conducted at room temperature (approximately 23°C). The cracked specimens were exposed to 28-day cycles of full saturation in the soil. Before the test began, the soil was fully saturated by raising the water level above the specimens until it reached the surface. Any water lost through evaporation was replenished by adding water as needed. Throughout the incubation period, the soil's pH was regularly monitored to ensure it remained within the target range.

6.4.3 Results and discussion

The SEM analysis of cracked surfaces from various mortar types is presented in Figure 93 (a) illustrates the crack surface of plain mortar exposed to flowing water, revealing clear evidence of calcium carbonate precipitation. Elemental analysis identified calcium (Ca), oxygen (O), and carbon (C) as the primary constituents of the deposits, all recognised as key components of calcium carbonate ($CaCO_3$) (Khan et al., 2023). This observation suggests that the particles on the crack surface are likely calcite or another polymorph of calcium carbonate. To confirm this, X-ray diffraction (XRD) analysis was conducted, verifying that the precipitates were indeed calcite, consistent with findings in prior studies (Lee et al., 2017) . Figure 93 (b) depicts the crack surface of plain mortar exposed to stagnant water, where precipitation was also observed. Energy-dispersive X-ray (EDX) analysis identified silicon (Si) and oxygen (O) as key elements within the material deposited in the cracks. These findings indicate the formation of calcium silicate hydrate (C-S-H), a product of continued cement hydration. This aligns with earlier research which demonstrates that autogenous healing in cementitious materials commonly involves the formation of C-S-H (Javeed *et al.*, 2024). Mortar specimens containing fly ash replacement (Figures 94(c, d)), the results reflect the distinct chemical properties of fly ash. The fly ash utilised in this study had low calcium content, resulting in elevated concentrations of silicon (Si) and oxygen (O) in both flowing and stagnant water conditions. The reduced presence of calcium carbonate indicates that self-healing in these specimens was predominantly driven by chemical processes rather than bacterial activity. This aligns with previous studies, which highlight that fly ash promotes autogenous healing by reducing calcium hydroxide (CH) and tricalcium aluminate (C_3A) content and supporting the formation of ettringite. The role of salt crystallisation pressure within cement pores further corroborates these observations, as noted in related studies [9]. Mortar specimens containing ground granulated blast furnace slag (GGBS) replacements showed clear differences in mineral formation depending on the water conditions they were exposed to. In specimens exposed to flowing water, analysis using scanning electron microscopy (SEM) and energy-dispersive X-ray (EDX) revealed that calcium carbonate was the dominant mineral forming on the crack

surfaces. This mineral likely formed due to chemical reactions supported by the movement of water; a process supported by findings in existing research. On the other hand, specimens exposed to stagnant water displayed a wider range of minerals, including calcium carbonate, ettringite, and calcium silicate hydrate (C-S-H). This variety can be attributed to the ongoing hydration of unreacted cement particles in the absence of water movement.

The data provided in the tables (27, 28, 29, 30, 31, and 32) highlights significant differences in calcium (Ca) content across the spectra, which directly affects their potential for bacterial self-healing. Spectrum 87, with the highest calcium content (28.98%), stands out as the most suitable for microbial-induced calcite precipitation (MICP). MICP plays a key role in bacterial self-healing, as calcium ions combine with carbonate ions produced by bacteria to form calcium carbonate ($CaCO_3$), sealing cracks and improving structural strength. These findings align with previous studies (Xu, Wang and Wang, 2018). Furthermore, Spectrum 87 also has moderate levels of silicon (13.91%) and oxygen (45.68%), which are essential for autogenous healing. These elements help form calcium silicate hydrate (C-S-H), an important compound for sealing cracks and enhancing structural integrity (Neville, 1995a). In contrast, Spectrum 54, with no calcium content (0%), shows limited potential for bacterial self-healing. While its high silicon content (33.46%) could support some degree of autogenous healing, the absence of calcium severely limits its ability to support MICP, a critical component of bacterial healing (H M Jonkers, no date). These results emphasize the importance of calcium in enabling bacterial self-healing processes. Spectrum 87 is identified as the most promising candidate for effective self-healing, while Spectrum 54 relies primarily on non-bacterial healing mechanisms.

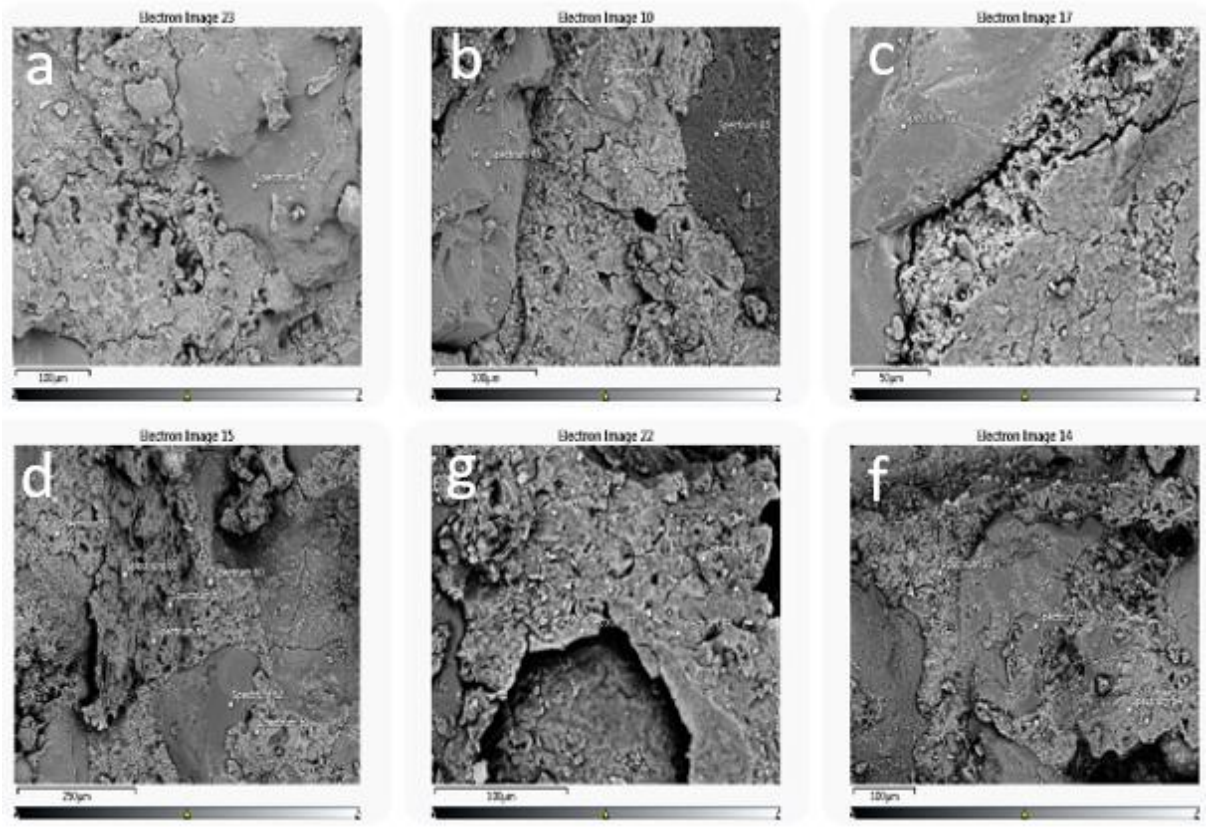

Figure 93: SEM images of different type of mortar: a. Plain mortar exposure to flowing water: b. plain mortar exposure to stagnant water: c. Fly ash mortar exposure to flowing water: d. fly ash mortar exposure to stagnant water:(f) GGBS mortar exposure to flowing water: g. GGBS mortar exposure to stagnant water.

Table 27: EDX data for plain mortar exposure to flowing water.

Element	Percentage (%): Spectrum 93
Carbon (C)	3.93
Oxygen (O)	36.52
Magnesium (Mg)	-
Aluminum (Al)	1.03
Silicon (Si)	2.99
Sulfur (S)	-
Potassium (K)	-
Calcium (Ca)	51.60
Iron (Fe)	3.94
Total Composition	100.00

Table 28: EDX data for plain mortar exposure to stagnant water

Element	Percentage (%): Spectrum 44
Carbon (C)	6.42
Oxygen (O)	57.53
Magnesium (Mg)	-
Aluminum (Al)	-
Silicon (Si)	35.19
Sulfur (S)	-
Calcium (Ca)	0.86
Iron (Fe)	-
Total Composition	100.00

Table 29: EDX Fly ash mortar exposure to flowing water

Element	Percentage (%): Spectrum 70
Carbon (C)	6.55
Oxygen (O)	53.84
Aluminum (Al)	16.45
Silicon (Si)	17.31
Potassium (K)	1.49
Calcium (Ca)	4.37
Iron (Fe)	-
Total	100.00

Table 30: EDX data for fly ash mortar exposure to stagnant water

Element	Percentage (%): Spectrum 58
Carbon (C)	-
Oxygen (O)	35.78
Magnesium (Mg)	-
Aluminum (Al)	-
Silicon (Si)	20.99
Potassium (K)	-
Calcium (Ca)	23.79
Iron (Fe)	-
Gold (Au)	19.44
Total	100.00

Table 31: EDX data for GGBS mortar exposure to flowing water.

Element	Percentage (%): Spectrum 87
Carbon (C)	5.38
Oxygen (O)	45.68
Magnesium (Mg)	-
Aluminum (Al)	3.74
Silicon (Si)	13.91
Potassium (K)	0.58
Calcium (Ca)	28.98
Iron (Fe)	1.74
Total	100.00

Table 32: EDX data for GGBS mortar exposure to stagnant water.

Element	Percentage (%): Spectrum 54
Carbon (C)	12.57
Oxygen (O)	54.22
Magnesium (Mg)	0.51
Aluminum (Al)	2.04
Silicon (Si)	8.69
Sulfur (S)	-
Calcium (Ca)	21.08
Iron (Fe)	0.89
Total Composition	100.00

6.5 Assessing the Impact of different type of soil on Self-Healing Concrete

Soil structure experiences the most significant improvement during consecutive cropping when organic farming practices are combined with reduced tillage. Additionally, incorporating a ley period has been shown to greatly enhance soil structure in heavily tilled areas. Researchers from the University of Derby Hamza *et al*. (2021) explored the potential of bio-concrete technology by using naturally occurring soil bacteria. Their study involved incubating samples in fully saturated conditions for 100 days, during which mortar supplemented only with nutrients achieved a healing rate of 50%. Building on this, the research aims to assess the impact of four different incubation environments on self-healing concrete: water (as a control), natural soil, organic soil, and a combination of organic and natural soils. Using techniques such as microscopy, chemical analysis, and crack sealing evaluations, the study seeks to uncover how different soil types influence the self-healing performance of concrete. By exploring the interaction between soil and concrete, the findings could pave the way for developing stronger and more sustainable construction materials for underground structures. This research ultimately aims to harness the natural properties of organic and natural soils to enhance concrete's self-healing capabilities, offering innovative solutions to improve the durability and lifespan of subterranean infrastructure.

6.5.1 Materials and Methods

6.5.1.1 Specimens Preparation and Crack Creation

This study involved the preparation of 12 mortar samples, meticulously crafted in line with BSEN 196-1 standards. Calcium lactate powder, sourced from SPECIAL INGREDIENTS in the UK, was incorporated as a nutrient for bacteria. Nine of these samples were exposed to varying soil conditions: organic soil from Levington Organic Blend in the UK, natural soil collected from the fields at the University of Derby, and a composite blend of organic and natural soils, all prepared according to BSEN 196-1 specifications. The remaining three samples were immersed in tap water, serving as a control group. Each specimen, measuring 4 × 4 × 16 cm, was reinforced with a central fibre mesh to prevent structural failure during crack formation. Detailed mixture proportions for the specimens are provided in Table 33. After a curing period of 28 days, cracks were induced in the samples using a three-point load test. After the curing process, cracks were induced in all specimens using a three-point bending test, following the crack creation techniques previously established in earlier studies. The study aims to explore the potential of organic soil in promoting effective crack healing in concrete specimens. This research provides valuable insights into bio-concrete technology and its potential to enhance the resilience and longevity of concrete structures, particularly those used in underground environments.

Table 33: Mortar specimens mix proportion.

Ingredients	PW	PO	PN	PC
Cement	500	500	500	500
Sand	1.5	1.5	1.5	1.5
Water	250	250	250	250
Nutrients	20	20	20	20

6.5.1.2 Incubation environment procedure

A sieve test, performed in accordance with BS EN 933 standards, was used to analyse the Particle Size Distribution (PSD) of the natural soil. Mortar specimens were divided into four groups (PW, PO, PN, and PC) and incubated with standard sand in different soil environments for 100 days as shows in figure 94. These environments included plain mortar in water (PW), mortar with nutrients in organic soil (PO), mortar with nutrients in natural soil (PN), and mortar with nutrients in a composite of organic and natural soils (PC). All specimens were kept fully saturated throughout the incubation period. Plain mortar specimens served as a control group to assess any natural remediation potential due to continuous hydration. The natural soil, sourced from fields near the University of Derby, was visually classified as a natural alluvial deposit consisting of soft to firm, dark brown silty clay with slight sandy characteristics. This type of clay is known to support a wide variety of naturally occurring bacterial species. The natural soil's pH ranged between 6.60 and 7.45, while the organic soil exhibited a more acidic pH range of 5.34 to 5.60. Following the cracking process, the specimens were carefully transferred into plastic containers. Dry soil was added in two layers: one beneath the specimens and another on top and in between them. Figure below provides an illustration of the specimen arrangement within the containers.

Figure 94: Prisms inside containers immersed in the soil

6.5.2 Soil analysis by (SEM and EDX)

SEM combined with EDX is a highly effective technique for analysing soil, including organic soil, by examining microscopic features such as surface structure, elemental composition, and particle morphology. Surface Morphology: SEM captures high-resolution images of soil particles, offering detailed insights into their size, shape, and surface characteristics, which are particularly relevant in organic soil studies. Microstructure Analysis: This method allows for a closer look at soil aggregates, pore structures, and the organisation of soil components, providing a deeper understanding of organic soil properties. Elemental Composition: EDX identifies and quantifies the elements present in soil particles by detecting characteristic X-rays emitted during SEM analysis. It also maps the spatial distribution of these elements, highlighting variations and differences between organic and non-organic soils.

In this study, a single soil sample was analysed to explore its components, including organic soil, for experimental purposes. The preparation for SEM involved adhering a carbon tape to a stud, lightly sprinkling dried clay onto the tape, and carefully removing any excess particles. The stud was then coated with Gold or Platinum to facilitate SEM imaging. For X-ray Diffraction (XRD) analysis, the clay samples were prepared by thinning them to 1–2 millimetres and polishing the surface to optimise X-ray exposure. This polishing step ensures greater accuracy and minimises distortions, particularly important when comparing organic and non-organic soils. The self-healing products derived from organic soil were analysed using SEM and EDX technologies to investigate their crystalline structure and chemical composition. This approach is essential for understanding and comparing the self-healing products formed in organic versus non-organic soils. Both soil types are visually depicted in Figure 95.

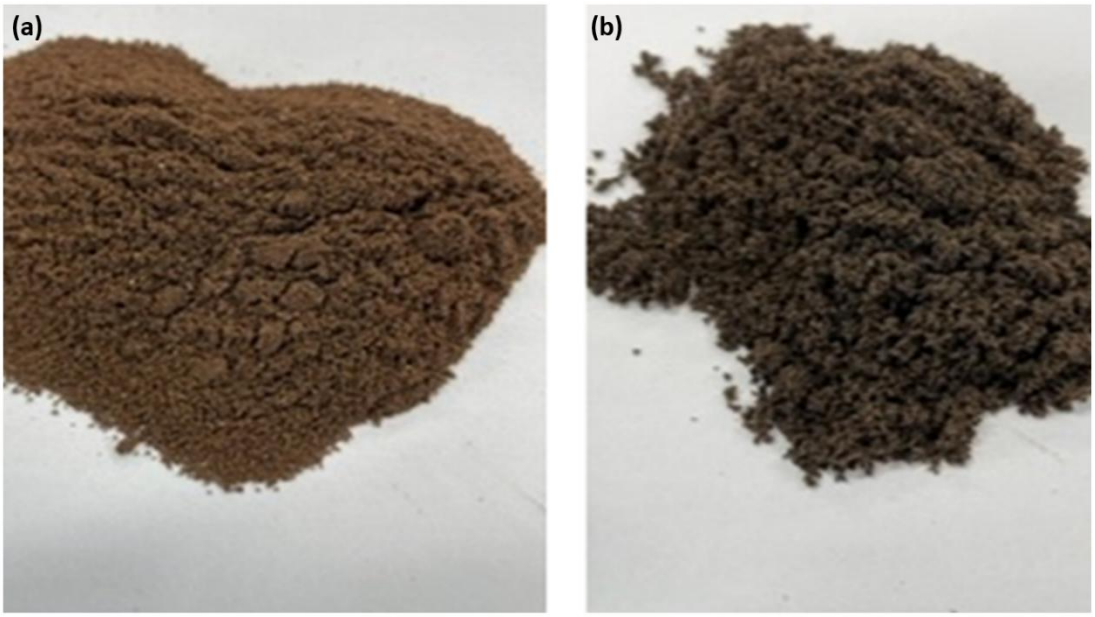

Figure 95: (a) Natural soil. (b) Organic soil

6.5.3 Results and discussion

6.5.3.1 Soil analysis SEM

Organic and natural soils exhibit distinct differences, and SEM analysis provides a detailed understanding of these variations. Recognising these differences is essential for evaluating how each soil type influences the performance of self-healing concrete, particularly in fostering microbial activity. SEM analysis offers valuable insights into the physical and chemical characteristics of both soil types, shedding light on their interaction with self-healing concrete (Amran *et al.*, 2022b). Figure 96 presents SEM images of natural and organic soils, highlighting noticeable differences in particle size and shape. The images show that natural soil contains larger, irregularly shaped particles, resulting in a coarser texture. In contrast, organic soil is composed of smaller, more uniform particles, indicating a finer texture. The shapes of the particles also differ significantly. Natural soil is characterised by angular, varied particles, which can lead to less uniform pore spaces. Organic soil, however, features more rounded and consistent particles, potentially creating interconnected and evenly distributed pores. In terms of porosity, the larger particles in natural soil produce wider gaps, leading to fewer but larger pores. On the other hand, organic soil's smaller, uniform particles contribute to a higher number of smaller pores, improving overall porosity and permeability. Additionally, the rougher surface texture of natural soil may impact microbial adhesion and colonisation, whereas the smoother surface of organic soil is likely to provide a more favourable environment for bacterial growth. These differences in particle size, shape, and texture significantly affect the soil's capacity to interact with and support microbial activity (Erktan, et al., 2020). The ability of water and nutrients to move through the soil, essential for reaching bacteria, is influenced by its porosity and permeability. Organic soil, with its finer particles and higher porosity, is better suited to promoting microbial activity compared to natural soil. This aligns with findings by (Lipiec *et al.*, 2006) who emphasised the importance of pore structure and infiltration in predicting water and nutrient flow within soil profiles.

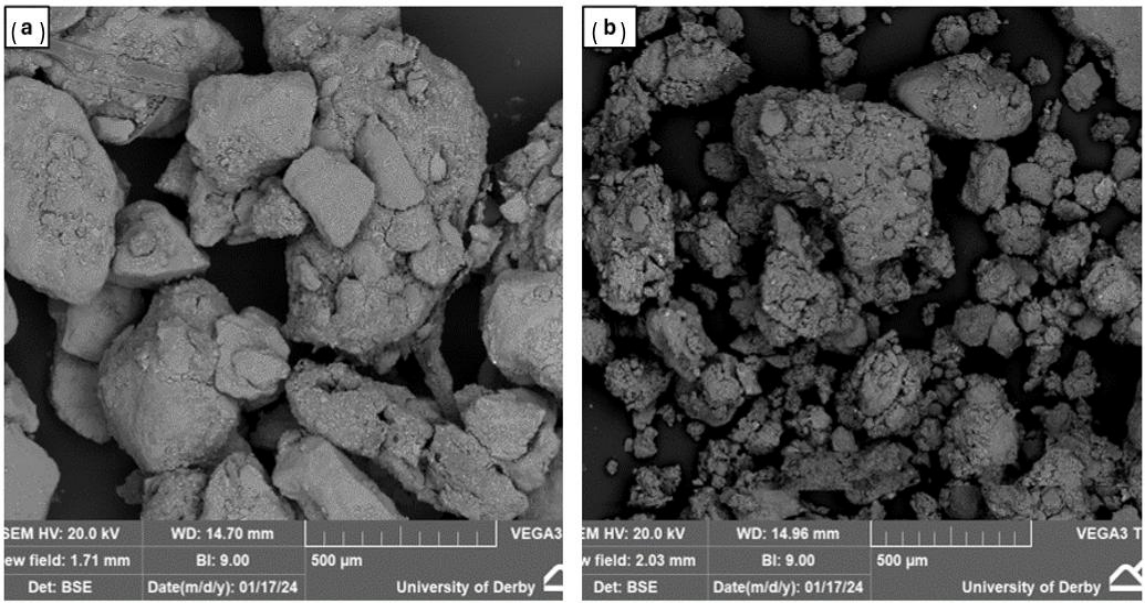

Figure 96: SEM analysis of soil structure (a) natural soil, (b) organic soil.

6.5.3.2 Soil analysis EDX

Figures 97 illustrate the Energy Dispersive X-ray (EDX) spectra for organic and natural soils, respectively, highlighting their elemental compositions through distinct peaks associated with various elements. The EDX spectrum for organic soil reveals a significant silicon (Si) peak, indicating a high concentration of this element. Oxygen (O) also exhibits a prominent peak, suggesting the presence of oxides or organic matter. Aluminium (Al) is notable and typically associated with clays and silicate minerals. Additionally, smaller peaks correspond to trace elements such as carbon (C), sodium (Na), magnesium (Mg), calcium (Ca), potassium (K), titanium (Ti), manganese (Mn), and iron (Fe). Similarly, the spectrum for natural soil shows major and minor elements, with silicon (Si) and oxygen (O) displaying the highest peaks, confirming their roles as dominant components. Aluminium (Al) is also evident, indicating the presence of common soil minerals. Trace elements, including carbon (C), sodium (Na), magnesium (Mg), calcium (Ca), potassium (K), titanium (Ti), manganese (Mn), and iron (Fe), are represented by smaller peaks. Unlike organic soil, the natural soil spectrum also includes sulfur (S), phosphorus (P), and chlorine (Cl) as minor peaks, indicating additional compounds or minerals absent in the organic soil. The key differences in elemental composition between the two soils are noteworthy. Organic soil contains higher concentrations of silicon (Si), oxygen (O), and aluminium (Al), along with a broader variety of trace elements. In contrast, natural soil shares high levels of silicon (Si) and oxygen (O) but features additional elements such as sulfur (S), phosphorus (P), and chlorine (Cl). These differences can be attributed to variations in organic matter, mineral composition, and environmental factors affecting soil formation. For self-healing concrete applications in underground structures, elements like calcium (Ca) and silicon (Si) are crucial, as they are essential for forming calcium silicate hydrate (C-S-H) gel, a key component of the self-healing mechanism. Both soil types contain calcium (Ca), which plays a role in the formation of self-healing compounds. However, the additional elements in natural soil, such as sulfur (S), phosphorus (P), and chlorine (Cl), may contribute to more complex chemical interactions that could enhance self-healing properties under certain conditions. The high silicon (Si) content in both soils is advantageous for forming C-S-H gel,

which is fundamental to the self-healing process. While both soils possess the necessary elements for self-healing, the presence of sulfur (S), phosphorus (P), and chlorine (Cl) in natural soil could make it more effective for specific self-healing mechanisms. According to Hamza *et al*. (2021) natural soil contains a diverse array of organic materials and a rich microbial community, both of which can significantly influence the self-healing capabilities of concrete structures. When concrete interacts with these microbial communities, the self-healing process may be enhanced. However, natural soil's larger and more irregular particle sizes can create wider gaps, potentially limiting the movement of bacteria and nutrients. This limitation could make organic soil, with its finer and more uniform particles, more advantageous in some scenarios. Additionally, as noted by Bueno Márquez *et al*. (2008) organic soil often originates from various sources, such as agricultural by-products, gardening waste, animal husbandry, food industry waste, sewage sludge, and urban solid waste. A recommended approach for processing these organic materials is composting, which stabilises the organic matter and its microbiological composition, enhancing its suitability for applications like self-healing concrete.

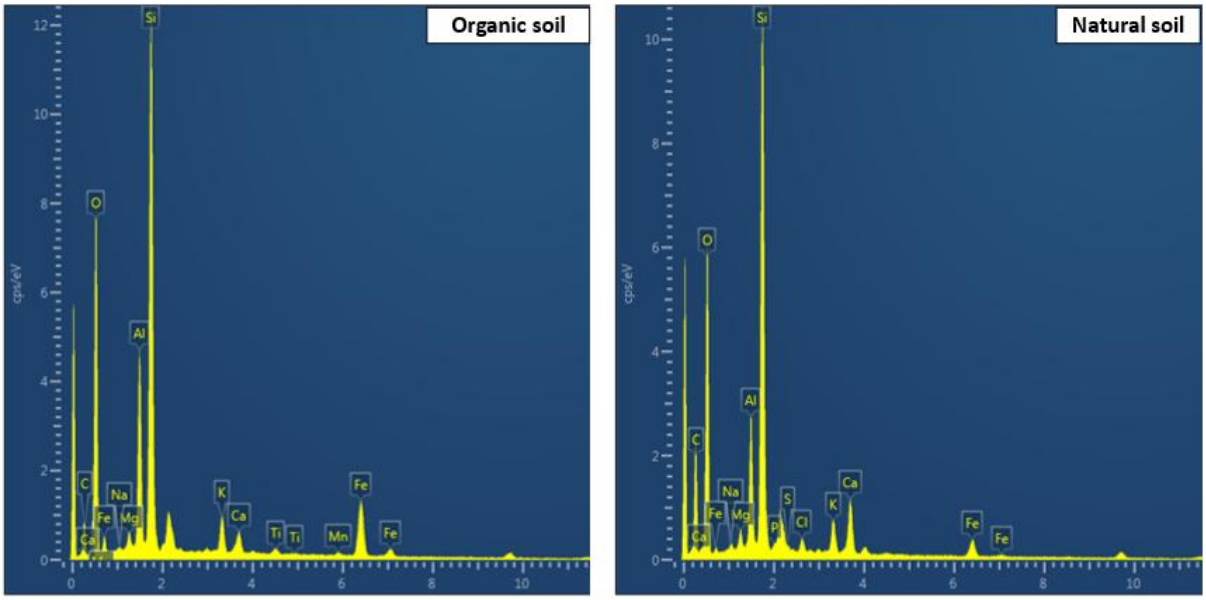

Figure 97: Energy-Dispersive X-ray Spectroscopy (EDX) analysis of organic and natural soil samples.

6.5.3.3 Effective of crack healing

After 100 days of incubation, the self-healing ability of the concrete specimens was carefully examined. Figure 98 highlights how cracks healed over time in self-healing concrete exposed to different conditions, including water, mixed soil, natural soil, and organic soil environments. In specimens incubated in water, the initial cracks were prominent, with sharp edges and distinct lines. However, after the incubation period, significant healing was observed, with the cracks becoming narrower and filled with precipitate. This highlights the potential of water alone to support self-healing, likely through autogenous mechanisms such as the continued hydration of unreacted cement particles and the formation of calcium carbonate, as previously reported by Şahmaran *et al*. (2013). Additionally, the calcium lactate powder within the specimens, combined with the ubiquitous presence of bacteria in air and water environments, may have contributed to microbial activity that facilitated the self-healing process. Airborne bacteria, originating from soil, vegetation, human activity, and aerosols, as well as aquatic bacteria, play essential roles in nutrient cycling, decomposition, and maintaining ecosystem balance (Liu *et*

al., 2021). Research has shown that bacteria are present and actively multiply in tap water, with concentrations ranging from 10^3 to 10^6 cells/ml (Hammes *et al.*, 2010). Based on this, the study hypothesises that innovative bio-concrete technologies could address challenges such as reduced workability, lower mechanical properties, low healing efficiency, poor survivability of bacteria and capsules in harsh concrete environments, high costs, and limited full-scale testing. In the mixed soil environment, the specimens initially had well-defined cracks before incubation. However, after the incubation period, significant healing was observed, with the cracks filled by materials identified as calcium carbonate or limestone. This healing process is largely due to the diverse nutrients and microorganisms present in mixed soil, which combines the benefits of both natural and organic soils. The mixed soil environment creates ideal conditions for microbial-induced calcite precipitation (MICP), where bacteria naturally produce calcium carbonate as part of their metabolic processes. The organic components in the soil enhance microbial activity by providing essential nutrients, while the natural soil helps maintain structural stability. Together, these factors create a supportive environment that optimizes the self-healing process. In the organic soil environment, the cracks were initially sharp and clearly defined. However, after incubation, a significant amount of healing was observed, with the cracks filling in and eventually closing. Organic soil, rich in nutrients and microbial life, provides a highly favourable environment for self-healing. The high microbial activity in this setting accelerates the production of calcium carbonate, a key factor in the repair process. The combination of a nutrient-rich composition and an active microbial community makes organic soil particularly effective in promoting self-healing.

Incubation in a water environment (PW).

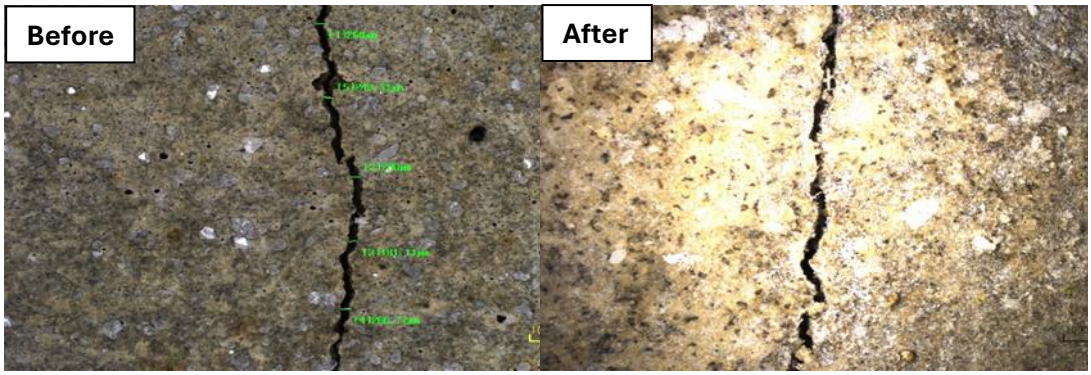

Incubation in a natural soil environment (PN).

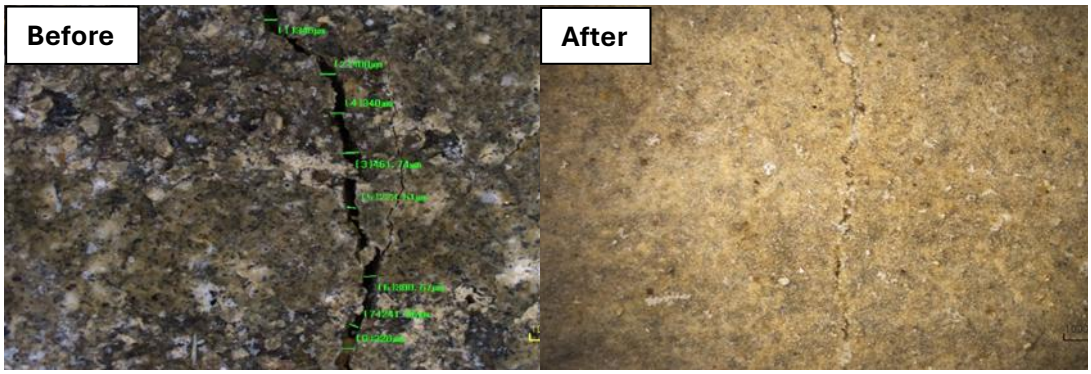

Incubation in a mix soil environment (PC)

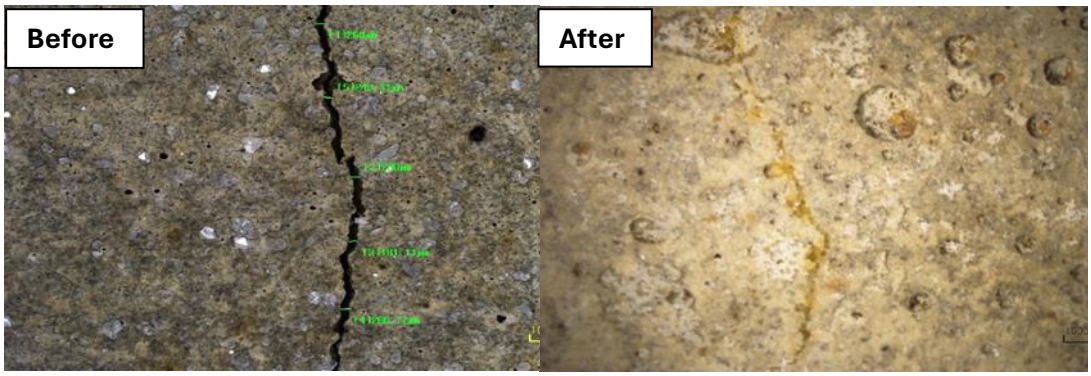

Incubation in an organic soil (PO)

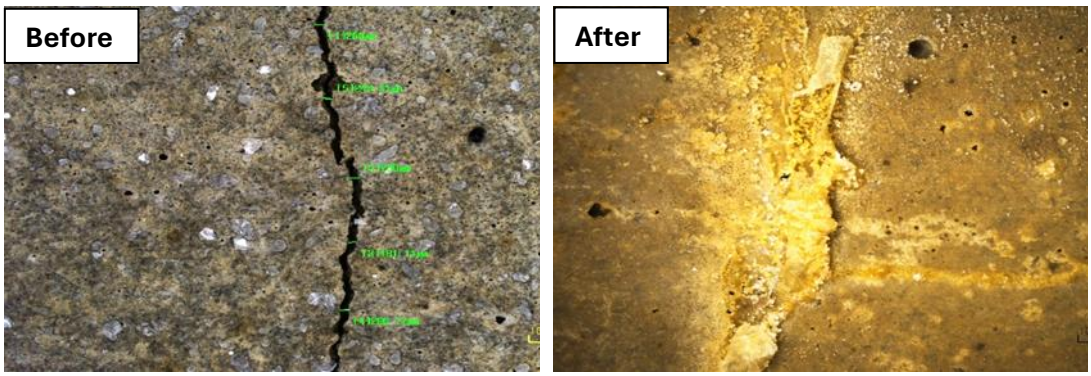

Figure 98: Microscopic analysis of crack healing before and after 100 days.

6.5.3.4 Scanning electron microscope analysis (SEM)

Figure 99 provides SEM images capturing the microstructural changes in concrete cracks under different soil conditions, emphasizing the role of calcium carbonate ($CaCO_3$) precipitation in self-healing mechanisms. In natural soil conditions, SEM imagery highlights the early phase of crack formation, with visibly wide gaps. Over time, calcium carbonate crystals begin to form within these cracks, appearing as irregular, block-like structures that progressively bridge the crack faces. This process significantly reduces the width of the cracks, demonstrating the effectiveness of natural soil in promoting self-healing through $CaCO_3$ deposition (De Muynck et al., 2010b). For specimens incubated in water, SEM analysis reveals a different crack-healing pattern. While the initial stage resembles the natural soil samples, the cracks in water-exposed specimens show finer and more uniformly distributed calcium carbonate crystals over time. This even precipitation process effectively seals the cracks, restoring the structural integrity of the concrete (Wiktor et al., 2011). Organic soil, characterized by a porous and granular structure, indicates a rich presence of organic matter, as seen in the SEM images. Cracks in these samples display extensive $CaCO_3$ precipitation, filling voids and forming a dense, interconnected network. This comprehensive crack filling is attributed to the enhanced nutrient content and microbial activity in organic soil, which accelerates the formation of calcium carbonate and improves the self-healing process (Tziviloglou *et al.*, 2016). Concrete specimens exposed to mixed soil exhibit a combination of features seen in both natural and organic soils. SEM imagery shows cracks partially filled with diverse shapes and sizes of calcium carbonate crystals, forming a complex matrix that bridges the crack faces effectively. The varied mineral and organic composition in mixed soil promotes robust calcium carbonate precipitation, supporting efficient self-healing of the concrete (Wang *et al.*, 2014). The findings from the SEM analysis underscore the pivotal role of soil environments in influencing the self-healing capacity of concrete through calcium carbonate deposition. Environments enriched with organic matter and microbial activity significantly enhance the healing process, contributing to the longevity and durability of concrete structures. These observations align with prior research emphasizing the role of suitable conditions in optimizing self-healing mechanisms in concrete (Su *et al.*, 2024).

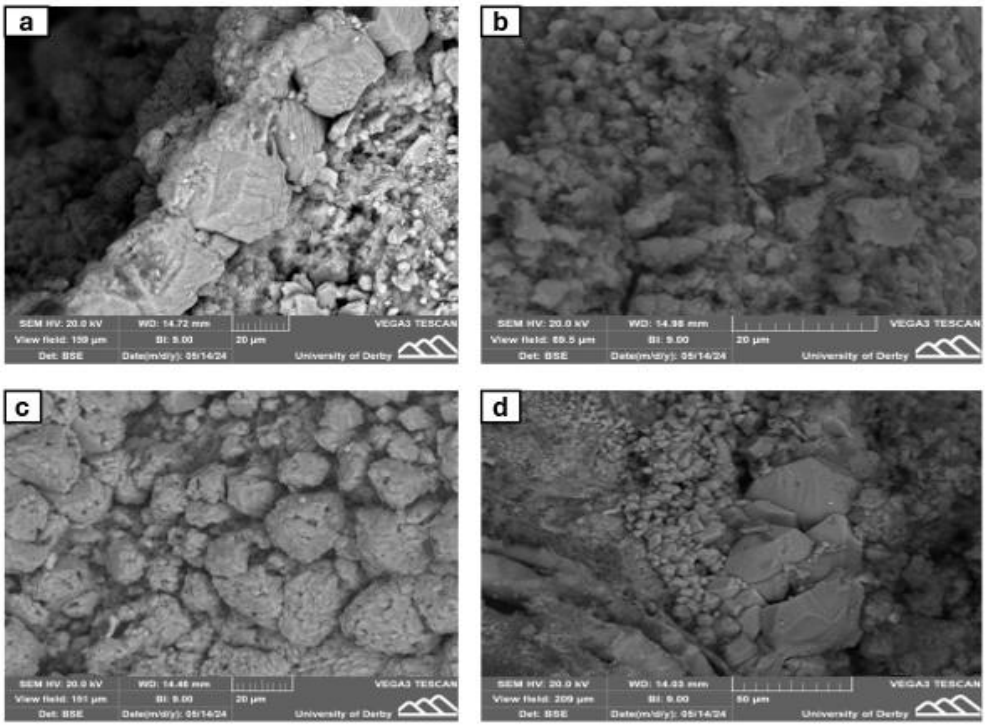

Figure 99: SEM analysis of a. Natural soil incubation environment, b. water incubation environment, c. mix soil incubation environment, d. organic soil incubation environment.

6.5.3.5 Energy dispersive X-ray spectroscopy (EDX)

The Energy-Dispersive X-ray Spectroscopy (EDX) results from different incubation environments show clear differences in elemental composition, influenced by both environmental conditions and bacterial activity, as illustrated in Figure 100. Additional insights can be drawn from the EDX data presented in Tables 34, 35, 36, and 37, which outline the elemental composition of concrete samples incubated in water, natural soil, mixed soil, and organic soil. These analyses focus primarily on calcium carbonate formation, a key indicator of the bacterial self-healing process. In samples incubated in water, EDX spectra indicate moderate calcium carbonate formation. For example, Spectrum 7 recorded 24.03% carbon (C), 49.50% oxygen (O), and 26.47% calcium (Ca). While this suggests the presence of carbonate compounds, the calcium content was lower compared to other environments. In contrast, samples exposed to natural soil showed higher calcium concentrations but relatively lower oxygen and carbon levels, indicating more active calcium carbonate precipitation. Spectrum 1 recorded 10.99% carbon (C), 39.32% oxygen (O), and 49.69% calcium (Ca), suggesting that natural soil provides a favourable setting for bacterial self-healing. These findings align with previous studies, which highlight how microbial-induced calcite precipitation (MICP) is significantly influenced by environmental conditions, with natural soil providing an ideal medium for bacterial activity and carbonate formation (De Muynck et al., 2010a). In the mixed soil environment, EDX data confirm a chemical composition that supports bacterial activity and calcium carbonate precipitation. Spectrum 11 recorded 16.64% carbon (C), 48.05% oxygen (O), and 35.31% calcium (Ca), reinforcing the idea that mixed soil is well-suited to promoting the self-healing process. Similarly, Wang *et al.* (2019) found that nutrient-rich environments enhance bacterial metabolism, facilitating better calcium carbonate formation and improving healing efficiency in bio-concrete. Meanwhile, the organic soil environment showed the highest levels of carbon and oxygen, indicating strong calcium carbonate formation and bacterial activity. Spectrum 9 recorded 18.46% carbon (C), 57.09% oxygen (O), and 24.45% calcium (Ca), suggesting that

organic soil provides the most favourable conditions for microbial-induced calcite precipitation. These results are consistent with research by H M Jonkers et al. (2010), which demonstrated that organic-rich environments encourage bacterial growth and accelerate calcium carbonate formation, further enhancing the self-healing potential of bio-concrete.

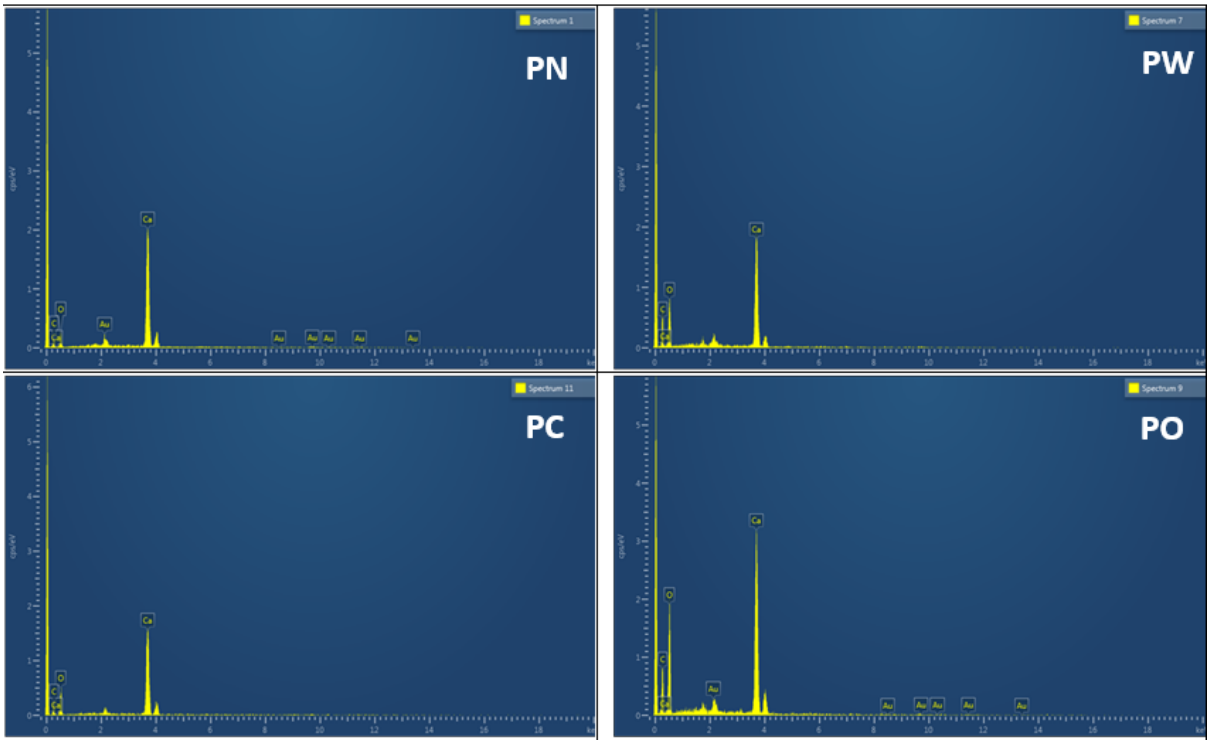

Figure 100: Energy-Dispersive X-ray Spectroscopy (EDX) analysis results of the white precipitated product formed within healed fractures in various mortar mixtures.

Table 34: EDX data for natural soil incubation.

Spectrum	Carbon (C)	Oxygen (O)	Calcium (Ca)	Total
Spectrum 1	10.99	39.32	49.69	100.00

Table 35: EDX data for spectrums of water environment incubation.

Spectrum	Carbon (C)	Oxygen (O)	Calcium (Ca)	Total
Spectrum 7	24.03	49.50	26.47	100.00

Table 36: EDX data of mix soil environment.

Spectrum	Carbon (C)	Oxygen (O)	Calcium (Ca)	Total
Spectrum 11	16.64	48.05	35.31	100.00

Table 37: EDX data for organic soil.

Spectrum	Carbon (C)	Oxygen (O)	Calcium (Ca)	Total
Spectrum 9	18.46	57.09	24.45	100.00

6.6 Assessing the impact of carbonation on self-healing concrete

6.6.1 Overview

This study takes a pre-setting approach, allowing cement to hydrate before being exposed to a CO2-rich environment over three days. The main aim is to understand how carbonation affects the surface of concrete and how exposure to carbonated water alters its chemical environment—findings that form the first phase of this project. The study also explores how quickly these changes can create the ideal conditions for advancing bio-concrete technology by encouraging soil bacteria to grow and thrive on the concrete surface. This work builds on findings from an earlier study of Macpherson (2009). On a broader scale, it is important to note that extracting groundwater often releases carbon dioxide (CO2) because groundwater typically contains CO2 levels 10 to 100 times higher than those in the atmosphere. As a result, the release of CO2 during groundwater extraction is almost unavoidable.

6.6.2 Materials and methods

6.6.2.1 Specimen preparation and crack creation

This study aimed to explore how carbonation affects bio-concrete technology. The experiment used Portland cement (BSEN 196-1) and GGBS cement (BSEN 196-2), both provided by HANSON HEIDELBERG CEMENT GROUP in the UK. To ensure proper CO2 diffusion and sample preparation, a water-to-cement ratio of 0.3 was chosen. The mixture was then compacted into 40 mm × 40 mm × 160 mm prisms, with a load applied for 30 seconds to consolidate the specimens. To investigate bio-concrete, six mortar prisms were prepared with calcium lactate powder added as a nutrient to support microbial activity. These were split into two groups: three were placed in containers with standard water, and the other three in containers with carbonated water. A second set of six prisms was made using GGBS cement and followed the same process. This systematic approach ensured a thorough examination of how carbonation could enhance bio-concrete. The calcium lactate powder, a key ingredient, was sourced from SPECIAL INGREDIENTS LTD in the UK.

The process for creating cracks in the specimens followed methods used earlier in this project. After a 24-hour setting period, the prisms were removed from their moulds and cured in water for 28 days. Carbonated water was replaced every two days to maintain its CO2 content, as the gas would otherwise dissipate, causing the water's properties to revert to standard conditions. After curing, the specimens were air-dried at room temperature and prepared for crack initiation through mechanical testing. A three-point bending test was carried out by placing each prism on two parallel beams. Cracks were then covered with cotton material that allowed water to pass through but blocked soil particles, ensuring clean and controlled conditions for further testing. The specimens were placed in 5-litre containers. Each container was rinsed with either standard water or carbonated water (1 litre per container) and then sealed to maintain a consistent CO2 environment. The containers were kept at a steady room temperature of 20°C, ensuring uniform conditions across all samples. This approach allowed for a clear understanding of how carbonation interacts with bio-concrete, particularly in supporting microbial processes for self-healing.

6.6.2.2 Incubation environment

This study used natural soil collected from the University of Derby's field to create an environment that closely reflects real underground conditions for concrete. To better understand the soil's characteristics, a sieve test was carried out following BS EN 933 standards

to analyse its Particle Size Distribution (PSD). The soil was identified as a natural alluvial deposit, appearing as soft to firm, dark brown silty clay with some sandy elements. This type of soil is known to support a diverse range of naturally occurring bacteria, which play an important role in biological self-healing processes. The soil's pH, measured using a handheld pH tester, ranged between 6.60 and 7.45, like the pH of the tap water used in other specimen groups. Once the mortar specimens were cracked, they were carefully placed in plastic containers, with dry soil added in two layers: one beneath the specimens and another covering and surrounding them. Each container held three specimens, and the incubation process was carried out at room temperature, around 23°C. Mortar specimens were prepared using standard sand and divided into three groups: PM (Plain Mortar), MN (Mortar with Nutrients), and MG (Mortar with Nutrients and GGBS replacement). All specimens were incubated in fully saturated soil for 56 days. The plain mortar served as a control group to observe natural self-healing (autogenous healing) that might occur due to ongoing hydration. To keep the soil fully saturated, water was maintained above the specimens, reaching the soil surface, and any loss due to evaporation was regularly topped up. During the incubation period, the soil's pH was closely monitored to ensure it remained within the required range for the study.

6.6.3 Results and discussion

The results in figure 101 shows that the mortar specimens exposed to carbonated water, including those with added nutrients and 35% GGBS replacement, showed no self-healing. Several factors likely contributed to this outcome. One key issue is the low pH environment created by carbonated water, which may have interfered with the activity of bacteria essential for microbial-induced calcium carbonate precipitation (MICP). As Jonkers *et al*. (2010) pointed out, bacterial activity in self-healing concrete is highly sensitive to pH, with optimal conditions typically falling between 7 and 9. Carbonated water often falls outside this range, making it difficult for bacteria to metabolize nutrients and produce calcium carbonate effectively. Another contributing factor is the 35% replacement of cement with GGBS, which reduces the calcium hydroxide content in the mix—a crucial ingredient for carbonation and self-healing. Research by De Muynck *et al*. (2008) has shown that binders with lower calcium hydroxide levels are less effective at self-healing due to the reduced availability of calcium ions needed to form calcium carbonate. Moreover, carbonated water, rich in dissolved carbon dioxide, reacts with the calcium hydroxide in the cement to form calcium carbonate during the carbonation process. This reaction significantly reduces the calcium hydroxide available, which is a key source of calcium ions needed for self-healing. This depletion is even more pronounced in mixes with GGBS, where calcium hydroxide levels are already lower, making it even harder for the self-healing process to take place effectively. While carbonation can help with surface-level calcium carbonate formation, it's generally not effective for addressing deeper or wider cracks, such as those observed in this study. For cracks larger than 0.3 mm, the process is often insufficient to fully close the gaps. The frequent replacement of carbonated water every two days may have further disrupted the chemical environment, making it harder for consistent healing processes to take place. Additionally, GGBS can slow down the hydration process, which limits the potential for autogenous healing, a process that relies on unhydrated cement particles reacting with water to seal cracks.

The black discoloration around the cracks in the mortar prisms is most likely a result of natural microbial activity, mineral reactions, or organic matter from the soil. Since these prisms were buried in soil for 56 days, bacteria and fungi had the perfect conditions to grow, forming dark biofilms or reacting with the cement. At the same time, minerals like iron or manganese from the soil could have oxidized, leaving dark stains. While high-tech analysis like SEM and EDX could confirm the exact cause, they are not necessary here. The exposure conditions and visible changes already tell us that natural biological and chemical processes are at play. A simple pH test or microbial culture would be enough to check if bacteria were responsible for the staining.

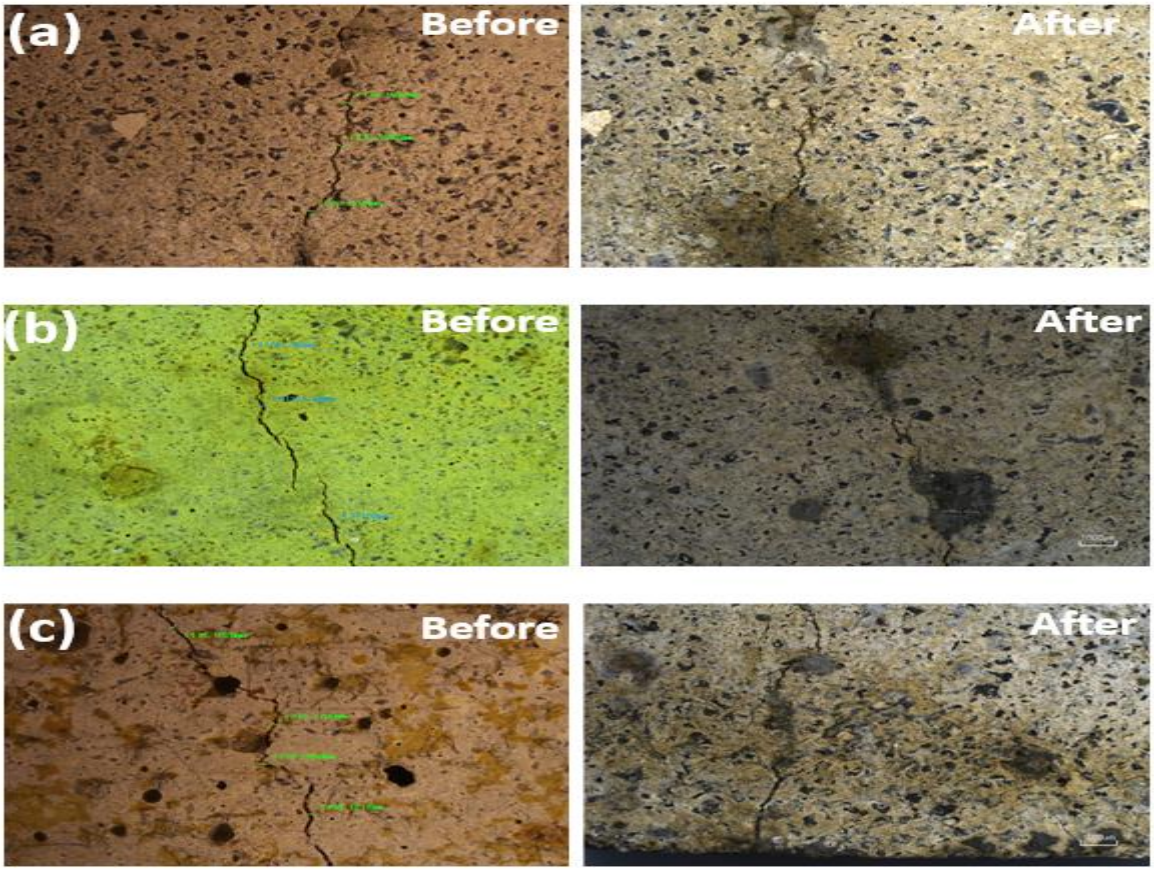

Figure 101: (a) Plain mortar with nutrients exposure to carbonated water. (b) %35 GGBS replacement with nutrients exposure to carbonated water. (c) Plain mortar exposure to carbonated water

6.7 Assessing the effectiveness of different capsules on self-healing concrete technology

6.7.1 Overview

This study explored how adding different types of capsules—calcium alginate and calcium carbonate—could improve the self-healing ability of concrete. The aim was to understand how these capsules, acting as carriers for healing agents or nutrients, helped concrete repair itself over time. Calcium alginate capsules, being biodegradable, released healing agents gradually, allowing the healing process to continue for longer. In contrast, calcium carbonate capsules provided an immediate source of minerals to seal cracks, enabling faster and more efficient healing. By testing these capsules under different conditions, the study offered valuable insights into how they could enhance concrete durability, extend its lifespan, and contribute to more sustainable construction.

6.7.2 materials and method

6.7.2.1 Specimens' preparation and crack creation

In line with BS EN 196-1, various mortar samples were prepared for this study, including plain mortar (control), mortar with calcium carbonate capsules, and mortar with calcium alginate capsules. Every material was thoughtfully selected and documented to ensure the highest quality and alignment with the study's goals. This careful approach was essential for investigating the self-healing properties of the mortar and ensuring reliable, repeatable results. The calcium carbonate capsules used in the mixes had particle sizes between 4.000 µm and 8.637 µm, while the calcium alginate capsules measured between 2,755.850 µm and 2,846.839 µm. These size ranges were specifically chosen to achieve even distribution and maximize the capsules' effectiveness in the mortar matrix. The mortar specimens were prepared in accordance with the established experimental protocol using Hanson Sulphate Resisting Cement (CEM III/A + SR), CEM II, sand, tap water, and calcium lactate powder as a nutrient. A consistent water-to-cement ratio of 0.5 was maintained across all mixtures to ensure uniformity in the experimental conditions. The specific proportions of the mortar mixtures are presented in Table 38. Each sample was cast into 40 mm × 40 mm × 160 mm prisms, with fibre mesh embedded in the centre to prevent complete failure. A total of nine samples were prepared for each type of mortar to ensure robust data for analysis. After 24 hours, the samples were demoulded and placed in water to cure for 28 days, allowing full hydration. Once curing was complete, the samples were removed from the water, air-dried at room temperature, and prepared for crack generation through mechanical testing. The process used to create cracks was consistent with methods employed in earlier studies within this project, ensuring the results could be compared accurately. This systematic and deliberate preparation ensured the samples were ready for the self-healing experiments that followed. The sizes and shapes of the capsules are discussed in more detail during the second phase of this project.

Table 38: Mortar mix percentages

Material	Plain Mortar (Control)	Mortar with Calcium Carbonate Capsules	Mortar with Calcium Alginate Capsules
Cement (CEM II) (g)	450	450	450
Sand (g)	1350	1350	1350
Water (g)	225	225	225
Calcium Carbonate Capsules (g)	N/A	22.5	N/A
Calcium Alginate Capsules (g)	N/A	N/A	22.5

6.7.3 Incubation environment

The incubation environment in this study was designed to match the conditions of previous research to ensure consistency. The soil, collected from the University of Derby's field, was first sieved to remove larger particles and standardize its composition. This step helped create a more uniform and controlled setting for the experiment. The mortar specimens were then incubated in this soil for 28 days, allowing enough time for bacterial activity to take place, nutrients to be released, and calcium carbonate to form, simulating natural conditions as closely as possible.

6.7.4 Results and discussion

6.7.4.1 Effective of crack healing

Figure 102 shows a comparison between mortar specimens with calcium carbonate capsules, calcium alginate capsules, and those without any capsules. These images, taken using microscopy, reveal clear differences in how effectively each type of mortar heals cracks, mainly due to how the capsules release nutrients. Both types of capsules are designed to deliver calcium lactate powder, which acts as a food source for naturally occurring soil bacteria. These bacteria then convert the calcium lactate into calcium carbonate, which helps seal the cracks. The calcium carbonate capsules, being more brittle, break easily when cracks appear, allowing the nutrients to be released immediately at the damage site, promoting faster self-healing. This rapid release enables bacteria to start the healing process quickly, leading to more effective and faster crack closure. In contrast, calcium alginate capsules, made with a biodegradable matrix, release their nutrients more slowly. This gradual release delays the activation of bacterial activity, resulting in slower and less effective healing. This difference is evident in visual observations, where cracks in specimens with alginate capsules remain more noticeable compared to those with calcium carbonate capsules. These findings are consistent with the work of Wang *et al*. (2014), who emphasized the importance of rapid nutrient availability for efficient healing, and H M Jonkers et al. (2010), who highlighted the critical role of immediate interactions between nutrients and bacteria in supporting microbial-induced calcium carbonate precipitation (MICP). While calcium carbonate capsules outperformed in this study due to their quick nutrient delivery, calcium alginate capsules could still be valuable in applications requiring a sustained nutrient supply over time. Future research could focus on enhancing alginate capsule designs to improve their ability to release nutrients more effectively upon cracking while maintaining their longer-term release benefits, making them more adaptable for different environmental and structural conditions.

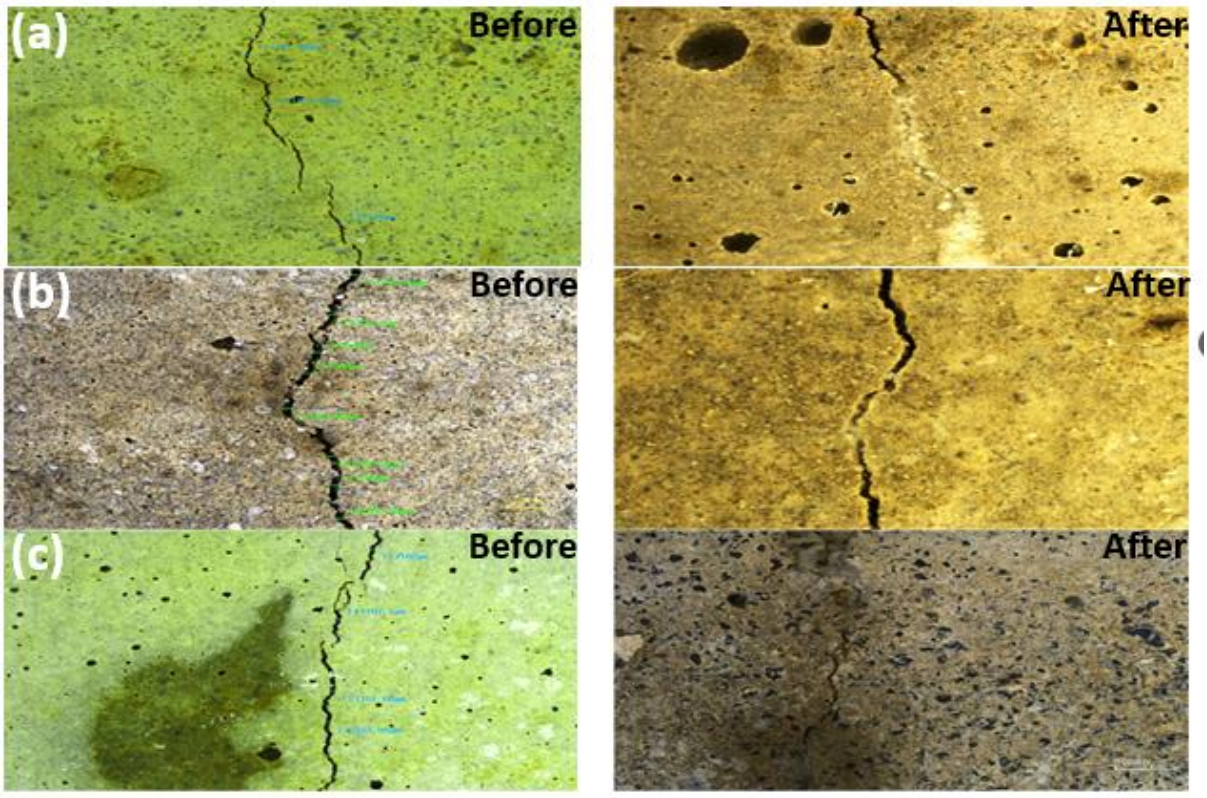

Figure 102: Microscopic analysis of crack healing was conducted before and after a 28-day incubation period within a soil environment. (a) Prisms with calcium carbonate capsules. (b) Prisms with calcium alginate capsules. (c) Plain prisms (Control)

6.7.4.2 SEM and EDX analysis

The SEM images in Figure 103 clearly show differences in crack healing across the three specimens, demonstrating the effectiveness of bacterial self-healing. In the prisms containing calcium carbonate capsules (a), cracks show significant healing, with dense crystal growth and bridging structures, suggesting that microbial-induced calcite precipitation (MICP) has actively filled the gaps. In contrast, the prisms with calcium alginate capsules (b) display only partial healing, with a more porous structure and scattered crystal deposits, indicating that some self-healing occurred but not as effectively as in (a). Meanwhile, the plain prisms without capsules (c) exhibit little to no healing, with cracks remaining open and the surface appearing rough and fibrous, lacking any calcium carbonate deposits. These observations highlight that calcium carbonate capsules offer the most effective self-healing, as they enhance bacterial activity and promote better crack closure, while calcium alginate capsules provide moderate healing, and the control sample shows no meaningful self-repair. The Energy-Dispersive X-ray Spectroscopy (EDX) analysis in the figure 104 provides valuable insights into the composition of the capsules and the role they play in the self-healing process of concrete. The calcium carbonate capsules mainly contain calcium (44.58%), oxygen (50.98%), and carbon (4.43%), making them highly effective in delivering essential nutrients that support bacterial activity. Calcium serves as a key nutrient for naturally occurring soil bacteria, allowing them to facilitate microbial-induced calcite precipitation (MICP) and seal cracks in the concrete (Wiktor et al., 2011). On the other hand, Figure 105 shows calcium alginate capsules, which have a more porous and fragmented structure. These capsules contain a wider range of elements, including oxygen (38.44%), silicon

(22.59%), aluminium (12.32%), iron (13.81%), and magnesium (2.88%), but a much lower calcium content (1.83%). Despite this, they still serve as nutrient carriers by gradually releasing essential compounds like calcium lactate, which helps keep bacterial activity sustained over time. In this study, naturally occurring soil bacteria were used for the self-healing process, with calcium carbonate capsules providing an immediate nutrient boost, while calcium alginate capsules ensured a steady supply of nutrients, creating a balanced system that supports effective crack healing. The analysis of Spectra 3, 27, and 41 in Tables 39, 40, and 41 further helps determine whether the healing process in the concrete was driven by bacterial activity or purely chemical reactions. Spectrum 3, which shows high levels of oxygen, silicon, aluminium, potassium, and iron but very little carbon and calcium, suggests that healing mainly occurred through chemical reactions like hydration or carbonation rather than microbial activity. The lack of significant carbon indicates minimal bacterial involvement, while the presence of aluminium and iron points to typical cementitious reactions rather than bio-mediated calcite formation. In contrast, Spectrum 27 reveals moderate amounts of carbon, along with oxygen, silicon, and calcium, suggesting that both chemical and microbial processes played a role in the healing process. The presence of calcium indicates that calcium carbonate precipitation occurred, which can happen naturally in concrete, but the moderate carbon content also hints at microbial involvement, meaning bacteria may have contributed to healing, but not as the sole mechanism. Spectrum 41, however, provides strong evidence of bacterial self-healing, as it shows a high concentration of calcium, a good amount of oxygen, and detectable levels of carbon—key indicators of microbial-induced calcite precipitation (MICP). The absence of silicon and aluminium further supports the idea that this healing process was primarily biological rather than a result of standard cement reactions.

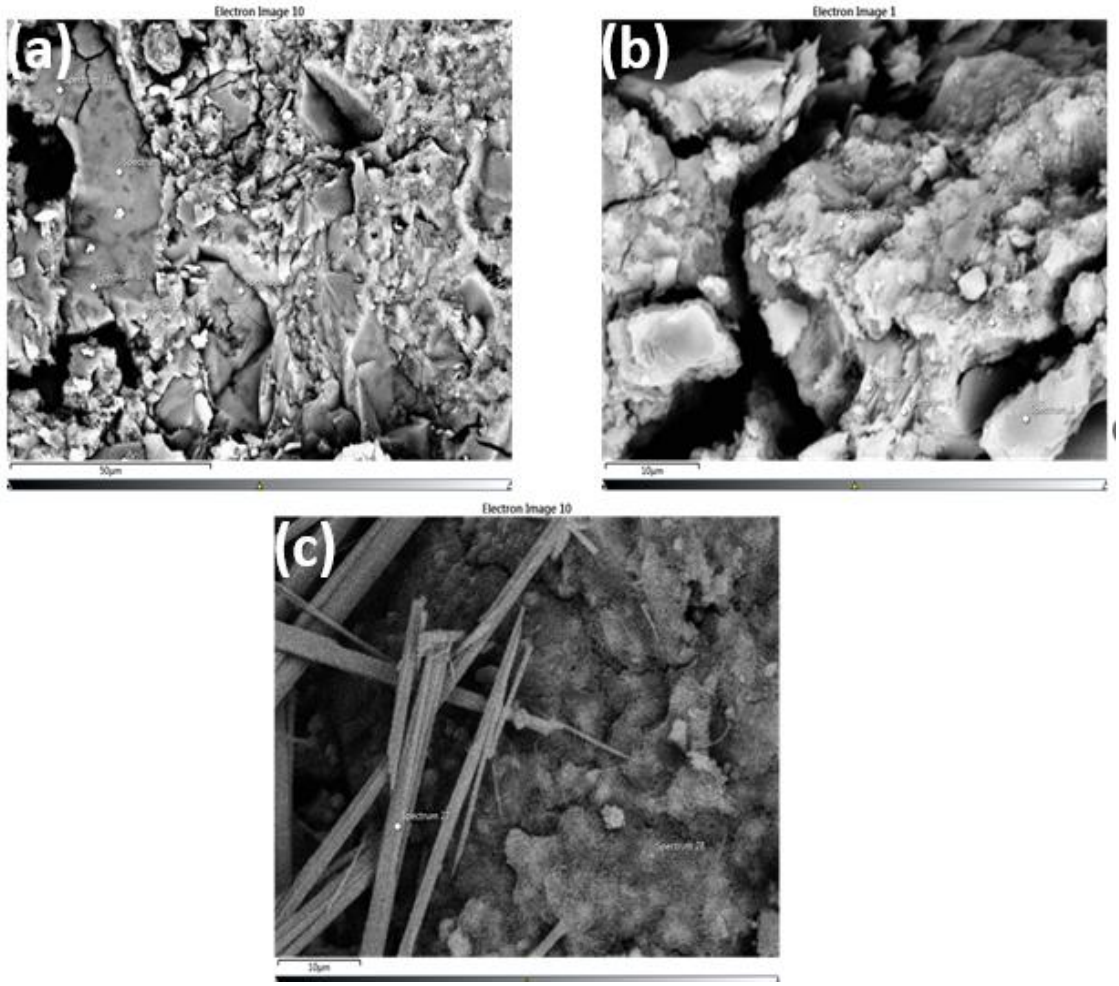

Figure 103: Scanning Electron Microscopy (SEM) analysis of: (a) Prisms incorporating calcium carbonate capsules. (b) Prisms incorporating calcium alginate capsules.
(c) Plain prisms without capsules.

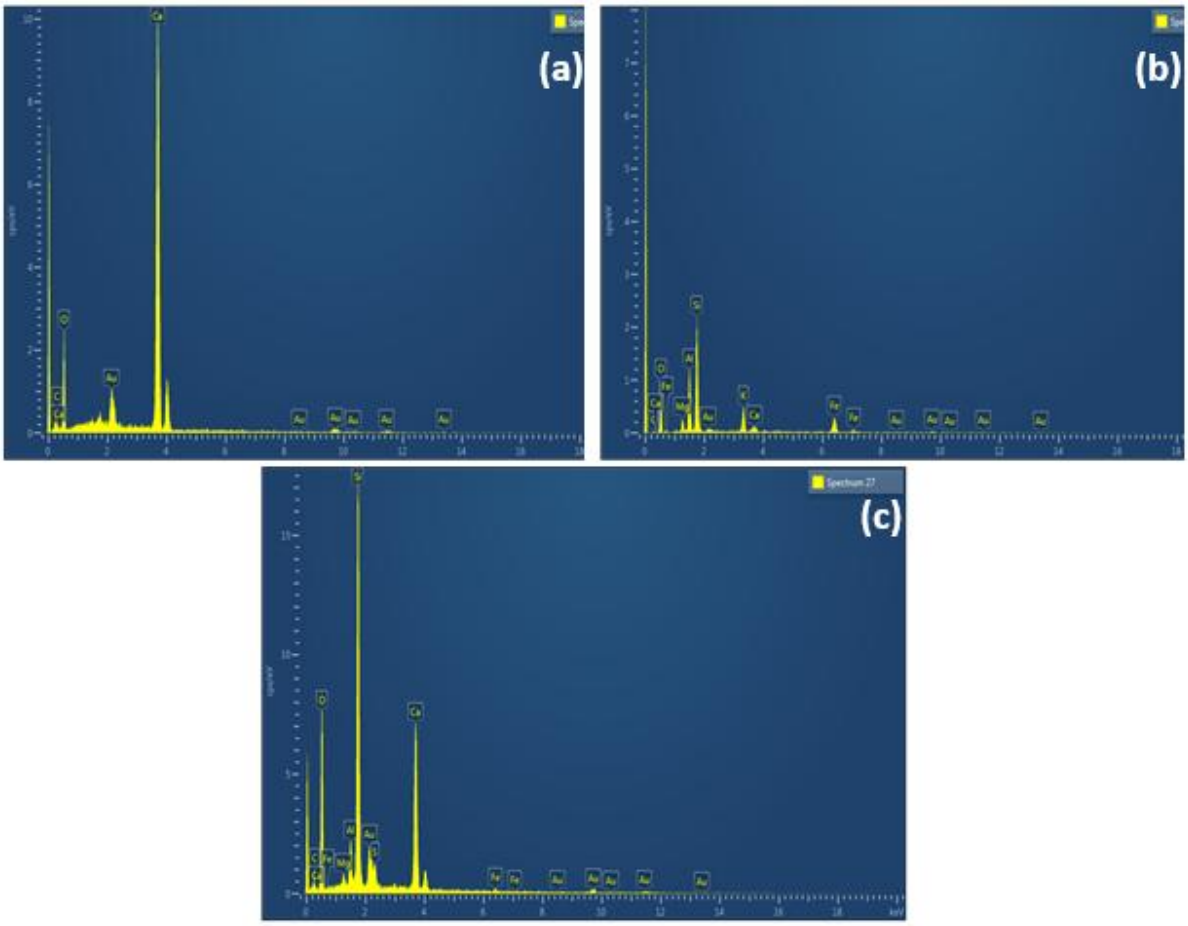

Figure 104: Energy-Dispersive X-ray Spectroscopy (EDX) analysis results of the white precipitated product formed in: (a) Prisms containing calcium carbonate capsules. (b) Prisms containing calcium alginate capsules. (c) Plain prisms without additional modifications.

Table 39: Prisms with calcium carbonate capsules (EDX)

Element	Percentage (%): Spectrum 41
Carbon (C)	4.43
Oxygen (O)	50.98
Magnesium (Mg)	-
Aluminum (Al)	-
Silicon (Si)	-
Sulfur (S)	-
Calcium (Ca)	44.58
Iron (Fe)	-
Total Composition	100.00

Table 40: Prisms with calcium alginate capsules (EDX)

Element	Percentage (%): Spectrum 3
Carbon (C)	0.14
Oxygen (O)	38.44
Magnesium (Mg)	2.88
Aluminum (Al)	12.32
Silicon (Si)	22.59
Potassium (K)	7.99
Calcium (Ca)	1.83
Iron (Fe)	13.81
Total Composition	100.00

Table 41: Plain prisms with no capsules (EDX)

Element	Percentage (%): Spectrum 27
Carbon (C)	15.64
Oxygen (O)	49.11
Magnesium (Mg)	0.54
Aluminum (Al)	1.98
Silicon (Si)	17.36
Sulfur (S)	1.37
Calcium (Ca)	13.36
Iron (Fe)	0.64
Total Composition	100.00

7 Chapter 7: Conclusion and future work

7.1 Overview

This thesis has explored how to enhance the sustainability of underground structures through a soil-driven bio-protection system for concrete. The research focused on understanding the bio self-healing mechanism and how different incubation environments influence its performance. Key factors such as the chemical environment of concrete, including pH levels, calcium ion concentrations, and electrical conductivity, were examined. These factors are critical for optimizing self-healing concrete technologies and ensuring their effectiveness. The second part of the study investigated the development of calcium carbonate capsules with improved size optimization. The goal was to identify capsule sizes that had minimal impact on the physical and mechanical properties of concrete while enhancing its self-healing capabilities. These capsules were specifically designed to work alongside naturally occurring soil bacteria, providing essential nutrients without compromising the structural performance of the concrete. Finally, the research evaluated the effectiveness of self-healing concrete by conducting a series of experiments under various conditions. These included testing different types of cement and exposing the concrete to flowing water systems, accelerated carbonation, and various soil types. This approach aimed to simulate real-world underground conditions, helping to better understand how self-healing concrete performs in practical applications and under diverse environmental stresses. This chapter brings together the key findings from the research, offering a summary of the conclusions drawn from the studies presented in this thesis. It also highlights recommendations for future work to further explore the potential of bio self-healing concrete when incubated in soil. For a more detailed discussion of specific findings, readers are encouraged to refer to the conclusion sections at the end of each chapter, where the outcomes of each aspect of the research are analysed in depth. These findings provide a strong foundation for further investigation into the development and application of bio self-healing technologies for sustainable underground structures.

7.2 Conclusion

7.2.1 Phase 1 (bacteria form and participate on the concrete surface)

This study explored the influence of the chemical environment within concrete on the viability and activity of naturally occurring bacteria from surrounding organic soil, with the aim of promoting microbial-induced self-healing. Rather than embedding engineered bacterial strains directly into the concrete matrix, the research focused on leveraging indigenous soil bacteria by creating conditions conducive to their survival and function. Through a series of controlled laboratory experiments, the effects of cement type, water flow, carbonation, and pH variation were systematically investigated to identify key parameters that enable biological self-healing.

- Supplementary Cementitious Materials: Partial replacement of ordinary Portland cement with 30–50% ground granulated blast-furnace slag (GGBS) effectively reduced the initially high pH levels of concrete (typically >12.5) to a more biologically favourable range of 9.2–10.5. However, replacement levels beyond 50% began to negatively impact mechanical properties, indicating a need for balance between chemical modification and structural integrity.

- pH Measurement and Indicator Calibration: A novel image-based pH measurement approach was developed using ImageJ software and phenolphthalein as a surface indicator. This method demonstrated a strong linear correlation ($R^2 \approx 0.95$) between red channel intensity and pH values, with phenolphthalein showing a distinct colour transition around pH 9.5. In contrast, the universal pH indicator exhibited inconsistent RGB behaviour, making phenolphthalein the preferred choice for accurate surface pH analysis in cementitious materials.
- Carbonation and Water Flow Effects: Accelerated carbonation, achieved through 30-minute CO_2 exposure, was shown to reduce surface pH to approximately 9.5, aligning with the optimal range for bacterial activity. Additionally, continuous water flow over a period of 14 days enhanced the carbonation process, particularly in GGBS-modified mortars, further contributing to pH reduction and improved environmental conditions for bacterial survival.
- Bacterial Activity and Calcium Carbonate Precipitation: The optimal pH range for microbial-induced calcium carbonate precipitation (MICP) was identified as 9.0–10.0. At pH levels above 11, calcium carbonate formation occurred primarily through abiotic chemical processes, while pH levels below 8 significantly diminished bacterial activity and carbonate production. Under optimal conditions, calcium carbonate precipitation reached 3.1–4.2 g/m^2, leading to visible crack sealing of up to 0.35 mm within 28 days of soil exposure.

These findings confirm that modifying the chemical environment of concrete through strategic use of GGBS, controlled carbonation, and water exposure can successfully support bacterial activity from organic soil, enabling effective and low-cost, passive self-healing. Furthermore, the study validates the use of phenolphthalein and RGB-based image analysis as a reliable and accessible method for surface pH monitoring in bio-concrete research. This approach offers a promising direction for enhancing the durability and service life of underground concrete infrastructure through sustainable and nature-inspired techniques.

7.2.2 Phase 2 (Producing small capsules to reduce the impact of capsules on concrete properties)

This study evaluated the influence of capsule size, type, and dosage on the compressive strength and crack-healing performance of self-healing concrete. Three additives were examined: calcium alginate capsules (~2847 µm), calcium carbonate microcapsules (~3 µm), and calcium lactate powder (sub-micron scale). The findings demonstrate that capsule properties significantly impact both mechanical integrity and healing efficiency, and that an optimized balance can enhance the sustainability and performance of concrete.

- Calcium Alginate Capsules (~2847 µm): Calcium alginate capsules, with an average diameter of approximately 2847 µm, were effective in delivering nutrients necessary for sustaining long-term bacterial activity, thereby supporting the healing of larger or more persistent cracks. However, their inclusion led to a substantial reduction in compressive strength, ranging from 15% to 20% at 7 days. This pronounced decrease is largely attributed to their relatively large size, which disrupted the cementitious matrix and increased overall porosity. Furthermore, the irregular distribution of these capsules within the mix introduced localized weak zones, compromising the early-age mechanical performance. Despite these drawbacks, calcium alginate capsules remain

a promising option for durability-oriented applications, where extended self-healing functionality is of greater importance than initial strength retention.

- Calcium Carbonate Microcapsules (~3 μm): The addition of calcium carbonate microcapsules, with an approximate diameter of 3 μm, resulted in a moderate reduction in compressive strength of 5% to 7% at 7 days. Their small size contributed to uniform dispersion within the cement matrix, promoting microstructural refinement and reduced porosity. This compatibility with the cementitious environment allowed the microcapsules to maintain the structural integrity of the composite while facilitating a gradual release of nutrients. The controlled release mechanism supported bacterial-induced calcium carbonate precipitation (MICP), enhancing the self-healing potential without compromising mechanical performance significantly. Thus, calcium carbonate microcapsules offer a balanced solution between mechanical integrity and healing efficacy.
- Calcium Lactate Powder: Calcium lactate powder, being the finest of the additives investigated, exhibited the least impact on compressive strength, with reductions limited to 2%–4% at 7 days. Its fine particle size promoted homogeneous distribution within the mix, preserving early-age strength. However, the absence of encapsulation rendered the nutrient highly susceptible to premature leaching or immediate microbial consumption. As a result, its effectiveness in supporting long-term bacterial activity was limited, thereby reducing its suitability for applications requiring prolonged self-healing and durability enhancement. Nevertheless, calcium lactate remains a viable option when short-term strength retention is a priority and nutrient longevity is of lesser concern.
- Effect of Dosage: Reducing the dosage of additives to 3% by weight of cement proved beneficial in mitigating strength loss across all capsule types. At this optimized dosage, both calcium carbonate microcapsules and calcium lactate powder maintained favourable compressive strength profiles while effectively supporting microbial activity. In contrast, calcium alginate capsules continued to impose a noticeable reduction in mechanical performance, even at lower dosages. However, their superior nutrient retention and ability to promote healing in wider cracks underscore their value in long-term durability-focused designs. Therefore, dosage optimization plays a critical role in balancing mechanical properties with self-healing performance in bio-enhanced cementitious systems.

These results highlight that smaller capsule, particularly calcium carbonate microcapsules, offer a compelling balance between mechanical strength preservation and biological self-healing capacity. Their compatibility with the cement matrix and ability to facilitate sustained microbial activity make them ideal for general-purpose applications where both early strength and durability are critical. Conversely, larger capsules such as calcium alginate, while detrimental to early-age strength, remain highly effective for long-term healing and may be more suitable for infrastructure where crack resilience over time is paramount.

7.2.3 Phase 3(the effectiveness of self-healing concrete)

This study conducted a series of targeted investigations to evaluate the influence of various factors—including supplementary cementitious materials (GGBS and fly ash), accelerated carbonation, controlled water flow, and capsule type—on the performance of bio-self-healing concrete. Emphasis was placed on optimizing the chemical environment to support the viability

of naturally occurring bacteria from organic soil and enhancing calcium carbonate precipitation for durable crack repair.

- Effect of Supplementary Materials (GGBS and Fly Ash): GGBS replacement at 30–50% significantly altered the pH environment, lowering values from >13.5 to 9.2–10.5, thereby enhancing conditions for bacterial activity. SEM imaging revealed that GGBS-modified specimens exposed to soil exhibited greater healing ratios, with calcium carbonate deposits visibly bridging cracks up to 0.35 mm wide within 28 days. Comparatively, mortar specimens with nutrients but without GGBS exhibited reduced healing efficiency, and SEM analysis detected ettringite within cracks—suggesting a less favourable healing environment and insufficient carbonate precipitation.
- Water Flow System: Specimens exposed to a flowing water regime (0.1–0.3 L/min over 14 days) demonstrated a more substantial pH reduction and enhanced carbonation compared to stagnant conditions. This modification in the chemical environment led to improved microbial activity and increased calcium carbonate yield, particularly in GGBS-enhanced samples. However, excessive flow rates risked leaching essential ions, indicating the need for controlled flow conditions to balance chemical modification and nutrient retention.
- Accelerated Carbonation: A controlled accelerated carbonation process involving 30 minutes of CO_2 exposure was employed to simulate rapid environmental carbonation. This treatment effectively reduced the pH of the cementitious matrix to approximately 9.5, aligning with the optimal range for bacterial viability and metabolic activity. While the lowered pH was conducive to microbial-induced calcium carbonate precipitation (MICP), the carbonation process concurrently consumed free calcium ions within the matrix. This reduction in available calcium ions limited the extent of calcium carbonate formation, thereby slightly diminishing the overall healing efficiency in certain cases. Consequently, although accelerated carbonation can enhance microbial activity by creating favourable pH conditions, its implementation must be carefully balanced to avoid excessive calcium ion depletion, which could hinder the self-healing process.
- Soil Environment and Microbial Activity: The presence of organic soil with high microbial activity was found to be a critical factor in facilitating effective microbial-induced calcium carbonate precipitation (MICP) for crack healing. Under optimized environmental conditions—specifically a pH range of 9–10 and the inclusion of ground granulated blast furnace slag (GGBS)—specimens exposed to organic soil exhibited calcium carbonate precipitation in the range of 3.1–4.2 g/m^2 and demonstrated the ability to heal surface cracks up to 0.35 mm in width. Scanning electron microscopy (SEM) analysis confirmed the formation of dense calcium carbonate deposits within the crack interfaces of these specimens. Such deposits were absent in control samples that were not exposed to active soil environments. In contrast, specimens placed in sterile or low-organic soils exhibited minimal healing, underscoring the essential role of indigenous microbial populations in sustaining MICP and promoting long-term self-healing functionality.

These findings underscore the importance of chemical environment engineering in bio-self-healing concrete systems. The use of GGBS and controlled water flow enhances the pH conditions and microbial habitat needed for sustained healing. While accelerated carbonation supports pH adjustment, it must be carefully balanced to avoid calcium ion depletion. The role of organic soil is paramount, as it enables indigenous microbial

populations to thrive and facilitate crack sealing through MICP. The integration of these strategies presents a pathway toward durable, resilient, and sustainable concrete infrastructure, particularly in underground applications.

7.3 Future work and recommendations

This research has provided valuable insights into enhancing the bio-self-healing capabilities of concrete in soil environments, particularly for underground structures exposed to microbial-rich organic soils. Building on the outcomes of this study, several avenues for future research are proposed to strengthen both the scientific understanding and practical implementation of this technology in the construction industry.

- While this study focused on early-age healing efficiency, future investigations should emphasize long-term durability testing under varied environmental conditions, including wet-dry cycles, freeze-thaw exposure, and chemical attack (e.g. sulphates and chlorides). Understanding how self-healing systems perform over extended periods will be crucial to ensure structural reliability in real-world applications. Incorporating mechanical testing such as modulus of elasticity, permeability, and flexural strength alongside crack sealing observations will offer a more comprehensive durability profile.
- The image-based pH analysis developed in this study could be further enhanced using artificial intelligence (AI) and machine learning techniques to improve accuracy, automate data interpretation, and predict healing performance. AI algorithms trained on large datasets of crack images, healing progress, and RGB values can be used to develop predictive models for calcium carbonate formation, healing rates, and nutrient effectiveness. Such tools can support real-time monitoring and provide decision-making assistance for engineers in both laboratory and on-site applications.
- Although this research successfully demonstrated laboratory-scale bio-healing using organic soil, the next step involves conducting field trials in varied soil types, moisture conditions, and temperature ranges. These real-world validations will help assess how environmental fluctuations influence bacterial activity, nutrient availability, and healing efficiency. Field studies should also evaluate constructability, maintenance requirements, and cost-benefit analysis of implementing bio-concrete at scale.
- The promising performance of GGBS in modifying the chemical environment to support microbial activity suggests further investigation into other supplementary cementitious materials (SCMs) is warranted. Materials such as silica fume, Class C/F fly ash, metakaolin, rice husk ash, and volcanic ash may offer unique benefits by affecting porosity, calcium availability, and chemical buffering capacity. Future studies should explore how these materials interact with soil bacteria and influence both strength and healing performance across different environmental settings.
- Controlled water flow played a critical role in enhancing carbonation and bacterial viability in this study. Future work should focus on optimising flow rates to maximise nutrient distribution and bacterial activation without compromising matrix integrity. Moreover, integrating sensor-based monitoring systems with water flow setups could enable automated healing evaluation and better control over healing environments in service conditions.
- Although accelerated carbonation helped reduce pH and support bacterial activity, it also depleted free calcium ions needed for MICP. Further studies should focus on balancing carbonation with calcium retention, perhaps through formulation adjustments or external calcium supplementation. Testing alternative carbonation

approaches—such as staged or pulsed CO_2 exposure—and evaluating their effects on healing efficiency and concrete durability would be a logical next step.

- Soil type and quality are critical variables influencing the success of bio-concrete. Future research should involve quantitative soil characterisation (e.g. organic content, microbial load, pH, and moisture) to correlate healing performance with specific soil properties. There is also scoped to explore microbial enrichment techniques, such as adding microbial consortia or organic amendments, to enhance healing in less fertile soils.

References

Achal, V. *et al.* (no date) 'Biogenic treatment improves the durability and remediates the cracks of concrete structures', *ElsevierV Achal, A Mukerjee, MS ReddyConstruction and Building Materials, 2013•Elsevier* [Preprint]. Available at: https://www.sciencedirect.com/science/article/pii/S0950061813005795?casa_token=TQ95VzBi1_UAAAAA:F3w-_rJxNyf3jMOy4wTAUHdL5lT9U-Xgf5TSgYqRDTQ4VdphiQUPrKv1E91hu7XQsZHDIQY (Accessed: 2 October 2024).

Achal, V., Mukherjee, A. and Reddy, M.S. (2010) 'Microbial Concrete: Way to Enhance the Durability of Building Structures', *Journal of Materials in Civil Engineering*, 23(6), pp. 730–734. Available at: https://doi.org/10.1061/(ASCE)MT.1943-5533.0000159.

Achternbosch, M. *et al.* (2011) 'Climate-Friendly Production of Cement: A Utopian Vision?', *ingentaconnect.com* [Preprint]. Available at: https://www.ingentaconnect.com/content/oekom/gaia/2011/00000020/00000001/art00008 (Accessed: 28 February 2023).

Ahmad, J. *et al.* (2022) 'A Comprehensive Review on the Ground Granulated Blast Furnace Slag (GGBS) in Concrete Production', *Sustainability 2022, Vol. 14, Page 8783*, 14(14), p. 8783. Available at: https://doi.org/10.3390/SU14148783.

Almeida, F.C.R. and Klemm, A.J. (2018) 'Effect of GGBS on Water Absorption Capacity and Stability of Superabsorbent Polymers Partially Crosslinked with Alkalis', *Journal of Materials in Civil Engineering*, 30(12), p. 04018315. Available at: https://doi.org/10.1061/(ASCE)MT.1943-5533.0002511.

Alonso, C. *et al.* (2006) 'Ground water leaching resistance of high and ultra high performance concretes in relation to the testing convection regime', *Cement and Concrete Research*, 36(9), pp. 1583–1594. Available at: https://doi.org/10.1016/J.CEMCONRES.2006.04.004.

Al-Thawadi, S., Al-Thawadi, S.M. and Info, A. (2011) 'Ureolytic Bacteria and Calcium Carbonate Formation as a Mechanism of Strength Enhancement of Sand Biosynthesis of nanoparticles View project Ureolytic Bacteria and Calcium Carbonate Formation as a Mechanism of Strength Enhancement of Sand', *Journal of Advanced Science and Engineering Research*, 1, pp. 98–114. Available at: https://www.researchgate.net/publication/230603500 (Accessed: 1 April 2022).

Altoubat, S., Concrete, D.L.-A.M.J.-A. and 2001, undefined (no date) 'Creep, shrinkage, and cracking of restrained concrete at early age', *academia.eduSA Altoubat, DA LangeACI Materials Journal-American Concrete Institute, 2001•academia.edu* [Preprint]. Available at: https://www.academia.edu/download/74974350/Creep_Shrinkage_and_Cracking_of_Restrain20211121-28992-ljf46s.pdf (Accessed: 2 October 2024).

Amarakoon, G.G.N.N. and Kawasaki, S. (2016) 'Factors Affecting the Improvement of Sand Properties Treated with Microbially-Induced Calcite Precipitation', pp. 72–83. Available at: https://doi.org/10.1061/9780784480120.009.

Amer Algaifi, H. *et al.* (2020a) 'Insight into the role of microbial calcium carbonate and the factors involved in self-healing concrete', *Construction and Building Materials*, 254, p. 119258. Available at: https://doi.org/10.1016/J.CONBUILDMAT.2020.119258.

Amer Algaifi, H. *et al.* (2020b) 'Insight into the role of microbial calcium carbonate and the factors involved in self-healing concrete', *Construction and Building Materials*, 254, p. 119258. Available at: https://doi.org/10.1016/J.CONBUILDMAT.2020.119258.

Amran, M. *et al.* (2022a) 'Self-Healing Concrete as a Prospective Construction Material: A Review', *Materials*, 15(9). Available at: https://doi.org/10.3390/MA15093214.

Anglani, G., Tulliani, J.M. and Antonaci, P. (2020) 'Behaviour of Pre-Cracked Self-Healing Cementitious Materials under Static and Cyclic Loading', *Materials 2020, Vol. 13, Page 1149*, 13(5), p. 1149. Available at: https://doi.org/10.3390/MA13051149.

Arya, C. and Ofori-Darko, F.K. (1996) 'Influence of crack frequency on reinforcement corrosion in concrete', *Cement and Concrete Research*, 26(3), pp. 345–353. Available at: https://doi.org/10.1016/S0008-8846(96)85022-8.

Atiş, C.D. (2003) 'Accelerated carbonation and testing of concrete made with fly ash', *Construction and Building Materials*, 17(3), pp. 147–152. Available at: https://doi.org/10.1016/S0950-0618(02)00116-2.

'Bacteria-based self-healing concrete' (2011), 56(1).

Bangert, F. *et al.* (2003) 'Environmentally induced deterioration of concrete: physical motivation and numerical modeling', *Engineering Fracture Mechanics*, 70(7–8), pp. 891–910. Available at: https://doi.org/10.1016/S0013-7944(02)00156-X.

Banthia, N., Research, R.G.-C. and concrete and 2006, undefined (no date) 'Influence of polypropylene fiber geometry on plastic shrinkage cracking in concrete', *ElsevierN Banthia, R GuptaCement and concrete Research, 2006•Elsevier* [Preprint]. Available at: https://www.sciencedirect.com/science/article/pii/S0008884606000056?casa_token=baiXEL0ZsGkAAAAA:ijLXwrgAnZ-a-GVj7Xou2ktGtpqE0B55JvNmzuwgHN2_WVYV8MfdtTumNsxJ0NiLq1aTK1fQ (Accessed: 2 October 2024).

Basheer, P. *et al.* (no date) 'Predictive models for deterioration of concrete structures', *ElsevierPAM Basheer, SE Chidiact, AE LongConstruction and Building Materials, 1996•Elsevier* [Preprint]. Available at: https://www.sciencedirect.com/science/article/pii/0950061895000925 (Accessed: 27 August 2024).

Baumgartner, L.K. *et al.* (no date) 'Sulfate reducing bacteria in microbial mats: Changing paradigms, new discoveries'. Available at: https://doi.org/10.1016/j.sedgeo.2005.12.008.

de Belie, N. *et al.* (2018a) 'A Review of Self-Healing Concrete for Damage Management of Structures', *Advanced Materials Interfaces*, 5(17), p. 1800074. Available at: https://doi.org/10.1002/ADMI.201800074.

de Belie, N. *et al.* (2018b) 'A Review of Self-Healing Concrete for Damage Management of Structures', *Advanced Materials Interfaces*, 5(17), p. 1800074. Available at: https://doi.org/10.1002/ADMI.201800074.

De Belie, N. and Wang, J. (2016) 'Bacteria-based repair and self-healing of concrete', *Journal of Sustainable Cement-Based Materials*, 5(1), pp. 35–56. Available at: https://doi.org/10.1080/21650373.2015.1077754.

Belleghem, B. Van *et al.* (no date) 'Capillary water absorption in cracked and uncracked mortar–A comparison between experimental study and finite element analysis', *Elsevier* [Preprint]. Available at: https://www.sciencedirect.com/science/article/pii/S0950061816300861 (Accessed: 9 January 2024).

Bennacef, C. *et al.* (2023) 'Influence of Alginate Properties and Calcium Chloride Concentration on Alginate Bead Reticulation and Size: A Phenomenological Approach', *Polymers*, 15(20), p. 4163. Available at: https://doi.org/10.3390/POLYM15204163.

Bentur, A. and Mitchell, D. (2008) 'Material performance lessons', *Cement and Concrete Research*, 38(2), pp. 259–272. Available at: https://doi.org/10.1016/J.CEMCONRES.2007.09.009.

Beycioğlu, A., Çomak, B. and Akçaabat, D. (2017) 'Evaluation of pH Value by Using Image Processing', 132. Available at: https://doi.org/10.12693/APhysPolA.132.1142.

Biondini, F. and Frangopol, D.M. (2016) 'Life-Cycle Performance of Deteriorating Structural Systems under Uncertainty: Review', *Journal of Structural Engineering*, 142(9), p. F4016001. Available at: https://doi.org/10.1061/(ASCE)ST.1943-541X.0001544.

Blaiszik, B.J. *et al.* (2010) 'Self-Healing Polymers and Composites', *http://dx.doi.org/10.1146/annurev-matsci-070909-104532*, 40, pp. 179–211. Available at: https://doi.org/10.1146/ANNUREV-MATSCI-070909-104532.

de Brito, J. and Kurda, R. (2021) 'The past and future of sustainable concrete: A critical review and new strategies on cement-based materials', *Journal of Cleaner Production*, 281, p. 123558. Available at: https://doi.org/10.1016/J.JCLEPRO.2020.123558.

Broomfield, J. (2023) *Corrosion of steel in concrete: understanding, investigation and repair*. Available at: https://www.taylorfrancis.com/books/mono/10.1201/9781003223016/corrosion-steel-concrete-john-broomfield (Accessed: 10 October 2024).

Bueno Márquez, P. *et al.* (2008) *Compostaje*. Available at: https://books.google.com/books?hl=en&lr=&id=APuzwas6rrcC&oi=fnd&pg=PA4&ots=BTOuN4mtU7&sig=imV9G1nJY5S2sLCgek3IBVA6Uo8 (Accessed: 23 May 2024).

Bulletins, D.R.-E. and 1977, undefined (no date) 'The role of soil invertebrates in nutrient cycling', *JSTOR* [Preprint]. Available at: https://www.jstor.org/stable/20112575?casa_token=HPrJmaLBRDoAAAAA:uqccC5xfWTmB7CnIXtV3kWG4jOisuHlqWhxkp_U81ECI1yxg8W_OkOp1sBdQX_nvlwrZR-wSrYqSrHOuabD6xRFBTYXfU7lKxk2GfQgSLGklOUPU9CY (Accessed: 30 March 2022).

Cao, H.T. *et al.* (1997) 'The effect of cement composition and pH of environment on sulfate resistance of Portland cements and blended cements', *Cement and Concrete Composites*, 19(2), pp. 161–171. Available at: https://doi.org/10.1016/S0958-9465(97)00011-5.

Ch Madhavi, T. and Annamalai, S. (2016) 'ELECTRICAL CONDUCTIVITY OF CONCRETE', 11(9). Available at: www.arpnjournals.com (Accessed: 1 November 2022).

Chahal, N. *et al.* (no date) 'Influence of bacteria on the compressive strength, water absorption and rapid chloride permeability of fly ash concrete', *Elsevier* [Preprint]. Available at: https://www.sciencedirect.com/science/article/pii/S0950061811003965?casa_token=X7tXXRS

VvIIAAAAA:kqGHIBEUA_s_43cPqvuWMsHhb_WKuji3wXYBZrmFQV-X2gXEqsL6cfO200EyJH4Z0kRaUq9E (Accessed: 5 September 2022).

Chai, J.C., Onitsuk, K. and Hayashi, S. (2009) 'Cr(VI) concentration from batch contact/tank leaching and column percolation test using fly ash with additives', *Journal of Hazardous Materials*, 166(1), pp. 67–73. Available at: https://doi.org/10.1016/J.JHAZMAT.2008.11.010.

Chalee, W. *et al.* (no date) 'Utilization of fly ash concrete in marine environment for long term design life analysis', *Elsevier* [Preprint]. Available at: https://www.sciencedirect.com/science/article/pii/S0261306909005093 (Accessed: 28 February 2023).

Chandra, S. and Berntsson, L. (2002) *Lightweight aggregate concrete*. Available at: https://books.google.com/books?hl=en&lr=&id=9mmcbg9qgG0C&oi=fnd&pg=PP1&dq=Chandra,+S.,+%26+Berntsson,+L.+(2002).+Lightweight+Aggregate+Concrete:+Science,+Technology,+and+Applications.+William+Andrew+Publishing.&ots=ewYVraD7KX&sig=wORbYZ2CggWPF9hGf-krVI02on0 (Accessed: 7 October 2024).

Chandra Sekhara Reddy, T. and Ravitheja, A. (2019) 'Macro mechanical properties of self healing concrete with crystalline admixture under different environments', *Ain Shams Engineering Journal*, 10(1), pp. 23–32. Available at: https://doi.org/10.1016/J.ASEJ.2018.01.005.

'Chapter 7 GUIDELINE SAMPLE PREPARATION' (no date).

Cheng, A. *et al.* (2005a) 'Influence of GGBS on durability and corrosion behavior of reinforced concrete', *Materials Chemistry and Physics*, 93(2–3), pp. 404–411. Available at: https://doi.org/10.1016/J.MATCHEMPHYS.2005.03.043.

Cheng, A. *et al.* (2005b) 'Influence of GGBS on durability and corrosion behavior of reinforced concrete', *Materials Chemistry and Physics*, 93(2–3), pp. 404–411. Available at: https://doi.org/10.1016/J.MATCHEMPHYS.2005.03.043.

Cheng, A. *et al.* (2013) 'Effects of leaching behavior of calcium ions on compression and durability of cement-based materials with mineral admixtures', *mdpi.com*, 6, pp. 1851–1872. Available at: https://doi.org/10.3390/ma6051851.

composites, C.M.-C. and concrete and 2009, undefined (no date) 'The greening of the concrete industry', *ElsevierC MeyerCement and concrete composites, 2009•Elsevier* [Preprint]. Available at: https://www.sciencedirect.com/science/article/pii/S0958946509000031?casa_token=3qETOk1LafEAAAAA:O6ZCM5ykjwCNrzv93zoJwv8_CKH13YBTouHc2Tm_yOkks1QleecLk4GftkY6-2WY_9KvFrtiAg (Accessed: 27 August 2024).

'Control of cracking in concrete structures' (2001), p. 46.

Cope, J. *et al.* (2002) 'Effect of restraint, volume change, and reinforcement on cracking of mass concrete', *civilwares.free.fr* [Preprint]. Available at: http://civilwares.free.fr/ACI/MCP04/2072r_95.pdf (Accessed: 7 October 2024).

Coppola, L., Coffetti, D. and Crotti, E. (2018) 'Innovative carboxylic acid waterproofing admixture for self-sealing watertight concretes', *Construction and Building Materials*, 171, pp. 817–824. Available at: https://doi.org/10.1016/J.CONBUILDMAT.2018.03.201.

Cuenca, E. *et al.* (no date) 'A methodology to assess crack-sealing effectiveness of crystalline admixtures under repeated cracking-healing cycles', *ElsevierE Cuenca, A Tejedor, L FerraraConstruction and Building Materials, 2018•Elsevier* [Preprint]. Available at: https://www.sciencedirect.com/science/article/pii/S095006181831345X?casa_token=knlCnqIrVM0AAAAA:fbkS6KY739AlG_FvGgmLzfUDxbmWlGztQkVleXM9InjNUsjjpSTt3zlac4-4LxvKoAvSBC0_Mg (Accessed: 22 May 2024).

Cuenca, E. and Ferrara, L. (2017) 'Self-healing capacity of fiber reinforced cementitious composites. State of the art and perspectives', *KSCE Journal of Civil Engineering 2017 21:7*, 21(7), pp. 2777–2789. Available at: https://doi.org/10.1007/S12205-017-0939-5.

Davies, R. *et al.* (2018) 'Large scale application of self-healing concrete: Design, construction, and testing', *Frontiers in Materials*, 5, p. 51. Available at: https://doi.org/10.3389/FMATS.2018.00051/BIBTEX.

DeJong, J. *et al.* (2014) 'Bacteria, Biofilms, and Invertebrates: The Next Generation of Geotechnical Engineers?', pp. 3959–3968. Available at: https://doi.org/10.1061/9780784413272.384.

Dejong, J.T. *et al.* (2013) 'Biogeochemical processes and geotechnical applications: Progress, opportunities and challenges', *Bio- and Chemo- Mechanical Processes in Geotechnical Engineering - Geotechnique Symposium in Print 2013*, pp. 143–157. Available at: https://doi.org/10.1680/BCMPGE.60531.014.

Dhami, N.K., Reddy, M.S. and Mukherjee, M.S. (2013a) 'Biomineralization of calcium carbonates and their engineered applications: A review', *Frontiers in Microbiology*, 4(OCT). Available at: https://doi.org/10.3389/FMICB.2013.00314/FULL.

Dhami, N.K., Reddy, M.S. and Mukherjee, M.S. (2013b) 'Biomineralization of calcium carbonates and their engineered applications: A review', *Frontiers in Microbiology*, 4(OCT), p. 314. Available at: https://doi.org/10.3389/FMICB.2013.00314/BIBTEX.

Dhir, R.K.. and Jones, R.M.. (1999) 'WATER PERMEABILITY AND AUTOGENOUS HEALING OF CRACKS IN CONCRETE', p. 696. Available at: https://doi.org/10.1680/IICSDAC.28241.0047.

Diep, T. and Thao, P. (2011) 'QUASI-BRITTLE SELF-HEALING MATERIALS: NUMERICAL MODELLING AND APPLICATIONS IN CIVIL ENGINEERING'.

Dong, B. *et al.* (2013) 'A microcapsule technology based self-healing system for concrete structures', *Journal of Earthquake and Tsunami*, 7(3). Available at: https://doi.org/10.1142/S1793431113500140.

Dong, B. *et al.* (2015) 'Smart releasing behavior of a chemical self-healing microcapsule in the stimulated concrete pore solution', *Cement and Concrete Composites*, 56, pp. 46–50. Available at: https://doi.org/10.1016/J.CEMCONCOMP.2014.10.006.

Dong, B. *et al.* (2017) 'Performance recovery concerning the permeability of concrete by means of a microcapsule based self-healing system', *Cement and Concrete Composites*, 78, pp. 84–96. Available at: https://doi.org/10.1016/J.CEMCONCOMP.2016.12.005.

Dong, B. *et al.* (no date) 'Performance recovery concerning the permeability of concrete by means of a microcapsule based self-healing system', *ElsevierB Dong, G Fang, Y Wang, Y Liu, S Hong, J Zhang, S Lin, F XingCement and Concrete Composites, 2017•Elsevier* [Preprint].

Available at:
https://www.sciencedirect.com/science/article/pii/S0958946516308186?casa_token=EX1TbcfTE5AAAAAA:-oidpUX4u_LFCNTek_CscOYiKXkQCEI9Me09lQ6Qvm6c55Dw67ZxngBrolFBDQA7yot8Q5GFRQ (Accessed: 2 October 2024).

Doyle, J. and Cooper, J.S. (2023) 'Physiology, Carbon Dioxide Transport', *StatPearls* [Preprint]. Available at: https://www.ncbi.nlm.nih.gov/sites/books/NBK532988/ (Accessed: 15 January 2025).

Dry, C. (1994a) 'Matrix cracking repair and filling using active and passive modes for smart timed release of chemicals from fibers into cement matrices', *Smart Materials and Structures*, 3(2), p. 118. Available at: https://doi.org/10.1088/0964-1726/3/2/006.

Dry, C. (1994b) 'Matrix cracking repair and filling using active and passive modes for smart timed release of chemicals from fibers into cement matrices', *Smart Materials and Structures*, 3(2), p. 118. Available at: https://doi.org/10.1088/0964-1726/3/2/006.

Duan, Y. *et al.* (2023) 'Investigating the Impact of Fly Ash on the Strength and Micro-Structure of Concrete during Steam Curing and Subsequent Stages', *Materials 2023, Vol. 16, Page 1326*, 16(4), p. 1326. Available at: https://doi.org/10.3390/MA16041326.

Ducret, A., Quardokus, E.M. and Brun, Y. V. (2016a) 'MicrobeJ, a tool for high throughput bacterial cell detection and quantitative analysis', *Nature microbiology*, 1(7), p. 16077. Available at: https://doi.org/10.1038/NMICROBIOL.2016.77.

Ducret, A., Quardokus, E.M. and Brun, Y. V. (2016b) 'MicrobeJ, a tool for high throughput bacterial cell detection and quantitative analysis', *Nature Microbiology 2016 1:7*, 1(7), pp. 1–7. Available at: https://doi.org/10.1038/nmicrobiol.2016.77.

Dupraz, S. *et al.* (2009) 'Experimental and numerical modeling of bacterially induced pH increase and calcite precipitation in saline aquifers', *Chemical Geology*, 265(1–2), pp. 44–53. Available at: https://doi.org/10.1016/J.CHEMGEO.2009.05.003.

Engineering, M.B.-P. and 2011, undefined (no date) 'Sustainable cements for green buildings construction', *Elsevier* [Preprint]. Available at: https://www.sciencedirect.com/science/article/pii/S1877705811049289 (Accessed: 28 February 2023).

Epelde, L. *et al.* (2008) 'Functional diversity as indicator of the recovery of soil health derived from Thlaspi caerulescens growth and metal phytoextraction', *Applied Soil Ecology*, 39(3), pp. 299–310. Available at: https://doi.org/10.1016/J.APSOIL.2008.01.005.

Erktan, A., Or, D. and Scheu, S. (2020) 'The physical structure of soil: Determinant and consequence of trophic interactions', *Soil Biology and Biochemistry*, 148, p. 107876. Available at: https://doi.org/10.1016/J.SOILBIO.2020.107876.

Erşan, Y.Ç., de Belie, N. and Boon, N. (2015) 'Microbially induced CaCO3 precipitation through denitrification: An optimization study in minimal nutrient environment', *Biochemical Engineering Journal*, 101, pp. 108–118. Available at: https://doi.org/10.1016/J.BEJ.2015.05.006.

Esaker, M. *et al.* (2021) 'Self-healing of bio-cementitious mortar incubated within neutral and acidic soil', *Materials and Structures/Materiaux et Constructions*, 54(2), pp. 1–16. Available at: https://doi.org/10.1617/S11527-021-01690-1/FIGURES/12.

Fang, C. *et al.* (no date) 'Corrosion influence on bond in reinforced concrete', *ElsevierC Fang, K Lundgren, L Chen, C ZhuCement and concrete research, 2004•Elsevier* [Preprint]. Available at: https://www.sciencedirect.com/science/article/pii/S0008884604001607?casa_token=2YiTBtBAPn8AAAAA:2vvf3jvvDAZvUklMb5MX3KzMbR6ha_RWCtcaeL4n_XMk7UZYrP4oGFT1w7XZqZdsQmpU9KtlfQ (Accessed: 10 October 2024).

Feiteira, J., Gruyaert, E. and de Belie, N. (2016) 'Self-healing of moving cracks in concrete by means of encapsulated polymer precursors', *Construction and Building Materials*, 102, pp. 671–678. Available at: https://doi.org/10.1016/J.CONBUILDMAT.2015.10.192.

Femenias, Y.S., Angst, U. and Elsener, B. (2017) 'PH-monitoring in mortar with thermally-oxidized iridium electrodes', *RILEM Technical Letters*, 2, pp. 59–66. Available at: https://doi.org/10.21809/RILEMTECHLETT.2017.37.

Ferris, F.G. *et al.* (2004) 'Kinetics of calcite precipitation induced by ureolytic bacteria at 10 to 20°C in artificial groundwater', *Geochimica et Cosmochimica Acta*, 68(8), pp. 1701–1710. Available at: https://doi.org/10.1016/S0016-7037(03)00503-9.

Fraay, A.L.A., Bijen, J.M. and de Haan, Y.M. (1989) 'The reaction of fly ash in concrete a critical examination', *Cement and Concrete Research*, 19(2), pp. 235–246. Available at: https://doi.org/10.1016/0008-8846(89)90088-4.

Fujita, Y. *et al.* (2004) 'Strontium incorporation into calcite generated by bacterial ureolysis', *Geochimica et Cosmochimica Acta*, 68(15), pp. 3261–3270. Available at: https://doi.org/10.1016/J.GCA.2003.12.018.

Gadd, G.M. and Dyer, T.D. (2017a) 'Bioprotection of the built environment and cultural heritage', *Microbial Biotechnology*, 10(5), p. 1152. Available at: https://doi.org/10.1111/1751-7915.12750.

Gadd, G.M. and Dyer, T.D. (2017b) 'Bioprotection of the built environment and cultural heritage', *Microbial Biotechnology*, 10(5), p. 1152. Available at: https://doi.org/10.1111/1751-7915.12750.

Gardner, D. *et al.* (2018) 'A survey on problems encountered in current concrete construction and the potential benefits of self-healing cementitious materials', *Case Studies in Construction Materials*, 8, pp. 238–247. Available at: https://doi.org/10.1016/J.CSCM.2018.02.002.

Gauvry, E. *et al.* (2021) 'Effects of temperature, pH and water activity on the growth and the sporulation abilities of Bacillus subtilis BSB1', *International journal of food microbiology*, 337. Available at: https://doi.org/10.1016/J.IJFOODMICRO.2020.108915.

Ghosh, S.K. (2009) 'Self-Healing Materials: Fundamentals, Design Strategies, and Applications', *Self-Healing Materials: Fundamentals, Design Strategies, and Applications*, pp. 1–291. Available at: https://doi.org/10.1002/9783527625376.

Giang, P.H.H. *et al.* (no date) 'Self-healing materials and structures for geotechnical and geo-environmental applications'. Available at: https://doi.org/10.1680/ECSMGE.60678.VOL2.071.

Gilford, J. *et al.* (2014) 'Dicyclopentadiene and sodium silicate microencapsulation for self-healing of concrete', *Journal of Materials in Civil Engineering*, 26(5), pp. 886–896. Available at: https://doi.org/10.1061/(ASCE)MT.1943-5533.0000892.

Gojević, A. *et al.* (2021) 'The Effect of Crystalline Waterproofing Admixtures on the Self-Healing and Permeability of Concrete', *Materials 2021, Vol. 14, Page 1860*, 14(8), p. 1860. Available at: https://doi.org/10.3390/MA14081860.

Goldstein, J.I. *et al.* (2017) 'Scanning electron microscopy and x-ray microanalysis', *Scanning Electron Microscopy and X-ray Microanalysis*, pp. 1–550. Available at: https://doi.org/10.1007/978-1-4939-6676-9.

Gollapudi, U.K. *et al.* (1995) 'A new method for controlling leaching through permeable channels', *Chemosphere*, 30(4), pp. 695–705. Available at: https://doi.org/10.1016/0045-6535(94)00435-W.

González-Muñoz, M.T. *et al.* (2010) 'Bacterial biomineralization: new insights from Myxococcus-induced mineral precipitation', *Geological Society, London, Special Publications*, 336(1), pp. 31–50. Available at: https://doi.org/10.1144/SP336.3.

Grieve, T.K.e.a., Non-structural cracks in concrete, ed. - Google Search (no date). Available at: https://www.google.co.uk/search?q=Grieve%2C+T.K.e.a.%2C+Non-structural+cracks+in+concrete%2C+ed.&sca_esv=83baeecfea64ff8d&sxsrf=ADLYWIL1fHnk3snVZykKrNtuI5d-5-mung%3A1728562637115&source=hp&ei=zcUHZ6v5BLeohbIP2NndqQg&iflsig=AL9hbdgAAAAAZwfT3bel8QdCNJyxcPzkcxJ1_ge1o1Y1&ved=0ahUKEwjrk9LP5YOJAxU3VEEAHdhsN4UQ4dUDCBg&uact=5&oq=Grieve%2C+T.K.e.a.%2C+Non-structural+cracks+in+concrete%2C+ed.&gs_lp=Egdnd3Mtd2l6IjhHcmlldmUsIFQuSy5lLmEuLCBOb24tc3RydWN0dXJhbCBjcmFja3MgaW4gY29uY3JldGUsIGVkLjIHECEYoAEYCkjWElDZCljZCnABeACQAQCYAasBoAGrAaoBAzAuMbgBA8gBAPgBAvgBAZgCAqACswGoAgrCAgcQIxgnGOoCwgIHEC4YJxjqApgDBZIHAzEuMaAHxAM&sclient=gws-wiz (Accessed: 10 October 2024).

Gruyaert, E. *et al.* (2016a) 'Capsules with evolving brittleness to resist the preparation of self-healing concrete', *Materiales de Construccion*, 66(323). Available at: https://doi.org/10.3989/MC.2016.07115.

Gruyaert, E. *et al.* (2016b) 'Capsules with evolving brittleness to resist the preparation of self-healing concrete', *Materiales de Construcción*, 66(323), pp. e092–e092. Available at: https://doi.org/10.3989/MC.2016.07115.

Guadagno, L. *et al.* (2019) 'Self-healing epoxy nanocomposites via reversible hydrogen bonding', *Composites Part B: Engineering*, 157, pp. 1–13. Available at: https://doi.org/10.1016/J.COMPOSITESB.2018.08.082.

Gupta, S., Pang, S.D. and Kua, H.W. (2017a) 'Autonomous healing in concrete by bio-based healing agents – A review', *Construction and Building Materials*, 146, pp. 419–428. Available at: https://doi.org/10.1016/J.CONBUILDMAT.2017.04.111.

Gupta, S., Pang, S.D. and Kua, H.W. (2017b) 'Autonomous healing in concrete by bio-based healing agents – A review', *Construction and Building Materials*, 146, pp. 419–428. Available at: https://doi.org/10.1016/J.CONBUILDMAT.2017.04.111.

Hamdan, N. *et al.* (2011) 'Carbonate mineral precipitation for soil improvement through microbial denitrification', pp. 3925–3934. Available at: https://doi.org/10.1061/41165(397)401.

Hammes, F. *et al.* (2010) 'Assessing biological stability of drinking water without disinfectant residuals in a full-scale water supply system', *Journal of Water Supply: Research and Technology-Aqua*, 59(1), pp. 31–40. Available at: https://doi.org/10.2166/AQUA.2010.052.

Hamza, O. *et al.* (2020) 'The effect of soil incubation on bio self-healing of cementitious mortar', *Materials Today Communications*, 24, p. 100988. Available at: https://doi.org/10.1016/J.MTCOMM.2020.100988.

Hamza, O. *et al.* (2021) 'RM4L2020 International Conference Paper number: 122 20-22 September 2021 Online Evaluation of the self-healing of cracked mortars incubated within', 122, pp. 20–22. Available at: https://www.researchgate.net/profile/Adam-Souid/publication/354860007_Evaluation_of_the_self-healing_of_cracked_mortars_incubated_within_sterilized_and_non-sterilized_natural_soil/links/6151a314522ef665fb6205ae/Evaluation-of-the-self-healing-of-cracked-mortars-incubated-within-sterilized-and-non-sterilized-natural-soil.pdf (Accessed: 23 May 2024).

Hamza, O. *et al.* (no date) 'Bio-protection of cementitious materials below ground: The significance of natural soil environments', *Elsevier* [Preprint]. Available at: https://www.sciencedirect.com/science/article/pii/S2666165924000127 (Accessed: 5 February 2024).

Harbottle, M. *et al.* (no date) 'Combined physical and biological gel-based healing of cementitious materials', *Citeseer* [Preprint]. Available at: https://citeseerx.ist.psu.edu/viewdoc/download?doi=10.1.1.890.4473&rep=rep1&type=pdf (Accessed: 14 April 2022).

Hartland, Stanley. (2004) 'Surface and interfacial tension : measurement, theory, and applications', p. 619.

Hermawan, H. *et al.* (2021) 'Understanding the Impacts of Healing Agents on the Properties of Fresh and Hardened Self-Healing Concrete: A Review', *Processes 2021, Vol. 9, Page 2206*, 9(12), p. 2206. Available at: https://doi.org/10.3390/PR9122206.

Hilloulin, B. *et al.* (2015) 'Design of polymeric capsules for self-healing concrete', *Cement and Concrete Composites*, 55, pp. 298–307. Available at: https://doi.org/10.1016/J.CEMCONCOMP.2014.09.022.

Hilloulin, B. *et al.* (2016) 'Mechanical regains due to self-healing in cementitious materials: Experimental measurements and micro-mechanical model', *Cement and Concrete Research*, 80, pp. 21–32. Available at: https://doi.org/10.1016/J.CEMCONRES.2015.11.005.

Hilloulin, B. *et al.* (no date) 'Design of polymeric capsules for self-healing concrete Design of polymeric capsules for self-healing concrete 1 2'. Available at: https://doi.org/10.1016/j.cemconcomp.2014.09.022ï.

Hohberg, I. *et al.* (2000) 'Development of a leaching protocol for concrete', *Waste Management*, 20(2–3), pp. 177–184. Available at: https://doi.org/10.1016/S0956-053X(99)00324-4.

Homma, D., Mihashi, H. and Nishiwaki, T. (2009a) 'Self-healing capability of fibre reinforced cementitious composites', *Journal of Advanced Concrete Technology*, 7(2), pp. 217–228. Available at: https://doi.org/10.3151/JACT.7.217.

Homma, D., Mihashi, H. and Nishiwaki, T. (2009b) 'Self-healing capability of fibre reinforced cementitious composites', *Journal of Advanced Concrete Technology*, 7(2), pp. 217–228. Available at: https://doi.org/10.3151/JACT.7.217.

Hommel, J. *et al.* (2016) 'Investigating the Influence of the Initial Biomass Distribution and Injection Strategies on Biofilm-Mediated Calcite Precipitation in Porous Media', *Transport in Porous Media*, 114(2), pp. 557–579. Available at: https://doi.org/10.1007/S11242-015-0617-3/FIGURES/13.

Hoseini, O. *et al.* (2018) 'International Journal of Molecular and Clinical Microbiology Visualization of acidic and alkaline pH effect on biofilm formation of Staphylococcus aureus isolates by Atomic force m International Journal of Molecular and Clinical Microbiology Visualization of acidic and alkaline pH effect on biofilm formation of Staphylococcus aureus isolates by Atomic force microscope', *International Journal of Molecular and Clinical Microbiology*, 8(1), pp. 942–949. Available at: https://www.researchgate.net/publication/336847666 (Accessed: 28 October 2024).

Huang, W. *et al.* (2010) 'Morphology controllable synthesis of ZnO crystals—pH-dependent growth', *Materials Chemistry and Physics*, 123(1), pp. 104–108. Available at: https://doi.org/10.1016/J.MATCHEMPHYS.2010.03.067.

Hulagabali, M., Prabhakara, D.R. and Hulagabali, A. (2018) 'Assessment of Water Absorption Capacity of Concrete with GGBS Replacement', *International Journal of Recent Research in Civil and Mechanical Engineering (IJRRCME)*, 5, pp. 1–9. Available at: www.paperpublications.org (Accessed: 26 February 2024).

Hung, C.C., Su, Y.F. and Hung, H.H. (2017) 'Impact of natural weathering on medium-term self-healing performance of fiber reinforced cementitious composites with intrinsic crack-width control capability', *Cement and Concrete Composites*, 80, pp. 200–209. Available at: https://doi.org/10.1016/J.CEMCONCOMP.2017.03.018.

Hung, C.C., Su, Y.F. and Su, Y.M. (2018) 'Mechanical properties and self-healing evaluation of strain-hardening cementitious composites with high volumes of hybrid pozzolan materials', *Composites Part B: Engineering*, 133, pp. 15–25. Available at: https://doi.org/10.1016/J.COMPOSITESB.2017.09.005.

Jacobsen', S., Marchand, J. and Homain, H. (1995a) 'ooo8-8846(95)00174-3 SEM OBSERVATIONS OF THE MICROSTRUCTURE OF FROST DETERIORATED AND SELF-HEALED CONCRETES', *Cement and Concrete Research*, 25(8), pp. 1781–1790. Available at: https://doi.org/10.1016/0008-8846(95)00174-3.

Jacobsen', S., Marchand, J. and Homain, H. (1995b) 'ooo8-8846(95)00174-3 SEM OBSERVATIONS OF THE MICROSTRUCTURE OF FROST DETERIORATED AND SELF-HEALED CONCRETES', *Cement and Concrete Research*, 25(8), pp. 1781–1790. Available at: https://doi.org/10.1016/0008-8846(95)00174-3.

Jacobsen, S. and Sellevold, E.J. (1996) 'Self healing of high strength concrete after deterioration by freeze/thaw', *Cement and Concrete Research*, 26(1), pp. 55–62. Available at: https://doi.org/10.1016/0008-8846(95)00179-4.

Jaffer, S.J. and Hansson, C.M. (2009) 'Chloride-induced corrosion products of steel in cracked-concrete subjected to different loading conditions', *Cement and Concrete Research*, 39(2), pp. 116–125. Available at: https://doi.org/10.1016/J.CEMCONRES.2008.11.001.

Janke, L. *et al.* (2005) 'Applications of shape memory alloys in civil engineering structures—Overview, limits and new ideas', *Materials and Structures*, 38(5), pp. 578–592. Available at: https://doi.org/10.1007/BF02479550.

Javeed, Y. *et al.* (2024) 'Microbial self-healing in concrete: A comprehensive exploration of bacterial viability, implementation techniques, and mechanical properties', *Journal of Materials Research and Technology*, 29, pp. 2376–2395. Available at: https://doi.org/10.1016/J.JMRT.2024.01.261.

Jefferson, A. *et al.* (2010) 'A new system for crack closure of cementitious materials using shrinkable polymers', *Cement and Concrete Research*, 40(5), pp. 795–801. Available at: https://doi.org/10.1016/J.CEMCONRES.2010.01.004.

Jiang, Z. *et al.* (2014) 'Self-healing of cracks in concrete with various crystalline mineral additives in underground environment', *Journal of Wuhan University of Technology-Mater. Sci. Ed. 2014 29:5*, 29(5), pp. 938–944. Available at: https://doi.org/10.1007/S11595-014-1024-2.

Jonkers, H.M. *et al.* (2010) 'Application of bacteria as self-healing agent for the development of sustainable concrete', *Ecological Engineering*, 36(2), pp. 230–235. Available at: https://doi.org/10.1016/J.ECOLENG.2008.12.036.

Jonkers, H M (no date) *Bacteria-based self-healing concrete*.

Jonkers, Henk M (no date) *Self Healing Concrete: A Biological Approach*.

Joseph, C. *et al.* (2010) 'Experimental investigation of adhesive-based self-healing of cementitious materials', *icevirtuallibrary.comC Joseph, AD Jefferson, B Isaacs, R Lark, D GardnerMagazine of Concrete Research, 2010•icevirtuallibrary.com*, 62(11), pp. 831–843. Available at: https://doi.org/10.1680/macr.2010.62.11.831.

Joseph, C. *et al.* (2015) 'Experimental investigation of adhesive-based self-healing of cementitious materials', *http://dx.doi.org/10.1680/macr.2010.62.11.831*, 62(11), pp. 831–843. Available at: https://doi.org/10.1680/MACR.2010.62.11.831.

Kadapure, S.A. *et al.* (2019) 'Mechanical and durability performance of sustainable bacteria blended fly ash concrete: an experimental study', *Taylor & Francis*, 13(1), pp. 45–53. Available at: https://doi.org/10.1080/19397038.2019.1644386.

Kan, L. *et al.* (2010) 'Self-Healing Characterization of Engineered Cementitious Composite Materials.', *acemrl.engin.umich.edu* [Preprint]. Available at: http://acemrl.engin.umich.edu/wp-content/uploads/sites/412/2018/10/Self-Healing-Characterization-of-Engineered-Cementitious-Composites-ECC.pdf (Accessed: 31 March 2022).

Kanellopoulos, A., Giannaros, P. and Al-Tabbaa, A. (2016) 'The effect of varying volume fraction of microcapsules on fresh, mechanical and self-healing properties of mortars', *Construction and Building Materials*, 122, pp. 577–593. Available at: https://doi.org/10.1016/J.CONBUILDMAT.2016.06.119.

Kardogan, B. *et al.* (2021) 'Compatibility and biomineralization oriented optimization of nutrient content in nitrate-reducing-biogranules-based microbial self-healing concrete', *mdpi.comB*

Kardogan, K Sekercioglu, YÇ ErşanSustainability, 2021•mdpi.com [Preprint]. Available at: https://doi.org/10.3390/su13168990.

Khan, M.B.E., Dias-da-Costa, D. and Shen, L. (2023) 'Effect of crack orientation on bacterial self-healing of bio-mortar in marine environment', *Materials Today Sustainability*, 24, p. 100608. Available at: https://doi.org/10.1016/J.MTSUST.2023.100608.

Kosarli, M. *et al.* (2019) 'Microcapsule-based self-healing materials: Healing efficiency and toughness reduction vs. capsule size', *Composites Part B: Engineering*, 171, pp. 78–86. Available at: https://doi.org/10.1016/J.COMPOSITESB.2019.04.030.

Kosmatka, S., Kerkhoff, B. and Panarese, W. (2003) 'Design and control of concrete mixtures'. Available at: https://trid.trb.org/View/863024 (Accessed: 2 October 2024).

Kovler, K. and Roussel, N. (2011) 'Properties of fresh and hardened concrete', *Cement and Concrete Research*, 41(7), pp. 775–792. Available at: https://doi.org/10.1016/J.CEMCONRES.2011.03.009.

Kuang, Y. and Ou, J. (2008) 'Self-repairing performance of concrete beams strengthened using superelastic SMA wires in combination with adhesives released from hollow fibers', *Smart Mater. Struct*, 17, pp. 25020–25027. Available at: https://doi.org/10.1088/0964-1726/17/2/025020.

Larosche, C.J. (2009) 'Types and causes of cracking in concrete structures', *Failure, Distress and Repair of Concrete Structures*, pp. 57–83. Available at: https://doi.org/10.1533/9781845697037.1.57.

Lauer, K.R. and Slate, F.O. (1957) 'Autogenous healing of cement paste', *Materiales de Construcción*, 7(080), pp. 51–51. Available at: https://doi.org/10.3989/MC.1957.V07.I080.2137.

Law, D.W. and Evans, J. (2013) 'Effect of Leaching on pH of Surrounding Water', *Materials Journal*, 110(3), pp. 291–296. Available at: https://doi.org/10.14359/51685662.

Law, D.W. and Evans, J. (no date a) *Effect of Leaching on pH of Surrounding Water*, *ACI Materials Journal*. Available at: https://www.researchgate.net/publication/272026952.

Law, D.W. and Evans, J. (no date b) 'Effect of Leaching on pH of Surrounding Water', *ACI Materials Journal*, 110(3). Available at: https://www.researchgate.net/publication/272026952 (Accessed: 27 August 2024).

Lee, B.Y. and Kurtis, K.E. (2017) 'Effect of pore structure on salt crystallization damage of cement-based materials: Consideration of w/b and nanoparticle use', *Cement and Concrete Research*, 98, pp. 61–70. Available at: https://doi.org/10.1016/J.CEMCONRES.2017.04.002.

Lee, H.X.D., Wong, H.S. and Buenfeld, N.R. (2016) 'Self-sealing of cracks in concrete using superabsorbent polymers', *Cement and Concrete Research*, 79, pp. 194–208. Available at: https://doi.org/10.1016/J.CEMCONRES.2015.09.008.

Lee, M.G., Wang, Y.C. and Chiu, C. te (2007) 'A preliminary study of reactive powder concrete as a new repair material', *Construction and Building Materials*, 21(1), pp. 182–189. Available at: https://doi.org/10.1016/J.CONBUILDMAT.2005.06.024.

Lee, Y.S. and Park, W. (2018a) 'Current challenges and future directions for bacterial self-healing concrete', *Applied Microbiology and Biotechnology*, 102(7), pp. 3059–3070. Available at: https://doi.org/10.1007/S00253-018-8830-Y/TABLES/3.

Lee, Y.S. and Park, W. (2018b) 'Current challenges and future directions for bacterial self-healing concrete', *Applied Microbiology and Biotechnology*, 102(7), pp. 3059–3070. Available at: https://doi.org/10.1007/S00253-018-8830-Y/TABLES/3.

Li, V.C., Lim, Y.M. and Chan, Y.W. (1998) 'Feasibility study of a passive smart self-healing cementitious composite', *Composites Part B: Engineering*, 29(6), pp. 819–827. Available at: https://doi.org/10.1016/S1359-8368(98)00034-1.

Li, W. *et al.* (2013) 'Self-Healing Efficiency of Cementitious Materials Containing Microcapsules Filled with Healing Adhesive: Mechanical Restoration and Healing Process Monitored by Water Absorption', *PLOS ONE*, 8(11), p. e81616. Available at: https://doi.org/10.1371/JOURNAL.PONE.0081616.

Li, Z. *et al.* (2019) 'Feasibility of Using 3D Printed Polyvinyl Alcohol (PVA) for Creating Self-Healing Vascular Tunnels in Cement System', *Materials (Basel, Switzerland)*, 12(23), p. 3872. Available at: https://doi.org/10.3390/MA12233872.

Lipiec, J. *et al.* (2006) 'Soil porosity and water infiltration as influenced by tillage methods', *Soil and Tillage Research*, 89(2), pp. 210–220. Available at: https://doi.org/10.1016/J.STILL.2005.07.012.

Liu, E. *et al.* (2017) 'Mapping high pH levels in hydrated calcium silicates', *Cement and Concrete Research*, 95, pp. 232–239. Available at: https://doi.org/10.1016/J.CEMCONRES.2017.02.001.

Liu, G. *et al.* (no date) 'Assessing the origin of bacteria in tap water and distribution system in an unchlorinated drinking water system by SourceTracker using microbial community', *ElsevierG Liu, Y Zhang, E van der Mark, A Magic-Knezev, A Pinto, B van den Bogert, W LiuWater Research, 2018•Elsevier* [Preprint]. Available at: https://www.sciencedirect.com/science/article/pii/S0043135418302392 (Accessed: 22 May 2024).

Liu, H. *et al.* (2017) 'Influence of microcrack self-healing behavior on the permeability of Engineered Cementitious Composites', *Cement and Concrete Composites*, 82, pp. 14–22. Available at: https://doi.org/10.1016/J.CEMCONCOMP.2017.04.004.

Lothenbach, B., Scrivener, K. and Hooton, R.D. (2011) 'Supplementary cementitious materials', *Cement and Concrete Research*, 41(12), pp. 1244–1256. Available at: https://doi.org/10.1016/J.CEMCONRES.2010.12.001.

Lowenthal, R.E. and Marais, G.V.R. (1976) 'Carbonate chemistry of aquatic systems'. Ann Arbor Science Publishers, Inc.,Ann Arbor, MI.

Luan, L. *et al.* (2023) 'Integrating pH into the metabolic theory of ecology to predict bacterial diversity in soil', *Proceedings of the National Academy of Sciences of the United States of America*, 120(3), p. e2207832120. Available at: https://doi.org/10.1073/PNAS.2207832120.

Lun, D. *et al.* (2021) 'Effect of Fly Ash on Leaching Characteristics of Cement-Stabilized Macadam Base', *Materials (Basel, Switzerland)*, 14(20). Available at: https://doi.org/10.3390/MA14205935.

Lv, L. *et al.* (2016) 'Synthesis and characterization of a new polymeric microcapsule and feasibility investigation in self-healing cementitious materials', *Construction and Building Materials*, 105, pp. 487–495. Available at: https://doi.org/10.1016/J.CONBUILDMAT.2015.12.185.

Macpherson, G.L. (2009) 'CO2 distribution in groundwater and the impact of groundwater extraction on the global C cycle', *Chemical Geology*, 264(1–4), pp. 328–336. Available at: https://doi.org/10.1016/j.chemgeo.2009.03.018.

Maddalena, R., Taha, H. and Gardner, D. (2021) 'Self-healing potential of supplementary cementitious materials in cement mortars: Sorptivity and pore structure', *Developments in the Built Environment*, 6, p. 100044. Available at: https://doi.org/10.1016/J.DIBE.2021.100044.

Maes, M., van Tittelboom, K. and de Belie, N. (2014) 'The efficiency of self-healing cementitious materials by means of encapsulated polyurethane in chloride containing environments', *Construction and Building Materials*, 71, pp. 528–537. Available at: https://doi.org/10.1016/J.CONBUILDMAT.2014.08.053.

Martys, N.S. and Ferraris, C.F. (1997) 'Capillary transport in mortars and concrete', *Cement and Concrete Research*, 27(5), pp. 747–760. Available at: https://doi.org/10.1016/S0008-8846(97)00052-5.

Matczuk, D. and Siczek, A. (2021) 'Effectiveness of the use of urease inhibitors in agriculture: a review**', *Int. Agrophys*, 35, pp. 197–208. Available at: https://doi.org/10.31545/intagr/139714.

materials, P.P.-C. and building and 1996, undefined (no date) 'Cathodic protection and cathodic prevention', *ElsevierP PedeferriConstruction and building materials, 1996•Elsevier* [Preprint]. Available at: https://www.sciencedirect.com/science/article/pii/0950061895000178 (Accessed: 10 October 2024).

Mcpolin, D.O. *et al.* (2007) 'New test method to obtain pH profiles due to carbonation of concretes containing supplementary cementitious materials', *ascelibrary.orgDO McPolin, PA Basheer, AE Long, KT Grattan, T SunJournal of Materials in Civil Engineering, 2007•ascelibrary.org*, 19(11), pp. 936–946. Available at: https://doi.org/10.1061/(ASCE)0899-1561(2007)19:11(936).

Meharie, M.G. *et al.* (2017) 'Factors Affecting the Self-Healing Efficiency of Cracked Concrete Structures', *http://www.sciencepublishinggroup.com*, 3(6), p. 80. Available at: https://doi.org/10.11648/J.AJASR.20170306.12.

Mehta, P., Title), P.M.-(No and 2006, undefined (no date) 'Concrete: microstructure, properties, and materials', *cir.nii.ac.jp* [Preprint]. Available at: https://cir.nii.ac.jp/crid/1130000797867624064 (Accessed: 7 October 2024).

Meraz, Md Montaseer *et al.* (2023) 'Self-healing concrete: Fabrication, advancement, and effectiveness for long-term integrity of concrete infrastructures', *Alexandria Engineering Journal*, 73, pp. 665–694. Available at: https://doi.org/10.1016/J.AEJ.2023.05.008.

Milla, J., Hassan, M.M. and Rupnow, T. (2017) 'Evaluation of Self-Healing Concrete with Microencapsulated Calcium Nitrate', *Journal of Materials in Civil Engineering*, 29(12), p. 04017235. Available at: https://doi.org/10.1061/(ASCE)MT.1943-5533.0002072.

Minnebo, P. *et al.* (2017) 'A Novel Design of Autonomously Healed Concrete: Towards a Vascular Healing Network', *Materials 2017, Vol. 10, Page 49*, 10(1), p. 49. Available at: https://doi.org/10.3390/MA10010049.

Mohammed, T.U. *et al.* (2001) 'Effect of Crack Width and Bar Types on Corrosionof Steel in Concrete', *Journal of Materials in Civil Engineering*, 13(3), pp. 194–201. Available at: https://doi.org/10.1061/(ASCE)0899-1561(2001)13:3(194).

MohdSam, A.R. *et al.* (no date) 'Effectiveness of tropical soil bacteria as self-healing agent in concrete'. Available at: https://doi.org/10.1088/1755-1315/220/1/012049.

Montanucci, P. *et al.* (2015) 'Insights in Behavior of Variably Formulated Alginate-Based Microcapsules for Cell Transplantation', *BioMed Research International*, 2015, p. 965804. Available at: https://doi.org/10.1155/2015/965804.

Moraes, L.E. *et al.* (2017) 'Short communication: Urea hydrolysis in dairy cattle manure under different temperature, urea, and pH conditions', *Journal of Dairy Science*, 100(3), pp. 2388–2394. Available at: https://doi.org/10.3168/JDS.2016-11927.

Mosley, W.H., Bungey, J.H. and Hulse, R. (1999) 'Reinforced Concrete Design', *Reinforced Concrete Design* [Preprint]. Available at: https://doi.org/10.1007/978-1-349-14911-7.

Mousa, M.R. *et al.* (2021) 'Determination of the Optimal Parameters for Self-Healing Efficiency of Encapsulated bacteria in Concrete Simulated Subtropical Climate'. Available at: https://doi.org/10.21949/1503647.

Muhammad, N.Z. *et al.* (2016) 'Tests and methods of evaluating the self-healing efficiency of concrete: A review', *Construction and Building Materials*, 112, pp. 1123–1132. Available at: https://doi.org/10.1016/J.CONBUILDMAT.2016.03.017.

Müller, B. *et al.* (2018) 'Wide-range optical pH imaging of cementitious materials exposed to chemically corrosive environments', *RILEM Technical Letters*, 3, pp. 39–45. Available at: https://doi.org/10.21809/RILEMTECHLETT.2018.72.

Muntean, A., Böhm, M. and Kropp, J. (2011) 'Moving carbonation fronts in concrete: A moving-sharp-interface approach', *Chemical Engineering Science*, 66(3), pp. 538–547. Available at: https://doi.org/10.1016/J.CES.2010.11.011.

De Muynck, W. *et al.* (2008) 'Bacterial carbonate precipitation as an alternative surface treatment for concrete', *Construction and Building Materials*, 22(5), pp. 875–885. Available at: https://doi.org/10.1016/J.CONBUILDMAT.2006.12.011.

de Muynck, W., de Belie, N. and Verstraete, W. (2010) 'Microbial carbonate precipitation in construction materials: A review', *Ecological Engineering*, 36(2), pp. 118–136. Available at: https://doi.org/10.1016/J.ECOLENG.2009.02.006.

De Muynck, W., De Belie, N. and Verstraete, W. (2010a) 'Microbial carbonate precipitation in construction materials: A review', *Ecological Engineering*, 36(2), pp. 118–136. Available at: https://doi.org/10.1016/J.ECOLENG.2009.02.006.

De Muynck, W., De Belie, N. and Verstraete, W. (2010b) 'Microbial carbonate precipitation in construction materials: A review', *Ecological Engineering*, pp. 118–136. Available at: https://doi.org/10.1016/j.ecoleng.2009.02.006.

Neville, A. (1995a) *Properties of concrete*. Available at: https://www.academia.edu/download/52236036/properties-of-concrete-by-am-neville.pdf (Accessed: 7 October 2024).

Neville, A. (1995b) *Properties of concrete*. Available at: https://www.academia.edu/download/52236036/properties-of-concrete-by-am-neville.pdf (Accessed: 10 October 2024).

Ng, W. *et al.* (no date) 'An overview of the factors affecting microbial-induced calcite precipitation and its potential application in soil improvement', *CiteseerWS Ng, ML Lee, SL HiiInternational Journal of Civil and Environmental Engineering, 2012•Citeseer* [Preprint]. Available at: https://citeseerx.ist.psu.edu/document?repid=rep1&type=pdf&doi=9618280c491a48ba578acba478d1432cd0315bab (Accessed: 6 August 2024).

Nie, J. *et al.* (2019) 'Bio-based epoxidized natural rubber/chitin nanocrystals composites: Self-healing and enhanced mechanical properties', *Composites Part B: Engineering*, 172, pp. 152–160. Available at: https://doi.org/10.1016/J.COMPOSITESB.2019.04.035.

Nielsen, S.D. *et al.* (2019a) 'Optical sensing of ph and o2 in the evaluation of bioactive self-healing cement', *ACS Omega*, 4(23), pp. 20237–20243. Available at: https://doi.org/10.1021/acsomega.9b02541.

Nielsen, S.D. *et al.* (2019b) 'Optical sensing of ph and o2 in the evaluation of bioactive self-healing cement', *ACS Omega*, 4(23), pp. 20237–20243. Available at: https://doi.org/10.1021/ACSOMEGA.9B02541.

Nishiwaki, T. *et al.* (2006) 'Development of Self-Healing System for Concrete with Selective Heating around Crack', *Journal of Advanced Concrete Technology*, 4(2), pp. 267–275. Available at: https://doi.org/10.3151/JACT.4.267.

Nishiwaki, T. *et al.* (2012) 'Experimental Study on Self-Healing Capability of FRCC Using Different Types of Synthetic Fibers', *Journal of Advanced Concrete Technology*, 10(6), pp. 195–206. Available at: https://doi.org/10.3151/JACT.10.195.

Nishiwaki, T. *et al.* (2014) 'Self-Healing Capability of Fiber-Reinforced Cementitious Composites for Recovery of Watertightness and Mechanical Properties', *Materials 2014, Vol. 7, Pages 2141-2154*, 7(3), pp. 2141–2154. Available at: https://doi.org/10.3390/MA7032141.

Ortolan, V.K., Mancio, M. and Tutikian, B.F. (2016) 'Evaluation of the influence of the pH of concrete pore solution on the corrosion resistance of steel reinforcement', *Journal of Building Pathology and Rehabilitation*, 1(1). Available at: https://doi.org/10.1007/S41024-016-0011-8.

Palla, R. *et al.* (2017) 'High strength sustainable concrete using silica nanoparticles', *Construction and Building Materials*, 138, pp. 285–295. Available at: https://doi.org/10.1016/J.CONBUILDMAT.2017.01.129.

Papadakis, V. *et al.* (no date) 'Supplementary cementing materials in concrete: Part II: A fundamental estimation of the efficiency factor', *ElsevierVG Papadakis, S Antiohos, S TsimasCement and Concrete research, 2002•Elsevier* [Preprint]. Available at: https://www.sciencedirect.com/science/article/pii/S0008884602008293?casa_token=lxBzYtikL5IAAAAA:zwgEYoF0D3D9GKGZ3NImUlVqbjxv_hIrn0nZKiWmWowboy-M4k12vvvgC3h5Q3zL3NpNbe2hMw (Accessed: 21 August 2024).

Pareek, K. *et al.* (2017) 'Ambient temperature hydrogen storage in porous materials with exposed metal sites', *International Journal of Hydrogen Energy*, 42(10), pp. 6801–6809. Available at: https://doi.org/10.1016/J.IJHYDENE.2017.01.209.

Pareek, S. *et al.* (2014) 'Feasibility of externally activated self-repairing concrete with epoxy injection network and Cu-Al-Mn superelastic alloy reinforcing bars', *Smart Materials and Structures*, 23(10), p. 105027. Available at: https://doi.org/10.1088/0964-1726/23/10/105027.

Park, B., Materials, Y.C.-C. and B. and 2018, undefined (no date) 'Self-healing capability of cementitious materials with crystalline admixtures and super absorbent polymers (SAPs)', *Elsevier* [Preprint]. Available at: https://www.sciencedirect.com/science/article/pii/S0950061818322396?casa_token=hyc4qrnkAZ0AAAAA:0hGSQuWsvq9ovZah1oblvEvcbmymqQhf0FC06-vOixVC1KdRgg6hr1CE1zOAtYjwKd4M91f6vIC9 (Accessed: 31 March 2022).

Park, M.K., Lee, S. and Kim, Y.S. (2022) 'Effects of pH and Osmotic Changes on the Metabolic Expressions of Bacillus subtilis Strain 168 in Metabolite Pathways including Leucine Metabolism', *Metabolites*, 12(2). Available at: https://doi.org/10.3390/METABO12020112/S1.

Park, S.H. *et al.* (2012) 'Tensile behavior of Ultra High Performance Hybrid Fiber Reinforced Concrete', *Cement and Concrete Composites*, 34(2), pp. 172–184. Available at: https://doi.org/10.1016/J.CEMCONCOMP.2011.09.009.

Paul, V.G., Wronkiewicz, D.J. and Mormile, M.R. (2017) 'Impact of elevated CO2 concentrations on carbonate mineral precipitation ability of sulfate-reducing bacteria and implications for CO2 sequestration', *Applied Geochemistry*, 78, pp. 250–271. Available at: https://doi.org/10.1016/J.APGEOCHEM.2017.01.010.

Pavía, S. and Condren, E. (2008) 'Study of the Durability of OPC versus GGBS Concrete on Exposure to Silage Effluent', *Journal of Materials in Civil Engineering*, 20(4), pp. 313–320. Available at: https://doi.org/10.1061/(ASCE)0899-1561(2008)20:4(313).

Pelletier, M.M. *et al.* (no date) *Self-healing concrete with a microencapsulated healing agent*.

Phanyawong, S. *et al.* (2017) 'Polymeric microcapsules with switchable mechanical properties for self-healing concrete: synthesis, characterisation and proof of concept', *Smart Materials and Structures*, 26(4), p. 045025. Available at: https://doi.org/10.1088/1361-665X/AA516C.

Poursaee, A. *et al.* (no date) 'Corrosion of steel bars in OPC mortar exposed to NaCl, MgCl2 and CaCl2: Macro-and micro-cell corrosion perspective', *ElsevierA Poursaee, A Laurent, CM HanssonCement and Concrete Research, 2010•Elsevier* [Preprint]. Available at: https://www.sciencedirect.com/science/article/pii/S0008884609002828?casa_token=kdgRNEwz9yQAAAAA:dDfQQq_9DNbAwiKzZiw68-sqlc3MN6y_dQNATQ6Gn8vhjgq34_e56UR9uw2oIQa3IsG94P95vg (Accessed: 10 October 2024).

Pu, Q. *et al.* (no date) 'Evolution of pH and chemical composition of pore solution in carbonated concrete', *ElsevierQ Pu, L Jiang, J Xu, H Chu, Y Xu, Y ZhangConstruction and Building materials, 2012•Elsevier* [Preprint]. Available at: https://www.sciencedirect.com/science/article/pii/S0950061811005265?casa_token=I6SuA595D10AAAAA:ukpvwrjkShPMm4j3XXpI41CPJfSzCfd29wdNFb5XWTSb2QTxf06aq2gcBUk-TOa2jogVYkBl3Q (Accessed: 27 August 2024).

Puchkov, E. (2016) 'Image Analysis in Microbiology: A Review', *Journal of Computer and Communications*, 04(15), pp. 8–32. Available at: https://doi.org/10.4236/JCC.2016.415002.

Qian, S. *et al.* (2009) 'Self-healing behavior of strain hardening cementitious composites incorporating local waste materials', *Cement and Concrete Composites*, 31(9), pp. 613–621. Available at: https://doi.org/10.1016/J.CEMCONCOMP.2009.03.003.

Qureshi, T.S., Kanellopoulos, A. and Al-Tabbaa, A. (2016) 'Encapsulation of expansive powder minerals within a concentric glass capsule system for self-healing concrete', *Construction and Building Materials*, 121, pp. 629–643. Available at: https://doi.org/10.1016/J.CONBUILDMAT.2016.06.030.

Rajczakowska, M. *et al.* (2019) 'Autogenous Self-Healing: A Better Solution for Concrete', *Journal of Materials in Civil Engineering*, 31(9), p. 03119001. Available at: https://doi.org/10.1061/(ASCE)MT.1943-5533.0002764.

Razmi, N. *et al.* (2023) 'Monitoring the effect of pH on the growth of pathogenic bacteria using electrical impedance spectroscopy', *Results in Engineering*, 20, p. 101425. Available at: https://doi.org/10.1016/J.RINENG.2023.101425.

Reda, M.A. and Chidiac, S.E. (2022) 'Performance of Capsules in Self-Healing Cementitious Material', *Materials*, 15(20). Available at: https://doi.org/10.3390/MA15207302.

Reeburgh, W.S. (2007) 'Oceanic Methane Biogeochemistry', *Chemical Reviews*, 107(2), pp. 486–513. Available at: https://doi.org/10.1021/CR050362V.

Rodriguez-Navarro, C. *et al.* (2003) 'Conservation of ornamental stone by Myxococcus xanthus-induced carbonate biomineralization', *Applied and Environmental Microbiology*, 69(4), pp. 2182–2193. Available at: https://doi.org/10.1128/AEM.69.4.2182-2193.2003/ASSET/E77F1730-7C1B-4F02-BC71-E7A9EBCCBC97/ASSETS/GRAPHIC/AM0431483009.JPEG.

de Rooij, M. *et al.* (eds) (2013) 'Self-Healing Phenomena in Cement-Based Materials', 11. Available at: https://doi.org/10.1007/978-94-007-6624-2.

Rooij, M de *et al.* (2013) 'Self-Healing Phenomena in Cement-Based Materials: State-of-the-Art Report of RILEM Technical Committee 221-SHC: Self-Healing Phenomena in Cement-Based Materials'. Edited by Mario de Rooij et al., 11. Available at: https://doi.org/10.1007/978-94-007-6624-2.

Şahmaran, M. *et al.* (no date) 'Self-healing of mechanically-loaded self consolidating concretes with high volumes of fly ash', *ElsevierM Şahmaran, SB Keskin, G Ozerkan, IO YamanCement and Concrete Composites, 2008•Elsevier* [Preprint]. Available at: https://www.sciencedirect.com/science/article/pii/S0958946508000838?casa_token=k5HXopzbG_UAAAAA:2yIpaO2sEnNcyxvfG2LWZhQUIML0jjYd2Aseb3BiTST7IFGGi3qHfcCGgmeb9Rpc0eahS6wLXQ (Accessed: 22 May 2024).

Sahmaran, M., Yildirim, G. and Erdem, T.K. (2013) 'Self-healing capability of cementitious composites incorporating different supplementary cementitious materials', *Cement and Concrete Composites*, 35(1), pp. 89–101. Available at: https://doi.org/10.1016/J.CEMCONCOMP.2012.08.013.

Sandaruwan, H.H.P.B. *et al.* (2024) 'Next-generation methods for precise pH detection in ocular chemical burns: a review of recent analytical advancements', *Analytical Methods* [Preprint]. Available at: https://doi.org/10.1039/D4AY01178C.

Sari, Y.D. (2015) 'Soil Strength Improvement by Microbial Cementation', *Marine Georesources and Geotechnology*, 33(6), pp. 567–571. Available at: https://doi.org/10.1080/1064119X.2014.953234.

Schlangen, E., Heide, N. ter and Breugel, K. van (2006) 'CRACK HEALING OF EARLY AGE CRACKS IN CONCRETE', *Measuring, Monitoring and Modeling Concrete Properties*, pp. 273–284. Available at: https://doi.org/10.1007/978-1-4020-5104-3_32.

Schmets, A. (2007) *Proceedings of the First International Conference on Self Healing Materials 18 - 20 April, 2007, Noordwijk aan Zee, The Netherlands*, *Betase BV IOP*. Dordrecht: Springer. Available at: http://www.mse.umd.edu/undergrad/490_materials_design/490_fall_2004/final_report-f04.pdf (Accessed: 22 March 2022).

Selvarajoo, T. *et al.* (2020) 'Mechanical response of a vascular self-healing cementitious material system under varying loading conditions', *Construction and Building Materials*, 254. Available at: https://doi.org/10.1016/J.CONBUILDMAT.2020.119245.

Senot, S. *et al.* (2012) 'Self Healing of Concrete Structures - Novel Approach Using Porous Network Concrete', *Journal of Advanced Concrete Technology*, 10(5), pp. 185–194. Available at: https://doi.org/10.3151/JACT.10.185.

Shrestha, R. *et al.* (2022) 'The effect of low-pH concrete on microbial community development in bentonite suspensions as a model for microbial activity prediction in future nuclear waste repository', *Science of The Total Environment*, 808, p. 151861. Available at: https://doi.org/10.1016/J.SCITOTENV.2021.151861.

Siad, H. *et al.* (2018) 'Advanced engineered cementitious composites with combined self-sensing and self-healing functionalities', *Construction and Building Materials*, 176, pp. 313–322. Available at: https://doi.org/10.1016/J.CONBUILDMAT.2018.05.026.

Sibhat, M. *et al.* (2024) 'Advancement in sodium carbonation pathways for sustainable carbon capture and utilization: A review', *Results in Engineering*, 23, p. 102536. Available at: https://doi.org/10.1016/J.RINENG.2024.102536.

Sidiq, A., Gravina, R. and Giustozzi, F. (2019) 'Is concrete healing really efficient? A review', *Construction and Building Materials*, 205, pp. 257–273. Available at: https://doi.org/10.1016/J.CONBUILDMAT.2019.02.002.

Silva-Castro, G.A. *et al.* (2015) 'Bioprecipitation of calcium carbonate crystals by bacteria isolated from saline environments grown in culture media amended with seawater and real brine', *BioMed Research International*, 2015. Available at: https://doi.org/10.1155/2015/816102.

Sisomphon, K., Copuroglu, O. and Koenders, E.A.B. (2012) 'Self-healing of surface cracks in mortars with expansive additive and crystalline additive', *Cement and Concrete Composites*, 34(4), pp. 566–574. Available at: https://doi.org/10.1016/J.CEMCONCOMP.2012.01.005.

Sisomphon, K., Copuroglu, O. and Koenders, E.A.B. (2013) 'Effect of exposure conditions on self healing behavior of strain hardening cementitious composites incorporating various

cementitious materials', *Construction and Building Materials*, 42, pp. 217–224. Available at: https://doi.org/10.1016/J.CONBUILDMAT.2013.01.012.

Snoeck, D., Smetryns, P.A. and de Belie, N. (2015) 'Improved multiple cracking and autogenous healing in cementitious materials by means of chemically-treated natural fibres', *Biosystems Engineering*, 139, pp. 87–99. Available at: https://doi.org/10.1016/J.BIOSYSTEMSENG.2015.08.007.

Son, H., Materials, H.K.-C.S. in C. and 2022, undefined (no date) 'Effect of nutrient types on the hydration of cementitious materials with co-cultured bacteria', *ElsevierHM Son, H KimCase Studies in Construction Materials, 2022•Elsevier* [Preprint]. Available at: https://www.sciencedirect.com/science/article/pii/S221450952200256X (Accessed: 29 August 2024).

Song, E.M. *et al.* (2014) 'Surface modification of CaCO3 nanoparticles by alkylbenzene sulfonic acid surfactant', *Colloids and Surfaces A: Physicochemical and Engineering Aspects*, 461(1), pp. 1–10. Available at: https://doi.org/10.1016/J.COLSURFA.2014.07.020.

Song, H. *et al.* (no date) 'Predicting carbonation in early-aged cracked concrete', *ElsevierHW Song, SJ Kwon, KJ Byun, CK ParkCement and Concrete Research, 2006•Elsevier* [Preprint]. Available at: https://www.sciencedirect.com/science/article/pii/S0008884605003418?casa_token=7rTBEny6QFgAAAAA:st44IaxTAJHn1pKZVfoYYCySVxmE5YIm7THgUBUJSbC_KnwoCQdfzrU7yc1PMI_FWPXcOwYT (Accessed: 2 October 2024).

Soroushian, P. and Bayasi, Z. (1991) 'Fiber Type Effects on the Performance of Steel Fiber Reinforced Concrete', *Materials Journal*, 88(2), pp. 129–134. Available at: https://doi.org/10.14359/1883.

Souid, A. *et al.* (2019) 'Experimental data of bio self-healing concrete incubated in saturated natural soil', *Data in Brief*, 26, p. 104394. Available at: https://doi.org/10.1016/J.DIB.2019.104394.

Souradeep, G. and Kua, H.W. (2016a) 'Encapsulation Technology and Techniques in Self-Healing Concrete', *Journal of Materials in Civil Engineering*, 28(12), p. 04016165. Available at: https://doi.org/10.1061/(ASCE)MT.1943-5533.0001687.

Souradeep, G. and Kua, H.W. (2016b) 'Encapsulation Technology and Techniques in Self-Healing Concrete', *Journal of Materials in Civil Engineering*, 28(12), p. 04016165. Available at: https://doi.org/10.1061/(ASCE)MT.1943-5533.0001687.

de Souza Oliveira, A. *et al.* (2021) 'An overview of a twofold effect of crystalline admixtures in cement-based materials: from permeability-reducers to self-healing stimulators', *Journal of Building Engineering*, 41, p. 102400. Available at: https://doi.org/10.1016/J.JOBE.2021.102400.

Stocks-Fischer, S., Galinat, J.K. and Bang, S.S. (1999a) 'Microbiological precipitation of CaCO3', *Soil Biology and Biochemistry*, 31(11), pp. 1563–1571. Available at: https://doi.org/10.1016/S0038-0717(99)00082-6.

Stocks-Fischer, S., Galinat, J.K. and Bang, S.S. (1999b) 'Microbiological precipitation of CaCO3', *Soil Biology and Biochemistry*, 31(11), pp. 1563–1571. Available at: https://doi.org/10.1016/S0038-0717(99)00082-6.

Stutzman, P.E., Feng, P. and Bullard, J.W. (2016) 'Phase Analysis of Portland Cement by Combined Quantitative X-Ray Powder Diffraction and Scanning Electron Microscopy', *Journal of research of the National Institute of Standards and Technology*, 121, pp. 47–107. Available at: https://doi.org/10.6028/JRES.121.004.

Su, Y. *et al.* (2024) 'A new bacteria-based self-healing system triggered by sulfate ion for cementitious material', *Journal of Building Engineering*, 86, p. 108886. Available at: https://doi.org/10.1016/J.JOBE.2024.108886.

Sun, L., Yu, W.Y. and Ge, Q. (2011) 'Experimental Research on the Self-Healing Performance of Micro-Cracks in Concrete Bridge', *Advanced Materials Research*, 250–253, pp. 28–32. Available at: https://doi.org/10.4028/WWW.SCIENTIFIC.NET/AMR.250-253.28.

Tang, Y. and Xu, J. (2021) 'Application of microbial precipitation in self-healing concrete: A review on the protection strategies for bacteria', *Construction and Building Materials*, 306, p. 124950. Available at: https://doi.org/10.1016/J.CONBUILDMAT.2021.124950.

Termkhajornkit, P. *et al.* (2009) 'Self-healing ability of fly ash–cement systems', *Cement and Concrete Composites*, 31(3), pp. 195–203. Available at: https://doi.org/10.1016/J.CEMCONCOMP.2008.12.009.

'Test Method for Flexural Strength of Concrete (Using Simple Beam with Third-Point Loading)' (2018). Available at: https://doi.org/10.1520/C0078_C0078M-18.

Title), M.F.-(No and 1974, undefined (no date) 'Handbook of concrete engineering', *cir.nii.ac.jp* [Preprint]. Available at: https://cir.nii.ac.jp/crid/1130282270748059904 (Accessed: 7 October 2024).

van Tittelboom, K. *et al.* (2010) 'Use of bacteria to repair cracks in concrete', *Cement and Concrete Research*, 40(1), pp. 157–166. Available at: https://doi.org/10.1016/J.CEMCONRES.2009.08.025.

van Tittelboom, K. *et al.* (2011) 'Self-healing efficiency of cementitious materials containing tubular capsules filled with healing agent', *Cement and Concrete Composites*, 33(4), pp. 497–505. Available at: https://doi.org/10.1016/J.CEMCONCOMP.2011.01.004.

van Tittelboom, K., de Belie, N., *et al.* (2012) 'Acoustic emission analysis for the quantification of autonomous crack healing in concrete', *Construction and Building Materials*, 28(1), pp. 333–341. Available at: https://doi.org/10.1016/J.CONBUILDMAT.2011.08.079.

van Tittelboom, K., Gruyaert, E., *et al.* (2012) 'Influence of mix composition on the extent of autogenous crack healing by continued hydration or calcium carbonate formation', *Construction and Building Materials*, C(37), pp. 349–359. Available at: https://doi.org/10.1016/J.CONBUILDMAT.2012.07.026.

van Tittelboom, K. *et al.* (2015a) 'The efficiency of self-healing concrete using alternative manufacturing procedures and more realistic crack patterns', *Cement and Concrete Composites*, 57, pp. 142–152. Available at: https://doi.org/10.1016/J.CEMCONCOMP.2014.12.002.

van Tittelboom, K. *et al.* (2015b) 'The efficiency of self-healing concrete using alternative manufacturing procedures and more realistic crack patterns', *Cement and Concrete*

Composites, 57, pp. 142–152. Available at: https://doi.org/10.1016/J.CEMCONCOMP.2014.12.002.

Van Tittelboom, K. and De Belie, N. (2013) 'Self-Healing in Cementitious Materials—A Review', *Materials 2013, Vol. 6, Pages 2182-2217*, 6(6), pp. 2182–2217. Available at: https://doi.org/10.3390/MA6062182.

van Tittelboom, K. and de Belie, N. (2013a) 'Self-healing in cementitious materials-a review', *Materials*, 6(6), pp. 2182–2217. Available at: https://doi.org/10.3390/MA6062182.

van Tittelboom, K. and de Belie, N. (2013b) 'Self-Healing in Cementitious Materials—A Review', *Materials 2013, Vol. 6, Pages 2182-2217*, 6(6), pp. 2182–2217. Available at: https://doi.org/10.3390/MA6062182.

Tittelboom, K. Van, Materials, N.D.B.- and 2013, undefined (1994) 'Self-healing in cementitious materials—A review', *mdpi.comK Van Tittelboom, N De BelieMaterials, 2013•mdpi.com*, 6, pp. 2182–2217. Available at: https://doi.org/10.3390/ma6062182.

Toohey, K.S. *et al.* (2007) 'Self-healing materials with microvascular networks', *Nature materials*, 6(8), pp. 581–585. Available at: https://doi.org/10.1038/NMAT1934.

TR22 Non-structural cracks in concrete PDF (no date). Available at: https://www.concretebookshop.com/tr22-non-structural-cracks-in-concrete-pdf-1779-p.asp (Accessed: 9 June 2025).

Tran, D.T. *et al.* (2024) 'Calcium alginate elastic capsules for microalgal cultivation', *RSC Advances*, 14(22), p. 15441. Available at: https://doi.org/10.1039/D4RA00519H.

Tran, P., Lander, S.M. and Prindle, A. (2024) 'Active pH regulation facilitates Bacillus subtilis biofilm development in a minimally buffered environment', *mBio*, 15(3). Available at: https://doi.org/10.1128/MBIO.03387-23.

Tziviloglou, E. *et al.* (no date) 'Bacteria-based self-healing concrete to increase liquid tightness of cracks', *ElsevierE Tziviloglou, V Wiktor, HM Jonkers, E SchlangenConstruction and Building Materials, 2016•Elsevier* [Preprint]. Available at: https://www.sciencedirect.com/science/article/pii/S0950061816310078 (Accessed: 28 October 2024).

Umar, M., Kassim, K.A. and Ping Chiet, K.T. (2016) 'Biological process of soil improvement in civil engineering: A review', *Journal of Rock Mechanics and Geotechnical Engineering*, 8(5), pp. 767–774. Available at: https://doi.org/10.1016/J.JRMGE.2016.02.004.

Vijay, K., Murmu, M. and Deo, S. V. (2017) 'Bacteria based self healing concrete – A review', *Construction and Building Materials*, 152, pp. 1008–1014. Available at: https://doi.org/10.1016/J.CONBUILDMAT.2017.07.040.

Violetta, B.K. and Yuers, K.L. (2015) 'ACI 212 . 3R-16 Report on Chemical Admixtures for Concrete', 28, pp. 0–15.

Wang, J. *et al.* (2017) 'Bacillus sphaericus LMG 22257 is physiologically suitable for self-healing concrete', *Applied microbiology and biotechnology*, 101(12), pp. 5101–5114. Available at: https://doi.org/10.1007/S00253-017-8260-2.

Wang, J. *et al.* (2018a) 'Self-healing properties of reactive powder concrete with nanofillers', *Smart Materials and Structures*, 27(11). Available at: https://doi.org/10.1088/1361-665X/AAE59F.

Wang, J. *et al.* (2018b) 'Self-healing properties of reactive powder concrete with nanofillers', *Smart Materials and Structures*, 27(11), p. 115033. Available at: https://doi.org/10.1088/1361-665X/AAE59F.

Wang, J. *et al.* (no date a) 'Application of hydrogel encapsulated carbonate precipitating bacteria for approaching a realistic self-healing in concrete', *Elsevier* [Preprint]. Available at: https://www.sciencedirect.com/science/article/pii/S095006181400631X (Accessed: 7 March 2023).

Wang, J. *et al.* (no date b) 'Application of hydrogel encapsulated carbonate precipitating bacteria for approaching a realistic self-healing in concrete', *ElsevierJY Wang, D Snoeck, S Van Vlierberghe, W Verstraete, N De BelieConstruction and building materials, 2014•Elsevier* [Preprint]. Available at: https://www.sciencedirect.com/science/article/pii/S095006181400631X?casa_token=8MO2BLrg3aQAAAAA:1VCTo19LPqmVqarRYdcjfCl-yjq8Zdhj07bCE3uJkMzHNpIUO60_wjMKytXXuSwcL147nojxWQ (Accessed: 2 October 2024).

Wang, J. *et al.* (no date c) 'Application of hydrogel encapsulated carbonate precipitating bacteria for approaching a realistic self-healing in concrete', *ElsevierJY Wang, D Snoeck, S Van Vlierberghe, W Verstraete, N De BelieConstruction and building materials, 2014•Elsevier* [Preprint]. Available at: https://www.sciencedirect.com/science/article/pii/S095006181400631X (Accessed: 28 October 2024).

Wang, J.Y., Snoeck, D., van Vlierberghe, S., *et al.* (2014) 'Application of hydrogel encapsulated carbonate precipitating bacteria for approaching a realistic self-healing in concrete', *Construction and Building Materials*, 68, pp. 110–119. Available at: https://doi.org/10.1016/J.CONBUILDMAT.2014.06.018.

Wang, J.Y., Snoeck, D., Van Vlierberghe, S., *et al.* (2014) 'Application of hydrogel encapsulated carbonate precipitating bacteria for approaching a realistic self-healing in concrete', *Construction and Building Materials*, 68, pp. 110–119. Available at: https://doi.org/10.1016/J.CONBUILDMAT.2014.06.018.

Wang, J.Y., Soens, H., *et al.* (2014) 'Self-healing concrete by use of microencapsulated bacterial spores', *Cement and Concrete Research*, 56, pp. 139–152. Available at: https://doi.org/10.1016/J.CEMCONRES.2013.11.009.

Wang, X. *et al.* (2019) 'Laboratory and field study on the performance of microcapsule-based self-healing concrete in tunnel engineering', *Construction and Building Materials*, 220, pp. 90–101. Available at: https://doi.org/10.1016/J.CONBUILDMAT.2019.06.017.

Whiffin, V., Journal, L.V.P.-G. and 2007, undefined (2007) 'Microbial carbonate precipitation as a soil improvement technique', *Taylor & FrancisVS Whiffin, LA Van Paassen, MP HarkesGeomicrobiology Journal, 2007•Taylor & Francis*, 24(5), pp. 417–423. Available at: https://doi.org/10.1080/01490450701436505.

White, S.R. *et al.* (2001) 'Autonomic healing of polymer composites', *Nature 2001 409:6822*, 409(6822), pp. 794–797. Available at: https://doi.org/10.1038/35057232.

Whitman, W., ... D.C.-P. of the and 1998, undefined (1998) 'Prokaryotes: the unseen majority', *National Acad Sciences*, 95, pp. 6578–6583. Available at: https://www.pnas.org/doi/abs/10.1073/pnas.95.12.6578 (Accessed: 27 February 2023).

Wiktor, V., composites, H.J.-C. and concrete and 2011, undefined (no date) 'Quantification of crack-healing in novel bacteria-based self-healing concrete', *Elsevier* [Preprint]. Available at: https://www.sciencedirect.com/science/article/pii/S0958946511000618?casa_token=fMZV2-cU6owAAAAA:jduZ_ZYdEE0Xl5tnpzmhV1tCeRYWi6sKqp0MiAmtaVGoYBcKiXT8lNDyEiTQq1F-_gYaFQ62 (Accessed: 1 September 2022).

Williams, S.L., Kirisits, M.J. and Ferron, R.D. (2017) 'Influence of concrete-related environmental stressors on biomineralizing bacteria used in self-healing concrete', *Construction and Building Materials*, 139, pp. 611–618. Available at: https://doi.org/10.1016/J.CONBUILDMAT.2016.09.155.

Wu, M. *et al.* (2019) 'Growth environment optimization for inducing bacterial mineralization and its application in concrete healing', *Construction and Building Materials*, 209, pp. 631–643. Available at: https://doi.org/10.1016/J.CONBUILDMAT.2019.03.181.

Wu, M., Johannesson, B., *et al.* (no date) 'A review: Self-healing in cementitious materials and engineered cementitious composite as a self-healing material', *Elsevier* [Preprint]. Available at: https://www.sciencedirect.com/science/article/pii/S0950061811005198 (Accessed: 27 February 2023).

Wu, M., Hu, X., *et al.* (2019) 'Growth environment optimization for inducing bacterial mineralization and its application in concrete healing', *Elsevier* [Preprint]. Available at: https://www.sciencedirect.com/science/article/pii/S0950061819306725 (Accessed: 27 February 2023).

Wu, M., Johannesson, B. and Geiker, M. (2012a) 'A review: Self-healing in cementitious materials and engineered cementitious composite as a self-healing material', *Construction and Building Materials*, 28(1), pp. 571–583. Available at: https://doi.org/10.1016/J.CONBUILDMAT.2011.08.086.

Wu, M., Johannesson, B. and Geiker, M. (2012b) 'A review: Self-healing in cementitious materials and engineered cementitious composite as a self-healing material', *Construction and Building Materials*, 28(1), pp. 571–583. Available at: https://doi.org/10.1016/J.CONBUILDMAT.2011.08.086.

Wu, M., Johannesson, B. and Geiker, M. (2012c) 'A review: Self-healing in cementitious materials and engineered cementitious composite as a self-healing material', *Construction and Building Materials*, 28(1), pp. 571–583. Available at: https://doi.org/10.1016/J.CONBUILDMAT.2011.08.086.

Wu, M., Johannesson, B. and Geiker, M. (2012d) 'A review: Self-healing in cementitious materials and engineered cementitious composite as a self-healing material', *Construction and Building Materials*, 28(1), pp. 571–583. Available at: https://doi.org/10.1016/J.CONBUILDMAT.2011.08.086.

Xiong, W. *et al.* (2015) 'A novel capsule-based self-recovery system with a chloride ion trigger', *Scientific Reports 2015 5:1*, 5(1), pp. 1–6. Available at: https://doi.org/10.1038/srep10866.

Xu, J., Wang, X. and Wang, B. (2018) 'Biochemical process of ureolysis-based microbial CaCO 3 precipitation and its application in self-healing concrete', *Applied microbiology and biotechnology*, 102(7), pp. 3121–3132. Available at: https://doi.org/10.1007/S00253-018-8779-X.

Xu, J. and Yao, W. (2014) 'Multiscale mechanical quantification of self-healing concrete incorporating non-ureolytic bacteria-based healing agent', *Cement and Concrete Research*, Complete(64), pp. 1–10. Available at: https://doi.org/10.1016/J.CEMCONRES.2014.06.003.

Yamanaka, T. (2003) 'The effect of pH on the growth of saprotrophic and ectomycorrhizal ammonia fungi in vitro', *Mycologia*, 95(4), pp. 584–589. Available at: https://doi.org/10.1080/15572536.2004.11833062.

Yang, Y. *et al.* (2009) 'Autogenous healing of engineered cementitious composites under wet-dry cycles', *Cement and Concrete Research*, 39(5), pp. 382–390. Available at: https://doi.org/10.1016/J.CEMCONRES.2009.01.013.

Yang, Z. *et al.* (2011) 'A self-healing cementitious composite using oil core/silica gel shell microcapsules', *Cement and Concrete Composites*, 33, pp. 506–512. Available at: https://doi.org/10.1016/j.cemconcomp.2011.01.010.

Yargicoglu, E.N. and Reddy, K.R. (2015) 'Review of biological diagnostic tools and their applications in geoenvironmental engineering', *Reviews in Environmental Science and Biotechnology*, 14(2), pp. 161–194. Available at: https://doi.org/10.1007/S11157-014-9358-Y.

Zadeike, D. *et al.* (2024) 'Exploring Calcium Alginate-Based Gels for Encapsulation of Lacticaseibacillus paracasei to Enhance Stability in Functional Breadmaking', *Gels (Basel, Switzerland)*, 10(10). Available at: https://doi.org/10.3390/GELS10100641.

Zeigler, D.R. and Perkins, J.B. (2021) 'The Genus Bacillus', *Practical Handbook of Microbiology*, pp. 249–278. Available at: https://doi.org/10.1201/9781003099277-24.

Zeng, H. *et al.* (2022) 'Effect of limestone powder and fly ash on the pH evolution coefficient of concrete in a sulfate-freeze–thaw environment', *Journal of Materials Research and Technology*, 16, pp. 1889–1903. Available at: https://doi.org/10.1016/J.JMRT.2021.12.033.

Zhang, L. *et al.* (2016) 'Study on the reinforcing mechanisms of nano silica to cement-based materials with theoretical calculation and experimental evidence':, *http://dx.doi.org/10.1177/0021998316632602*, 50(29), pp. 4135–4146. Available at: https://doi.org/10.1177/0021998316632602.

Zhang, W. *et al.* (2020) 'Self-healing cement concrete composites for resilient infrastructures: A review', *Composites Part B: Engineering*. Elsevier Ltd. Available at: https://doi.org/10.1016/j.compositesb.2020.107892.

Zhang, X. *et al.* (2021) 'Effects of carrier on the performance of bacteria-based self-healing concrete', *Construction and Building Materials*, 305, p. 124771. Available at: https://doi.org/10.1016/J.CONBUILDMAT.2021.124771.

Zhang, X.H., Wang, X.W. and Xu, Y.S. (2022) 'Groundwater environment and related potential engineering disasters of deep underground space in Shanghai', *Bulletin of Engineering Geology and the Environment*, 81(5). Available at: https://doi.org/10.1007/S10064-022-02692-1.

Zhang, Z., Qian, S. and Ma, H. (2014) 'Investigating mechanical properties and self-healing behavior of micro-cracked ECC with different volume of fly ash', *Construction and Building Materials*, 52, pp. 17–23. Available at: https://doi.org/10.1016/J.CONBUILDMAT.2013.11.001.

Zhao, J. *et al.* (2022) 'Fungal colonization and biomineralization for bioprotection of concrete', *Journal of Cleaner Production*, 330. Available at: https://doi.org/10.1016/j.jclepro.2021.129793.

Zhou, Z. *et al.* (2011) 'Influence of Slag and Fly Ash on the Self-Healing Ability of Concrete', *Advanced Materials Research*, 306–307, pp. 1020–1023. Available at: https://doi.org/10.4028/WWW.SCIENTIFIC.NET/AMR.306-307.1020.

Zhu, D.Y., Rong, M.Z. and Zhang, M.Q. (2015) 'Self-healing polymeric materials based on microencapsulated healing agents: From design to preparation', *Progress in Polymer Science*, Complete(49–50), pp. 175–220. Available at: https://doi.org/10.1016/J.PROGPOLYMSCI.2015.07.002.

van der Zwaag, S. (2007) 'An Introduction to Material Design Principles: Damage Prevention versus Damage Management', *Springer Series in Materials Science*, 100, pp. 1–18. Available at: https://doi.org/10.1007/978-1-4020-6250-6_1.